Table des matières

Liste des figures

Liste des abréviations

°C	Degré Celsius
$^{\bullet}$OH	radical hydroxyle
$^{1}O_2$	Oxygène singulet
5'dRP	5' désoxyribose phosphate
6-4PP	Photoproduits pyrimidine (6-4) pyrimidone
8-oxoG	8-oxo-7,8-dihydroguanine
Å	Angström
ADN	Acide désoxyribonucléique
ADP	Adénosine diphosphate
ALC1	de l'anglais « *Amplified in liver cancer 1* »
AP	site abasique (apurinique or apyrimidique)
APE1	AP endonucléase 1
APLF	de l'anglais « *Aprataxin and PNKP like factor* »
ARH3	de l'anglais « *ADP-ribosyl-hydrolase* 3 »
ARN POLIIo	de l'anglais « *elongating RNA polymerase II complex* »
ARN	Acide ribonucléique
ART	domaine de transfert de l'ADP-ribose
ATM	de l'anglais « *Ataxia telangiectasia mutated* »
ATP	Adénosine triphosphate
ATR	de l'anglais « *Ataxia telangiectasia and Rad3 related*»
BER	réparation par excision de bases
BHD1-3	domaines en épingle à cheveux 1-3
BRCA1/2	de l'anglais « *Breast cancer 1/2 susceptibility protein*»
BRCT	de l'anglais « *breast cancer susceptibility protein, BRCA-1, C-terminal* »
Brg1	de l'anglais « *Brahma-related gene-1*»

CAK	de l'anglais « *Cyclin activating kinase* »
CBS	Carcinomes baso-cellulaires
C-C	cytosine-cytosine
CHD2/4	de l'anglais « *Chromodomain helicase DNA binding protein 2/4* »
CHFR	de l'anglais « *Checkpoint with forkhead and ring finger domains* »
CHIP	Immunoprécipitation de la chromatine
CHO	de l'anglais « *Chinese hamster ovary* »
Co-IP	Co-immunoprécipitation
COP9	de l'anglais « *Constitutive photomorphogenesis 9* »
CPD	dimères cyclobutaniques de pyrimidine
CS	Syndrome de Cockayne
CSA	de l'anglais « *Cockayne syndrome A protein* »
CSB	de l'anglais « *Cockayne syndrome B protein* »
CSC	Carcinomes spino-cellulaires
C-T	cytosine-thymine
Cul4A	de l'anglais « *Cullin4A* »
DDB1	de l'anglais «UV-*damaged DNA binding protein 1*»
DDB2	de l'anglais « UV-*damaged DNA binding protein 2*»
DNA-PK	de l'anglais « *DNA-dependent protein kinase* »
DSBR	réparation de cassures double-brins
e^-	électron
ERCC1	de l'anglais « *Excision repair cross-complementing rodent repair deficiency, complementation group 1*»
F1-3	doigts de zinc 1 à 3
FACS	cytométrie en flux
FACT	de l'anglais « *Facilitates chromatin transcription* »
FapyG	formamidopyrimidine (2,6-diamino-4-hydroxy-5-formamidopyrimidine)
FEN1	de l'anglais « *Flap endonuclease-1* »

FHA	de l'anglais « *Forkhead-associated domain* »
G1	de l'anglais « *Gap 1*»
G-C	guanine-cytosine
GCN5	de l'anglais « *General control of amino acid synthesis protein 5* »
GG-NER	réparation globale du génome par excision de nucléotides
G-T	guanine-thymine
H	Histone
H^+	proton
H_2O_2	peroxyde d'hydrogène
HAT	Histone acétyltransférase
HCR	réactivation dans les cellules hôtes
HD	domaine hélicoïdal
hFPG1	de l'anglais « *human Formamidopyrimidine-glycosylase 1*»
HMGN1	de l'anglais « *High mobility group nucleosome binding domain containing protein 1*»
HR	réparation par recombinaison homologue
HR23B	de l'anglais « *Human homolog of radiation sensitive 23 B protein* »
INO80	de l'anglais « *Inositol requiring mutant 80* »
IP	Immunoprécipitation
J/m^2	joule par mètre carré
Ku70/80	de l'anglais « *70/80 kDa subunit of Ku antigen* »
Lys	lysine
MAR	monomère d'ADP-ribose
MARylation	mono(ADP-ribosyl)ation
MRE11	de l'anglais « *Meiotic recombination 11* »
NAD^+	forme oxydée du ***nicotinamide adénine dinucléotide***
NBS1	de l'anglais « *Nijmegen Breakage Syndrome 1* »
NEIL1-3	de l'anglais « *Nei like glycosylase 1-3* »

NER	réparation par excision de nucléotides
NHEJ	réparation par ligation des extrémités non-homologues
NLS	signal de localisation nucléaire
NTH1	de l'anglais « *Endonuclease three homolog 1»*
$O_2^{\bullet}$	anion superoxyde
OGG1	8-oxoguanine DNA glycosylase 1
p	protéine
PAR	polymères d'ADP-riboses
PARG	poly(ADP-ribose) glycohydrolase
PARP	poly(ADP-ribose) polymérase
PARylation	poly(ADP-ribosyl)ation
PBM	de l'anglais « *PAR binding motif »*
PBZ	de l'anglais « *PAR-binding zinc finger »*
PCNA	de l'anglais « *Proliferating-cell-nuclear-antigen »*
PIP	de l'anglais « *PCNA-interacting protein »*
PNKP	de l'anglais « *Polynucleotides phosphate kinase »*
RAD4	de l'anglais « *Radiation sensitive 4 protein »*
Rbx1	de l'anglais « *Ring box protein 1 »*
RFC	de l'anglais « *Replication factor C »*
RING	de l'anglais « *Really Interesting New Gene »*
RNF111	de l'anglais « *Ring Finger Protein 111 »*
RNF146	de l'anglais « *Ring Finger Protein 146 »*
RNF168	de l'anglais « *Ring Finger Protein 168 »*
ROS	espèces réactives de l'oxygène
RPA	de l'anglais « *Replication protein A »*
SMARCA5	de l'anglais « *SWI/SNF-related matrix-associated actin-dependent regulator of chromatin subfamily A member 5 »*
SSBR	réparation des cassures simple-brin

STAGA	de l'anglais « *SPT3-TAF9-GCN5 acetylase complex* »
SWI/SNF	de l'anglais « *Switch/sucrose nonfermentable chromatin remodeling protein* »
TARG1	de l'anglais « *Terminal ADP-ribose glycohydrolase 1* »
TC-NER	réparation couplée à la transcription par excision de nucléotides
TFIIH	Facteur de transcription IIH
TFIIS	Facteur de transcription IIS
TGD	de l'anglais « *Transglutaminase homology domain* »
T-T	dimère de thymine
TTD	de l'anglais « *Trichothiodystrophie* »
UBA	de l'anglais « *Ubiquitin-associated domains* »
USP7	de l'anglais « *Ubiquitin specific protease 7* »
UV	radiations ultraviolettes
UVA-C	radiations ultraviolettes de type A à C
UV-DDB	de l'anglais « *UV-damaged DNA binding protein* »
UVRAG	de l'anglais « *UV radiation resistance-associated gene* »
$UV^{S}S$	de l'anglais « *UV-sensitive syndrome* »
UVSSA	de l'anglais *«UV Stimulated Scaffold Protein A»*
WD	motif tryptophane-acide aspartique
WGR	domaine tryptophane-glycine-arginine
WWE	domaine tryptophane-tryptophane-acide glutamique
XAB2	de l'anglais « *XPA-binding protein 2* »
XP	de l'anglais « *Xeroderma pigmentosum* »
XPA-XPG	de l'anglais « *Xeroderma pigmentosum, complementation group A to G* »
XRCC1/4	de l'anglais « *X-ray repair cross complementing protein ¼* »
γ-H2AX	de l'anglais « *H2A histone family, member X* »

Remerciements

La fin des études doctorales est un moment idéal pour regarder en arrière et pour faire le bilan de tout ce qu'on a fait, de tout ce qu'on aurait souhaité faire et surtout de ce qu'on a réussir faire grâce à l'aide de personnes extraordinaires.

Je tiens d'abord remercie à mon directeur de recherche Girish Shah. J'ai eu la chance de travailler pour lui pendant huit heureuses années de ma vie et je ne pouvais pas demander un meilleur mentor. Girish est patient, travaillant, jamais fatigué à discuter des résultats ou à apprendre. Il est aussi une des personnes les plus enthousiastes que j'ai connues. Pour lui, écrire un article et partager les résultats avec la communauté scientifique est comme un jour de célébration. Je lui dois ma gratitude pour m'avoir donné l'opportunité de développer un nouveau projet dans laboratoire et de me laisser le temps et l'espace de m'épanouir comme étudiant. Il m'a toujours encouragé à participer à des congrès afin d'échanger des idées, d'avoir des rétroactions pour mon projet et d'apprendre des meilleurs acteurs de notre champ de recherche.

Je voudrais remercier tous les membres présents et passés du laboratoire de Girish qui ont contribués à mon bien-être tant scientifique que personnel. Je n'oublierais jamais nos discutions pendant les pauses-café, qu'elles fussent scientifiques ou non-scientifiques, mais non moins importantes ou enrichissantes. Je tiens à remercier particulièrement Rashmi qui est devenue avec les années plus qu'une collègue, une vraie amie. Grâce à Rashmi, plusieurs de mes idées ont pris forme et je n'ai pas perdu mon temps dans des projets farfelus. J'admire sa patience lorsqu'elle planifie les expériences et la passion qu'elle met dans leur réalisation. Son travail est sans relâche jusqu'à l'obtention des résultats. Elle a toujours été à l'écoute que ce soit pour des expériences scientifiques ou des problèmes quotidiens. À travers elle, j'ai aussi découvert une nouvelle et vaste culture. Merci!

Thanks Nupur for obliging me to speak English every day. Without knowing, you have contributed to my development as a researcher. I owe you a lot and I hope to pay you back by teaching you French.

Je remercie Nancy, avec laquelle j'ai partagé la paillasse les deux premières années de mon doctorat. Nancy m'a poussé à la limite de mes connaissance et a toujours été disponible pour des discutions scientifiques, qui ont abouties, plusieurs fois, dans des expériences réussis. Je remercie Alicia qui a corrigé mes applications pour des bourses de recherche, mon mémoire et cette thèse. Alicia est une très bonne amie, toujours disponible pour tout le monde, toujours là pour nous aider. Elle a accompli des miracles. Merci!

Je remercie les membres du jury qui ont acceptés de donner de leur temps, très précieux, afin de lire et corriger ma thèse. Je remercie Marc qui a corrigé la thèse. Grâce à lui, elle est plus facile à lire et à comprendre. En attendant la bouteille de champagne, je lui dis à l'instant merci.

Merci à tous les organismes qui ont subventionnés mes études, tant au niveau maîtrise que doctorat : Le Fonds de recherche du Québec-Santé (FRQ-S), le Conseil de recherches en sciences naturelles et en génie du Canada (CRSNG), la Faculté de médecine de l'Université Laval, l'Association des chercheuses et chercheurs étudiant à la Faculté de médecine de l'Université Laval (ACCEM) et les Instituts de recherche en santé du Canada (IRSC). Par l'attribution de bourse de doctorat, de stage et de congres, ils m'ont permis de réaliser mon projet de recherche et de le présenter dans les conférences nationales et internationales.

Finalement, je remercie ma famille, ma belle-famille, mes amis d'ici et d'ailleurs. Je suis extrêmement reconnaissante envers ma mère Elena qui, depuis mon enfance, m'a encouragée à étudier. Elle a travaillé de longues heures dans une usine de confections de vêtements pour que je ne sois pas obligée de le faire. Merci, Cristian d'avoir cru en moi, de m'avoir encouragé et épaulé toutes ces années. Tu es mon fan numéro un! Merci Stéphan, d'avoir eu la « patience » d'attendre ta maman à finir ses études à son rythme. Merci à Sébastian qui espère avoir sa maman à la maison, juste pour lui, maintenant que ses études doctorales sont finies.

Que cette thèse soit un plaisir pour vous tous!

Avant-propos

Avant cette thèse, des résultats montraient que la protéine PARP1 liait l'ADN endommagé par les rayons ultraviolets et était activée très rapidement suite aux dommages produits par les UV : les dommages directs réparés par la voie de réparation par excision de nucléotides (NER) et les dommages indirects éliminés par la réparation par excision de bases (BER). Dans une étude subséquente, il a été mis en évidence que l'absence de la PARP1 retardait la réparation des dommages directs induits dans un gène rapporteur viral. Mon projet dans le laboratoire du Dr Girish Shah, avait comme objectif de caractériser le mécanisme par lequel la PARP1 et son activité catalytique étaient impliquées dans la NER. Les travaux de recherche m'ont permis de contribuer à titre de première et co-première auteure à la conception de trois publications dont les résultats sont présentés aux chapitres 3, 4 et 5 de ce manuscrit. Ces publications ont été rendues possibles grâce à l'aide de plusieurs personnes. Leur contribution sera détaillée avant la présentation de chaque manuscrit.

Le **chapitre 1** présente les connaissances actuelles sur la réparation des dommages induits par les UV ainsi que sur les rôles de la PARP1 dans différentes voies de réparation de l'ADN. Le **chapitre 2** établit le contexte qui a déclenché la recherche sur le rôle de la PARP1 dans la NER et les objectifs que nous avons établis afin de valider notre hypothèse.

Au **chapitre 3** nous avons identifié le facteur DDB2 comme partenaire de la PARP1 durant la phase de reconnaissance des dommages de la NER. Nous avons démontré par une multitude d'essais *in vitro* et *in vivo* que le DDB2 stimulait l'activité catalytique de la PARP1 qui est requise pour un recrutement efficace de la XPC aux sites de dommages. Le manuscrit intitulé **« Role of poly(ADP-ribose) polymerase-1 in the removal of UV-induced DNA lesions by nucleotide excision repair »** (Mihaela Robu, Rashmi G. Shah, Nancy Petitclerc, Julie Brind'Amour, Febitha Kandan-Kulangara et Girish M. Shah) publié dans la revue *Proceedings of the National Academy of Sciences of the United States of America* a été réalisé grâce à l'aide de chacun des co-auteurs cités ci-dessus. La version PDF de l'article est disponible à l'annexe 1 de cette thèse.

Par la suite nous avons déchiffré la base structurale de l'interaction entre la PARP1 et le DDB2 à la chromatine. Pour ce faire, nous avons développé deux techniques présentées dans le **chapitre 4**. La première technique associe le fractionnement cellulaire à la technique d'immunofluorescence afin d'extraire des protéines solubles tout en conservant des protéines qui lient fortement la chromatine. La deuxième technique consiste en la création d'un oligonucléotide avec un seul dommage de type UV et entouré de multiples sites de reconnaissance pour des enzymes de restriction. Grâce à ces outils, nous avons démontré la co-localisation *in vivo* de la PARP1 endogène avec un dommage CPD ou avec le DDB2. De plus, nous avons montré que la PARP1 avait une empreinte asymétrique sur l'ADN endommagé par les UV, de -12 à +9 nucléotides autour de la lésion. Le manuscrit intitulé « **Characterization of the interactions of PARP-1 with UV-damaged DNA in vivo and in vitro »** (Nupur K. Purohit[#], Mihaela Robu[#], Rashmi G. Shah[#], Nicholas E. Geacintov and Girish M. Shah) a été publié dans la revue *Scientific Reports.* Sa version PDF est disponible à l'annexe 2 de cette thèse.

Au **chapitre 5,** nous avons démontré le rôle indépendant du DDB2 de la PARP1 dans les fonctions de la XPC. La PARP1 interagit avec la XPC dans le nucléoplasme même en absence de dommage, ce qui est en contradiction avec son interaction après irradiation avec le DDB2 au niveau de la chromatine. Suite à l'irradiation, le complexe PARP1-XPC se déplace vers la chromatine grâce à l'activité catalytique de la PARP1. Nos résultats indiquent que la PARP1 et le DDB2 coopèrent afin d'assurer un recrutement efficace de la XPC aux sites de dommages, ainsi que son transfert sur la lésion. Le manuscrit « **Poly(ADP-ribose) polymerase 1 escorts XPC to UV-induced DNA lesions during nucleotide excision repair »** (Mihaela Robu[#], Rashmi G. Shah[#], Nupur K. Purohit, Pengbo Zhou, Hanspeter Naegeli et Girish M. Shah) a été soumis à la revue *Proceedings of the National Academy of Sciences of the United States of America* pour publication.

J'ai aussi contribué en tant que co-auteure à la publication des deux articles de synthèse. L'article « **Resistance to PARP-Inhibitors in Cancer Therapy** » (Alicia Montoni, Mihaela Robu, Emilie Pouliot et Girish M Shah) a été publié dans la revue *Frontiers in Pharmacology* en janvier 2013. L'article ***«*** **PARP Inhibitors in Cancer**

Therapy: Magic Bullets but Moving Targets » (Girish M Shah, Mihaela Robu, Nupur K Purohit, Jyotika Rajawat, Lucio Tentori et Grazia Graziani) a été publié en novembre 2013 in *Frontiers in Oncology*. Les versions PDF des articles sont disponibles dans les annexes 3 et 4.

Finalement, dans le **chapitre 6**, les résultats majeurs de cette thèse seront discutés et des perspectives pouvant donner une vision plus approfondie sur les rôles de la PARP1 et de la PARylation dans la NER seront proposées.

Chapitre 1

Introduction

Une des réponses précoces des cellules de mammifère aux dommages à l'ADN est l'activation de l'enzyme nucléaire poly(ADP-ribose) polymérase 1 (PARP1). La PARP1 activée utilise le substrat nicotinamide adénine dinucléotide (NAD^+) pour former des polymères d'ADP-ribose (PAR) sur des protéines cibles, une modification post-traductionnelle appelée poly(ADP-ribosyl)ation ou PARylation. *Mes travaux de doctorat portent sur le rôle de la PARP1 et de la PARylation dans la détection et la réparation par excision de nucléotides (NER) des dommages directs induits à l'ADN par les radiations solaires ultraviolettes (UV). Cette introduction a pour but d'introduire et de décrire les rôles de la PARP1 dans la réparation de l'ADN et le fonctionnement des protéines impliquées dans la phase de reconnaissance des dommages directs induits à l'ADN par les radiations ultraviolettes du soleil.*

1.1 Les rayons ultraviolets

Les radiations UV forment une partie des radiations électromagnétiques du spectre solaire et peuvent être subdivisées selon la longueur d'onde en trois catégories : les UVA (315-400 nm), les UVB (280-315 nm) et les UVC (100-280 nm) représentés dans la figure 1.1. La couche d'ozone absorbe les radiations de moins de 310 nm, donc les rayons qui touchent la surface de la Terre sont formés majoritairement des UVA (90-95%) et d'une partie des UVB (5-10%) [1]. Malgré le fait que les UVC sont absorbés en totalité dans l'atmosphère par la couche d'ozone, des lampes à UVC sont utilisées comme modèle dans les laboratoires, car elles peuvent induire des dommages à l'ADN et aux protéines seulement après une courte exposition [2].

L'énergie de chaque type d'UV est inversement corrélée à sa longueur d'onde, donc les UVC sont les plus énergétiques, les UVA sont les moins énergétiques et les UVB ont des

caractéristiques situées entre les deux. Toutefois, la profondeur de pénétration dans la peau augmente avec la longueur d'onde: les UVA pénètrent jusqu'au niveau du derme alors que les UVB sont presque en totalité absorbés par l'épiderme où seulement 10 à 20% d'entre eux arrivent au niveau basal (Figure 1.1) [3].

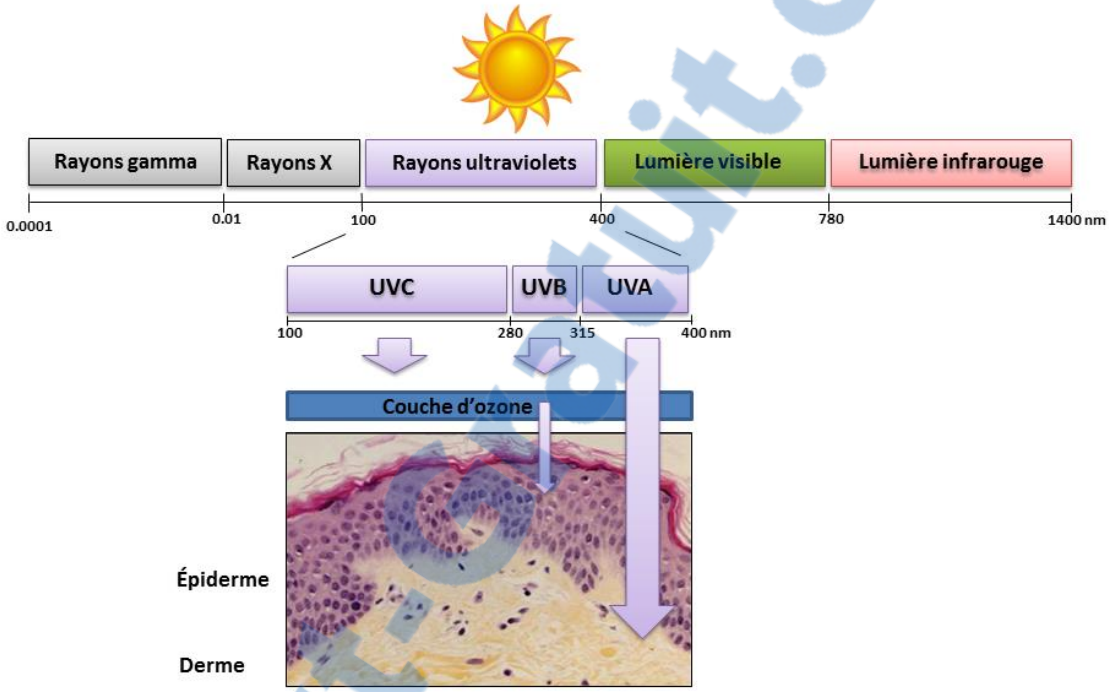

Figure 1.1 Les caractéristiques du spectre solaire.

Plusieurs types de radiations électromagnétiques divisées en fonction de la longueur d'onde composent le spectre solaire. Les rayons UVA et une partie des UVB se rendent jusqu'à la surface de la Terre et sont absorbés par la peau, alors que les UVC sont bloqués par la couche d'ozone. Modifié de D'Orazio *et al.*, 2013 [4].

Malgré le fait qu'elles représentent juste une petite fraction (5%) du spectre solaire, les radiations ultraviolettes sont considérées comme le carcinogène ubiquitaire et physique le plus important [5]. Ainsi, la surexposition aux UV au niveau de la peau cause de l'inflammation, de l'atrophie et un vieillissement dégénératif. Elle est le facteur le plus important dans l'apparition et le développement des cancers de la peau [4, 6]. Chaque

composante du rayonnement UV peut exercer une variété d'effets sur les cellules, les tissus et les molécules, incluant l'ADN.

1.2 Les dommages à l'ADN induits par les UV

Quand les rayons ultraviolets frappent la peau, une partie de leur énergie est absorbée par des chromophores (l'ADN et plusieurs autres chromophores endogènes capables de générer des espèces réactives de l'oxygène) ce qui peut causer des dommages à l'ADN. Les UV peuvent induire deux types de dommages : directs par la formation des dimères entre les pyrimidines adjacentes et indirects *via* des espèces oxydatives pouvant entraîner la formation de bases oxydées ou/et des cassures simple-brin (Figure 1.2).

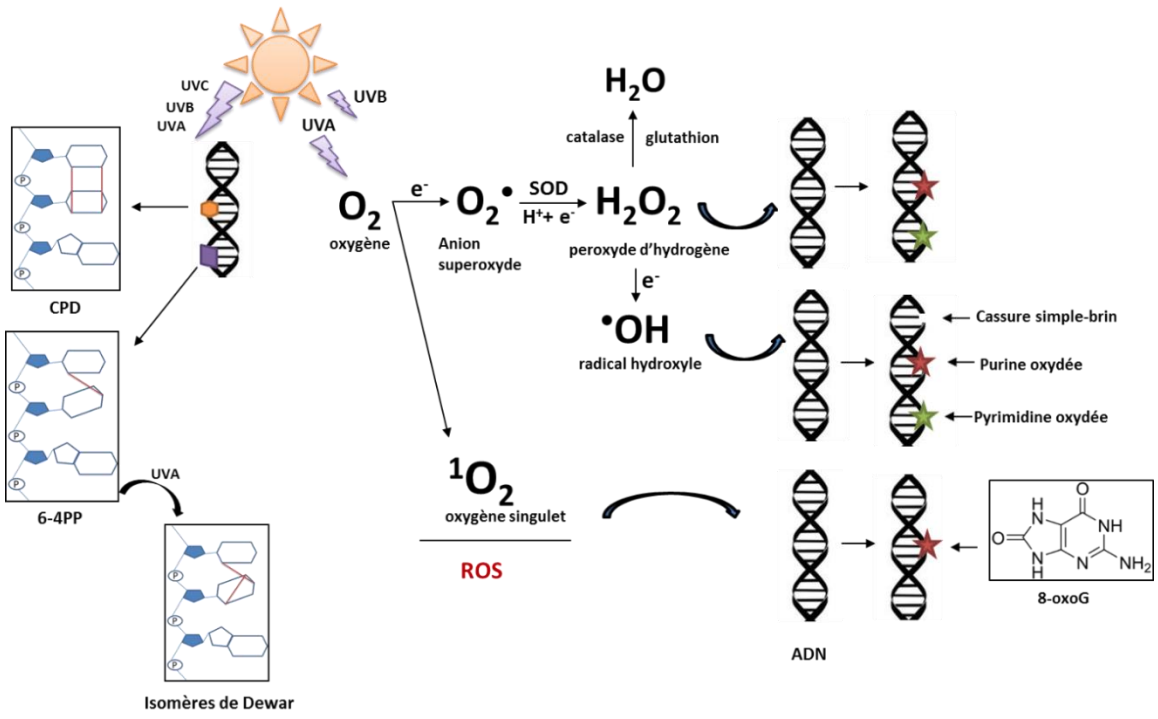

Figure 1.2 Dommages à l'ADN induits par les rayons ultraviolets.

Les UVA, les UVB et les UVC endommagent directement l'ADN avec la formation des dimères cyclobutyliques de pyrimidine (CPD) et des produits pyrimidine-pyrimidone (6-4PP). L'exposition des 6-4PP aux UVA mène à la formation des isomères de Dewar. Les UVA et les UVB peuvent aussi engendrer des dommages indirects à l'ADN, comme des 8-

oxoguanine (8-oxoG) et des cassures simple-brin via des espèces réactives de l'oxygène (ROS). SOD-« superoxyde dismutase », e^- - électrons, H^+ - protons.

1.2.1 Les dommages directs à l'ADN

En général, le type de dommage dépend de la longueur d'onde de la radiation. Les UVB et les UVC endommagent directement l'ADN qui absorbe efficacement des radiations avec une longueur d'onde comprise entre 200 et 290 nm. Les deux types de photoproduits causés par les UVC et les UVB sont les dimères cyclobutyliques de pyrimidine (CPD) et les photoproduits pyrimidine (6-4) pyrimidone (6-4PP) (Figure 1.2) [7].

Les CPD sont formés par la saturation de la liaison double située entre les carbones C4 et C5 des pyrimidines adjacentes (thymine (T) et/ou cytosine (C)) avec la formation d'une structure en anneau de cyclobutane (Figure 1.2) [8, 9]. La formation des CPD est un processus extrêmement rapide; deux thymines adjacentes peuvent se dimériser dans une picoseconde [10]. Une fois formés, les CPD sont des structures très stables, avec une demi-vie de quelques heures [7]. Le type de CPD induit (T-T, T-C, C-C ou C-T) dépend de la longueur d'onde du rayonnement UV, du contenu en bases cytosine et guanine, mais également du site dipyrimidique lui-même. Ainsi, étant donné que la thymine est la base la plus photoréactive, les lésions les plus fréquentes après expositions aux UVB et UVC sont les dimères de type thymine-thymine (T-T) suivi par les dimères thymine-cytosine (T-C) [11, 12].

Les 6-4PP, formés par le transfert de la liaison double entre les carbones C5 et C6 de la pyrimidine en 5' vers le carbone de la position 4 de la pyrimidine en 3', sont souvent des T-C, C-C et plus rarement des T-T. Le résultat est un intermédiaire instable qui est réarrangé spontanément en un 6-4PP par la formation d'un lien covalent entre le carbone C4 de la pyrimidone et le carbone C5 de la base pyrimidique (Figure 1.2) [13]. Étant donné que les 6-4PP présentent un maximum d'absorption à 320 nm, leur exposition ultérieure aux UVB ou aux UVA peut entraîner un changement conformationnel avec la formation des isomères de Dewar (Figure 1.2) [14].

Le rapport entre le nombre de CPD et le nombre de 6-4PP formés après irradiation aux UV est approximativement 3:1 [15]. Cette différence s'explique par la nature et la position des bases, mais aussi par la flexibilité de l'ADN. Les 6-4PP sont des lésions déformantes induisant à l'ADN un angle de 44° par rapport à sa conformation initiale, alors que les CPD créent juste une petite distorsion de 7 à 9° [16]. Cette caractéristique affecte leur distribution: les 6-4PP se forment principalement dans les régions inter-nucléosomales [17] alors que les CPD sont formés uniformément dans les régions inter- et intra-nucléosomales [18]. Dans la chromatine, les deux types de dommages occupent des régions différentes : les CPD sont distribués dans l'eu- et l'hétérochromatine, alors que les 6-4PP ont été détectés seulement dans les régions eu-chromatiniennes [19].

La distorsion induite à l'ADN par les 6-4PP associée à un environnement chromatinien plus permissif facilite leur reconnaissance par les protéines de réparation de l'ADN ce qui explique leur réparation rapide. Les CPD sont éliminés à un rythme plus lent que les 6-4PP et l'efficacité de réparation de ce type de dommage décroît dans l'ordre C-T > T-C > T-T [20]. Comme ils persistent plus longtemps dans l'ADN, ils sont considérés comme responsables de la plupart des effets nocifs des rayonnements UV allant du coup de soleil au vieillissement de la peau et au cancer. De plus, les CPD de type C-C et les 6-4PP de type C-T et C-C peuvent être convertis en uracile par déamination [21]. Ce processus peut expliquer la transition C vers T et les mutations en tandem CC vers TT appelées "signature UV" dans le gène suppresseur de tumeur p53 rencontré dans plus de la moitié des cancers de la peau [22].

La formation des dommages directs a été considérée longtemps comme spécifique des rayonnements UVB et UVC. Cependant, plusieurs études ont démontré que les UVA avec longueurs d'ondes situées entre 320 et 340 nm causent des dommages directs à l'ADN [23]. Les dimères engendrés de type thymine-thymine sont formés par l'absorption de l'énergie des UVA directement par l'ADN ou par l'intermédiaire d'un chromophore endogène (psoralène, fluoroquinolone, cétone aromatique) [24]. Les UVA ne produisent pas de lésion de type 6-4PP ou d'isomère de valence Dewar [7]. Bien que les dommages directs à l'ADN produits par les UVA dépassent en terme quantitatif les dommages de type oxydatifs

[24, 25], la capacité des UVA à induire des CPD est de 6000 fois inférieure à celle des UVB [11].

1.2.2 Les dommages indirects à l'ADN

La composante UVA et, dans une moindre mesure, la composante UVB de la lumière solaire sont capables d'induire une variété de dommages indirects à l'ADN (Figure 1.2), incluant des bases pyrimidiques oxydées (e.g thymine glycol, 5'-hydroxycytosine), des purines modifiées (7,8-dihydro-8-oxoguanine (8-oxoG) et 2,6-diamino-4-hydroxy-5-formamidopyrimidine (FapyG)) et des cassures simple-brin dans une proportion 0.4:1:0.45 [7]. La formation directe de cassures double-brin par les UV reste controversée [7, 26].

Les UVB sont peu efficaces dans l'induction des dommages oxydatifs qui représentent seulement 1% du nombre total de dommages induits par la même dose d'UVB [27]. De plus, le mécanisme impliqué dans la génération de ce type de dommages par les UVB est source de débat [13]. Par contre, ceux impliqués dans la formation des dommages oxydatifs par les UVA sont bien connus [28]. Les UVA provoquent des dommages indirects à l'ADN par l'intermédiaire de chromophores endogènes (mélanines, flavines, NADPH (« la forme réduite du nicotinamide adénine dinucléotide phosphate »), oxydases, protéines qui contiennent des groupements porphyrine ou hème). En absorbant l'énergie des UVA, ceux-ci sont excités dans des états instables, très énergétiques, appelés états triplets et ils réagissent directement avec les bases de l'ADN (photosensibilisation de type I) ou transfèrent leur énergie aux molécules d'oxygène (photosensibilisation de type II), menant ainsi à la formation d'espèces réactives de l'oxygène (ROS) comme l'oxygène singulet ($^1O_2$) et l'anion superoxyde ($O_2^{\bullet}$) [29]. L'anion superoxyde formera à la suite de réactions chimiques le peroxyde d'hydrogène (H_2O_2) et le radical hydroxyle ($^{\bullet}OH$). L'oxygène singulet agit spécifiquement sur la guanine conduisant à la formation des 8-oxoG [30]. Les espèces H_2O_2 et le $^{\bullet}OH$ vont modifier les purines et les pyrimidines sans distinction. Le radical $^{\bullet}OH$ attaque aussi l'unité ribose de l'ADN avec la formation de cassures simple-brin [31].

Les 8-oxoG ont longtemps été considérées comme le type de dommage le plus abondant produit par les UVA. Cependant, il a été démontré, en exposant des cellules CHO aux UVA, que les CPD, les 8-oxoG, les pyrimidines oxydées et les cassures simple-brin étaient formés dans une proportion de 10:3:1:1 [24]. Les 8-oxoG tendent à s'apparier avec une adénine au lieu d'une cytosine pendant la réplication et ce mésappariement peut provoquer, lors du deuxième cycle réplicatif, un changement de G-C par G-T [32]. Ce type de mutation a été répertorié dans des cancers de la peau, ce qui confère aux 8-oxoG un pouvoir mutagène. À part l'ADN, les radicaux libres attaquent d'autres macromolécules telles que les protéines et les lipides [27]. Les ROS produits par les UV persistent longtemps après irradiation. Cependant, leurs effets à long terme sur les macromolécules ne sont pas bien connus.

En conclusion, dépendamment de la longueur d'onde de la radiation et de la structure chimique des chromophores, les UV peuvent causer différents types de dommages : les UVC, les UVB et les UVA causent des dommages directs à l'ADN mais les UVB et les UVA induisent aussi des dommages indirects. Dans les deux cas, ces dommages interfèrent directement avec les processus cellulaires vitaux, comme la transcription et la réplication de l'ADN et peuvent provoquer des mutations et des aberrations chromosomiques qui augmentent le risque de cancer, induisent la sénescence et éventuellement la mort cellulaire. Ce n'est donc pas surprenant que plusieurs types de voies de réparation aient évolués pour assurer une réparation efficace des dommages induits par les UV.

1.3 La réparation des dommages induits par les UV

L'ADN est la molécule responsable du maintien et de la transmission de l'information génétique de tout organisme vivant. Pour la protéger contre des lésions qui peuvent éventuellement modifier l'information génétique, les organismes ont développé des voies de signalisation des dommages et de réparation de l'ADN. Les dommages indirects induits à l'ADN par les UV sont éliminés par la réparation par excision de bases (BER) et les dommages directs sont réparés par excision de nucléotides (NER).

1.3.1 La réparation des dommages indirects par excision de bases (BER)

Les cellules mettent en place des voies de protection de la cellule pour inactiver les ROS (enzymes et antioxydants naturels) ainsi que des voies de réparation pour éliminer les dommages à l'ADN qu'ils causent. Les mécanismes de défense contre les ROS sont constitués d'enzymes (catalase, glutathion) et d'antioxydants naturels (acide ascorbique, α-tocophérol) (Figure 1.2). Le glutathion neutralise la réactivité des radicaux libres, processus pendant lequel le glutathion lui-même est oxydé par le radical hydroxyle. Par ailleurs, le déséquilibre entre les deux formes de glutathion (oxydé/réduit) indique un stress oxydatif [12]. La catalase détoxifie le peroxyde d'hydrogène et la superoxide dismutase inactive les anions superoxydes [33].

Les dommages induits à l'ADN par les ROS (bases oxydées et cassures simple- brin) sont éliminés par la voie de réparation par excision de bases (BER) (Figure 1.3). Les différents types de bases oxydées sont reconnus chez les mammifères par une des glycosylases bifonctionnelles : les purines oxydées, surtout les guanines, sont des substrats pour les enzymes OGG1 («8-oxoguanine DNA glycosylase 1») et hFPG1 (« human Formamidopyrimidine-glycosylase 1 »), les pyrimidines oxydées sont reconnues par l'enzyme NTH1 (« Endonuclease three homolog 1 ») et les deux types de bases oxydées sont reconnus par les NEIL1-3 (« Nei like glycosylase 1-3 ») [34]. Ces enzymes ont à la fois une activité enzymatique glycosylase et lyase. Elles excisent la base endommagée et clivent le site abasique (apurinique/apyrimidique-AP) généré créant une cassure simple-brin avec un résidu 3' non-conventionnel. L'étape suivante de la BER consiste en l'élimination de ce résidu pour générer une extrémité 3'OH, le substrat des polymérases. L'AP endonucléase 1 (APE1) nettoie l'extrémité 3' créée par les OGG1/NTH1/hFPG1 et la kinase PNKP (« Polynucleotides phosphate kinase ») celle créée par les NEIL1-3. Une fois les résidus éliminés, la BER continue avec l'étape de synthèse. Dépendamment du nombre de nucléotides remplacés, la BER est divisée en deux sous-voies : la « short-patch BER » emploie la polymérase β pour insérer un seul nucléotide et la « long-patch BER » remplace de 2 à 8 nucléotides en amont de la lésion par l'activité de la polymérase β ou celle des polymérases réplicatives δ et ε associées au facteur de processivité PCNA (« Proliferating

cell nuclear antigen »). Dans ce cas, le rabat formé par le déplacement du brin contenant le dommage est éliminé par la FEN1 (« Flap Endonuclease 1 ») [35]. La ligation par le complexe ligase III/XRCC1 (« X-ray repair cross-complementing protein 1 ») dans le cas de « short-patch BER » et par la ligase I pour la sous-voie la « long-patch BER » complète la réparation des dommages oxydatifs par l'excision de bases [36].

Les mécanismes qui contrôlent le choix entre les deux sous-voies de la BER demeurent inconnus. Une étude propose que la sous-voie de réparation soit déterminée par le type de dommage. Par exemple, les sites AP oxydés ont un résidu 5' désoxyribose phosphate (5'dRP) modifié qui ne peut pas être éliminé par l'activité lyase de la polymérase β. Dans ce cas, le résidu sera coupé par la FEN1 comme part du rabat formé pendant l'étape de synthèse de la sous-voie « long patch BER » [35]. À ce mécanisme s'en ajoutent d'autres qui proposent que la concentration d'ATP, l'interaction entre les protéines, la concentration des protéines au site de réparation et l'étape du cycle cellulaire contrôlent le choix de la sous-voie [37]. En général la réparation par la sous-voie « long-patch BER » est considérée comme mineure, sauf quelques exceptions [38].

La BER a lieu en quatre étapes. Pour expliquer comment l'activité des protéines de la BER est coordonnée afin d'éliminer les bases endommagées, deux modèles sont proposés. Le premier modèle sépare la phase de reconnaissance de la BER des étapes suivantes, ce qui implique que la lésion sera reconnue deux fois: une fois par les glycosylases et une deuxième fois, après l'incision du brin, par la PARP1 [36]. Dans ce modèle, la réparation des cassures simple-brin (SSBR) est une sous-voie de la BER. L'arrivée séquentielle des protéines est facilitée par des facteurs accessoires comme le facteur XRCC1 et la protéine PARP1. Le facteur XRCC1 joue un rôle de plateforme d'échafaudage dans la BER, car il interagit avec les glycosylases OGG1 [39] et NEIL1 [40], les endonucléases APE1 [41] et PNKP [42], la polymérase β [43] et la ligase III [44].

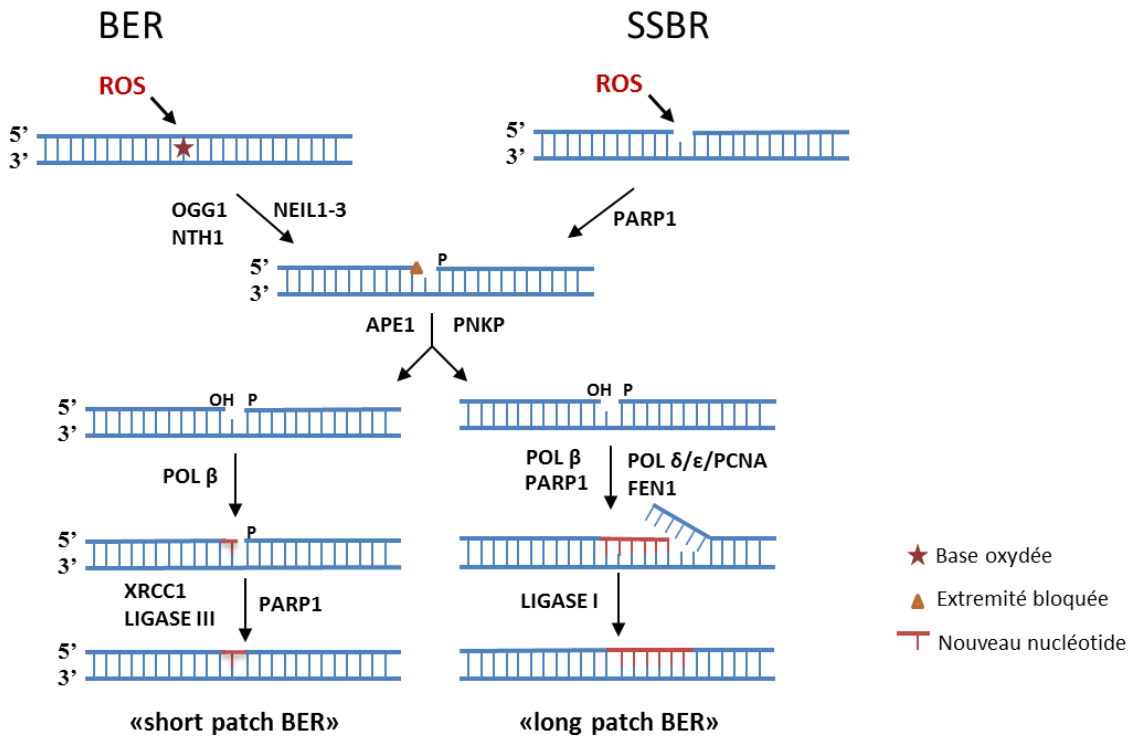

Figure 1.3 La réparation de bases oxydées et de cassures simple brin induites par les ROS.

Les bases oxydées sont reconnues par des glycolases bifonctionnelles, alors que les cassures simple brin sont reconnues par la PARP1. Une fois le dommage reconnu, le mécanisme BER/SSBR s'enchaine avec le nettoyage des extrémités du site abasique avec la formation des résidus en 3' et 5' qui permettront l'étape de synthèse d'un nouveau nucléotide (« short patch BER ») ou de plusieurs nucléotides (« long patch BER ») et enfin l'étape de ligation par les ligases III ou I. Modifié de Carter and Parson, 2016 [45].

Bien que le facteur XRCC1 n'ait pas d'activité enzymatique, il stimule l'activité enzymatique, la localisation et la stabilisation au site des dommages des protéines de la BER ainsi que le remodelage de la chromatine [46]. Le rôle du XRCC1 dans la BER est étroitement lié à celui de la PARP1, car plusieurs études indiquent que son recrutement aux dommages dépend de la présence de la PARP1 [47]. La PARP1 recrute plusieurs protéines de la BER et module leur activité [48]. Par exemple, elle s'associe avec les intermédiaires de réparation de la BER, les 5'dRP, et ce, en compétition directe avec l'APE1, elle stimule la synthèse du nouveau brin par la polymérase β et le clivage par la FEN1 du brin contenant la base

endommagée [49]. Malgré toutes ces observations, le rôle direct de la PARP1 dans la réparation des dommages oxydatifs reste controversé [50-52], car sa déplétion affecte seulement la réparation de certains types de dommages oxydatifs [53]. Le deuxième modèle « passer le bâton » propose que les protéines de la voie BER se relaient successivement au niveau de la lésion initialement reconnue par les glycosylases jusqu'à élimination complète de la lésion [54, 55]. Dans ce cas, la formation des complexes multi-protéiques par les protéines de la BER, dont la PARP1 ne fait pas partie [56] expliquera la rapidité avec laquelle les bases endommagées sont réparées [52].

Les rayons UV induisent aussi minoritairement des cassures simple-brin à l'ADN via l'attaque de la 2'-désoxyribose par le radical hydroxyle [57, 58]. Ces dommages sont éliminés par la SSBR en quatre étapes, dont les trois dernières sont communes pour la SSBR et la BER (Figure 1.3). La première étape, de détection et de signalisation du dommage, est réalisée par la PARP1 et probablement par la PARP2 [59]. La liaison de la PARP1 au niveau de la cassure stimule son activité catalytique [60]. Elle forme alors des polymères d'ADP-ribose sur plusieurs protéines présentes au site de dommage, incluant la PARP1 elle-même. Cette modification est absolument nécessaire pour le recrutement du XRCC1 au site de cassure simple-brin [61-63]. L'absence du recrutement du XRCC1, couplé avec un ralentissement de la cinétique de réparation des cassures simple-brin dans les cellules déficientes en PARP1 ou avec une PARP inactive soutient cette observation [64, 65]. Une fois le dommage reconnu les autres protéines de la voie BER seront recrutées [59].

1.3.2 La réparation des dommages directs par excision de nucléotides (NER)

La voie de réparation par excision de nucléotides est unique parmi les autres voies de réparation, car elle élimine une très grande variété de dommages non-reliés structuralement comme les dommages directs induits par les UV (les CPD et les 6-4PP), les adduits encombrants provoqués par des polluants comme le benzo(a)pyrène, les pontages intra-brin formés par des drogues comme le cisplatine et les cyclopurines produites par les ROS. Chez les mammifères, la NER est la seule voie de réparation qui élimine les lésions induites par les UV dans les parties photo-exposées de la peau [66]. Son importance est attestée par

l'hypersensibilité au soleil et la prédisposition à développer des cancers de la peau chez des patients atteints par la maladie *Xeroderma pigmentosum (*XP). D'autres maladies associées à une NER défectueuse sont le *Syndrome de Cockayne* (CS), le *« UV-sensitive syndrome* » ($UV^{S}S$) et la *Trichothiodystrophie* (TTD). Toutes ces maladies autosomales récessives sont caractérisées par des mutations dans des gènes codant pour des protéines impliquées dans la voie NER. Présentement, il existe sept groupes de complémentation *XP* (*XP-A* à *XP-G*), deux groupes *CS* (*CS-A* et *CS-B*), trois groupes *UVSS* et six groupes *TTD*. Un huitième groupe inclus dans la maladie *XP*, le *XP-V*, est dû à des mutations dans la polymérase η spécialisée dans la réparation des CPD pendant la réplication [67, 68]. La caractéristique commune de toutes ces maladies est la photosensibilité. Par conséquent, les dommages induits par les UV sont les plus étudiés et sont devenus paradigmatiques de la NER.

La réparation par excision de nucléotides est un processus coordonné qui utilise de façon séquentielle approximativement 30 protéines dans les étapes suivantes : (A) la reconnaissance des dommages, (B) la vérification du dommage et la formation d'un complexe ouvert, (C) l'incision du brin contenant le dommage et la synthèse d'un nouveau brin d'ADN suivi de la ligation (D) (Figure 1.4) [69].

1.3.2.1 La phase de reconnaissance des dommages

La première étape et aussi la plus cruciale dans toute voie de réparation de l'ADN est la détection des lésions. Chez les mammifères, en fonction de la localisation des dommages dans le génome, différentes protéines sont impliquées dans la reconnaissance des dommages menant à la séparation de la voie NER en deux sous-voies : la réparation couplée à la transcription (TC-NER) et la réparation globale du génome (GG-NER) (Figure 1.4, étape A) [70].

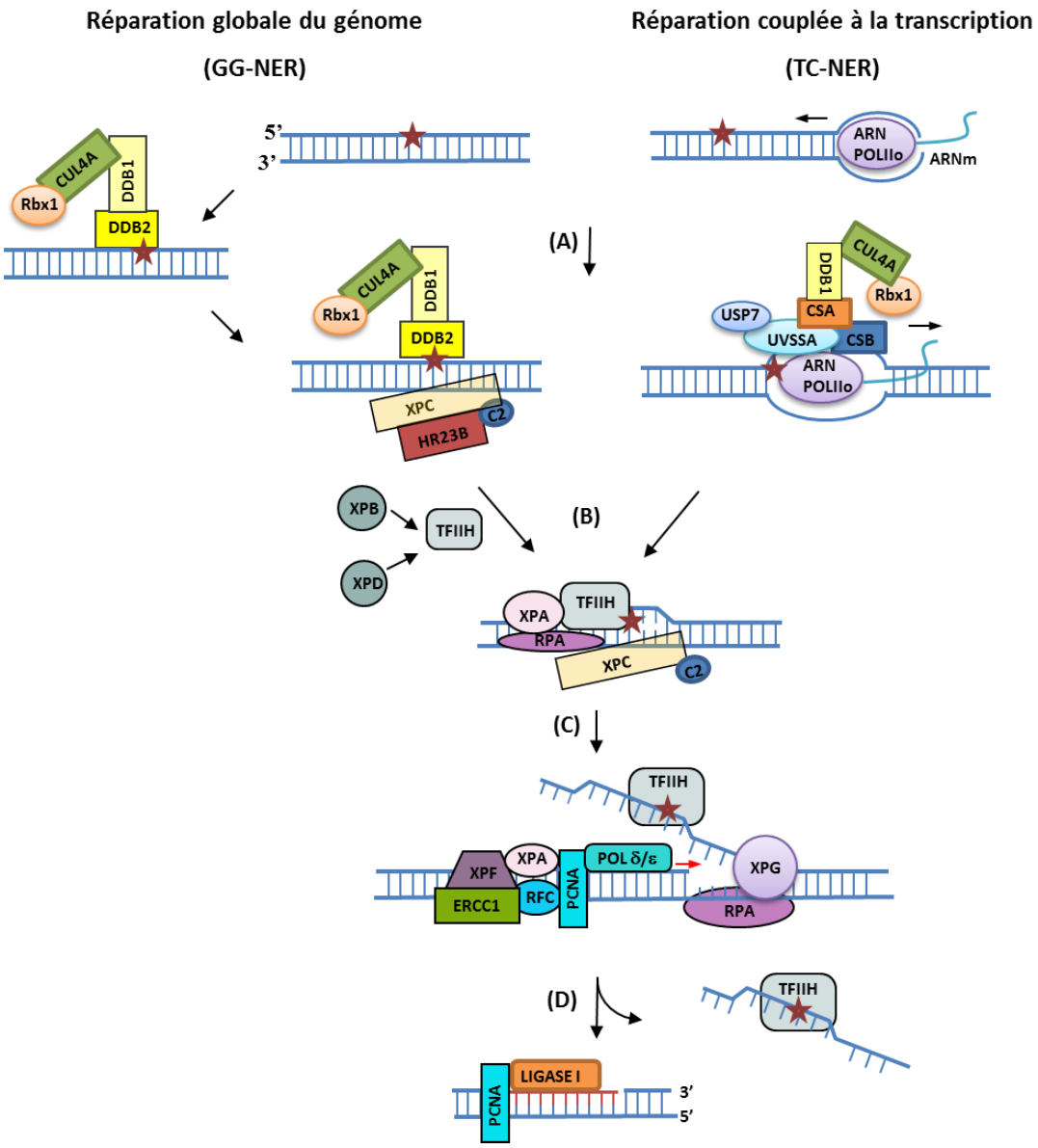

Figure 1.4 La réparation des dommages directs par excision de nucléotides.

Les complexes protéiques impliqués dans la reconnaissance de dommages (étape A) sont l'ARN POLIIo-CSB pour les dommages localisés sur le brin des gènes transcriptionnellement actifs (TC-NER) et les complexes UV-DDB (DDB2 et DDB1) et XPC-HR23B-centrin2 pour ceux situés dans le reste du génome (GG-NER). Une fois le dommage reconnu, les deux sous-voies de la NER convergent vers l'étape de recrutement du facteur de transcription TFIIH, lequel ouvre l'hélice d'ADN avec ses hélicases XPB et XPD (étape B). Le blocage de la XPD par la lésion permet l'ouverture complète de la «bulle» et le recrutement des protéines XPA, XPG et du complexe RPA qui mène à la formation du complexe ouvert, de pré-incision (étape B). La protéine XPF est recrutée par la XPA via son

partenaire ERCC1 et initie l'étape d'incision, en coupant en 5' de la lésion. Ceci engendre la formation d'un groupement 3'OH libre qui joue le rôle d'amorce pour les polymérases δ/ε. La synthèse du nouveau brin est probablement le signal qui déclenche l'activation de la XPG, la coupe en 3' et l'achèvement de la synthèse du nouveau brin (étape C). La réparation est complétée par les ligases III et I (étape D).

Initialement décrite comme la « réparation préférentielle » du génome [71], la TC-NER élimine les dommages situés sur le brin transcrit de gènes actifs. L'arrêt de l'ARN polymérase II pendant la phase d'élongation de la transcription devant les photo-lésions constitue le signal pour le recrutement de la protéine spécifique de la TC-NER, la CSB (« Cockayne syndrome protein B ») [72]. La CSB fait partie de la grande famille de protéines de remodelage de la chromatine dépendante de l'ATP, SWI/SNF. Son activité ATP-ase assure plusieurs de ses rôles dans la TC-NER : son association avec l'ADN, le remodelage de la chromatine et le recrutement des autres facteurs spécifiques de la réparation TC-NER [73]. En absence des dommages, e.g. avant irradiation, la CSB est libre dans le nucléoplasme. Suite à l'induction des dommages par les UV, la grande majorité des molécules de CSB (90%) migrent vers la chromatine. Pour se stabiliser sur le site du dommage, la CSB doit soustraire l'effet inhibiteur de son domaine N-terminal sur le domaine C-terminal qui est responsable de la liaison à l'ADN. Pour ce faire, elle utilise l'énergie obtenue par l'hydrolyse d'ATP [74]. La translocation de la protéine suivante, la CSA (« Cockayne syndrome protein A »), au site du dommage est dépendante du domaine C-terminal de la CSB [75, 76]. Son interaction avec la CSB active le complexe ubiquitine ligase [77] formé des protéines CSA, DDB1 («UV- damaged DNA binding protein 1 »), Cul4A (« Cullin 4A ») et Rbx1 (« RING box protein 1 ») [78], qui modifient alors les protéines CSB, CSA et l'ARN POLIIo avec des résidus ubiquitine [79]. Le rôle biologique de l'ubiquitinylation de la CSB reste controversé. Une étude montre que l'ubiquitinylation de la CSB et sa dégradation par le protéasome permet le redémarrage de la transcription [80] alors qu'une autre montre que l'accumulation de la CSB ubiquitinylée accélère la reprise de la transcription [81]. L'ubiquitinylation de l'ARN POLIIo mène à son recyclage, qui dépend de la protéine UVSSA (« UV Stimulated Scaffold Protein A»), vers la forme ARN POLIIa, responsable de l'initiation de la transcription [82]. Découverte récemment comme une des protéines responsable du syndrome de sensibilité aux UV, l'UVSSA fait partie *in vivo*, d'un complexe formé avec la

déubiquitinase USP7 (« ubiquitin specific processing protease 7 »). Après irradiation, ce complexe est recruté au dommage par la CSA pour enlever les chaines d'ubiquitine des protéines de la TC-NER grâce à l'activité déubiquitinase de l'USP7. *In vivo*, l'équilibre entre la dégradation de protéines ubiquitinylées par le complexe ubiquitine ligase CSA-DDB1-Cul4A-Rbx1 et leur stabilisation par l'activité du complexe UVSSA-USP7 assure le bon fonctionnement de la TC-NER.

Après la formation du complexe d'initiation (Figure 1.4, étape A), plusieurs scénarios ont été proposés pour expliquer comment les facteurs situés en aval de la phase de reconnaissance de la TC-NER ont accès à la lésion qui se trouve probablement dans le site actif de la polymérase arrêtée [83]. Le modèle le plus accepté est *le recul* de l'ARN POLIIo. Pour ce faire, les nucléosomes qui se trouvent en arrière de la polymérase doivent être enlevés ou déplacés. Il a été proposé que la CSB facilite ce processus [70] par le recrutement de l'histone acétyltransférase p300, de la HMGN1 (« High mobility group nucleosome binding domain containing protein 1 ») [84, 85] ou directement via son activité ATP-ase [86]. Par la suite, la CSA recrute la protéine XAB2 (« XPA-binding protein 2 ») et le facteur de transcription TFIIS [84]. La XAB2 est impliquée dans la transcription et l'épissage des ARN pré-messagers mais son rôle exact dans le TC-NER n'est pas encore connu [87]. Le TFIIS clive l'ARN pré-messager synthétisé en interagissant avec le site actif de l'ARN POLIIo ou il stimule le clivage de cet ARN par l'ARN POLIIo, elle-même [88]. Les autres scénarios proposés, comme le « by-pass » des lésions par l'ARN POLIIo ou la dégradation de la ARN POLIIo par le protéasome sont soit non prouvés expérimentalement, soit considérés comme solution de dernier recours [70].

La réparation globale du génome (GG-NER) répare comme son nom l'indique, les lésions dans tout le génome. La détection des dommages a lieu indépendamment de la transcription par le complexe hétérotrimérique XPC-HR23B-centrin 2 (Figure 1.4, GG-NER). La XPC (« Xeroderma pigmentosum C protein ») reconnaît et a beaucoup d'affinité pour les lésions qui causent une distorsion significative de l'hélice d'ADN [66]. La structure cristallographique de RAD4 (« Radiation sensitive 4 protein »), l'orthologue de la XPC chez les levures, ainsi que des études biochimiques, montrent que la XPC se lie à la jonction

double-brin-simple-brin de l'ADN et fait des contacts avec les nucléotides non-endommagés situés en face du dommage [89]. Cette caractéristique de la XPC de reconnaître les conséquences des dommages plutôt que la lésion elle-même, explique la grande variété de lésions ciblées et réparées par la GG-NER. Cependant, la même caractéristique limite la capacité de la XPC à détecter les lésions qui causent des distorsions mineures à la double hélice d'ADN comme le principal type de lésion induite par les UV, les CPD [90]. Dans ce cas, la XPC est aidée par le complexe « UV- damaged DNA binding complex » (UV-DDB) composé des facteurs DDB1 et DDB2 ou XPE (« Xeroderma pigmentosum E protein ») (Figure 1.4, étape A). Le DDB2 reconnaît et lie avec une très grande affinité les dommages d'ADN induits par les UV [77, 91]. *Comme la compréhension de la phase de reconnaissance des dommages de la GG-NER est cruciale pour cette étude, elle sera détaillée dans le sous-chapitre 1.4.*

Une fois le dommage reconnu les deux sous-voies de la NER se rejoignent et d'autres protéines sont ensuite recrutées afin d'assurer la suite de la réparation. Dans le cas de la GG-NER, une étape supplémentaire de vérification des dommages s'impose car le recrutement de la XPC sur le brin non-endommagé n'est pas un gage de l'existence d'un vrai dommage, tel que discuté dans la section 1.4.1.

1.3.2.2 La phase de vérification des dommages et la formation du complexe ouvert

Dépendamment de la sous-voie utilisée, la CSB ou la XPC déstabilise la double hélice d'ADN et recrute par interaction directe le facteur de transcription TFIIH (Figure 1.4, étape B) [84, 92-94]. Au cours de cette étape, le retournement des bases non-endommagées par la XPC sert de guide afin d'assurer le chargement correct du complexe TFIIH sur le brin endommagé [95]. Le TFIIH est à la fois un facteur de transcription et un facteur de réparation des dommages à l'ADN. Il est composé de dix sous-unités, dont les deux hélicases XPB et XPD qui jouent un rôle essentiel dans la NER. Des études biochimiques et structurales ont permis de caractériser le rôle de chacune d'entre elles. La XPB recrute le complexe TFIIH au site du dommage où son activité ATP-ase régulée par la XPC et l'unité p52 de la TFIIH [96] est absolument nécessaire [97]. Son activité hélicase dans la direction 3'-5' est minimale,

car le complexe TFIIH se déplace sur l'ADN en direction 5'-3' [98]. Contrairement à la XPB, les deux activités, hélicase et ATP-ase, de la XPD sont requises pour l'immobilisation du complexe sur l'ADN [99] et pour ouvrir l'ADN dans la direction 5'-3' permettant ainsi le recrutement des protéines suivantes de la voie NER [100]. La collision de la XPD avec un dommage de type CPD est suffisante pour inhiber son activité hélicase [99, 101]. Aussi, les études structurales de son orthologue procaryote montrent que les quatre domaines structuraux de la XPD forment une sorte de « tunnel » qui peut accommoder de l'ADN simple-brin [102, 103]. En se basant sur ces observations le modèle de XPD comme facteur de vérification des dommages pendant la NER a été proposé [99, 101, 104, 105]. Selon ce modèle, la XPD brise les liens d'hydrogène d'entre les deux brins d'ADN dont un passe par le « tunnel » en mode ATP-dépendant. L'intégrité des bases sera analysée par une sorte de poche de reconnaissance de la XPD qui peut accommoder seulement des bases d'ADN natives. Les lésions étant volumineuses, elles ne peuvent pas y entrer et elles bloquent l'activité hélicase de la XPD. Ce mécanisme est soutenu par l'observation du fait que le complexe ouvert recruté par la XPC se déplace seulement en direction 5' à 3' en utilisant l'activité ATP-ase du TFIIH [104]. Finalement, par des expériences de mutations ponctuelles, Mathieu *et al.* [106] ont prouvé l'existence de la poche de reconnaissance de lésion à l'entrée du « tunnel » et ont identifié les acides aminés critiques pour l'interaction avec la lésion en montrant que les mutants étaient incapables de s'arrêter au site de lésion. Suite aux actions des hélicases XPB et des XPD, le complexe TFIIH génère une structure ouverte d'approximativement 25 nucléotides [107]. La stabilisation du complexe ouvert nécessite d'autres facteurs, comme la XPA et le RPA.

La protéine XPA a été longtemps considérée comme un candidat potentiel pour le rôle de protéine de reconnaissance des dommages de la NER [108]. Cependant, son affinité pour l'ADN double-brin endommagé est plus faible que celle des protéines DDB2 et XPC [109] et son recrutement est dépendant de la présence de la XPC [92]. Malgré le fait qu'elle n'a aucune fonction catalytique connue, la XPA est critique pour la NER. Une fonction proposée pour la XPA est la formation et le positionnement correct du complexe de réparation de la NER [110]. En fait, la XPA interagit avec plusieurs protéines de la NER et module leur activité: les TFIIH, RPA, XPC, DDB2, ERCC1-XPF et PCNA [111]. Sa

localisation en 5’ de la lésion soutient l’hypothèse d’un mécanisme de chargement par la XPA du complexe XPF-ERCC1 pour initier les étapes subséquentes de la NER [112]. À part son rôle structural, la XPA assiste la XPD dans la vérification des dommages [105]. Lorsque l’ADN est endommagé, la XPA inhibe l’activité hélicase de la TFIIH tout en stimulant le relâchement du sous-complexe tri-protéique CAK (« cyclin activating kinase ») du TFIIH, facilitant ainsi la transition de la transcription vers la réparation de l’ADN [105]. De plus, étant donné sa haute affinité pour les nucléotides endommagés et situés dans un contexte de structure simple brin, la XPA joue elle-même un rôle direct dans la vérification de dommages [113]. Par conséquent, l’ADN sera clivé uniquement lorsqu’un vrai substrat de la NER est présent. Dans le cas contraire, le complexe ouvert est désassemblé avant le recrutement de l’endonucléase XPF/ERCC1.

Le complexe RPA (« Replication Protein A *»)* formé des protéines RPA70, RPA32 et RPA14 protège le brin non-endommagé et positionne, avec la XPA, les deux endonucléases XPF et XPG en 5 ' et 3' du dommage respectivement [114]. À ce moment, le complexe XPC-centrin2 quitte l’ADN pour être recyclé [92, 94] permettant ainsi le recrutement de l’endonucléase XPG [115].

1.3.2.3 La phase d’incision du dommage et de synthèse du nouveau brin

La protéine XPG, membre de la famille des FLAP-endonucléases, est recrutée au site de dommage par le complexe TFIIH [116]. Son premier rôle dans la NER est purement structural, elle empêche la dissociation de la XPD du complexe TFIIH [117]. L’endonucléase XPF est recrutée au site de dommage par la XPA via son partenaire ERCC1 [118, 119]. Même si les deux endonucléases ont la même spécificité et coupent l’ADN à la jonction double-brin-simple-brin, elles sont de polarités différentes: le complexe ERCC1-XPF coupe l’ADN en 5’ de la lésion et la XPG en 3’ (Figure 1.4, étape C). La première incision faite par le XPF-ERCC1 requiert la présence de la XPG, mais pas sa fonction catalytique [120]. Le résidu 3’OH généré peut être utilisé par les polymérases pour initier la synthèse d’un nouveau brin. Pour ce faire, l’endonucléase XPG recrute via son domaine PIP « PCNA-interacting protein » le complexe RFC-PCNA qui sera positionné en 5’ du dommage par le complexe

RPA. Ceci est accompagné par le recrutement des polymérases qui commencent la synthèse du nouveau brin [121]. En fonction du statut cellulaire, différentes polymérases sont impliquées. Dans les cellules en prolifération, la synthèse du nouveau brin est réalisée par la polymérase ε recrutée par la PCNA et une forme modifiée de la RFC contenant la protéine CTF18 (« Chromosome transmission fidelity protein 18 ») [122]. Dans les cellules quiescentes, cette étape est accomplie par les polymérases δ et κ. Le recrutement de la polymérase δ nécessite le complexe RFC-PCNA, alors que celui de la polymérase κ utilise la protéine d'échafaudage XRCC1 et la PCNA sous sa forme ubiquitinylée. En utilisant la technique de l'interférence à l'ARN, Ogi *et al.* [122] ont démontré que dans 50% des sites des dommages, l'ADN était synthétisé par les polymérases δ et κ et dans le reste par la polymérase ε. Afin de finaliser la synthèse du nouveau fragment, l'ADN doit être coupé en 3' de la lésion. Cette incision faite par la XPG réclame la présence et l'activité catalytique de la XPF [123]. Par la suite, la XPG est ubiquitinylée par le complexe ubiquitine ligase Cdt2 (« *Cell division cycle protein 2 »)* et dégradée par le protéasome [124]. L'utilisation de ce mécanisme, appelé « cut-patch-cut », évite l'activation des voies de signalisation des dommages et l'arrêt du cycle cellulaire [69]. Un fragment de 26-30 nucléotides contenant le facteur TFIIH lié au dommage est libéré à la fin de cette étape [125].

1.3.2.4 La phase de ligation du nouveau brin

Une fois la synthèse accomplie, le RFC et les polymérases quittent l'ADN (Figure 1.4, étape D). La PCNA reste attachée à la chromatine et recrute l'ADN ligase I [121]. Dans les cellules quiescentes, la ligase III est recrutée par la XRCC1 [126].

1.4 La phase de reconnaissance des dommages de la GG-NER

La réparation globale du génome emploie deux complexes protéiques, le XPC-HR23B-centrin2 et l'UV-DDB pour détecter et initier la réparation de 90% des dommages induits par les UV à travers le génome [70].

1.4.1 Un détecteur versatile : la protéine Xeroderma pigmentosum C

Protéine clé de la GG-NER, la XPC fait partie *in vivo* d'un complexe trimérique formé avec deux autres facteurs, le HR23B (« human homolog of Radiation sensitive 23B protein ») et la centrine 2. La sous-unité XPC est responsable de la reconnaissance de l'ADN endommagé et de la liaison du complexe hétérotrimérique à l'ADN. Le HR23B stimule la liaison des dommages par la XPC [127] et la protège contre la dégradation par le protéasome [128]. Il a quatre domaines fonctionnels : un domaine UbL (ubiquitine-like) pour lier le protéasome, deux motifs UBA (« ubiquitin-associated ») qui lient des chaînes d'ubiquitine et un domaine de liaison pour la XPC [129]. Curieusement, le HR23B se détache de la XPC une fois le dommage reconnu et ne participe pas à la NER [130]. Comme le site d'interaction de HR23B chevauche celui de la liaison entre l'ADN et la XPC [89], il a été proposé que son départ permettrait probablement à la XPC de se lier à l'ADN de façon stable. La centrine 2 lie le domaine C-terminal de la XPC et y reste probablement attachée pendant la NER. Elle stimule la réparation des dommages par la NER [131] mais son rôle biologique exact est inconnu.

La XPC est une protéine de 940 acides aminés avec des domaines de liaison à l'ADN et des domaines d'interaction protéine-protéine (Figure 1.5A). Des études fonctionnelles *in vitro* et *in vivo* ont montré que la présence de la XPC au site du dommage est nécessaire au recrutement des autres protéines de la GG-NER ainsi que pour réparation des lésions par cette sous-voie [92, 132]. Comme initiateur de la GG-NER, la protéine XPC doit être en mesure de détecter la grande variété de lésions à l'ADN qui représentent le substrat de la NER. Un premier indice du mécanisme moléculaire employé par la XPC pour réaliser un tel exploit a été fourni par des expériences biochimiques. La XPC lie des dommages qui sont des substrats pour la NER, comme les 6-4PP, les pontages intra-brins engendrés par le cisplatine, mais elle lie également les substrats des autres voies de réparation, comme des bases mal appariées, des lésions réparées par la BER incluant les 8-oxoG et même des liaisons d'ADN non endommagé mais en forme de bulle [133-135]. D'autres études ont précisé que la XPC liait préférentiellement les jonctions double brin- simple-brin d'ADN [136, 137], et que son affinité pour l'ADN simple-brin était réduite de moitié en présence d'une lésion [137]. Ces observations ont mené à la proposition d'un mécanisme indirect de

reconnaissance des dommages par la protéine XPC qui reconnait le manque d'appariement des nucléotides et/ou la déstabilisation de l'hélice d'ADN [134, 138]. Ce mécanisme a été confirmé par la résolution de la structure cristallographique de la RAD4, son orthologue chez *Saccharomyces cerevisiae* [89]. La protéine RAD4 utilise quatre domaines pour se lier à l'ADN endommagé, domaines conservés chez la XPC: le domaine TGD (« transglutaminase homology domain ») et les domaines en épingle à cheveux BHD1 à 3 (« β hairpin domain 1-3 »). Les domaines TGD et BHD1 ancrent la RAD4 sur l'ADN en liant l'ADN double-brin sur 11 paires de bases en 3' de la lésion, tandis que les domaines BHD2/3 lient le brin non-endommagé, interagissant avec les quatre nucléotides situés en face du dommage. Donc, la protéine couvre seulement la partie située en 3' de la lésion, laissant le côté 5' de la lésion libre. Lors d'insertion du doigt en épingle à cheveux (« β hairpin ») du domaine BHD3 à travers la double hélice, la paire de bases formant le dommage ainsi que les bases situées en face de lui sont retournées vers l'extérieur. Les bases non endommagées sont gardées dans la « paume » de la structure en forme de « main » formée par les domaines BHD2 et BHD3, alors qu'aucun contact entre la RAD4 et les deux nucléotides endommagés n'a été observé. Les deux autres paires de bases flanquant le dommage et liées par BHD2/3 restent à l'intérieur, dans la conformation d'ADN double brin. Le BHD3 comble l'espace vide et stabilise le complexe XPC sur l'ADN qui est maintenant plié dans un angle de 42°. Cette stratégie indirecte de détection des dommages basée sur la détection de distorsions de la double hélice d'ADN et la liaison du brin non-endommagé explique la polyvalence de la GG-NER à réparer une grande variété de lésions non-apparentées structurellement.

Toutefois, comme la structure cristallographique de RAD4 représentait la phase finale de l'étape de reconnaissance des dommages par la XPC, des études subséquentes ont tenté d'expliquer comment la XPC trouve ces distorsions induites par les dommages à l'ADN dans la chromatine. La résolution de la structure cristallographique de la RAD4 liant un ADN intact n'a pas donné la réponse tant attendue, car elle était identique à celle de RAD4 liant l'ADN endommagé [139]. Comme la discrimination entre ces deux types d'ADN ne résidait pas dans leur structure, plusieurs mécanismes ont été proposés (Figure 1.5B).

(a) « Interroge et ouvre ». La XPC scanne continuellement l'ADN à la recherche de dommages décrits par des liaisons multiples et transitoires avec les bases d'ADN [140]. Lors

de cette étape, elle utilise un « senseur minimal » formé des domaines BHD1 et BHD2, ainsi que le tour β situé entre BHD2 et BHD3. Grâce à sa charge négative, répulsive contre l'ADN, le tour β fournit la mobilité requise aux molécules de XPC dans leur quête de lésions dans le génome. Lorsqu'elle trouve la lésion, la XPC insère son doigt en épingle à cheveux du domaine BHD3 entre les nucléotides, elle plie l'ADN et forme un complexe de reconnaissance stable (Figure 1.5B, partie a) [141].

(b) « Barrière cinétique ». Dans ce modèle, la sélectivité de la XPC pour les sites endommagés est le résultat d'une compétition entre le temps de résidence à un site donné et la rapidité avec laquelle XPC tourne les bases vers l'extérieur [139, 142]. L'absence ou la faiblesse des liaisons entre les bases endommagées fait en sorte que le temps requis à la XPC pour ouvrir l'ADN endommagé (7 msec) est 4000 fois plus court que celui nécessaire à ouvrir l'ADN intact (Figure 1.5B, partie b).

(c) « Tords et ouvre ». La XPC diffuse rapidement sur l'ADN et par moment elle interroge brièvement (100-500 µsec) la stabilité de l'ADN par torsion. Si l'ADN est facilement tordu, cela indique à la XPC/RAD4 la présence de bases non appariées et probablement la présence d'une lésion. Ceci sera vérifié lors d'une étape lente qui inclut le mécanisme (b) : l'ouverture de l'ADN et la stabilisation du complexe XPC-ADN via le domaine BHD3 (Figure 1.5B, partie c) [143].

Une étude très récente qui se base sur la visualisation des mouvements des molécules de RAD4 sur de l'ADN immobilisé sur des billes, propose que la XPC utilise tous ces trois mécanismes pendant la recherche des dommages: glissement sur l'ADN avec ses domaines BHD1/2, vérification de la présence des dommages en pliant ou tordant l'ADN et ouverture de l'ADN et insertion de son domaine BHD3 lorsque la lésion est encombrante [144].

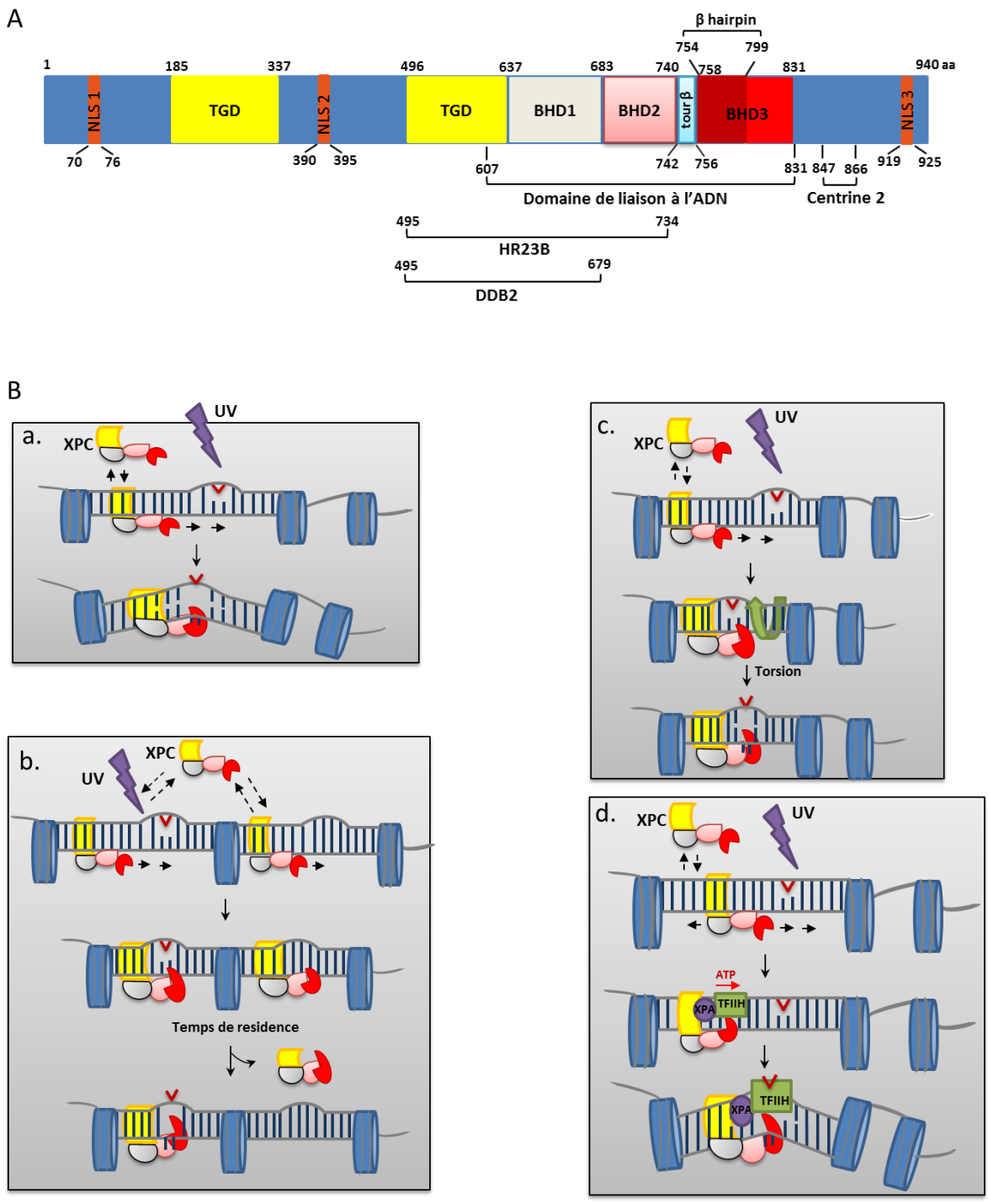

Figure 1.5 La XPC et ses mécanismes de recherche de dommages dans la chromatine.

A. Structure de la XPC indiquant ses domaines de liaison à l'ADN et les domaines d'interaction avec d'autres protéines. La XPC utilise quatre domaines pour lier l'ADN, le TGD et les BHD1/3, mais seulement deux pour chercher les dommages: le BHD1 et BHD2 avec son tour β. Le domaine TGD est également requis pour l'interaction entre XPC et les

protéines HR23B, DDB2 et XPA. Le domaine BHD1 contribue à l'interaction de la XPC avec le DDB2 et le HR23B. En utilisant les résidus situés dans la partie C terminale, la XPC s'associe à la centrine 2 et aux facteurs p62 et XPB du complexe TFIIH. **B.** Mécanismes de recherche de la XPC pour des lésions qui déforment la structure β de l'ADN et arrêtent XPC lorsqu'elle glisse sur l'ADN : (a) interroge et ouvre; (b) barrière cinétique et (c) tords et ouvre. (d). mécanisme de liaison coopérative pour la recherche des lésions peu encombrantes, comme les dommages de type thymine-thymine. Plus de détails sont donnés dans le texte.

Si ces mécanismes peuvent expliquer la reconnaissance des dommages qui déforment suffisamment l'ADN pour arrêter la XPC, ils ne s'appliquent pas pour les lésions qui déforment très peu ou pas l'hélice de l'ADN, comme les CPD. Malgré le fait qu'ils représentent 75% des dommages induits par les UV et 90% des dommages réparés par GG-NER, la XPC n'a pas d'affinité mesurable pour ce type de dommage. *In vitro*, XPC n'est pas ou est très peu capable d'initier leur réparation [133, 134, 145, 146]. Dans ce cas, un autre mécanisme appelé « liaison coopérative » a été proposé [147, 148] par lequel la spécificité réduite de la XPC pour les dommages de type CPD [90] pourrait être compensée par l'engagement d'autres protéines et/ou des modifications post-traductionnelles (Figure 1.5B, partie d). En effet, une étude récente démontre que lorsque le dommage est un CPD, la XPC emploie un mécanisme de « reconnaissance de la distance » par rapport au site de lésion. Son mouvement contraignant sur une distance de 1-2 kilobases autour des sites CPD agit comme signal pour les facteurs situés en aval qui vont procéder à sa vérification [144]. En employant ce mécanisme, les problèmes d'encombrement stérique possibles qui peuvent arriver entre la XPC et les autres facteurs de réparation sont évités. Il est aussi possible que le complexe ouvert se forme en amont du dommage et qu'il se déplace par la suite grâce à l'activité hélicase du complexe TFIIH [104].

1.4.2 Un complexe multifonctionnel : le complexe UV-DDB

Un candidat raisonnable qui facilite la reconnaissance des dommages de type CPD dans la chromatine est le complexe hétéro-dimérique UV-DDB constitué des facteurs DDB1 et DDB2. Le DDB2 (« UV-damaged DNA binding protein 2 »), codée par le gène XPE est

apparue récemment dans l'évolution et n'existe pas chez les eucaryotes inférieurs comme la levure. Les structures cristallographiques du complexe UV-DDB liant l'ADN avec une lésion de type 6-4PP ou CPD ont montré que les dommages sont exclusivement liés par le domaine WD40 de DDB2. Le DDB2 lie des dommages de type UV dans l'ADN nu [77, 91] ou dans une structure de type nucléosome [149]. Ce facteur lie aussi des sites abasiques et des bases mal appariées, mais il ne lie pas des gros adduits [150]. Pour ce faire, le DDB2 établit des contacts avec les deux brins d'ADN et utilise le doigt tri-peptidique (« β hairpin ») pour retourner la lésion vers l'extérieur. Par la suite, le dommage sera stabilisé dans une poche hydrophobe présente à sa surface par plusieurs résidus (Figure 1.6). Plus important, cette poche peut accueillir seulement deux nucléotides. Donc les CPD, les 6-4PP et les sites abasiques entrent dans cette poche, mais pas les gros adduits comme le 4-nitrosoqinolone. Comme dans le cas de la XPC, l'insertion de ce doigt et l'extrusion du dommage résulte dans le pliage de l'ADN sous en angle de 45°. Le DDB1 n'interagit pas directement avec l'ADN [151], mais il est essentiel pour la fonction du complexe, tel que démontré par l'existence des maladies XP-E caractérisées par des mutations affectant l'interaction du DDB2 avec le DDB1 [152]. Le facteur DDB1 est formé de trois domaines de type WD40 : BPA, BPB et BPC (« β propeller A to C ») [31]. Les domaines BPA et BPC forment un angle de 60° entre eux qui constitue l'interface de liaison du DDB2. La liaison du DDB1 au DDB2 est réalisée par le motif hélice-boucle-hélice situé dans la partie N-terminale du DDB2.

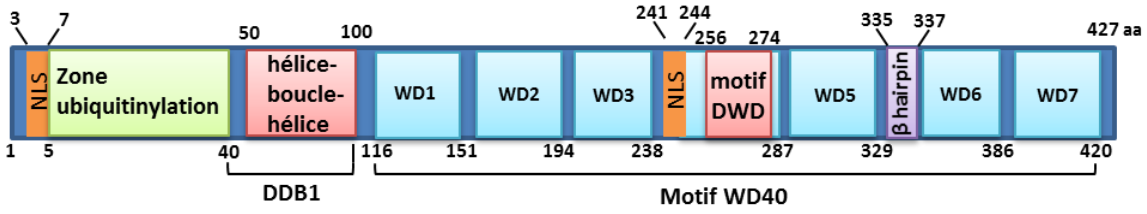

Figure 1.6 Structure du DDB2 montrant ses domaines importants et le site d'interaction avec le DDB1.

Le facteur DDB2 est une protéine globulaire formée de sept domaines WD possédant chacun 4 hélices. L'ADN traverse la cavité centrale des hélices WD40 le long d'un axe défini par les domaines WD 4 et 7. Les points de contacts entre le DDB2 et l'ADN se trouvent dans les régions intra-domaine. Le doigt en épingle à cheveux occupe l'espace entre les domaines

WD5 et WD6. Le motif DWD n'interagit pas avec l'ADN ou avec le DDB1. Les résidus accepteurs d'ubiquitine, ainsi que le motif d'interaction avec le facteur DDB1 sont concentrés dans la région N-terminale du DDB2.

Après irradiation, le facteur DDB2 est recruté très rapidement et indépendamment de la XPC sur les lésions (Figure 1.7) [153, 154]. Le complexe UV-DDB cherche les dommages en trois dimensions en sautant d'une molécule d'ADN à une autre, ce qui lui permet de scanner l'ADN rapidement tout en évitant les problèmes associés au glissement sur l'ADN, comme la présence des autres protéines et des nucléosomes [155]. Plusieurs études *in vitro* ont montré que l'affinité du complexe UV-DDB pour les dommages de type UV est de 100 à 1000 fois supérieure à celle de la XPC [156, 157]. La formation d'un dimère avec un autre complexe UV-DDB via leur domaine N-terminal l'immobilise au site du dommage et augmente son affinité pour l'ADN endommagé [158]. Une fois lié, le DDB2 stimule la translocation de la XPC du nucléoplasme vers la chromatine [159] et assure l'accumulation de la XPC non seulement aux sites CPD mais aussi aux sites 6-4PP [156, 160]. Cette observation est soutenue par le fait que les cellules provenant des personnes ayant des mutations dans le gène XPE codant pour le DDB2 réparent très peu les dommages de type CPD et lentement les dommages de type 6-4PP [154, 156]. En conclusion, ce premier modèle propose que le complexe UV-DDB reconnait les dommages induits par les UV *in vivo* et y recrute la XPC probablement par interaction directe [146, 154, 161]. Cependant, le mécanisme par lequel la lésion passe du DDB2 à la XPC n'est pas toujours bien compris. Une seule étude a réussi à montrer *in vitro* une interaction transitoire entre la XPC et l'UV-DDB au site de dommage impliquant les régions TGD et BHD1 de la XPC : l'association sur le TGD se produit indépendamment de l'ADN, tandis que la liaison du DDB2 avec le BHD1 de la XPC est stimulée par l'ADN endommagé. [162]. Il est proposé que cette courte interaction soit suffisante pour indiquer à la XPC l'existence d'un dommage réel et limite ainsi toute recherche futile de dommages.

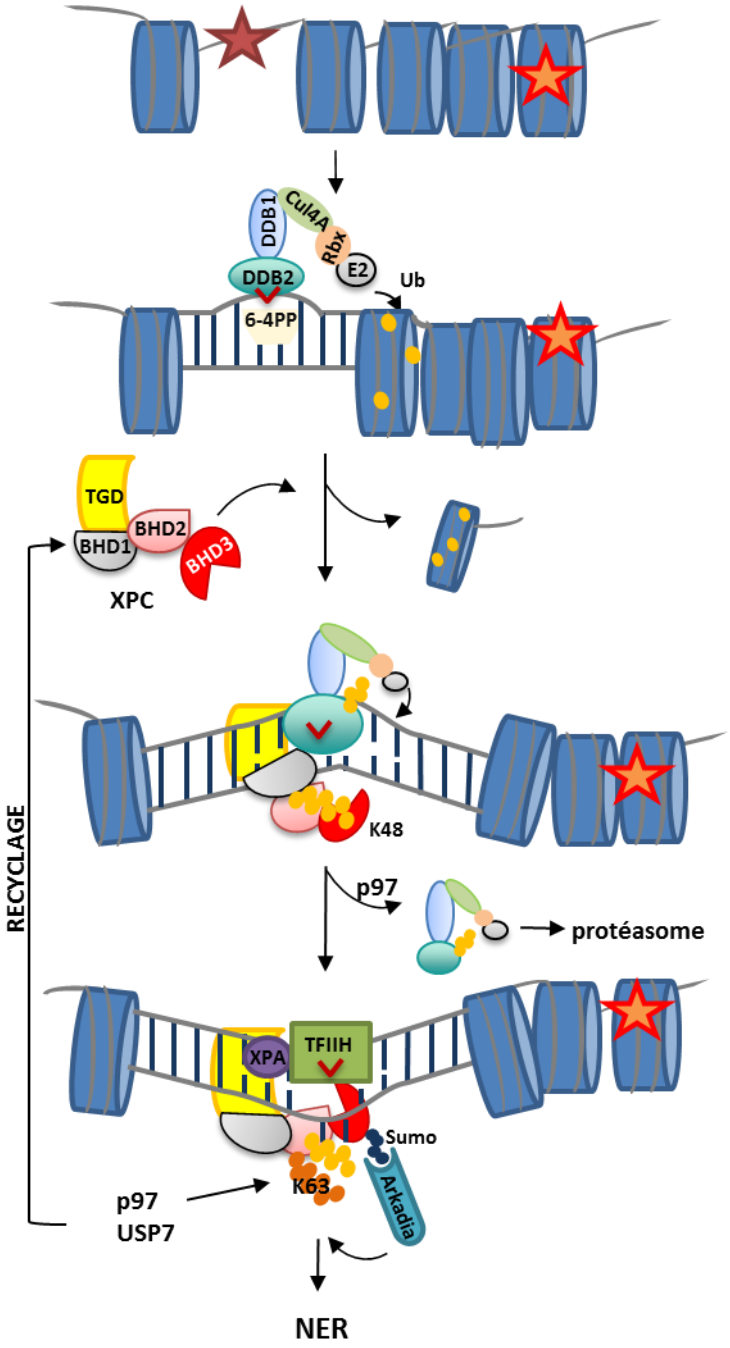

Figure 1.7 Le recrutement direct de la XPC au site des dommages par le complexe ubiquitine ligase UV-DDB.

Les détails sont donnés dans le texte. Les cercles jaune et orange représentent des résidus d'ubiquitine, les cercles bleu représentent les protéines Sumo et les étoiles, les dommages induits à l'ADN par les rayons UV.

À part son rôle de facteur de reconnaissance des dommages, l'UV-DDB forme un complexe ubiquitine ligase avec les protéines Cul4A et Rbx1. En absence des dommages, ce complexe est maintenu inactif par le complexe multi-protéique COP9 (« Constitutive photomorphogenesis 9 »), responsable de la déneddylation des Cul4 [78]. Suite à l'irradiation, la liaison du DDB2 aux dommages induit la libération du complexe COP9, ce qui permet la neddylation de la Cul4A. Cette modification est requise pour activer le complexe ubiquitine ligase qui modifie alors des substrats situés dans un rayon d'environ 100 Å [91]. Le complexe ubiquitine ligase pourrait aussi être assemblé au site de dommage par la protéine UVRAG («UV radiation resistance-associated gene »). Ce facteur promeut l'interaction du DDB1 avec la Cul4A, ainsi que la neddylation de la Cul4A au site de la lésion [163]. Les principales cibles du complexe ubiquitine ligase sont les histones, la XPC, le DDB2 ainsi que la Cul4A elle-même [78, 146, 164]. L'ubiquitinylation de la XPC augmente de deux fois son affinité pour l'ADN intact ou endommagé [146]. Par contre, le DDB2 ubiquitinylé perd son affinité pour l'ADN et est dégradé. L'importance critique de l'ubiquitinylation est prouvé par une diminution du recrutement de la XPC [165] et l'augmentation de l'instabilité chromosomique [166] lors d'une présence prolongée du DDB2 au site de dommages. De plus, la présence du DDB2 natif inhibe l'excision des 6-4PP ou des CPD de l'ADN, mais cette inhibition est levée suite à l'induction de l'ubiquitinylation [146, 147]. La région N-terminale du DDB2 (résidus 1-40) a été identifié comme site majeur accepteur d'ubiquitine (Figure 1.6) et plusieurs résidus y sont localisés (Lys 4, 5, 11, 22, 35, 36 et 40) [77]. Par conséquent, un mécanisme de transfert de la lésion du DDB2 vers la XPC dépendant de l'ubiquitinylation a été aussi proposé. La modulation de l'ubiquitinylation du DDB2 par la XPC est intrigante. En étant la cible préférée du complexe ubiquitine ligase Cul4-Rbx1, la XPC retarde la dégradation normalement rapide du DDB2 qui pourra participer à plusieurs séries de reconnaissance des dommages avant d'être dégradé [167].

Le complexe ubiquitine ligase UV-DDB-Cul4A-Rbx1 ne facilite pas seulement le transfert du dommage du DDB2 à la XPC, mais influence plusieurs de ses fonctions (Figure 1.7). Premièrement, l'ubiquitinylation change la distribution spatio-temporelle de la XPC [162]. La XPC native est recrutée aux dommages situés dans la région compacte intra-nucléosomale. En modifiant la XPC, le DDB2 contrecarre ce mouvement et recrute la XPC

dans les régions inter-nucléosomales où il se trouve, assurant ainsi la réparation rapide des dommages 6-4PP. Une fois le DDB2 dégradé, la XPC migrera vers les zones intra-nucléosomales pour réparer d'autres dommages, surtout des CPD, aidée par des facteurs encore inconnus. Deuxièmement, la sumoylation de la XPC par les SUMO1/3 (« Small ubiquitin-like modifier 1/3 ») dépend du DDB2 [168, 169] et est absolument nécessaire pour son ubiquitinylation ultérieure par la RNF111/Arkadia, une ubiquitine ligase dépendante de sumoylation (Figure 1.7) [169]. Cette modification est reconnu par la ségregase dépendante de l'ubiquitinylation p97 qui enlève de la chromatine non seulement la XPC mais aussi le DDB2, pour laisser la place aux endonucléases XPG et XPF [170]. Cela empêche ainsi leur fixation prolongée qui est source d'instabilité génétique [166]. Une fois dans le nucléoplasme, le sort de ces deux protéines est différent : le DDB2 est envoyé vers le protéasome et dégradé, tandis que la XPC est recyclée à son état natif grâce à l'activité de la déubiquitinase USP7 [171]. En conclusion, ce modèle propose que suite au recrutement de la XPC, l'ubiquitinylation facilite le transfert de la lésion du DDB2 à la XPC et assure son fonctionnement efficace pendant la NER.

Cependant, plusieurs observations ne concordent pas avec le modèle proposé. Par exemple, les structures cristallographiques de ces deux protéines montrent que chacune d'entre elles plie l'ADN, mais en des directions opposées [89, 91]. De plus, chacune d'entre elles introduit une structure en forme de doigt dans le même espace afin de vérifier la présence des dommages, ce qui est tout à fait impossible. Aussi, avec la technique d'EMSA (« Electrophoretic mobility shift assay »), on a observé que lorsque ces deux facteurs de reconnaissance des lésions étaient incubés avec de l'ADN endommagé, ils ne forment pas qu'un seul complexe, mais deux complexes séparés [157]. Finalement, une étude récente démontre que le UV-DDB arrive au dommage et part du dommage indépendamment de la XPC et il réside sur la lésion plus de temps que la XPC [172].

Pour concilier les données concernant le rôle du DDB2 dans la GG-NER *in vivo* avec ces observations, il a été proposé que le remodelage de la chromatine par le complexe UV-DDB constitue le signal indiquant à la XPC la présence des dommages (Figure 1.8). Le rôle du DDB2 dans le remodelage de la chromatine est très bien documenté. Premièrement, le

DDB2 plie l'ADN sous un angle de 40° lorsqu'il se lie au site de dommage [91]. Comme cet angle induit une distorsion de l'hélice d'ADN qui constitue le substrat préféré de la XPC, ceci pourrait être un signal pour l'attirer au dommage. Il a été montré que plus la distorsion est grande, plus le nombre de molécules de XPC liées augmente [173]. Deuxièmement, les chaînes d'ubiquitine déposées sur les histones par le complexe ligase UV-DDB-Cul4A-Rbx1 pourrait être reconnues par les domaines UBA de l'HR23B (Figure 1.8) [174, 175]. Troisièmement, le déplacement ou l'éviction des histones H3, H4 et H2A ubiquitinylées expose l'ADN et donne accès à la XPC au site de dommage (Figure 1.8) [176, 177]. Quatrièmement, l'UV-DDB recrute des facteurs de remodelage de la chromatine. Des études initiales sur le rôle de la chromatine dans la réparation des dommages par la NER ont montré que l'hyper-acétylation augmente la réparation des dommages induits par les UV [178-180]. Le DDB2 recrute des complexes impliqués dans l'acétylation des histones, comme le complexe p300 [181, 182] et l'acétyltransférase GCN5 (« General control of amino acid synthesis protein 5 ») composante du complexe STAGA (« SPT3-TAF9-GCN5 acetylase complex ») [180]. D'autres facteurs de remodelage de la chromatine dépendant de l'ATP, comme l'INO80 (« Inositol requiring mutant 80 ») [183] et la Brg1 (« Brahma-related gene 1 ») interagissent aussi avec le DDB2 [184]. Chez les mammifères, le recrutement de l'INO80 au site du dommage facilite le recrutement des protéines XPC et XPA et la réparation des dommages 6-4PP et CPD. Par contre, le recrutement de la Brg1 est dépendant de la présence du DDB2 et de la XPC; son rôle exact dans la NER est source de débat [184, 185]. Finalement, le DDB2 peut directement ouvrir la chromatine indépendamment de ses fonctions dans le complexe ubiquitine ligase [186]. Donc, ce deuxième modèle propose que le facteur DDB2, en stimulant le remodelage de la chromatine, crée un environnement favorable au recrutement de la XPC. Par contre, il n'explique pas comment la XPC trouve les distorsions induites par le DDB2 sur les sites endommagés. D'autres études seront nécessaires pour combler cette lacune dans la compréhension.

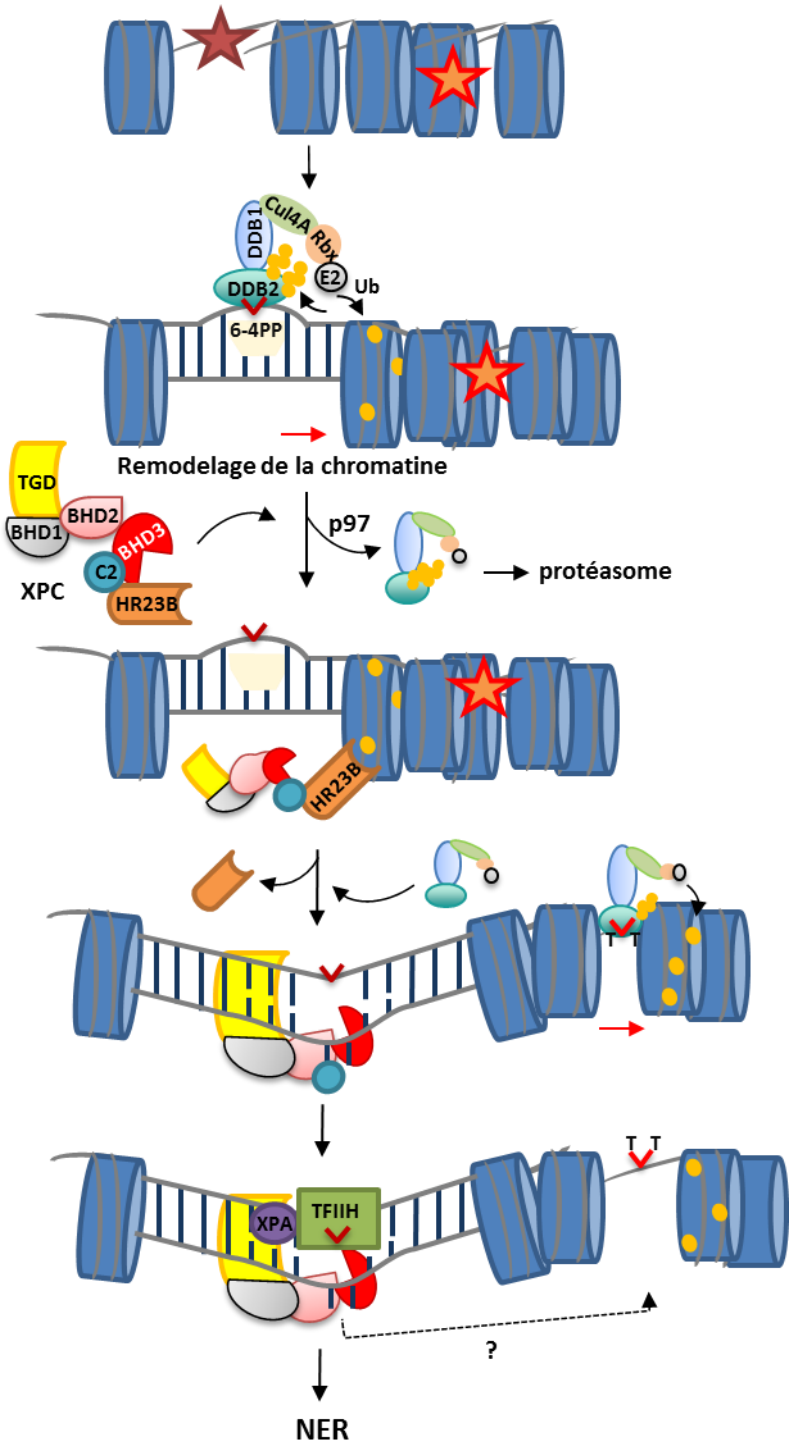

Figure 1.8 Le recrutement indirect de la XPC par le complexe UV-DDB via le remodelage de la chromatine.

Les détails sont donnés dans le texte. Les cercles jaune représentent les résidus d'ubiquitine et les étoiles représentent les photolésions.

En conclusion, la NER est un processus complexe qui implique le recrutement et le départ coordonnés d'environ 30 protéines. De plus en plus, les études récentes révèlent que les modifications post-traductionnelles, e.g. ubiquitinylation, sumoylation et éventuellement phosphorylation régulent le mouvement des protéines de la NER autour du site de la lésion. Dans ce contexte, il était important d'établir si la poly(ADP-ribosyl)ation, une modification post-traductionnelle catalysée par des membres de la famille des poly(ADP-ribose) polymérases, pourrait jouer un rôle dans la NER.

1.5 La poly(ADP-ribos)ylation (PARylation)

L'ADP-ribosylation est une modification post-traductionnelle qui consiste à transférer une (MARylation) ou plusieurs (PARylation) unités d'ADP-ribose sur des protéines acceptrices. La formation de poly(ADP-ribose) (PAR) a été rapportée pour la première fois en 1963 par Chambon *et al.* [187], qui ont observé que l'addition de nicotinamide mononucléotide stimulait l'incorporation de l'ATP radioactivement marqué dans des polymères par une protéine dont l'activité enzymatique dépendait de l'ADN. La structure des PAR a été résolue de façon indépendante par trois laboratoires [188-190] et l'enzyme responsable de leur synthèse a été nommée poly(ADP-ribose) polymérase (PARP) [191]. Les unités d'ADP-ribose sont liées par une liaison glycosidique 1"-2' ribose-ribose pour former des PAR très complexes pouvant atteindre 200 à 400 unités *in vitro* et *in vivo*, avec des points de branchement régulièrement espacés tous les 20-50 résidus [192-194]. Certains PAR ramifiés ont une structure secondaire hélicoïdale qui rappelle la structure de l'ADN et de l'ARN d'où le nom de troisième type d'acide nucléique [195]. Le rôle de ces différences structurales dans les PAR n'est pas bien compris mais elles pourraient probablement influencer la signalisation en aval, comme sélectionner une voie de réparation et/ou arrêter le cycle cellulaire [196].

Au moins quatre activités enzymatiques sont requises pour la synthèse des PAR. (1) Le clivage du substrat NAD^+ en nicotinamide, proton (H^+) et ADP-ribose par l'activité NAD glycohydrolase des PARPs. (2) Le transfert de la première unité d'ADP-ribose (MARylation) sur les résidus glutamate ou aspartate, mais aussi sur les résidus cystéine, arginine et lysine

des protéines cibles. (3) L'élongation de la chaîne de polymères par addition de résidus d'ADP-ribose via une liaison O-glycosidique ribose-ribose (PARylation). (4) Enfin, les ramifications qui supposent l'attachement des résidus d'ADP-ribose à l'extérieur de la portion linéaire du polymère [197, 198]. Comme toutes les autres modifications post-traductionnelles, l'ADP-ribosylation dépend de l'existence d'« écrivains » pour leur synthèse et d'« éditeurs » pour leur dégradation. De plus, plusieurs centaines de protéines « lectrices » ont été identifiées et caractérisées [199]. Le niveau des PAR dans les cellules est très faible, mais il peut augmenter de 10 à 500 fois en réponse aux dommages à l'ADN. Les PAR sont éliminés très rapidement par des « éditeurs », avec une demi-vie *in vivo* de 40 sec à 6 min [197].

1.5.1 Un « écrivain » : la poly(ADP-ribose) polymérase 1

L'ADP-ribosylation est catalysée par des membres de la famille des poly(ADP-ribose) polymérases (PARP). Cette famille contient 17 membres chez les humains, identifiés sur la base d'homologie avec le domaine catalytique du membre fondateur, la PARP1. Les membres de cette famille utilisent le substrat NAD^+ pour transférer des sous-unités d'ADP-ribose sur des protéines cibles [193]. Étant donné que seulement 4 de ces 17 membres, les PARP1, PARP2, PARP5A (tankyrase 1) et PARP5B (tankyrase 2), ont la capacité de former des PAR [200], une nouvelle nomenclature a été proposée pour la famille des poly(ADP-ribose) polymérases, qui est connue maintenant aussi sous le nom de « ADP-rybosyltransferase of the diphteria toxin-like type » (ARTD) [201].

La PARP1, le membre le plus connu et étudié de la famille constitue le sujet de ma thèse, sa structure et ses fonctions seront détaillées dans les sections et paragraphes suivants.

1.5.1.1 La structure de la PARP1

La PARP1, une des plus abondantes protéines nucléaires ($0,5\text{-}2\times10^6$ copies par cellule) [202] est responsable de la formation de la majorité des PAR (90%) dans les cellules

de mammifère [202, 203]. Chez les humains, la PARP1 est une protéine de 113 kDa organisée en 6 modules divisés en trois domaines fonctionnels distincts: le domaine de liaison à l'ADN, le domaine d'auto-modification et le domaine catalytique (Figure 1.9) [204].

Le domaine de liaison à l'ADN est unique à la PARP1 et s'étale du premier acide aminé jusqu'à l'acide aminé 373. Il contient trois doigts de zinc (F1-F3) et un signal de localisation nucléaire qui renferme un site de clivage par la caspase 3 (Figure 1.9A) [192]. Les doigts de zinc F1 et F2 sont strictement nécessaires pour la liaison à l'ADN et l'activation catalytique de la PARP1 [205, 206], ce qui explique probablement leur clivage pendant l'apoptose [207]. Les structures cristallographiques montrent un mode bipartite de liaison des doigts de zinc de la PARP1 : le « phosphate backbone grip » lie les résidus de sucre et de phosphate de trois nucléotides situées vers l'extrémité 3', alors que le « base stacking loop » fait des contacts avec les deux bases exposées. Il est à noter qu'aucun des doigts n'établit de liaison avec les extrémités 3' ou 5' de l'ADN [208, 209]. Ceci explique la capacité de la PARP1 à lier une grande variété de structures d'ADN natives ou endommagées indépendamment de leurs séquences, car des bases exposées peuvent être rencontrées aussi dans des structures d'ADN sans cassures, comme l'ADN en tige-boucle et cruciforme [210]. Par des mutations dirigées, il a été déterminé que pour la liaison de la PARP1 à l'ADN, les contacts avec le squelette de sucre-phosphate sont plus importants que les contacts avec les bases exposées [209].

Des analyses biochimiques et cellulaires ont démontré que chaque doigt de zinc exerce des fonctions distinctes. Le doigt F2 a 100 fois plus d'affinité pour l'ADN que le doigt F1, mais il n'est pas requis pour l'activation de la PARP1 *in vitro* par l'ADN avec cassure double-brin. En contraste, les acides aminés du doigt F1 qui sont en contact avec les bases non-appariées situées en 3' de la cassure sont requis pour initier l'activation de la PARP1 en formant des contacts avec les autres domaines de la PARP. Le doigt F2 est requis pour la liaison des cassures simple-brin d'ADN [209, 211, 212]. Étant donné son affinité élevée pour l'ADN, il est le premier à se lier en 3' de la cassure simple-brin. En tordant l'ADN, il expose un site cryptique situé en 5'de la cassure de liaison qui sera lié par le doigt F1. Pour éviter l'encombrement stérique, l'ADN est très déformé par rapport à la structure β et plié dans un

angle de 100°. La liaison directionnelle des doigts de zinc, avec le doigt F1 en 5' et le doigt F2 en 3' de la cassure, est la seule à assurer l'activation de la PARP1. Le doigt F3 lie l'ADN du même côté que le doigt F1, mais loin du site de cassure. Il transmet le signal de détection des dommages aux autres domaines de la PARP1, ce qui assure son activation ultérieure [213, 214].

Considéré longtemps comme le seul site accepteur de PAR, la partie centrale de la PARP1 située entre les acides aminés 374 et 523 a été nommée *le domaine d'auto-modification* (Figure 1.9A). Des études protéomiques récentes ont identifié des acides aminés accepteurs d'ADP-ribose dans chacun des trois domaines fonctionnels de la PARP1. Cependant, un tiers d'entre eux reste concentrés dans la région d'auto-modification (du résidu 456 au résidu 491) [215, 216]. La partie N-terminale du domaine d'auto-modification contient un motif «leucine zipper» très peu caractérisé, qui pourrait être impliqué dans la dimérisation de la PARP1 et/ou dans les interactions protéine-protéine. Le module BRCT («breast cancer susceptibility protein, BRCA-1, C-terminal») permet aussi à la PARP1 d'interagir avec ses partenaires. Il n'est pas essentiel pour son activation *in vitro* [193].

Le domaine catalytique de la PARP1 situé entre les acides aminés 524 à 1014, est composé du module WGR et du module de liaison du NAD^+ (Figure 1.9A). Le rôle du WGR, nommé d'après les acides aminés qui le composent, Tyr-Gly-Arg, a été mis en évidence récemment [209]. La structure cristallographique de la PARP1 lie à un modèle de cassure double-brin (oligonucléotide double-brin) montre que des résidus conservés du module WGR interagissent avec l'ADN en 5' de la cassure. Le WGR forme avec les doigts de zinc une interface qui couvre la cassure sur approximativement sept paires de bases. Cette interface permet la liaison et le changement conformationnel du domaine catalytique associé à l'activation de la PARP1 [208]. Le module de liaison du NAD^+ est composé du sous-domaine hélicoïdal (HD) et le sous-domaine de transfert de l'ADP-ribose (ART). Le sous-domaine HD est retrouvé seulement chez les membres de la famille activés par l'ADN endommagé : les PARP1 à 3 [193]. Il inhibe l'activité catalytique de la PARP1, sa délétion résultant d'une PARP1 hyperactive [217]. L'ART est responsable des quatre activités catalytiques de la PARP1 : l'hydrolyse du NAD^+, l'attachement initial d'un résidu d'ADP-ribose sur les

protéines acceptrices, l'élongation et les ramifications des PAR (Figure 1.9B). Il contient un site accepteur du NAD^+, nommé site donateur, et un site accepteur, de fixation de l'unité d'ADP-ribose sur lequel le prochain résidu d'ADP-ribose sera lié pendant la réaction d'élongation des PAR. Le site donateur est composé de trois pochettes de liaison, une pour le nicotinamide, une deuxième pour le phosphate et une troisième pour l'ADP-ribose [193]. Des données structurales ont révélé que le site accepteur de la PARP peut accueillir l'ADP-ribose acceptrice dans les deux orientations pouvant donner lieu à des polymères linéaires ou ramifiés. Dans le site de liaison du NAD^+, une séquence de 50 acides aminés forme la « signature de la PARP », la structure la plus conservée chez les membres de la famille de PARP [192].

1.5.1.2 Le mécanisme d'activation de la PARP1

L'activité basale de la PARP1 est très faible, mais en présence de différents types d'activateurs, tel que l'ADN endommagé, les nucléosomes, la chromatine et même les histones, elle augmente jusqu'à 500 fois [218]. Plusieurs études ont démontré que les doigts de zinc de PARP1 étaient essentiels pour son activation en présence d'ADN [209, 216, 218, 219]. Toutefois, le mécanisme par lequel les signaux de son domaine de liaison à l'ADN sont traduits par l'activation de son domaine catalytique n'est pas connu.

C'est seulement en 2012 que Langelier *et al.*, [208] ont mis en évidence pour la première fois que la formation des connexions entre les domaines de la PARP1 est à la base de son mécanisme d'activation. Par conséquent, la simple mutation d'un acide aminé critique à la formation des liaisons inter-domaines est suffisante pour inactiver PARP1 sans toutefois affecter sa liaison à l'ADN ou la formation d'une structure compacte [209, 220, 221]. L'interaction de la PARP1 comme monomère avec un modèle de cassure double-brin cause des modifications conformationnelles dans les doigts F1, F3 et le domaine WGR qui amènent le site catalytique à proximité du domaine de liaison à l'ADN [208]. Par la suite, l'effet auto-inhibiteur du sous-domaine HD doit être levé. Son dépliage local par réarrangement des hélices permet une liaison productive du substrat NAD^+ et change la flexibilité et la dynamique du sous-domaine ART, activant la PARP1 [217]. Il est intéressant de souligner

que l'ampleur du changement conformationnel du sous-domaine HD est directement corrélée avec le degré d'activation catalytique de la PARP1 [217], ce qui explique probablement les variations dans l'activation de la PARP1 observées avec différentes structures d'ADN. Le domaine d'auto-modification de la PARP1 est placé à proximité du domaine catalytique, ce qui explique la concentration de sites d'acceptation des PAR dans la région située entre le BRCT et le WGR [215].

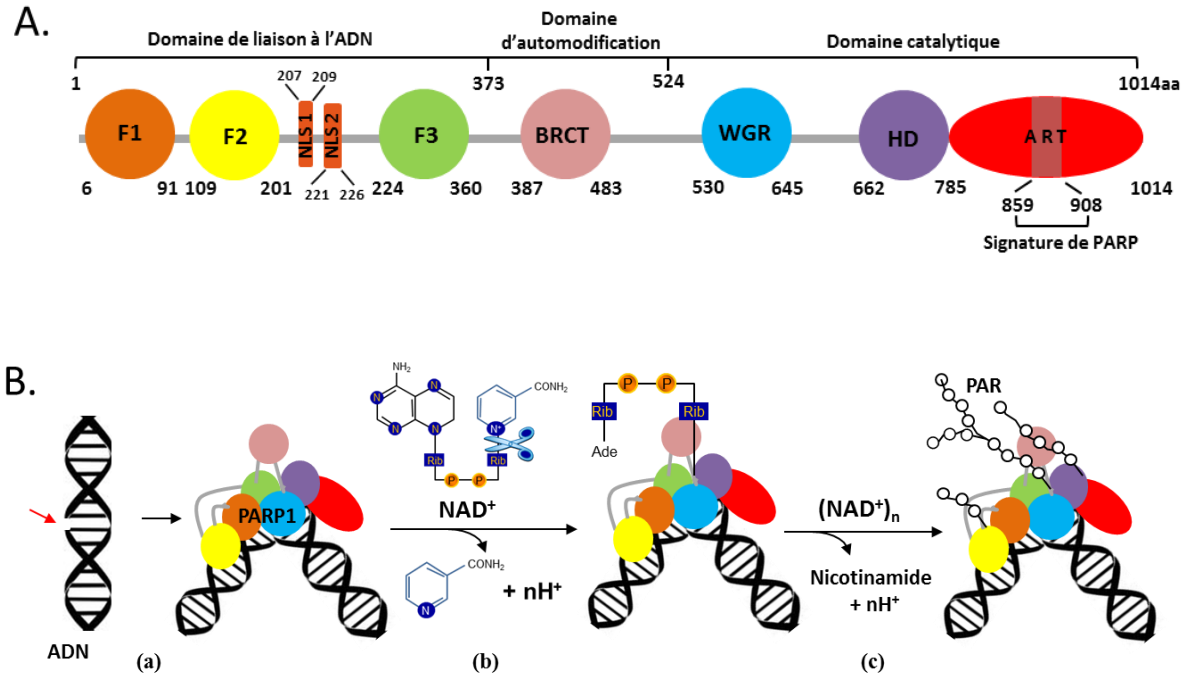

Figure 1.9 La PARP1 et ses activités catalytiques.

A. Structures de la PARP1 avec ses trois domaines fonctionnels. **B**. Activation de la PARP1 par les cassures simple brin d'ADN. (a) Liaison de la PARP1 sur l'ADN et formation d'une structure compacte; (b) clivage du substrat nicotinamide dinucléotide avec libération du nicotinamide et d'un proton puis initiation de la PARylation et (c) élongation et ramification des polymères d'ADP-ribose.

La formation de différentes connexions entre les domaines de la PARP1 en fonction de la structure des activateurs peut expliquer les variations de la PARylation. Le doigt F2

n’est pas nécessaire pour activer PARP1 aux cassures double-brin [209], mais il collabore avec F1 pour lier un oligonucléotide double-brin avec des bouts cohésives [222]. Les contacts établis entre le doigt F2 et l’ADN ne changent pas par rapport aux études précédentes [208, 209] mais la polarité du doigt F1 est inversée par rapport à l'ADN. Dans le même contexte, il a été montré que l’activation de la PARP1 aux cassures simple-brin requière la liaison directionnelle de F2 en 3’ et F1 en 5’ de la cassure [212]. Des études futures seront nécessaires afin de déterminer les interactions de la PARP1 avec d’autres types d’ADN endommagé, surtout dans le contexte de la chromatine.

Il est connu que la PARP1 est activée par les lésions induites par les UV, les sites apuriniques et apyrimidiques, les structures en tige-boucle et cruciforme [223], mais aussi par les histones [224] et certaines de ses modifications post-traductionnelles (phosphorylation, MARylation) [225, 226]. Il sera intéressant de déchiffrer la structure de la PARP1 liée à l’ADN endommagé mais sans cassure pour déterminer si ses interactions seront différentes en fonction de l’état de l’ADN, e.g. cassé ou intact, ainsi que les conséquences fonctionnelles de ces différences. Un premier indice est la structure du doigt F1 en présence et absence d’ADN qui montre un repositionnement des résidus clés pour l’activation de la PARP1 lorsqu’elle est liée à l’ADN [209]. Un deuxième indice est la torsion majeure de l’ADN au site d’une cassure simple brin, impossible à obtenir avec de l’ADN intact. De plus, déterminer si la PARP1 lie l’ADN comme dimère [227, 228] ou monomère [208, 221] en fonction de la structure de l’ADN est également importante avant d’accepter un modèle unique d’activation de la PARP1.

1.5.2 Les « éditeurs » : protéines qui dégradent les polymères d’ADP-ribose

Comme dans le cas de toute autre modification post-traductionnelle, la synthèse et la dégradation des polymères sont étroitement contrôlées [193]. La dégradation des PAR commence immédiatement après le début de leur synthèse assurant ainsi une signalisation correcte de la présence de dommages dans les cellules et de leur niveau: 85% ont une demi-vie de 40 secondes, et les 15% restants ont 6 minutes [229]. En dégradant rapidement les

PAR, les « éditeurs » empêchent la déplétion du NAD^+ liée à la mort cellulaire par nécrose ou l'accumulation des PAR libres liée à une forme d'apoptose nommée PARthanatos [230].

L'enzyme principale responsable de dégrader les PAR dans les cellules est la poly(ADP-ribose) glycohydrolase (PARG). L'absence de la PARG cause la mortalité chez l'embryon murin (E 3.5) attestant son importance pour la maintenance de la physiologie normale de la cellule [231, 232]. Chez les mammifères, un seul gène code pour plusieurs isoformes de PARG situés dans des compartiments cellulaires différentes : la PARG-110/111 est la forme nucléaire, les PARG-99 et PARG-102 sont des isoformes cytoplasmiques et la PARG-65 est la forme mitochondriale [233]. L'enzyme PARG comporte trois domaines fonctionnels : la région régulatrice, le domaine accessoire et le domaine Macro [193]. Situé en position N-terminale de la protéine, la région régulatrice contient un signal de localisation nucléaire (NLS), un motif d'interaction avec la PCNA (PIP) et un signal d'export nucléaire. Le NLS situé dans les premiers 20 acides aminés est absent chez les PARG 102 et 99 qui restent alors cytoplasmiques. Le motif PIP est impliqué dans le recrutement indépendamment des PAR de la PARG au site de dommages [234]. Le rôle du domaine accessoire est le moins compris; un rôle indirect dans la stabilisation du domaine Macro lui a été attribué [235]. Le domaine Macro est un module de liaison des PAR, qui dans la structure de la PARG, a évolué par l'ajout d'une boucle catalytique [236] contenant une séquence conservée de deux résidus glutamate consécutifs. La déplétion de ces résidus mène à la perte totale de l'activité catalytique de la PARG [236, 237]. La dégradation des polymères par la PARG libère des unités de mono-ADP-ribose, donc elle exerce surtout une activité exo-glycohydrolase. Pour ce faire, la PARG lie les unités d'ADP-ribose terminales des chaines, place le lien ribose-ribose entre les résidus glutamate clés et clive le lien ribose-ribose. PARG peut aussi cliver les polymères par son activité endo-glycohydrolase [238], mais ceci est inefficace [239]. Les PAR peuvent être aussi dégradés par l'ADP-ribosyl-hydrolase 3 (ARH3). Elle possède une activité exo-glycohydrolase qui agit sur des polymères libres [240].

Probablement à cause de l'encombrement stérique, ni la PARG, ni l'ARH3 ne peuvent cliver la dernière unité d'ADP-ribose, laissant ainsi une protéine mono-ADP-ribosylée.

Récemment, des protéines capables de cliver ce lien ont été décrites: la TARG1 (« terminal ADP-ribose glycohydrolase 1») et les Macro D1/D2. Elles agissent sur les résidus d'ADP-ribose attachés à des acides aminé acides, tels que le glutamate et l'aspartate, mais pas sur ceux liés à des résidus lysine ou arginine [241, 242]. La TARG1 peut aussi cliver le lien entre la première unité d'ADP-ribose et la protéine libérant la chaine de PAR entière [243]. L'hydrolyse de la première unité d'ADP-ribose est l'étape qui limite la dégradation des chaînes de PAR, durant quelques minutes [244].

1.5.3 Les « lectrices » : protéines acceptrices de polymères d'ADP-ribose

La PARylation a de nombreuses et diverses fonctions dans les cellules eucaryotes. Par conséquent, ce signal doit être reconnu rapidement et spécifiquement afin d'assurer une réponse cellulaire adéquate. Presque 800 des protéines qui acceptent des PAR après induction de dommages oxydatifs à l'ADN ou suite à la PARylation *in vitro* ont été identifiées par des études de protéomique [196]. Récemment, en associant la spectrométrie de masse à la création des analogues des PARP1 à 3 et du substrat NAD^+, une étude *in vitro* a montré que 167 protéines cibles parmi 800 étaient modifiées par la PARP1. De ces 167 protéines, 43 sont PARylés exclusivement par la PARP1, le reste étant des cibles communes des PARP1, PARP2 et PARP3 [245]. Ces découvertes techniques récentes ont aussi permis de caractériser le site d'interaction des PAR sur les protéines acceptrices. Ceci a multiplié la liste d'acides aminés qui sont la cible des PAR; aux acides aspartique et glutamique on a ajouté la lysine, la cystéine et l'arginine. Certains de ces sites peuvent être non-spécifiques, étant donné leur capacité à être modifiés de façon non-enzymatique par des PAR libres obtenus par l'activité de la PARG ou ARH3 [246]. De plus, des hydrolases qui enlèvent le dernier résidu d'ADP-ribose de résidus lysine ou cystéine n'ont pas été identifiées. Cependant, la PARylation des résidus lysine de queue des histones et de la PARP1, de la FEN1 et d'autres protéines a été montrée *in vitro* et *in vivo* après le traitement des cellules avec de l'H_2O_2 [247]. Sa signification et son rôle biologique restant à déterminer [248]. Le site de PARylation n'est pas toujours confié à quelques résidus. À ce jour, quatre classes distinctes de modules de lecture de PAR ont été identifiés : l'abondant PBM (« PAR binding motif »), le PBZ (« PAR-binding zinc finger »), le domaine Macro et le domaine WWE. À ceux-ci s'ajoutent des

domaines supplémentaires, comme le domaine BRCT, le FHA (« forkhead-associated domain »), le GAR (« Glycine-Arginine rich domain ») et le RRM (« RNA recognition motif ») [249].

La liaison des PAR chargés négativement sur les protéines cibles affecte profondément leurs fonctions normales : elles acquièrent d'autres fonctions leur permettant de répondre adéquatement aux stimuli. Parmi ceux-ci, on mentionne l'inhibition de l'interaction avec l'ARN, l'ADN ou des protéines partenaires, la relocalisation cellulaire, ainsi que l'inhibition/stimulation des activités enzymatiques [250]. Cela a mené au concept de « reprogrammation » des fonctions protéiques par la PARylation [251]. Il a été démontré *in vitro* et *in vivo* que les modules de liaison des PAR chevauchent souvent d'autres domaines protéiques importants, tel que le domaine de liaison à l'ADN ou les domaines d'interaction protéine-protéine [252]. Une fois PARylées, les protéines perdent leur affinité pour l'ADN par répulsion de charge. Les facteurs de remodelage de la chromatine FACT (« Facilitates chromatin transcription »), ISWI (« imitation SWI of drosophila melanogaster ») et KDM5B (« Lysine-specific demethylase 5B »), les protéines p53, Ku70/80 et la PARP1 également ne sont que quelques exemples de l'effet inhibiteur de la PARylation sur l'interaction des protéines avec l'ADN. De plus, la PARylation affecte les interactions protéine-protéine : la p21 PARylée n'interagit plus avec la PCNA [253] tout comme la p53 PARylée avec le récepteur d'export nucléaire Crm1 (« Chromosome region maintenance 1 »), s'accumulant dans le noyau [254].

La relocalisation cellulaire est un autre effet de la « reprogrammation» des fonctions protéiques. Suite à la micro-irradiation des cellules, la PARP1 est rapidement recrutée au site de dommages et activée [255]. Les polymères formés localement établissent une plateforme d'échafaudage pour les protéines ayant des modules de liaison de polymères comme celles mentionnés ci-dessus. Par exemple, la protéine d'échafaudage XRCC1 est recrutée sur le site de cassure simple-brin via son domaine BRCT ayant un module PBM [63]. L'histone chaperone APLF (« Apatraxin and PNK-like factor ») s'accumule autour des cassures grâce à ses modules PBZ [256]. Le facteur de remodelage de la chromatine ALC1 (« Amplified in liver cancer 1 ») exerce ses fonctions seulement après avoir été reconnu les PAR formés au

site de dommage avec son domaine Macro [257]. Fait intéressant, toutes les enzymes impliquées dans la dégradation de PAR possèdent un domaine Macro modifié dans leur structure, ce qui explique probablement leur localisation rapide au site de formation des PAR et la courte demi-vie des PAR. L'inhibition de l'activité de la PARP1, en utilisant des inhibiteurs spécifiques ou la déplétion des modules de liaison des PAR, abolit le recrutement de toutes les protéines susmentionnées.

Les PAR affectent aussi les autres modifications post-traductionnelles. Le cas le plus connu est le contrôle de la PARylation sur l'activité ubiquitine ligase du RNF146 (« Ring Finger Protein 146 ») ou Iduna. Le RNF146 possède un domaine WWE, riche en tryptophane-tryptophane-glutamate, qui reconnaît les chaînes PAR avec beaucoup d'affinité [258]. La PARylation du RNF146 entraine la modification conformationnelle de son domaine catalytique qui devient alors actif [259]. Par la suite, le RNF146 modifie, avec des chaînes d'ubiquitine des protéines de réparation de l'ADN, comme le XRCC1, la PARP1, l'ADN ligase III et la Ku70 [260] préalablement PARylées, assurant ainsi leur dégradation d'une manière contrôlée et au temps opportun. Dans ce cas, la PARylation des protéines sert de signal pour leur ubiquitinylation subséquente

Dépendamment du niveau de stress cellulaire, la PARP1 pourrait recruter des protéines spécifiques et/ou moduler leur fonction en catalysant la formation des chaînes de PAR de différentes longueurs et des ramifications. Par exemple, le recrutement et la liaison de la XRCC1 à l'ADN nécessite des polymères formés d'un minimum de 7 unités [261] alors que des polymères de 12 à 15 unités d'ADP-ribose sont requis pour le recrutement et l'activation de l'ALC1 [262]. La p53 lie des PAR courts (14 mer) mais aussi les longues chaines de PAR (plus de 55mer) [263]. Sa modification avec des PAR courts, au maximum de 20 unités [264] affecte la liaison à l'ADN avec une séquence consensus bloquant ainsi la transcription de gènes Bax (« Bcl-2–associated X protein ») et Fas [265]. La dégradation des PAR liés à la p53 pendant l'apoptose coïncide avec l'activation de la caspase 3, le clivage de la PARP1 et l'activation des gènes pro-apoptotiques [266]. Les polymères longs sont efficacement hydrolysés par les activités endo- et exo-glycohydrolase de la PARG, tandis que les petits PAR ne sont pas des bons substrats [267]. Cette dépendance de la longueur des

PAR pour l'activation catalytique de la PARG ajoute un niveau supplémentaire de contrôle, celui du temps de dissociation des PAR liés aux protéines. Donc, la longueur et la ramification des PAR pourraient jouer un rôle dans la signalisation de l'ampleur de dommages.

En conclusion, les modules de liaison des PAR ciblent les protéines acceptrices vers le site de synthèse des polymères et, en modulant leurs interactions avec l'ADN et leurs activités enzymatiques, permettent une régulation temporelle et spatiale de différentes réponses cellulaires, incluant la réparation de l'ADN.

1.5.4 La PARP1 et la réparation des dommages à l'ADN

Étudiée d'abord et avant tout comme réponse cellulaire aux dommages à l'ADN, la PARylation est impliquée dans plusieurs autres réponses cellulaires en absence de stress comme la transcription, la réplication, la maintenance de télomères, le métabolisme et l'architecture cellulaire, pour ne donner que quelques exemples [268, 269]. L'importance de la PARP1 dans la réparation des dommages à l'ADN est démontrée par sa haute affinité et son recrutement rapide au niveau des différents types de lésions, par ses nombreuses interactions avec des facteurs de réparation de l'ADN et par la sensibilité aux agents endommageant l'ADN des souris PARP1$^{-/-}$ déficientes en PARP1. Le développement des techniques de microscopie en temps réel a permis de démontrer qu'après l'induction de dommages à l'ADN (oxydation, alkylation, irradiation), une des réponses cellulaires rapides sont le recrutement et l'activation catalytique de la PARP1 aux sites de lésions [255]. L'effet principal de la présence localisée de la PARP1 et des polymères inclut la signalisation de la présence des dommages, le changement de la structure de la chromatine, le recrutement de protéines de réparation de l'ADN et l'élimination des dommages (Figure 1.10). Le signal peut être amplifié par le recrutement au site de lésion d'autres protéines de signalisation comme l'ATM (« Ataxia telangiectasis mutated ») [270] et l'ATR (« Ataxia telangiectasia and Rad3-related protein ») [271]. Récemment, il a été proposé que la PARylation des extrémités d'ADN par la PARP1 puisse être aussi un signal de présence de dommages, surtout après le départ de la PARP1 de la chromatine [272].

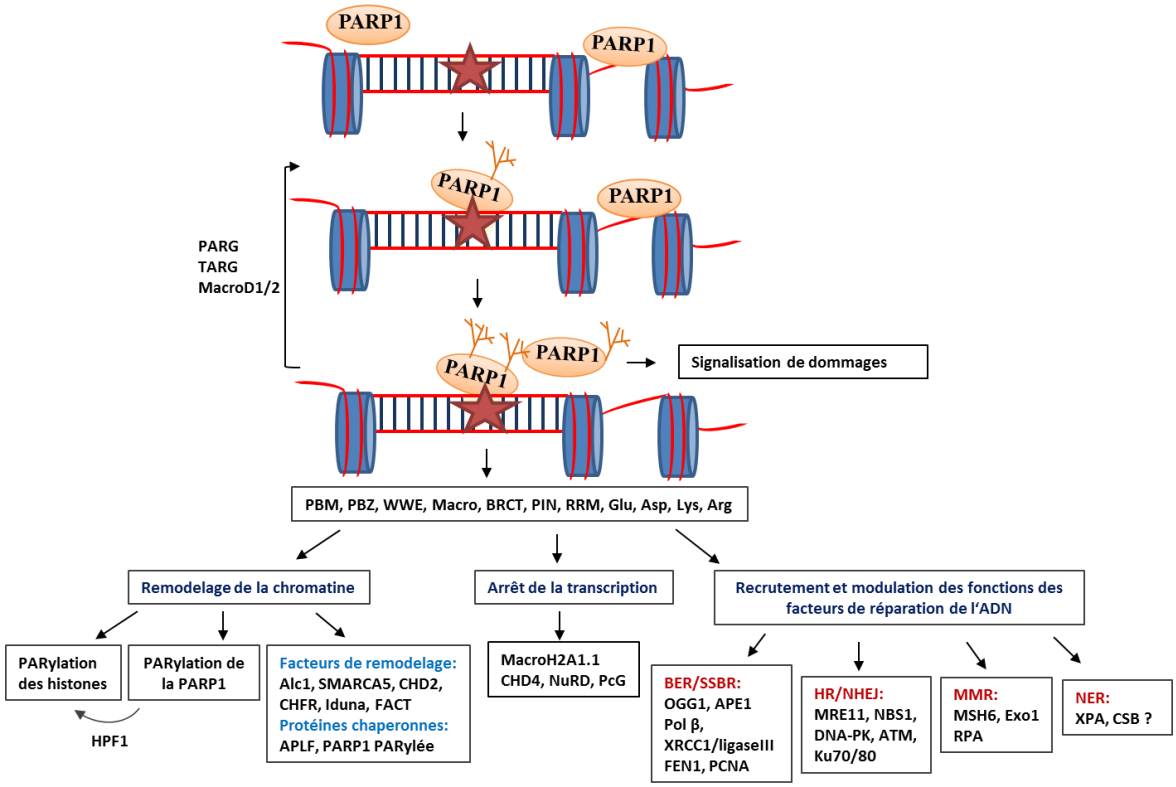

Figure 1.10 Les fonctions de la PARP1 dans la réparation des dommages à l'ADN.

La PARP1 peut être libre dans le nucléoplasme et liée à la chromatine. En réponse aux dommages à l'ADN, la PARP1 est activée et forme des polymères d'ADP-ribose. Ces polymères signalent la présence des dommages et recrutent des protéines de remodelage de la chromatine et des facteurs de réparation ayant des modules de lecture des PAR dans leur structure. Plus de détails sont fournis dans le texte. Modifié de Tallis *et al*., 2014 [273].

1.5.4.1 La PARP1 et le remodelage de la chromatine

Chez les eucaryotes la réparation de l'ADN a lieu dans la chromatine, structure formée par l'enchaînement répété des nucléosomes unis par l'ADN inter-nucléosomal. Selon le modèle « accès-réparation-restauration » l'ouverture transitoire de la chromatine par la mobilisation des histones facilite la reconnaissance rapide de la lésion et le recrutement de protéines de réparation des dommages à l'ADN, assurant une réparation efficace [274]. Ce processus est surtout important pour les voies de réparation qui comportent des complexes protéiques très larges : la NER et la réparation des cassures double-brin (DSBR). La

réorganisation de la chromatine a lieu soit par des modifications post-traductionnelles des histones, soit par le déplacement, l'éviction et/ou le changement des histones avec d'autres variantes par des facteurs de remodelage de la chromatine et des protéines chaperonnes [69].

Une multitude d'études *in vitro* et *in vivo* ont mis en évidence le rôle majeur de la PARP1 dans l'organisation de la structure chromatinienne. Déjà dans les années 80, des études de microscopie électronique avaient montré que la PARylation de la chromatine mène à sa décondensation [275, 276]. Comme cette structure ressemble à celle obtenue par la déplétion de l'histone H1 de la chromatine, il a été proposé que la PARylation de l'histone H1 était responsable de la formation d'une structure chromatinienne relâchée. L'histone H1 PARylée reste liée à la chromatine [275]. À noter que son domaine de liaison des PAR se trouve dans la partie C terminale impliquée dans la compaction de la chromatine [277]. Les histones du cœur nucléosomal sont aussi PARylées, mais l'histone H1 reste le meilleur accepteur des PAR *in vitro* et *in vivo* [278, 279]. Comme le site accepteur des PAR se trouve à l'interface avec l'ADN, la modification des histones sur des résidus glutamate, aspartate et lysine [280, 281] est suffisante pour déstabiliser la structure nucléosomale [282]. Par contre, d'autres études ont suggéré que la PARylation de la PARP1 est suffisante pour ouvrir la chromatine et que la modification des nucléosomes n'était pas obligatoire. La PARP1 fait partie intégrante de la structure chromatinienne, occupant la région inter-nucléosomale [219]. L'addition de la PARP1 native aux polynucléosomes promeut leur compaction en une structure serrée. Par conséquent, l'auto-modification de la PARP1 entraine la relaxation de cette structure, probablement via son expulsion par répulsion des charges [283]. Même une activation basale de la PARP1, par des polymères courts de 40 unités, est suffisante pour induire la décondensation de la chromatine [284]. Ces données *in vitro* ont été confirmées chez la Drosophile par Tulin *et al*., qui ont montrés la décondensation de la chromatine et l'activation de la transcription suite à l'activation de la PARP1 [285]. Comme la cible de choix de la PARylation est la PARP1 elle-même, son éviction de la chromatine, suite à son auto-modification, est le mécanisme privilégié pour expliquer l'ouverture de la chromatine [286, 287]. Des études récentes ajoutent un nouveau niveau de complexité en montrant que seules les molécules de PARP1 liant l'ADN intact seront expulsées par auto-PARylation, alors que la PARP1 PARylée et liée à l'ADN endommagé restera afin d'assurer la réparation

[60, 288]. Il faut préciser que ce mécanisme n'exclut pas la trans-PARylation des histones. La découverte d'une nouvelle protéine HPF1 (« Histone PARylation factor 1 ») [289] qui promeut la modification des histones en limitant l'hyper-auto-PARylation de la PARP1, soutient cet argument.

Un troisième mécanisme pour expliquer la relaxation dépendante de la PARP de la chromatine est basé sur la haute affinité des histones pour la PARP1 modifiée et chargée négativement [288, 290]. Dans ce mécanisme, la PARP1 PARylée joue le rôle de protéine chaperonne. Elle séquestre localement les histones, permettant ainsi l'ouverture de la structure nucléosomale et la réparation [282]. Une fois le dommage réparé, les PAR liés sur la PARP1 seront dégradés par la PARG et les histones pourront réintégrer la structure chromatinienne. Ce modèle est contesté par une étude récente *in vivo* qui observe une réduction de l'histone H1 au site de dommages induits par des lasers et non un enrichissement [291]. Les auteurs proposent que l'histone H1 PARylée soit probablement expulsée de la chromatine.

La PARP1 mobilise les histones aussi via le recrutement des facteurs de remodelage de la chromatine et protéines chaperonnes (Figure 1.10). Parmi ces facteurs, le plus étudié est l'ALC1 qui utilise l'ATP pour faire glisser les nucléosomes. Son recrutement au site de dommage *in vivo* et aux polynucléosomes *in vitro* est dépendant de la présence de PAR et de son domaine Macro [257]. De plus, selon des études biochimiques il a été montré que la PARP1 stimule son activité ATP-ase via la formation d'un complexe PARP1-ALC1-nucléosome [262]. D'autres facteurs de remodelage de la chromatine dont le recrutement est dépendant de la présence de la PARP1 et des PAR sont SMARCA5 (« SWI/SNF-related matrix-associated actin-dependent regulator of chromatin subfamily A member 5 ») et CHD2 (« chromodomain helicase DNA binding protein 2 ») [292, 293]. Le recrutement du CHD2 dépend de la présence de la PARP1. Le CHD2 déclenche le remodelage de la chromatine via l'incorporation de la variante d'histone H3.3 au site de cassures double-brin. Ceci induit l'assemblage du complexe de la voie de réparation par ligation d'extrémités non-homologues (NHEJ). La SMARCA5 joue un rôle important dans la réparation des cassures double-brin. Contrairement au CHD2, l'activité catalytique de la PARP1 est requise non seulement pour

le recrutement et la décondensation de la chromatine par SMARCA5, mais également pour son interaction avec RNF168 (« Ring Finger Protein 168 »). À son tour, la SMARCA5 favorise le recrutement de RNF168 et l'accumulation subséquente de BRCA1 (« Breast cancer 1 ») au site de lésion. Ces données lient physiquement et fonctionnellement la PARylation aux cascades de signalisation initiées par des ubiquitines ligases. Fait intéressant, deux autres ubiquitines ligases ayant des domaines de liaison de PAR jouent un rôle important dans la réparation de l'ADN : l'ubiquitine ligase CHFR (« Checkpoint with forkhead and ring finger domains ») et Iduna [260, 294]. La CHFR contient dans sa structure deux domaines PBZ qui reconnaissent les PAR formés sur le site de cassure double-brin. Sa déplétion retarde la conjugaison d'ubiquitine aux sites marqués par les γH2Ax. De plus, il induit la relaxation de la chromatine par le déplacement de la PARP1 et des histones [295]. Le départ de la PARP1 du site de dommage est essentiel à la réparation. Ceci peut être réalisé par la PARylation, mais aussi selon la dégradation de la PARP1 par ubiquitinylation. En ce sens, la déplétion de la CHFR ralentit le départ de la PARP1 située dans la chromatine, ce qui affecte la réparation des dommages. Aussi, la CHFR interagit seulement avec la PARP1 PARylée et pas avec la PARP1 native [294]. Tout comme la CHFR, la modification de la PARP1 par Iduna mène aussi à sa dégradation [260].

En plus des facteurs de remodelage, la PARP1 et la PARylation recrutent aussi des protéines chaperonnes. L'APLF (« Aprataxin and PNK-like factor ») est impliqué dans la réparation des cassures double et simple-brin [296]. Son substrat préférentiel est le complexe tétramérique H3/H4. Selon des études *in vitro*, il a été démontré que l'APLF conduit au désassemblage du complexe H3/H4 avec augmentation concomitante de la quantité d'ADN libre [297]. De plus, l'APLF interagit avec le facteur de remodelage ALC1 et favorise son interaction avec les histones [297]. En plus de son rôle dans le remodelage de la chromatine, l'APLF interagit avec Ku80 et stimule le recrutement de la XRCC4 et la réparation par la NHEJ [298]. Ensemble, ces résultats suggèrent que l'APLF cible les histones PARylées aux sites des cassures grâce à son domaine PBZ et facilite la réparation de l'ADN par le déplacement des histones ou leur échange avec des variantes d'histones, comme macroH2A1. L'histone variant macroH2A1.1 favorise la compaction transitoire de la chromatine au site de dommages et diminue le recrutement de la Ku70/80 [299]. Cette

compaction de la chromatine semble contredire le modèle « ouvrir-réparer-restaurer ». Cependant, elle est essentielle à l'arrêt de la transcription limitant ainsi l'augmentation du nombre de dommages. Plusieurs facteurs impliqués dans la répression de la transcription sont recrutés aux lésions dans un mode PAR-dépendant : le CHD4 (« chromodomain helicase DNA-binding protein 4 »), la sous-unité catalytique du complexe NuRD (« Nucleosome Remodeling Deacetylase ») et le complexe PcG (« Polycomb group protein ») [300, 301]. La présence de ces facteurs au site de dommages est accompagnée par la libération de l'ARN POLIIo qui crée l'espace nécessaire au recrutement des facteurs de réparation. Un autre exemple est la Spt16, la sous-unité catalytique du complexe FACT connue pour son rôle facilitateur de la transcription via le remodelage de la chromatine [302]. La PARylation de Spt16 réduit sa capacité de lier les nucléosomes, résultant dans l'inhibition de la transcription au site de dommage [303].

En conclusion, la PARP1 facilite la réparation par la compaction et/ou la décondensation de la chromatine en fonction des signaux physiologiques reçus par la cellule, donnant ainsi accès au site de dommage aux facteurs de réparation.

1.5.4.2 La PARP1 et la réparation des bases endommagées et des cassures simple-brin

Un des rôles les plus connus et étudiés de la PARP1 est la réparation des cassures simple-brin et des bases endommagées (SSBR/BER); la PARP1 étant maintenant considérée comme une des protéines de cette voie de réparation [304]. Plusieurs mécanismes d'action possibles ont été proposés pour la PARP1. Tout d'abord, elle peut signaler la présence des dommages, en se liant aux structures mimant des intermédiaires de réparation par la BER/SSBR, comme les sites abasiques, les gaps et les structures « en flap » [305]. L'activation de la PARP1 conduit par la suite à sa dissociation des cassures permettant la réparation par les autres facteurs de la BER [306-308]. La PARP1 participe à d'autres cycles de détection et de signalisation de cassures simple-brin une fois ses PAR dégradés par la PARG. En s'associant et en se dissociant de l'ADN, la PARP1 protège les cassures simple-brin contre la dégradation et prévient la formation de cassures double-brin [309]. Ce modèle

nommé « nick-protection » s'applique lorsque le nombre de cassures simple-brin excède la capacité de réparation de la cellule.

Des études biochimiques ont indiqué que la PARP1 et la PARylation pourraient jouer d'autres rôles dans la BER, comme le recrutement et la modulation des activités enzymatiques des facteurs de réparation associés à la BER. Par exemple, la PARP1 lie les sites abasiques [305] et stimule *in vitro* (jusqu'à 10 fois) l'activité endonucléase d'APE1 [310]. Comme les molécules de PARP1 sont 10 fois plus nombreuses que celles de l'APE1, il a été proposé que la PARP1 protège les cassures jusqu'à ce que l'APE1 soit disponible pour s'y lier et amorcer la BER. En effet, l'affinité de la PARP1 pour l'ADN et l'affinité de l'APE1 pour la PARP1 diminue lorsque l'APE1 ou des structures d'ADN mimant des intermédiaires de la BER sont ajoutés en excès aux extraits cellulaires [48, 311]. Lorsque le nombre de lésions dépasse celui des molécules d'APE1, la PARP1 se lie de façon covalente aux sites abasiques [312] et entraine la mort cellulaire. Comme alternative, la PARP1 pourrait commencer la réparation par la BER au moyen de son activité AP-lyase [305]. La formation des PAR, suite à l'incision du brin, recrute la PNKP qui nettoie l'extrémité 3'. Cependant ce type de BER, indépendant de l'APE1 est très rare, l'activité lyase de la PARP1 étant faible.

À part l'APE1, la PARP1 interagit avec d'autres protéines de la BER, comme la polymérase β, le complexe XRCC1/ligase III, la FEN1 et la PCNA [304]. L'activation de la PARP1 est aussi suivie du recrutement de la FEN1 [313] ce qui stimule l'activité de la polymérase β au site de dommages réparés par le « long patch-BER » [49]. Son interaction avec le facteur XRCC1 est la plus étudiée. Il est recruté au site de dommages en quelques secondes [61] par des PAR [261]. À son tour, le XRCC1 contribue à la stabilisation de la PARP1 au site de lésion, en limitant son auto-PARylation [62]. Par ce mécanisme, la PARP1 retarde son départ, assure la protection des cassures et module l'activité catalytique des facteurs de la BER. Cependant, des études récentes ont remis en question le rôle de la PARP1 dans la BER via le recrutement du XRCC1. Campalans *et al*., [39] ont montré que le recrutement lent du XRCC1 aux lésions oxydatives réparées par la BER était indépendant de la PARP1 et de la PARylation, alors que Reymelds *et al* [53] ont observé ce type de recrutement seulement au niveau des pyrimidines endommagées. Dans les deux études, le

XRCC1 est recruté rapidement par les PAR aux sites de cassures simple-brin. L'effet additif de l'inhibition de la PARP1 sur la survie cellulaire et la formation de cassures simple-brin dans les cellules déficientes en XRCC1 indique des rôles importants, mais distincts pour ces deux protéines dans la réparation par BER/SSBR [314].

Plusieurs observations soutiennent aussi un possible rôle de la PARP1 dans la BER/SSBR via le remodelage de la chromatine. La présence des lésions dans une structure polynucléosomale a un impact négatif sur la BER : l'APE1 reconnaît seulement les lésions orientées vers l'extérieur du cœur nucléosomal, l'activité de la polymérase β est réduite et celle du complexe XRCC1/ligase III est complètement bloquée [46]. *In vivo*, la PARP1 reconnaît les dommages oxydatifs situés dans les régions hétéro-chromatiniennes et promeut l'accumulation du XRCC1 dans ces régions [315]. L'ouverture de la chromatine, par la PARylation et par l'activité du complexe XRCC1-ligase III qui a la capacité de défaire les nucléosomes [46], pourrait faciliter le recrutement des facteurs de la BER/SSBR, comme l'OGG1 qui interagit physiquement avec la PARP1 [316] et réside exclusivement dans les régions eu-chromatiniennes [39].

Si le rôle de PARP1 dans le recrutement des protéines de la BER/SSBR est bien établi, son implication directe dans leur réparation reste controversée. L'utilisation des inhibiteurs de la PARP retarde la réparation des cassures simple-brin et des bases endommagées [317, 318] mais elle est tout à fait normale dans les cellules déficientes en PARP1 [52, 306, 319]. Ceci suggère que la PARP1 a des rôles accessoires dans la BER, comme la réparation des intermédiaires de la BER par la sous-voie « long patch BER» et le remodelage de la chromatine. D'autres études seront nécessaires afin de déchiffrer le rôle exact de la PARP1 dans la voie BER/SSBR.

1.5.4.3 PARP1 et la réparation de cassures double-brin

Étant donné la sensibilité aux drogues qui induisent l'effondrement des fourches de réplication des cellules déficientes en PARP1 [320], plusieurs études ont analysé ses rôles possibles dans la réparation dépendante de la réplication des cassures double-brin. Il a été

démontré que la PARP1 facilite le redémarrage des fourches de réplication bloquées et la réparation par recombinaison homologue des fourches effondrées et converties en cassures double-brin. PARP1 lie les fourches de réplication arrêtées, et elle est activée par ces fourches [321, 322] et son auto-PARylation sert de signal pour le complexe MRE11-Rad50-NBS1 [255, 321]. Le recrutement du complexe est facilité par la présence des domaines de liaison des PAR : la MRE11 a un domaine PBM et la NBS1 un domaine BRCT [323]. En plus de recruter la MRE11, la PARP1 limite aussi son activité de résection nécessaire à l'assemblage de la nucléoprotéine Rad51 [324]. Le traitement des cellules $PARP1^{-/-}$ à l'hydroxyurée augmente la formation des foyers Rad51 [321] et à l'inverse, son activation exacerbée par la déplétion de la PARG réduit leur formation [325]. La PARP1 stimule la réparation de fourches effondrées par la HR en bloquant l'association au niveau de la fourche de la Ku70 et de la ligase IV [326]. De plus, en facilitant le recul de la fourche [327] ou en stimulant la réparation des cassures simple-brin [328, 329] la PARP1 limite la formation de cassures double-brin.

Les cassures double-brin sont réparées majoritairement par la ligation d'extrémités non-homologues (NHEJ). Il y a deux voies de réparation par la NHEJ : la NHEJ classique, dépendante de la Ku, utilise les protéines Ku70/80, DNA-PK et ligase IV/XRCC4/XLF et la voie alternative de la NHEJ, indépendante de la Ku, implique les protéines MRE11, l'histone H1 et le complexe XRCC1/ligase III. La contribution de la PARP1 dans la réparation par la NHEJ classique reste à établir, car d'une part la PARP1 rivalise avec la Ku pour la liaison des cassures d'ADN [330, 331] et d'autre part les souris doublement déficientes en PARP1 et en DNA-PK sont plus sensibles que celles à mutation simple [332]. Cependant, une étude récente propose un rôle pour la PARP1 dans la NHEJ classique après avoir observé que l'inhibition ou la déplétion de PARP1 dans les cellules humaines réduit le recrutement de la XRCC4 aux cassures induites par des lasers et affecte la réparation d'un plasmide modèle *in vitro*. Le mécanisme impliqué serait l'association de la PARP1 aux cassures après le départ de la Ku70/80 et le recrutement du facteur de remodelage CHD2 qui, en ouvrant la chromatine, favoriserait l'assemblage du complexe NHEJ [292]. L'implication de la PARP1 dans la voie alternative de la NHEJ est plus évidente, car les cellules déficientes en Ku ne réparent pas les cassures double-brin en absence de la PARP1 [331]. PARP1 contribue au

recrutement de la MRE11 et de l'histone H1 et à son tour, l'histone H1 stimulerait la réparation des cassures double-brin par la voie alternative de la NHEJ [333].

1.5.4.4 La PARP1 et la réparation par excision de nucléotides

Plusieurs observations soutiennent un possible rôle de la PARP1 dans la NER. Tout d'abord, une série d'études faites dans les années 80 avait montré la diminution des réserves intracellulaires de NAD^+, l'incorporation de NAD^+ radioactif et la formation de PAR suite à l'irradiation de cellules aux UVC, un traitement qui induit exclusivement des dommages directs réparés par la NER [334-336]. Comme, il était généralement accepté que la PARP1 était exclusivement activée par des cassures d'ADN [337], son activation rapide par les UVC a été liée à l'étape d'excision du brin endommagé de la NER. L'absence ou la diminution de son activation dans les cellules XP déficientes en protéines impliquées dans cette phase de réparation et donc incapable d'exciser l'ADN, appuyait cette proposition.

Cependant, des collègues de mon laboratoire ont démontré qu'en réponse aux UVC, PARP1 s'active de façon monophasique, très rapidement (15 secondes), avant la formation des cassures simple-brin [338]. La PARP1 s'active de façon biphasique en réponse aux rayons UVB, une première activation très rapide (après quelques secondes) en réponse aux dommages directs et suivie par une seconde activation plus tardive (1-2 h) en réponse aux dommages oxydatifs. En utilisant la technique d'irradiation locale (qui permet de créer des zones d'irradiation locale de 3-5 µm entourées de régions non irradiées), ils ont montré aussi que la formation des PAR au site de lésions UV coïncidait avec l'arrivée des protéines de la NER impliquées dans la phase de reconnaissance des dommages. De plus, ils ont démontré que la PARP1 pouvait se lier à l'ADN irradié aux UVB, enrichie en dommages de type T-T [338]. Donc, l'activation de la PARP1 par les UVC observée précédemment par d'autres chercheurs n'était pas due à la formation de cassures simple-brin, mais à la liaison de la PARP1 aux CPD.

L'activation rapide de la PARP1 suggérait son implication dans la phase de reconnaissance des dommages de la NER. Comme cette étape est différente selon la

localisation du dommage (gène transcrit activement comparé au reste du génome), des collègues de mon laboratoire ont vérifiés laquelle des deux sous-voies de la NER, GG-NER ou TC-NER, était la plus affectée par l'absence de la PARP1 [339]. En utilisant des cellules XP-C, déficientes en GG-NER, des cellules CS-B, déficiente en TC-NER et la technique de réactivation dans les cellules hôtes (HCR) il a été mis en évidence que: 1) l'absence de la PARP1 des fibroblastes humains réduisait la HCR du gène rapporteur endommagé par les UV jusqu'au niveau comparable à celui des cellules XP-C et CS-B et 2) l'absence de la PARP1 dans les cellules XP-C et CS-B diminue davantage la réactivation du gène rapporteur irradié aux UV. Ces résultats suggéraient l'implication de la PARP1 dans les deux sous-voies de la phase de reconnaissance des dommages de la NER. Cependant, cette technique mesure les conséquences de la réparation et non la réparation en soi. De plus, le génome viral a une organisation plus simple que le génome des mammifères. Ainsi, la preuve directe de la participation de la PARP1 dans la NER consiste à évaluer la réparation des lésions directes dans le génome de cellules eucaryotes.

Toutefois, dans leur grande majorité, les études qui ont évalué le rôle de la PARP1 dans la NER ont démontré que l'absence de la PARP1 et/ou de son activité n'affectaient pas la cinétique de réparation des dommages directs induits par les UVC [336, 340, 341] malgré le fait que certains ont observé un retardement dans les stades précoces de la réparation [342, 343]. Par contre, la viabilité réduite des fibroblastes humains déficients en PARP1 après irradiation aux UVC [339] peut être considérée comme une preuve de l'implication de la PARP1 dans la NER. Cette étude est appuyée par l'observation que l'inhibition de la PARP1 par la surexpression de son domaine de liaison à l'ADN [344] ou par utilisation des inhibiteurs spécifiques [345], diminue la vitesse de réparation des CPD dans les cellules de hamster et les cellules BRCA1 $^{-/-}$, déficientes dans la NER [346, 347]. Des études préliminaires réalisées dans notre laboratoire montraient une réduction de la cinétique de réparation des dommages directs à l'ADN induits par irradiation dans deux modèles: des souris sans poils irradiées aux UVB après inhibition de la PARP1 par l'inhibiteur chimique DHQ et des fibroblastes de peau humains synchronisés en G1 et irradiés aux UVC en absence de la PARP1 [348, 349]. Malgré toutes ces nombreuses observations, aucun rôle direct de la PARP1 dans la réparation des dommages par la NER n'a été établi. Enfin, des études *in vitro*

et in silico montrent que des protéines de la NER, e.g. les XPC, DDB1, CSB et XPA, ont des domaines de liaison des PAR [252, 350, 351]. La PARylation de la CSB, après le traitement de cellules avec de l'H_2O_2, diminue son activité ATP-ase [350].

En conclusion, la PARP1 et la PARylation jouent des rôles clés dans la réparation de l'ADN endommagé, comme la signalisation des dommages, le remodelage de la chromatine et le recrutement des facteurs de réparation, contribuant ainsi au maintien de l'intégrité du génome et à la survie cellulaire. Il n'est donc pas étonnant que l'inhibition de son activité catalytique soit devenue une cible de choix pour améliorer l'efficacité des thérapies anti-cancéreuses.

1.5.4.5 La PARP1 et la thérapie du cancer

Une des caractéristiques des cellules cancéreuses est l'instabilité génétique. Pour plusieurs cancers il y a un lien direct entre l'instabilité génétique et une voie de réparation défectueuse. Par exemple, des mutations dans des gènes codant pour des protéines de la voie HR, sont liées au développement de 37-52% des cancers d'ovaire de haut grade [352]. Ces défauts dans les voies de réparation sont ciblés par plusieurs thérapies anti-cancéreuses qui exploitent la vulnérabilité des cellules cancéreuses aux agents qui endommagent l'ADN.

Les nombreuses fonctions de la PARP1 dans la réparation de l'ADN, mais surtout son rôle dans la réparation des cassures simple-brin ont été initialement ciblées pour augmenter l'action cytotoxique des agents anticancéreux (témozolomide, cisplatine, camptothécine) [353]. En 2005, après la publication simultanée par deux groupes des résultats montrant que l'inhibition de l'activité catalytique de la PARP tue sélectivement les tumeurs déficientes en BRCA1/2 [354, 355], le développement des inhibiteurs de la PARP1 a connu un essor important. Ces observations ont été suivies par la démonstration que les tumeurs ayant des mutations dans d'autres protéines de la voie HR étaient aussi hypersensibles aux inhibiteurs de la PARP, probablement en raison de l'augmentation de l'instabilité génétique [356]. Une centaine d'essais cliniques utilisent présentement des inhibiteurs de la PARP en monothérapie ou en combinaison avec des agents chimio- ou radio-

thérapeutiques (https://clinicaltrials.gov), la plupart ciblant des cancers avec des mutations génétique ou fonctionnelle pour BRCA1/2.

Cependant, le mécanisme derrière ce phénomène appelé létalité synthétique n'est toujours pas connu [357]. La létalité synthétique décrit une situation qui a lieu lorsque la perte ou la mutation simultanée des deux gènes ou protéines est fatale alors que la mutation/perte d'un seul de ces deux gènes n'est pas létale. Initialement, il a été proposé que l'inhibition de la PARP empêche la réparation des cassures simple-brin qui seront converties en cassures double-brin lors de la réplication. Dans les cellules de type sauvage, ces dommages sont réparés alors qu'ils sont fatals pour les cellules déficientes en BRCA1/2 [357]. Cependant, plusieurs observations n'étaient pas compatibles avec cette proposition. La déplétion de la PARP1 ou son inhibition n'augmente pas le nombre de cassures simple-brin dans les cellules de phénotype sauvage ou déficientes en BRCA [52, 358]. De plus, la déplétion de la XRCC1, protéine clé de la BER/SSBR, dans les cellules déficientes en BRCA n'affecte pas la survie cellulaire, ce qui suggère que le rôle de la PARP1 dans la BER/SSBR a un impact mineur sur la mort de cellules déficiente en HR [357]. Par conséquent, d'autres mécanismes ont été proposés: (a) Le piégeage de la PARP1 sur l'ADN endommagé. La PARP1 piégée [357] bloquerait l'accès au site du dommage aux facteurs de réparation tel que proposé par Satoh et Lindahl [359]. Ce mécanisme explique pourquoi l'inhibition de la PARP est plus cytotoxique pour les cellules déficientes en BRCA qu'une absence de la PARP1 [52]. (b) Un retardement dans le recrutement de BRCA1. BRCA1 est recruté par deux voies : par l'interaction avec les γH2Ax et via son partenaire BARD1 qui lie des PAR [360]. L'inhibition de la PARP expliquerait la sensibilité des cellules mutées pour BRCA1 mais pas celle des cellules ayant des mutations dans d'autres gènes de la voie HR. (c) L'activation de la NHEJ. Tel que discuté dans le sous-chapitre précédent, les protéines PARP1 et Ku sont en compétition pour la liaison des cassures double-brin [331]. L'inactivation de la PARP mènera à la réparation des cassures double brin par la NHEJ qui favorise l'instabilité génomique et les réarrangements chromosomiques [361]. (d) Diverses combinaisons des mécanismes susmentionnés [353]. Des études supplémentaires seront nécessaires afin de déchiffrer le(s) mécanisme(s) conduisant à la létalité synthétique entre

l’inhibition de PARP et un HR défective, qui devrait prendre en considération les autres membres de la famille PARP et les multiples fonctions cellulaires de la PARP1.

En conclusion, Une meilleure compréhension des fonctions biologiques, physiologiques et pathologiques des PARP sera indispensable pour déterminer laquelle de ces fonctions ou quelle combinaison de ces fonctions explique l’effet observé afin d’améliorer la sélection des tumeurs qui bénéficieraient le plus de l’utilisation des inhibiteurs de PARP et de limiter les problèmes de résistance [362].

Chapitre 2

Contexte et objectifs de la recherche

L'ADN est soumis continuellement aux actions des agents environnementaux et des produits métaboliques qui portent atteinte à son intégrité. Ils peuvent induire de l'instabilité génétique, des mutations, et conduire à la mort cellulaire. Parmi eux, les UV sont considérés comme le carcinogène physique le plus important. La moitié des cancers de la peau d'origine kératinocytaire, les carcinomes baso-et spino-cellulaires (CBC, CSC), se développent dans les zones photo-exposées. Selon les statistiques de la Société Canadienne du Cancer l'incidence des cancers de la peau est équivalente à celles de tous les autres cancers réunis et les CBC et les CSC occupant le premier rang (environ 40%) de tous les nouveaux cas de cancer au Canada [363]. Pour empêcher leur développement, deux réponses cellulaires sont cruciales: la réparation de l'ADN endommagé par les UV et la mort des cellules trop endommagées. Une des enzymes activées par les dommages induits à l'ADN par les UV et ayant un rôle dans ces deux réponses est la PARP1. Mes travaux portent sur le rôle de la PARP1 dans la réparation des dommages directs induits à l'ADN par les UV.

Plusieurs études, en commençant avec celles des années 80, ont démontré l'activation de la PARP1 après l'irradiation des cellules aux UVC et UVB. Par la suite, il a été démontré que la PARP1 reconnaît, lie et est activée par les dommages directs, de type T-T, induits par les UV et réparés par la NER [338]. Cependant, les opinions étaient partagées quant au rôle joué par la PARP1 dans la réparation de ces dommages. Quelques études ont rapporté que la PARP1 et son activité catalytique n'avait aucun effet [336, 340, 342] d'autres ont affirmé qu'elle stimulait [364] ou inhibait la réparation des dommages directs induits par les UV [344, 345]. Par conséquent, des études supplémentaires s'avéraient nécessaires afin de prouver sans équivoque la participation de la protéine PARP1 dans la NER des cellules eucaryotes et de déchiffrer le mécanisme exact par lequel cette protéine influence la réparation des dommages directs causés par les UV.

Notre hypothèse est que la protéine PARP1 par son interaction physique avec des protéines de la NER et/ou par sa capacité à modifier ces protéines par son produit, les PAR, est impliquée dans la détection de l'ADN endommagé par les UV et le recrutement de protéines jouant un rôle dans l'étape de reconnaissance des dommages de la NER.

Pour démontrer cette hypothèse, les objectifs spécifiques de mon doctorat sont :

(1) Analyser si l'effet de la PARP1 sur la cinétique de réparation des photo-lésions est universel.
(2) Analyser l'interaction de la PARP1 avec des protéines de la NER et vérifier le rôle de l'activité de la PARP1 dans ces interactions.
(3) Identifier les protéines acceptrices de PAR parmi les protéines de la NER.
(4) Montrer le recrutement de la PARP1 au niveau du site des dommages induits par les UV *in vivo*.

Chapitre 3

Role of poly(ADP-ribose) polymerase-1 in the removal of UV-induced DNA lesions by nucleotide excision repair

Mihaela Robu, Rashmi G. Shah, Nancy Petitclerc, Julie Brind'Amour[1], Febitha Kandan-Kulangara and Girish M. Shah[*]

Laboratory for Skin Cancer Research, CHUL (CHUQ) Hospital Research Centre of Laval University, Laval University, Québec (QC) Canada G1V 4G2

[1]Present address: Terry Fox Laboratory, Vancouver (BC) Canada V5Z 1L3

*Corresponding Author: GM Shah (418) 656 4141/x48259, e-mail: girish.shah@crchul.ulaval.ca

3.1 Avant-propos

Lorsque j'ai amorcé mes études, le rôle de la PARP1 dans la réparation de dommages directs induits à l'ADN par les rayons ultraviolets était un sujet controversé. Les résultats préliminaires obtenus pendant ma maîtrise indiquaient que la PARP1 stimulait la réparation des dommages directs du génome des fibroblastes humains synchronisés en G1. Afin de déchiffrer le mécanisme d'action de la PARP1, nous avons cherchés ses partenaires parmi les protéines de la phase de reconnaissance des dommages de la NER. La caractérisation de l'interaction entre la PARP1 et une de ces protéines, le facteur DDB2, après irradiation aux UVC a fait l'objet d'un article publié en janvier 2013 dans la revue *Proceeding of the National Academy of Sciences of the United States of America*, lequel est disponible en version PDF à l'annexe 1 de cette thèse.

Les techniques que j'ai mises au point pendant ma maîtrise (l'analyse de la réparation de l'ADN par cytométrie en flux et par immunofluorescence, le fractionnement cellulaire), nous ont permis de démontrer le rôle stimulateur de la PARP1 dans la réparation des dommages directs induits par les UV (Figures 3.1A et C-E). L'effet inhibiteur de la PARP1 sur la réparation des CPD après l'inactivation de son activité catalytique dans la peau des souris avait été observé par Julie Brind'Amour (Figure 3.1B) avant mon arrivée dans le laboratoire du Dr Shah. Je suis également l'auteure des immunoprécipitations montrant l'interaction de la PARP1 avec le facteur DDB2 et la modification de DDB2 avec des PAR *in vivo* (Figure 3.2C, 3.3A, 3.4C, S3.1D-E), des essais d'immunofluorescence montrant le recrutement de myc-DDB2 (Figure S3.2D) et de la XPC (Figure 3.4E) aux dommages et des fractionnements cellulaires montrant la cinétiques de formation des PAR et le recrutement des protéines de la NER à la chromatine (Figures 3.2A, E, 3.3E, 3.4A, F, S3.3E). Rashmi Shah a réalisé les essais *in vitro* montrant la stimulation de l'activité de PARP1 par le DDB2 (Figures 3.3C, D, F et S3.3 B-D), la PARylation du DDB2 *in vitro* (Figures 3.3B et S3.3A) et leur interaction (Figures 3.2B, 3.2D et 3.4B). Nancy Petitclerc a caractérisé l'interaction entre la PARP1 endogène et le DDB2 exogène couplé à une étiquette myc (Figures S3.2 A-C, E). Les clones GMRSiP exprimant une PARP1 exogène couplée à une étiquette FLAG dans des cellules rendues déficientes en PARP1 endogène par interférence à l'ARN, utilisées dans les

Figures 3.2B, 3.2D et S3.1B ont été créés par Febitha Kandan-Kulangara. En tant que première auteure, j'ai participé à la rédaction du manuscrit, à sa révision et j'ai fait le montage des figures.

3.2 Résumé

Une des réponses précoces des cellules de mammifères aux dommages à l'ADN est l'activation catalytique de l'enzyme nucléaire poly(ADP-ribose) polymérase-1 (PARP-1). La PARP-1 activée forme des polymères d'ADP-ribose (pADPr ou PAR) qui modifient post-traductionnellement des protéines cibles, telles que la PARP-1 elle-même et des protéines de réparation de l'ADN. Bien que ce métabolisme soit connu pour être impliqué dans plusieurs voies de réparation, ici, nous montrons son rôle dans la voie versatile de réparation par excision de nucléotides (NER) qui élimine une grande variété de dommages à l'ADN, y compris ceux induits par les UV. Nous montrons que l'inhibition de la PARP ou la déplétion spécifique de la PARP-1 diminue l'efficacité de réparation des lésions d'ADN induites par les UV du génome de fibroblastes de peau humaine ou de l'épiderme de souris. En utilisant des cellules compétentes et déficientes en NER et des essais *in vitro* nous montrons que le facteur DDB2, une protéine clé de la phase de reconnaissance des lésions de la sous-voie de réparation globale du génome de la NER (GG-NER), s'associe à la PARP-1 sur la chromatine après irradiation aux UV, stimule son activité catalytique et est modifiée par des pADPr. L'inhibition de la PARP supprime l'interaction du DDB2 avec PARP-1 ou la XPC et diminue la localisation de la XPC à l'ADN endommagé par les UV, qui est l'étape clé menant aux étapes situées en aval de la GG-NER. Ainsi, la PARP-1 collabore avec le DDB2 pour augmenter l'efficacité de l'étape de reconnaissance des lésions de la GG-NER.

3.3 Abstract

Among the earliest responses of mammalian cells to DNA damage is catalytic activation of a nuclear enzyme poly(ADP-ribose) polymerase-1 (PARP-1). Activated PARP-1 forms the polymers of ADP-ribose (pADPr or PAR) that post-translationally modify its target proteins, such as PARP-1 and DNA repair related proteins. While this metabolism is known to be implicated in other repair pathways, here, we show its role in the versatile nucleotide excision repair pathway (NER) that removes a variety of DNA damages including those induced by UV. We show that PARP inhibition or specific depletion of PARP-1 decreases the efficiency of removal of UV-induced DNA damage from human skin fibroblasts or mouse epidermis. Using NER-proficient and deficient cells and *in vitro* PARP-1 assays, we show that DDB2, a key lesion recognition protein of the global genomic sub-pathway of NER (GG-NER), associates with PARP-1 in the vicinity of UV-damaged chromatin, stimulates its catalytic activity and is modified by pADPr. PARP inhibition abolishes UV-induced interaction of DDB2 with PARP-1 or XPC, and also decreases localization of XPC to UV-damaged DNA, which is a key step that leads to downstream events in GG-NER. Thus, PARP-1 collaborates with DDB2 to increase the efficiency of the lesion recognition step of GG-NER.

3.4 Introduction

Mammalian cells respond very rapidly to different types of DNA damage by activation of an abundant and ubiquitous nuclear enzyme poly(ADP-ribose) polymerase-1 (PARP-1). The activated PARP-1 utilizes NAD^+ to form polymers of ADP-ribose (pADPr or PAR) which modify PARP-1 itself and selected target proteins, such as histones and DNA repair proteins [365]. This post-translational modification, i.e., PARylation has been implicated in cellular responses ranging from DNA repair to cell death. Among mammalian DNA repair pathways, PARP-1 has been implicated in the base excision repair, homologous recombination and non-homologous end-joining pathways [304, 366], but we do not know its role in the most versatile nucleotide excision repair (NER) pathway that removes a wide variety of DNA lesions including UV-induced thymine dimers (T-T) and other cyclobutane pyrimidine dimers (CPD) as well as 6-4 photoproducts (6-4PP) [68].

The core mammalian NER pathway uses more than 30 proteins to recognize the damaged site on DNA, remove 24-32 nucleotides long single-stranded DNA containing the lesion, fill the gap using the non-damaged strand as a template and finally ligate the nick [68]. There are two sub-pathways of NER: the transcription-coupled NER (TC-NER) removes lesions from the actively transcribed strands of the genes; and the global genomic NER (GG-NER) repairs lesions from the entire genome. These two pathways differ in the initial step of lesion recognition: TC-NER is initiated when elongating RNA polymerase II stalls at the lesion, whereas GG-NER is initiated when the lesion is recognized in the chromatin context by DDB2 (XPE), which through its participation in UV-DDB-E3 ligase complex ubiquitinates and localizes the key GG-NER protein XPC to the damaged site [146, 186, 367].

Although the roles for different core NER proteins have been well-characterized with bacterial and yeast model systems, we still cannot fully explain the accuracy and rapidity with which mammalian NER is targeted to a very few damaged bases that are surrounded by a large number of unmodified bases in chromatin. In this context, some of the post-translational modifications, such as phosphorylation, acetylation, ubiquitination and

sumoylation are known to help different steps of NER [368]. Here, we examined whether PARylation that occurs rapidly after PARP-1 is activated by UV-induced DNA lesions [338], could be involved in improving the efficiency of mammalian NER. Earlier studies examined the effect of impaired PARP-1 function on mammalian NER but obtained contradictory results [345, 369, 370], because the repair of UV-induced CPD was unaffected by PARP inhibition in HeLa cells [369] whereas it was reduced in trans-dominantly PARP-1 inhibited CHO cells [370] or in the PARP-1 impaired triple negative breast cancer cell lines [345]. In view of other confounding factors such as DNA repair defects in CHO or breast cancer cells, we used RNAi or PARP inhibition approaches in multiple mammalian NER proficient models to show that PARP-1 is required for an efficient removal of UV-induced T-T and 6-4PP from genomic DNA. We also show that the catalytic activity of PARP-1 in collaboration with DDB2 leads to an improved function of DDB2 and XPC during the lesion recognition step of mammalian GG-NER.

3.5 Results

PARP inhibitors delay removal of UV-induced DNA lesions

To explore the role of catalytic activation of PARP-1 in NER, we first examined the effect of PARP inhibitor PJ-34 on the efficiency of removal of UVC-induced T-T or 6-4PP from genomic DNA of two different human skin fibroblasts using a flow cytometry based assay [371] (Fig. 3.1A). In this assay, the histograms for T-T or 6-4PP at early time points after irradiation (5-15 min) represent initial damage, and movement of histograms at later time points (6-63h) towards untreated cells represents the extent of repair. In the SV-40 immortalized GMU6 human skin fibroblasts, a significant removal of T-T at 24h was seen only in the normal but not in the PJ-34 treated cells (Fig. 3.1A, left panel). The quantification of average T-T signal confirmed that 43% damage removed by 24h from normal GMU6 cells was significantly more than 27% damage removed by PJ-34 treated cells ($n=4-7$, $P<0.05$). Next, we examined the effect of PJ-34 on the capacity of hTert-immortalized BJ-EH2 human foreskin fibroblasts to remove UVC-induced T-T and 6-4PP lesions up to 63h and 6h, respectively (Fig. 3.1A, middle and right panels). Unlike normal BJ cells that removed all

the T-T signal by 63h, PJ-34 treated cells removed significantly less (50%) damage, which was further confirmed by quantifying average T-T signal from multiple assays (n=6, $P<0.05$). For removal of 6-4PP lesions, while the final repair by 6h was not affected, the early phase of removal of damage at 1h was significantly suppressed by PJ-34; and quantification of signal confirmed that 45% of damage removed by normal BJ cells was significantly more than 20% damage removed by PJ-34 treated cells (n=3, $P<0.01$). Lastly, the removal of UVB-induced T-T from epidermis of SKH-1 hairless mice was also reduced up to 48h by PARP inhibitor 1,5-dihydroxyisoquinoline (Fig. 3.1B). Thus, PARP inhibitors significantly decreased the efficiency of removal of UV-induced DNA photolesions in multiple models.

PARP-1 depletion decreases efficiency of removal of UV-induced DNA damage

PARP inhibitors affect activity of all the members of PARP family, hence we examined whether the effect of PARP inhibition on repair of UV-damaged DNA was due to its effect on PARP-1 or on other PARPs. We used GMSiP human skin fibroblasts, in which PARP-1 has been stably and significantly depleted by shRNA without affecting the expression of PARP-2 [372]. We assessed their capacity to: (a) form PAR in response to UVC; and (b) repair the UVC-induced T-T lesions. In the pADPr-immunoblot, a strong signal for heterogeneous bands of PARylated proteins above 116 kDa [373] could be seen in the matched PARP-1 replete GMU6 cells but not in the GMSiP cells (Fig. 3.1C), confirming that PARP-1 is the major, if not the only producer of pADPr in UV-treated cells. Using flow cytometry assay, we noted a marked failure of GMSiP cells to remove T-T from 15 min to 24h (Fig. 3.1D), which is in stark contrast to a significant repair seen in GMU6 cell (Fig. 3.1A, left panel). To exclude the possible differences in the cell cycle phases influencing the repair capacity of these cells [371], we synchronized GMU6 and GMSiP cells in G1 phase and compared their time-course of removal of T-T up to 24h by flow cytometry (Fig. 3.1E) and immunofluorescence microscopy (Fig. 3.1F). By both the techniques, we observed that PARP-1-depleted cells were inefficient at removal of T-T damage. The quantification of T-T signal from flow-cytometry assays confirmed that while GMU6 cells removed 54% of the initial damage, GMSiP cells barely removed any damage (~2%) (n=3, $P<0.01$). The immunofluorescence microscopy confirmed this trend because GMU6 cells removed 58% of

the T-T signal per nuclei by 24h as compared to 15% damage removed by GMSiP cells ($n>125$ nuclei, $P<0.01$). Since PARP-1 depletion was sufficient to abolish UV-induced PAR synthesis and impair repair of UV-induced DNA damage, similar to that seen in PARP inhibited cells, PARP-1 is likely to be the main PARP implicated in this repair process.

Characterization of UV-induced interaction between PARP-1 and DDB2

We had earlier shown that PARP-1 rapidly binds to UV-damaged DNA *in vitro* or in UV-irradiated cells, and it is activated to form PAR within seconds after irradiation at the site of DNA damage [338]. Since DDB2, the early GG-NER protein, is also known to translocate very rapidly at the site of UV-damaged DNA [374], we examined by co-immunoprecipitation (co-IP) studies whether DDB2 and PARP-1 interact with each other in the vicinity of UV-damaged chromatin using cellular fractions that represent chromatin-bound proteins (Ch-fraction) rather than the whole cell extract (Fig. S3.1A). The cell fractionation technique to isolate Ch-fraction was validated by confirming the expected UV-induced relocalization of DDB2 to this fraction in both NER-proficient GM637 and NER-deficient XP-C cells (Fig. 3.2A, 4, 8 and 12), although total cellular DDB2 levels remained unchanged before and after irradiation (Fig. 3.2A, 1, 5 and 9). We further confirmed that UV irradiation promoted the recruitment of downstream NER proteins XPC and XPA to the Ch-fraction of GM637 cells, whereas XP-C cells did not relocalize XPA to the Ch fraction (Fig. 3.2A). For the IP studies, we used GMRSiP cells that express FLAG-tagged human PARP-1 (Fig. S3.1B-C). The IP of Ch-extracts (input) of these cells prepared before or 10 min after UVC irradiation with PARP-1 antibody revealed a significant UV-induced association of DDB2 with PARP-1, which was confirmed in an inverse co-IP with DDB2 antibody (Fig. 3.2B, lanes 4 and 8). Mock IPs with control IgGs confirmed specificity of antibody-based IPs (Fig. S3.1D). To determine if the interaction between these two proteins is direct or mediated via DNA, DDB2-IP was carried out in the presence of 200 µg/ml ethidium bromide to loosen the protein-DNA interactions. The failure of ethidium bromide to prevent co-IP of PARP-1 with DDB2 indicated a direct interaction between these two proteins (Fig. 3.2C, and mock control Fig. S3.1E).

To determine the possible role of catalytic activation of PARP-1 in this interaction, the GMRSiP cells were irradiated in the presence or absence of PARP-inhibitor PJ-34. The FLAG-IP of Ch-fractions before or after irradiation confirmed UV-induced interaction of DDB2 and PARP-1 without PARP inhibitor (Fig. 3.2D, DDB2-lane 4). Interestingly, while PJ-34 treatment did not prevent UV-induced accumulation of DDB2 in the input Ch-fraction prior to IP, it significantly suppressed its ability to associate with PARP-1 (Fig. 3.2D, DDB2-lanes 6 and 8). In an independent model of GMU6 cells expressing mycDDB2 (Fig. S3.2A-C), we confirmed by local UVC irradiation (Fig. S3.2D) and co-IP of Ch-fractions with PARP-1 or myc antibodies (Fig. S3.2E) that PARP-inhibitor PJ-34 did not affect early accumulation of mycDDB2 but blocked its co-IP with PARP-1. We examined whether PARP-inhibitor that disrupts the interaction between DDB2 and PARP-1 also affects the departure of DDB2 from the damaged site, which is a necessary step for the continuation of GG-NER [375]. Immunoblotting for DDB2 in the Ch-fractions isolated up to 2h after irradiation revealed that DDB2 levels which accumulated from 5-15 min declined rapidly by 60 min in the normal cells, but remained high until 120 min in PARP inhibited cells (Fig. 3.2E). Thus, although the initial recruitment of DDB2 to UV-induced chromatin is independent of PARP-1, its subsequent direct association with PARP-1 as well as its eventual departure from the damaged site is dependent on the catalytic activity of PARP-1 that would PARylate proteins near the damaged DNA.

DDB2 stimulates catalytic activity of PARP-1 and becomes a target for PARylation

The influence of catalytic activity of PARP-1 on DDB2 prompted us to examine whether DDB2 is PARylated in response to UV (Fig. 3.3A-B). First, the pADPr-IP of GMU6-mycDDB2 cells pulled down more of mycDDB2 after UVC-exposure, indicating that it is either PARylated or interacts with other PARylated proteins (Fig. 3.3A). That DDB2 could be directly PARylated was tested in an *in vitro* Dot-blot assay, which showed that pADPr could bind to mycDDB2 (Fig. 3.3B, top panel). The binding of pADPr to its known acceptors PARP-1 and XPA [376] served as positive controls. To confirm that the recipient of pADPr was indeed the designated protein in the immunopurified mycDDB2 preparation, we ran a SouthWestern type of blot in which immunopurified mycDDB2 and purified GST-

DDB2 were resolved on SDS-PAGE, blotted and reacted with pADPr (Fig. 3.3B, bottom panel). The mycDDB2 and purified GST-DDB2 displayed one major pADPr-accepting band at 50 or 75 kDa, which corresponds to their respective bands in the DDB2 immunoblots. A strong signal for PARylated PARP-1 at 113 kDa was a positive control, and lack of pADPr binding by proteinase K (Fig. 3.3B) or DNase I and anti-myc antibody (Fig. S3A) served as negative controls. Thus, DDB2 is an acceptor of pADPr.

We next examined whether interaction of DDB2 with PARP-1 has any influence on the activity of PARP-1. In an *in vitro* PARP-1 activation assay [373], we first observed using bovine PARP-1 and non-labeled NAD (Fig. S3.3B) or immunopurified human FLAG-PARP-1 and biotinylated NAD (Fig. S3.3C) that the catalytic activation of PARP-1 by UV-damaged DNA was stimulated in the presence of mycDDB2, as seen from a heterogeneous smear above 113 kDa for PARylated PARP-1. Moreover, the effect of DDB2 on stimulating PARP-1 activation and formation of pADPr-modified PARP-1 was more pronounced with UV-damaged DNA than with the unirradiated DNA (Fig. 3.3C, lanes 2-3). Interestingly, the PARylation of myc-DDB2 (50 kDa) was evident from the smearing of signal between 50-75 kDa in both pADPr and myc-blots in this reaction (lane 3). Controls show that PJ-34 suppressed PARP-1 activation (lanes 4-6) and mycDDB2 could not activate PARP-1 without DNA (lane 1). A dose-response for purified GST-DDB2 in the assay showed that ~1/12th amount of GST-DDB2 gave an optimum activation of PARP-1, i.e., 67 pmol GST-DDB2 for 860 pmol PARP-1 per assay (Fig. 3.3D and Fig. S3.3D).

Next, we examined whether the interaction with DDB2 stimulates activity of PARP-1 in UV irradiated cells. In the pADPr immunoblot, the signal for PARylated proteins in the first 60 min after UVC irradiation was extremely weak in DDB2-deficient XP-E cells as compared to DDB2-replete GMU6 cells (Fig. 3.3E), although PARP-1 levels were comparable in both the cell types (Fig. S3.3E). This deficiency could be rescued in XP-E cells by transient transfection of mycDDB2 expression vector, because despite being irradiated with UVC at the same time, the XP-E cells that did not express transfected mycDDB2 (non-red nuclei) showed a basal level of pADPr synthesis (green signal), which was significantly stimulated in the cells that expressed mycDDB2 (red nuclei) (Fig. 3.3F and

chart). The PJ-34 treatment abolished this additional pADPr synthesis. Collectively these results indicate that DDB2 stimulates the catalytic activity of PARP-1 by UVC-damaged DNA and in turn, PARP-1 PARylates DDB2.

XPC and the interaction of PARP-1 with DDB2

To determine whether XPC that is known to co-IP with DDB2 [146] plays a role in PARP-1 and DDB2 interaction, we used XP-C cells because they could recruit DDB2 to the damaged DNA but not XPA and other downstream GG-NER proteins due to non-functional XPC (Fig. 3.2A). Since PARP-1 activation and pADPr synthesis played a key role in DDB2-PARP-1 interaction, we first examined whether XP-C cells could make pADPr in response to UVC. The time course of pADPr immunoblot revealed that the appearance and extent of PARylated proteins in UV-irradiated XP-C and NER-proficient GM637 cells was comparable (Fig. 3.4A). Using co-IP studies in XP-C cells for PARP-1 (Fig. 3.4B) or pADPr (Fig. 3.4C), we observed that UVC-irradiation promoted an interaction between PARP-1 and DDB2 (Fig. 3.4B) and caused direct or indirect PARylation of DDB2 (Fig. 3.4C). Since these interactions were not as robust as in normal cells (Fig. 3.2B-C and Fig. 3.3A), our results indicate that there may be an XPC-dependent and independent interaction between PARP-1 and DDB2.

Since PARP inhibitor disrupts the interaction between DDB2 and PARP-1 and blocks the departure of DDB2 from the UV-damaged DNA, we determined whether it would also affect the downstream actions of DDB2, such as its interaction with XPC or modification and stabilization of XPC to UV-damaged DNA [146, 367]. Using DDB2-IP of GMU6 cells, we observed that PJ-34 significantly suppressed UV-induced association of DDB2 with XPC (Fig. 3.4D, lanes 6 and 8). Moreover, a slowly migrating heterogeneously modified XPC, often characterized as ubiquitinated XPC [146], was significantly increased in response to UV and suppressed in the PJ-34 treated cells (Fig. 3.4D, lanes 6 and 8). A possible consequence of this effect of PARP inhibition was evident on the recruitment and stabilization of XPC at the site of DNA damage after local UVC irradiation. In the normal GMU6 cells, the signal for XPC colocalized with subnuclear T-T by 10 min and sharply

intensified by 30 min. In the PJ-34 treated cells, XPC was weakly localized with T-T at 10 min, and failed to focus properly by 30 min (Fig. 3.4E). The quantification of XPC and T-T in the subnuclear spots revealed that PARP inhibition significantly reduced the colocalization of XPC with T-T (Fig. 3.4E, chart). This was further confirmed by effect of PARP inhibitor on the presence of XPC in Ch-fractions of UV-irradiated GMU6 cells (Fig. 3.4F). In the normal cells, the XPC levels gradually declined from the peak values at 5-15 min up to 4h, whereas in PARP inhibited cells, XPC levels declined rapidly by 30-60 min. In addition, the band for modified XPC was significantly increased from 5-15 min in the normal cells but not in the PJ-34 treated cells (Fig. 3.4F). Thus, PARP inhibition disrupted the interaction of XPC with DDB2 and decreased its stabilization at the lesion site.

3.6 Discussion

We show that in response to UV irradiation, PARP inhibited cells have: (a) an impaired capacity to remove UV-induced DNA photolesions; (b) a decreased level of interaction of DDB2 with XPC or PARP-1; (c) an increased tendency for DDB2 to persist at the UV-damaged chromatin; and (d) a decreased level of recruitment, modification and localization of XPC to the damaged site. In addition, we show that: (e) DDB2 and PARP-1 directly interact in the vicinity of ~~the~~ DNA lesion; (f) DDB2 stimulates catalytic activity of PARP-1; and (g) DDB2 is modified by PAR. Our results strongly indicate that PARP-1 is the principle player in above responses, because cells specifically depleted of PARP-1 do not form detectable amounts of PARylated proteins in response to UV, and are also inefficient at repair of UV-damaged genomic DNA. Our results are consistent with earlier reports that impaired PARP-1 function increases UV-induced skin cancer in mice [377], decreases cellular capacity to repair UV-induced DNA damage from viral reporter gene [378] or genomic DNA of CHO or triple negative breast cancer cells [345, 370], and decreases the clonogenicity in response to UV [378].

Our results together with previous reports suggest several possible ways in which PARP-1 can collaborate with DDB2 to increase the efficiency of GG-NER. (i) The PARylated PARP-1 or free PAR chains could serve as a scaffold on which PARylated DDB2

can interact with XPC, such as that suggested for their role with XRCC-1 in the base excision repair [379]. Hence, PARP inhibitor or absence of PARP-1 could reduce participation of XPC in NER. (ii) The catalytic activation of PARP-1 and resultant PARylation of DDB2 could promote chromatin remodelling by DDB2. In fact, PARP inhibitor or PARP-1 depletion was recently shown to block chromatin remodelling of UV-damaged chromatin [186]. In addition, the departure of DDB2 from the UV-induced lesion site was shown to be dependent on chromatin remodelling [177], hence our result showing a delayed departure of DDB2 from UV-damaged chromatin in PARP inhibited cells supports an argument that catalytic function of PARP-1 plays a role in DDB2-mediated chromatin remodelling. This would be in agreement with the reported role of PARylated ALC-1 or APLF-1 in stimulating their chromatin remodelling activity in DNA repair [380]. (iii) The catalytic activity of PARP-1 and PAR formed locally around the lesion could be involved in the ubiquitination activity of UV-DDB-E3 ligase complex, just as PARylation of targets has been shown to facilitate their modification by ubiquitin E3 ligase RNF146/ Iduna [379]. The ubiquitination of different proteins by UV-DDB-E3 ligase produces varying end-results, e.g., ubiquitination of its own members DDB2, cullin 4A, and Rbx1 leads to a disengagement of the ligase complex from the damaged site; that of the histones H2A, H3 and H4 leads to chromatin remodelling [177, 381]; and that of XPC helps in its recruitment and stabilization at the damaged site [381]. While previous study has shown chromatin destabilization effect of PARP inhibition [186], here we show its effect on reduced mobility of DDB2 and decreased modification and stabilization of XPC, all of which could be explained by inefficient ubiquitination activity of UV-DDB-E3 ligase complex. (iv) Finally, a strong effect of PARP inhibition in suppression of the initial phase of repair of 6-4PP in BJ-hTert cells could be due to specific influence of PARP-1 activation on NER at a given site of chromatin, because recently ubiquitination of XPC was shown to promote its relocalization from intra- to inter-nucleosomal region to prioritize the repair at the latter site [367].

Based on our results and previous work, we propose a model for the role of PARP-1 and DDB2 at the lesion recognition step of GG-NER (Fig. 3.5). Immediately after UV irradiation, PARP-1, due to its sheer abundance and known capacity to be rapidly activated in response to different types of DNA damage [368], is likely to be one of the first proteins

to arrive at the lesion and be basally activated within seconds of DNA damage (step 1). The arrival of DDB2, which occurs in a similar time frame as PARP-1, will cause a stronger activation of PARP-1, which will result in PARylation of many proteins including PARP-1 and DDB2. This will foster a direct association of DDB2 and PARP-1 that resists separation by ethidium bromide during IP (step 2). Since both proteins are known to independently bind to DNA containing CPD lesions, it is likely that these proteins would interact with the damaged DNA as well as with each other (step 2). One possible scenario to explain the downstream events is that the PARylated DDB2 as part of UV-DDB-E3 complex will remodel the chromatin (step 3A), ubiquitinate DDB2 to reduce its affinity for the lesion (step 3B) and ubiquitinate XPC to promote its stabilization at the damaged site (step 4), which will result in an efficient GG-NER (step 5). As indicated in the model, many of the steps in this model have been shown by us and others [186], implying the role for PARP-1 in collaboration with DDB2 at the lesion recognition step to improve the efficiency of mammalian GG-NER. It will be interesting to examine if PARP-1 also plays other roles in NER.

3.7 Figures and legends

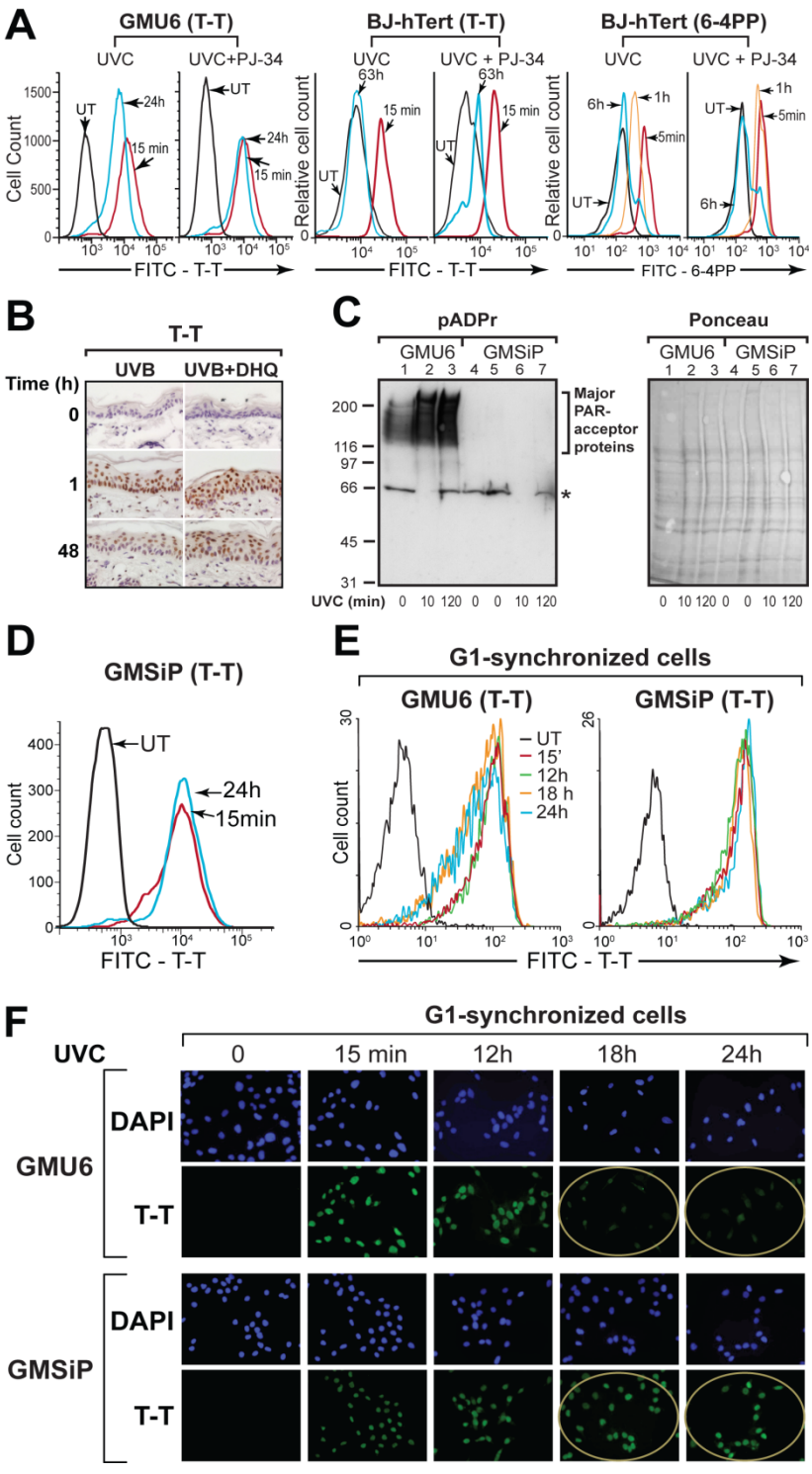

Figure 3.1 Impaired PARP-1 function delays removal of T-T and 6-4PP from genomic DNA.

(**A**) PARP inhibition decreases repair of T-T and 6-4PP. The GMU6 and BJ-hTert fibroblasts were treated with 10 μM PJ-34 (or control) prior to UVC-irradiation at 10 (for T-T) or 30 (for 6-4PP) J/m^2. Repair was monitored before (untreated: UT) or after irradiation at specified times. Representative histograms from one of 4-6 experiments with similar results are shown. (**B**) PARP inhibition delays removal of UV-induced DNA lesions from mouse epidermis. Mice were exposed to 1,600 J/m^2 UVB, and PARP inhibitor DHQ was applied every 3h to inhibit PARP activation up to 12h. Skin was processed for immunohistological analysis of T-T. Data shown here is from one of 4 experiments with identical results. (**C**) PARP-1-depleted GMSiP cells are deficient in formation of pADPr upon UV exposure. The chromatin-bound protein fractions from GMSiP and PARP-1 replete GMU6 cells at specified time after irradiation with 30 J/m^2 UVC were immunoblotted for PARylated proteins, as shown here for one of three experiments with identical results. Asterisk indicates nonspecific reaction with BSA, and Ponceau staining was a loading control. (**D-F**) PARP-1 depletion decreases repair of UV-induced T-T in non-synchronized or in G1 synchronized human skin fibroblasts. GMU6 and GMSiP cells were non-synchronized (panel D) or synchronized in G1 phase with 0.5 μM mimosine (panels E-F) prior to irradiation with 10 (panels D-E) or 100 (panel F) J/m^2 UVC. Repair was monitored at specified times by flow cytometry (panels D-E) or fluorescence microscopy (panel F). Data is from one of 3-4 experiments with similar results.

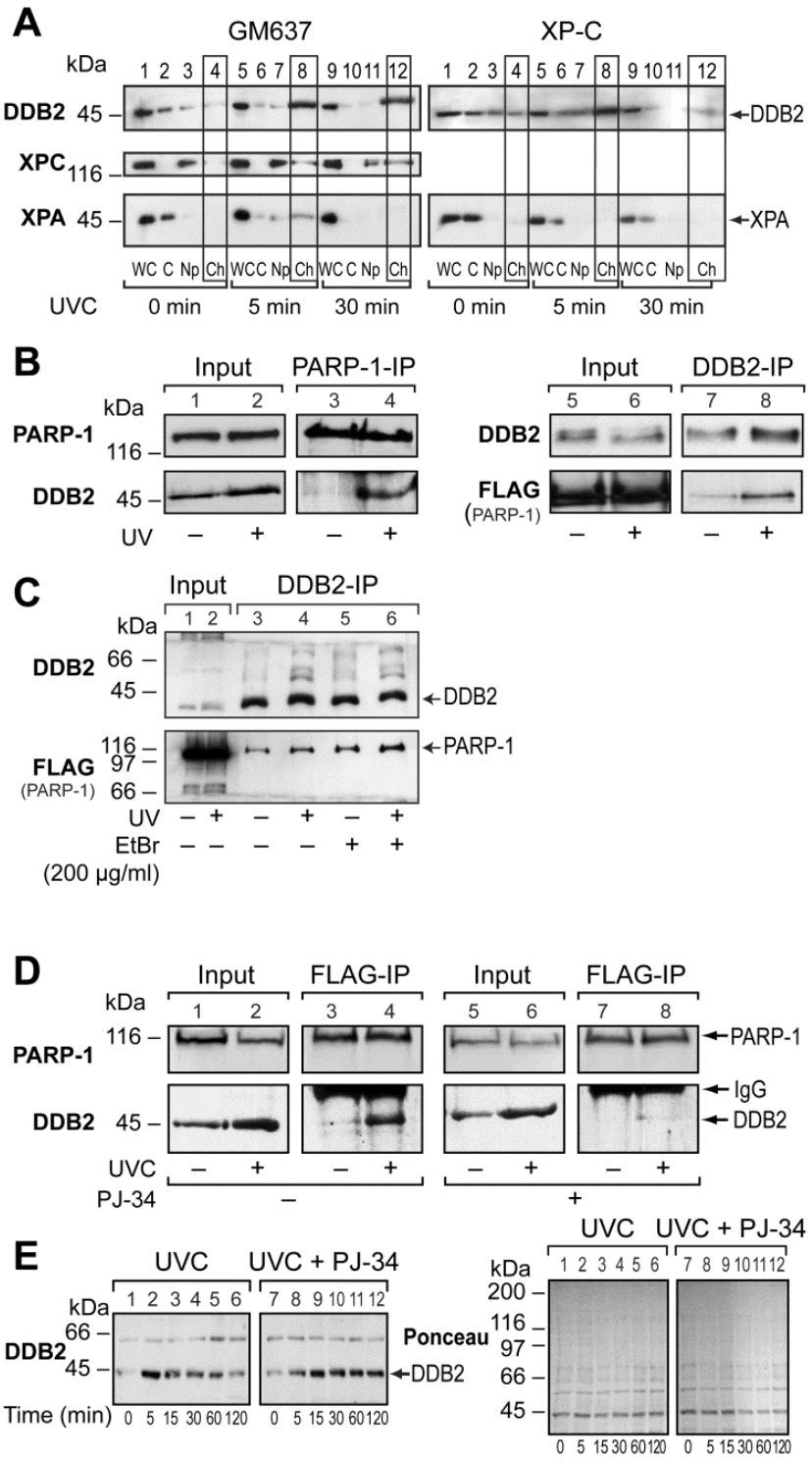

Figure 3.2 Cooperation between PARP-1 and DDB2 at UVC-irradiated chromatin.

(**A**) UVC-induced recruitment of NER proteins to chromatin-bound protein (Ch) fractions. Different cellular fractions (WC: whole cells, C: cytoplasm; Np: nucleoplasm and Ch:

chromatin-bound) prepared from the NER-proficient GM637 and NER-deficient XP-C cells at 0 (unirradiated), 5 and 30 min after UVC-irradiation were immunoblotted for DDB2, XPC and XPA. (**B**) UV-induced association of PARP-1 and DDB2. The co-IPs were carried out with Ch-fractions (input) derived from control or UVC (30 J/m^2) irradiated FLAG-PARP-1 expressing GMRSiP cells with antibodies to PARP-1 or DDB2. Input and IP-eluates were immunoblotted for the presence of PARP-1/FLAG and DDB2. Results are from one of six experiments with identical results. (**C**) Interaction of PARP-1 and DDB2 is not mediated via DNA. The Ch-fractions (input) of GMRSiP cells prepared before or 10 min after exposure to 30 J/m^2 UVC were incubated with or without ethidium bromide prior to and during IP for DDB2, followed by immunoblotting for DDB2 and FLAG-PARP-1. Results are representative of two experiments with identical results. (**D**) PARP inhibitor disrupts co-IP of PARP-1 and DDB2. GMRSiP were treated with 10 μM PJ-34 (or control) prior to UVC irradiation at 30 J/m^2. The Ch-fractions (input) prepared at 10 min after irradiation were subjected to IP for FLAG followed by detection of PARP-1 and DDB2. Data are from one of three experiments with identical results. (**E**) PARP inhibition delays the departure of DDB2. The Ch-fractions isolated from GMU6 cells at specified times after UVC irradiation with 10 J/m^2 (or control) in the presence or absence of 10 μM PJ-34 were immunoblotted for DDB2. Ponceau staining was used as a loading control.

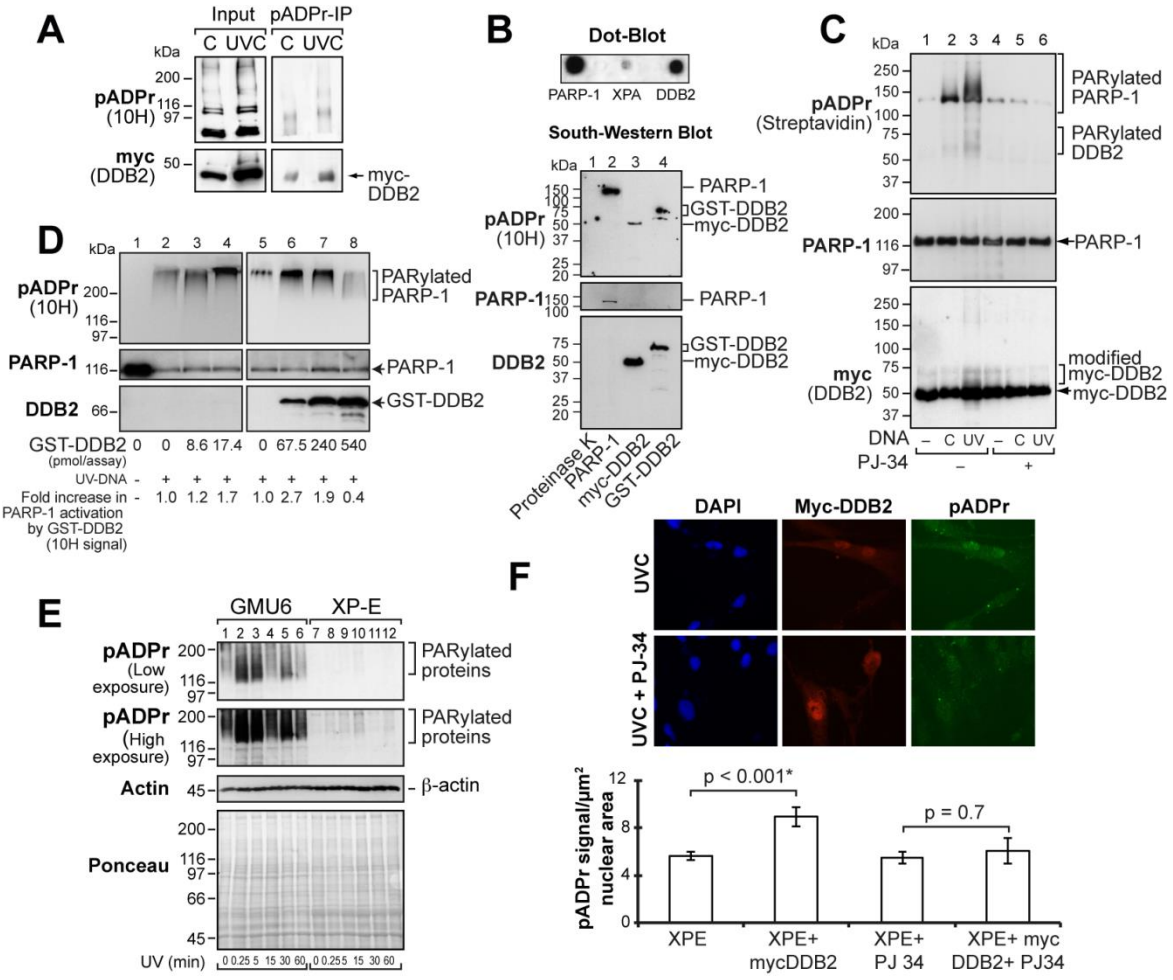

Figure 3.3 DDB2 stimulates PARP-1 activation and is a target for PARylation.

(**A**) The pADPr-IP was carried out with Ch-fractions isolated from GMU6-mycDDB2 cells before or 10 min after exposure to 10 J/m^2 UVC and immunoblotted for PARylated proteins and myc. (**B**) DDB2 binds to pADPr. Top panel: Dot-blot. Purified bovine PARP-1 and immunopurified XPA and DDB2 were spotted and reacted with pADPr prior to immunoprobing for pADPr. Bottom panel: SouthWestern Blot: Immunopurified mycDDB2, purified GST-DDB2, purified bovine PARP-1 and proteinase K were resolved on SDS-PAGE, blotted and reacted with pADPr followed by immunoprobing for pADPr, PARP-1 and DDB2. The results are representative of two experiments with similar results. (**C-D**) DDB2 stimulates catalytic activity of PARP-1 in response to UVC-damaged DNA. *In vitro* PARP-1 activation assays were performed with purified bovine PARP-1, immunopurified

mycDDB2 (panel C) or different amounts of purified GST-DDB2 (panel D), control or UV-irradiated covalently closed circular DNA, untagged or biotinylated NAD and PJ-34, as specified. Aliquots were immunoblotted for PARP-1 (PARP-1), pADPr (10H or streptavidin) and DDB2 (myc or DDB2). Purified GST-DDB2 is undetectable by antibody at lower concentrations and shows minor degradation bands at higher levels. The results are representative of three experiments with similar results. (**E**) XP-E cells are inefficient at forming pADPr upon UV exposure. GMU6 and XP-E cells were irradiated with 10 J/m^2 UVC and whole cell extracts prepared at various times were immunoblotted for pADPr. Actin probing and Ponceau staining served as loading controls. (**F**) DDB2 stimulates catalytic activation of PARP-1 *in vivo*. XP-E cells were transiently transfected with myc-DDB2 expression vector for 24h, treated with 10 μM PJ-34 (or control) prior to irradiation with 10 J/m^2 UVC. Samples were processed at 5 min for immunofluorescent visualization of mycDDB2 (red), pADPr (green) and DNA (DAPI-blue). The chart provides an average pADPr signal per unit nuclear area (Mean + S.E) of XP-E cells that expressed the transfected mycDDB2 or not. The image and chart are derived from the data of multiple nuclei from different fields of two independent experiments.

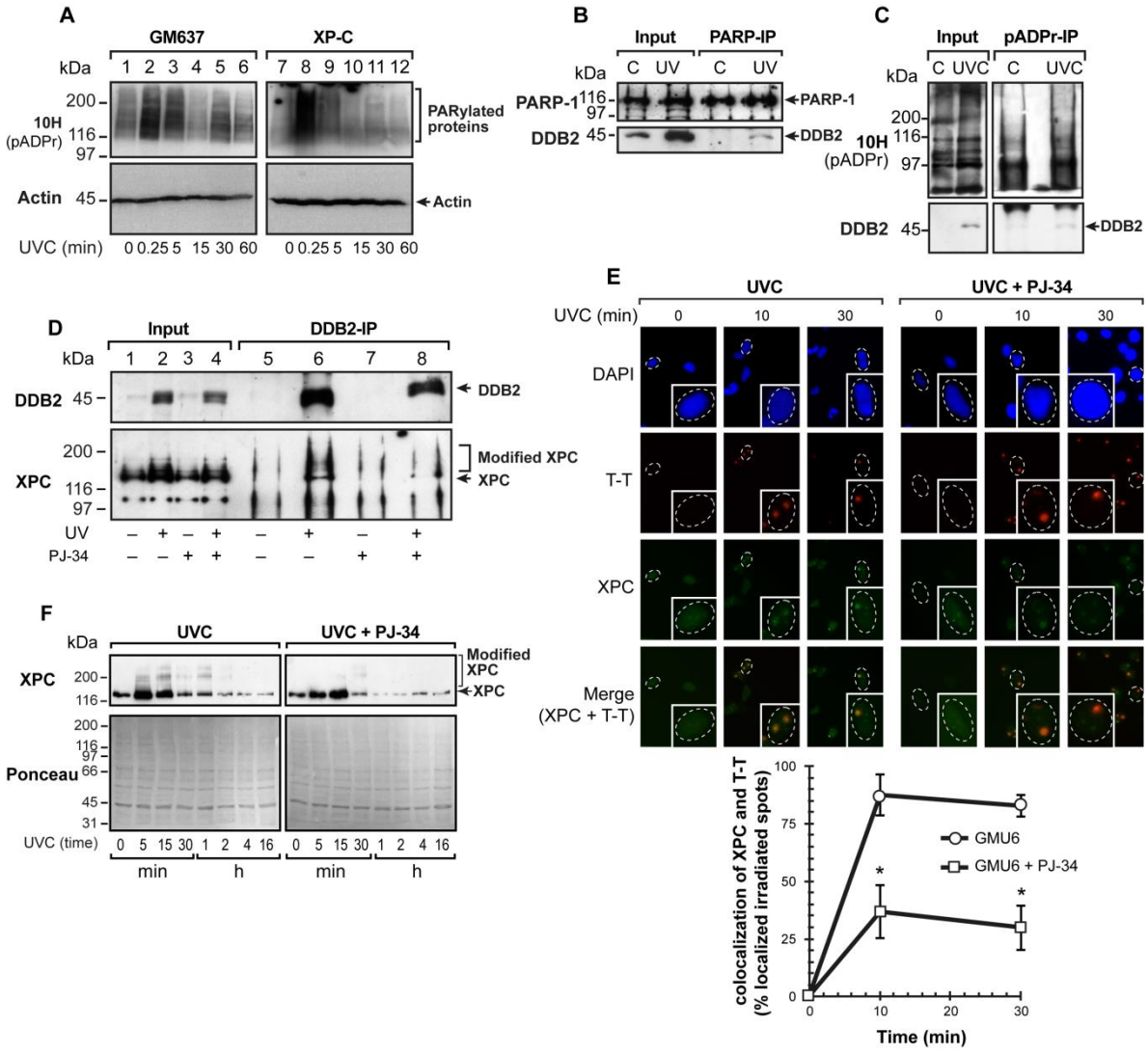

Figure 3.4 Effect of PARP inhibition on XPC-related events in response to UV.

(**A**) UV-induced pADPr synthesis in XP-C cells. GM637 and XP-C cells were irradiated with 10 J/m^2 UVC and whole cell extracts prepared at various time points were immunoblotted for pADPr. Actin was used as a loading control. (**B-C**) UV-induced interaction of PARP-1 with DDB2, and pADPr modification of DDB2 in XP-C cells. The Ch-fractions (input) derived from control or UVC (30 J/m^2) irradiated XP-C cells were subjected to IP for PARP-1 or pADPr, and immunoblotted for PARP-1, pADPr (10H) and DDB2. Results shown here are from one of three experiments with identical results. (**D**) PARP inhibitor disrupts UV-induced co-IP of DDB2 with XPC. GMU6 cells were treated with 10 μM PJ-34 (or control) and Ch-fractions prepared before or 10 min after UVC irradiation at 30 J/m^2 were subjected to IP for DDB2 followed by detection of XPC. Results are representative of 2-3 experiments

with identical results. (**E**) Aberrant XPC localization in PARP-inhibited cells. GMU6 cells were locally irradiated with 100 J/m^2 UVC with or without PJ-34. Immunofluorescence microscopy allowed detection of XPC (green) and T-T (red) in DAPI-stained nuclei. The chart represents the percent of T-T spots, which are also positive for XPC, as pooled from three experiments, each in triplicates (n=100-150 spots, data points are mean $\pm$ SE). (**F**) PARP inhibition decreases UVC-induced modification and stabilization of XPC. GMU6 cells treated with 10 μM PJ-34 (or control) were irradiated with 10 J/m^2 UVC and Ch-fractions prepared at different time points were immunoblotted to detect unmodified and modified forms of XPC. Ponceau staining served as a loading control. Results shown here are from one of four experiments with identical results.

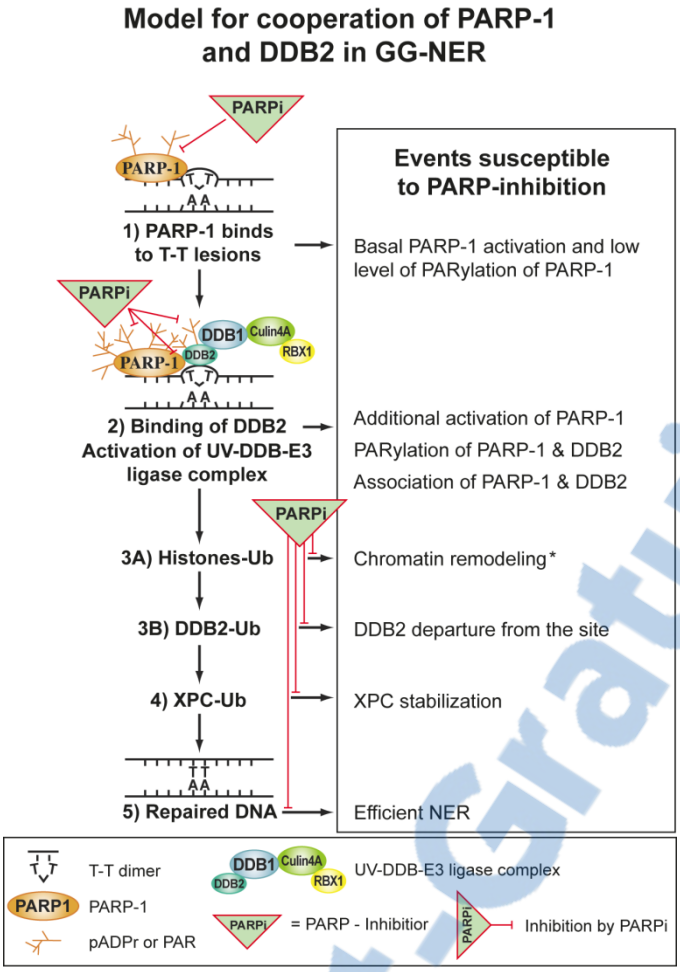

Figure 3.5 Model for cooperation of PARP-1 and DDB2 in GG-NER.

See Discussion for details. Based on the present data and previous study (denoted by *: reference [186]), different NER related end-results that are susceptible to PARP inhibition are indicated in the box.

Supplementary figures

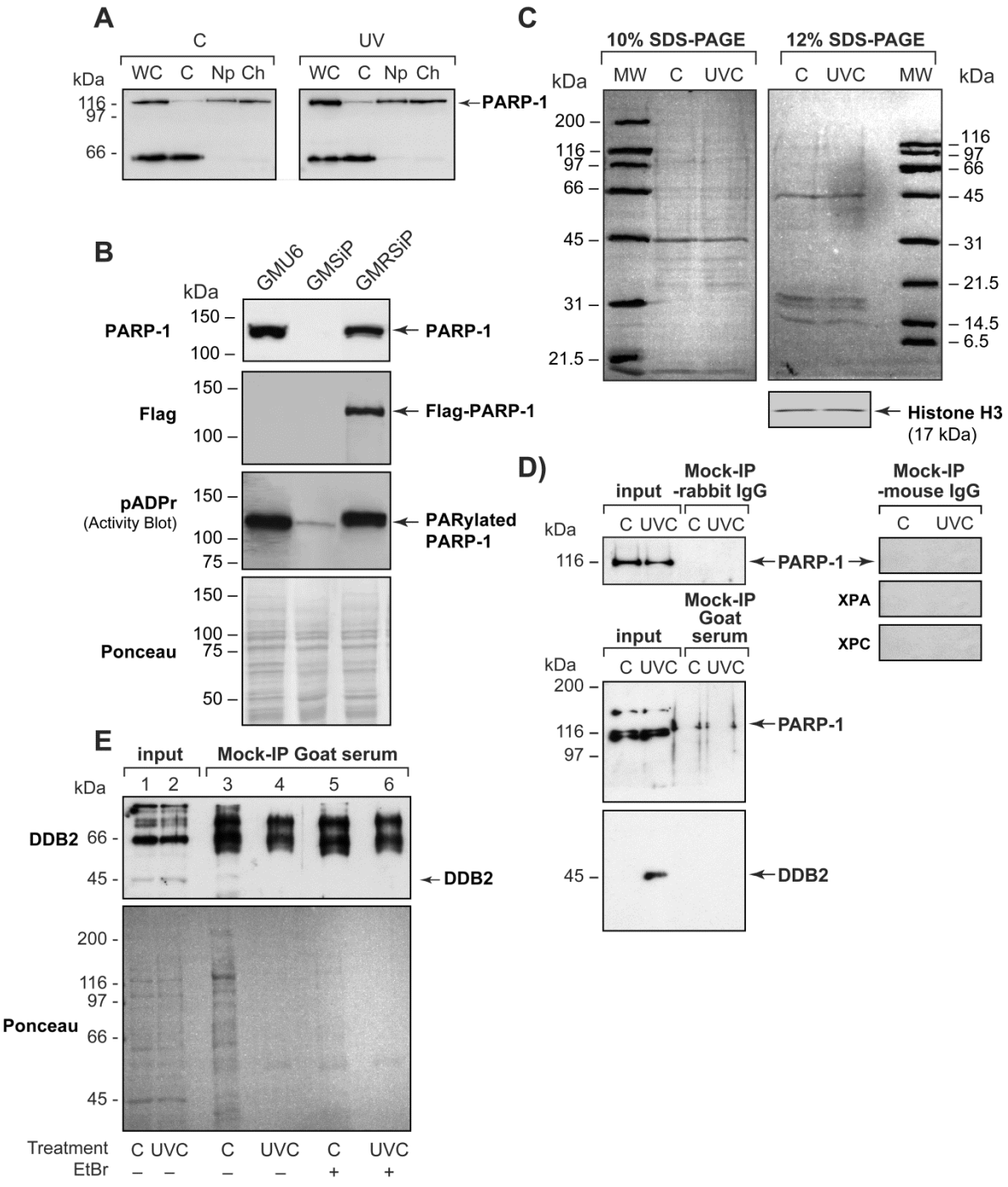

Figure S3.1 Preparation of Ch-fractions, FLAG-PARP1 expressing GMRSiP cells, and controls for IP.

(**A**) Isolation of cell fraction containing chromatin-bound proteins (Ch-fraction). GM637 were irradiated with 30 J/m^2 UVC (or control) and harvested 10 min later to prepare whole cell extracts "WC" which were fractionated to cytoplasmic "C", nucleoplasmic "Np" and chromatin-bound "Ch" fractions as per the protocol in the extended experimental procedures. All fractions were immunoblotted for nuclear PARP-1 and cytoplasmic Beclin-1. (**B**) Creation of FLAG-PARP-1 expressing GMRSiP cells. From the NER proficient GM637 cells, PARP-1 was stably depleted by DNA vector-based RNAi to first create GMSiP cells, whereas GMU6 are its matched pair of PARP-1 replete cells (reference # [372]). GMRSiP cells were created by a stable expression of FLAG-tagged RNAi-resistant hPARP-1 in GMSiP cells. One clone each of GMU6, GMSiP and GMRSiP were immunoblotted to detect the cellular or introduced FLAG-tagged PARP-1. The ability of reintroduced FLAG-PARP-1 to make polymer was verified by PARP-1-Activity blot. Ponceau staining was used as a loading control. (**C**) Verification for equal protein content in the input Ch-fractions of different samples before IP. The protein content of all Ch fractions was estimated by Bradford assay and for all IP studies equalized amounts of Ch-proteins from different samples were taken, as shown here for the blots of pre-IP Ch fractions from control or UV-irradiated GMRSiP cells stained with Ponceau or immunoblotted for histone H3. (**D -E**) Mock IPs with rabbit and mouse IgG, goat serum showed an absence of non-specific pull-down of relevant NER proteins. Where specified, 200 µg/ml ethidium bromide was continuously present from one hour before until final wash steps of IP with goat serum.

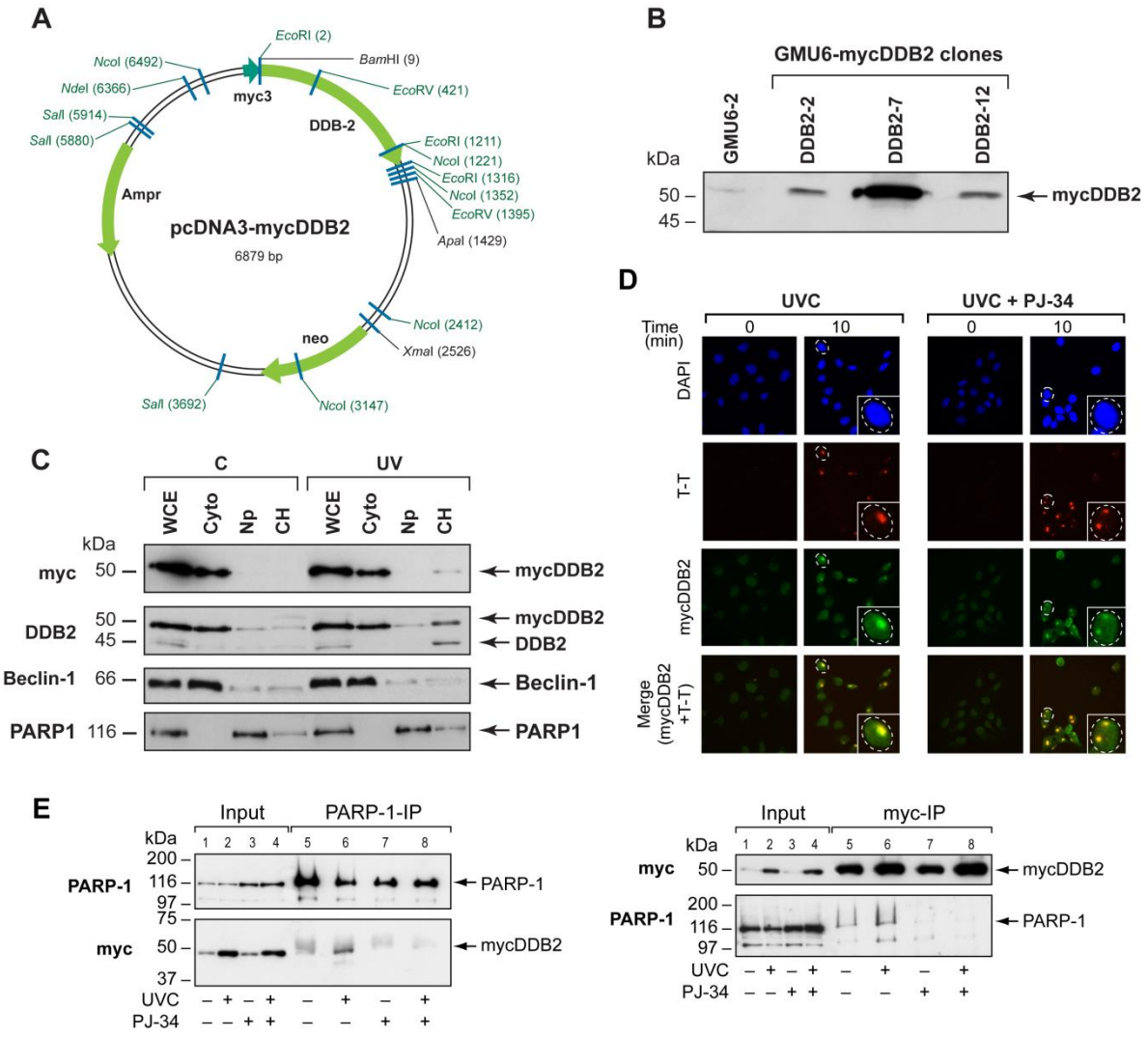

Figure S3.2 Creation of GMU6-mycDDB2 clones, mycDDB2 localization and co-IP with PARP-1.

(**A**) The pcDNA3-mycDDB2 eukaryotic expression vector map (Addgene). (**B**) The GMU6-mycDDB2 expressing clones. Three stable clones GMU6-mycDDB2 # 2, 7 and 12 were isolated from GMU6-2 cells after stable transfection with pcDNA3-mycDDB2 and the level of expression of mycDDB2 in these clones was determined by immunoblotting for myc. (**C**) UV-induced recruitment of mycDDB2 in the Ch fraction of GMU6-mycDDB2 clone 7. Cells were irradiated to 10 J/m^2 UV (10 min) and Ch-fractions were prepared as described in Fig. S1A. The movement of exogenous mycDDB2 was identical to the endogenous DDB2, as seen after immunoblotting for myc and DDB2. Probing for beclin-1 and PARP-1 served as

cytoplasmic and nuclear markers, respectively. (**D**) PARP inhibition does not block initial recruitment of DDB2. The GMU6-mycDDB2 cells were treated with 10 μM PJ-34 (or control) for 15 min, followed by local irradiation with 100 J/m^2 UVC, and processed after 10 min for indirect immunofluorescence visualization of T-T (red) and mycDDB2 (green). The results presented here are from one of four experiments with identical results. (**E**) PARP inhibitor disrupts co-IP of PARP-1 and DDB2. GMU6-mycDDB2 cells were treated with 10 μM PJ-34 (or control) prior to UVC irradiation at 10 J/m^2. Cells were harvested at 10 min and Ch-fractions were subjected to IP for PARP-1 and myc (for mycDDB2) followed by detection of PARP-1 and mycDB2. Results are representative of 2-3 experiments with identical results.

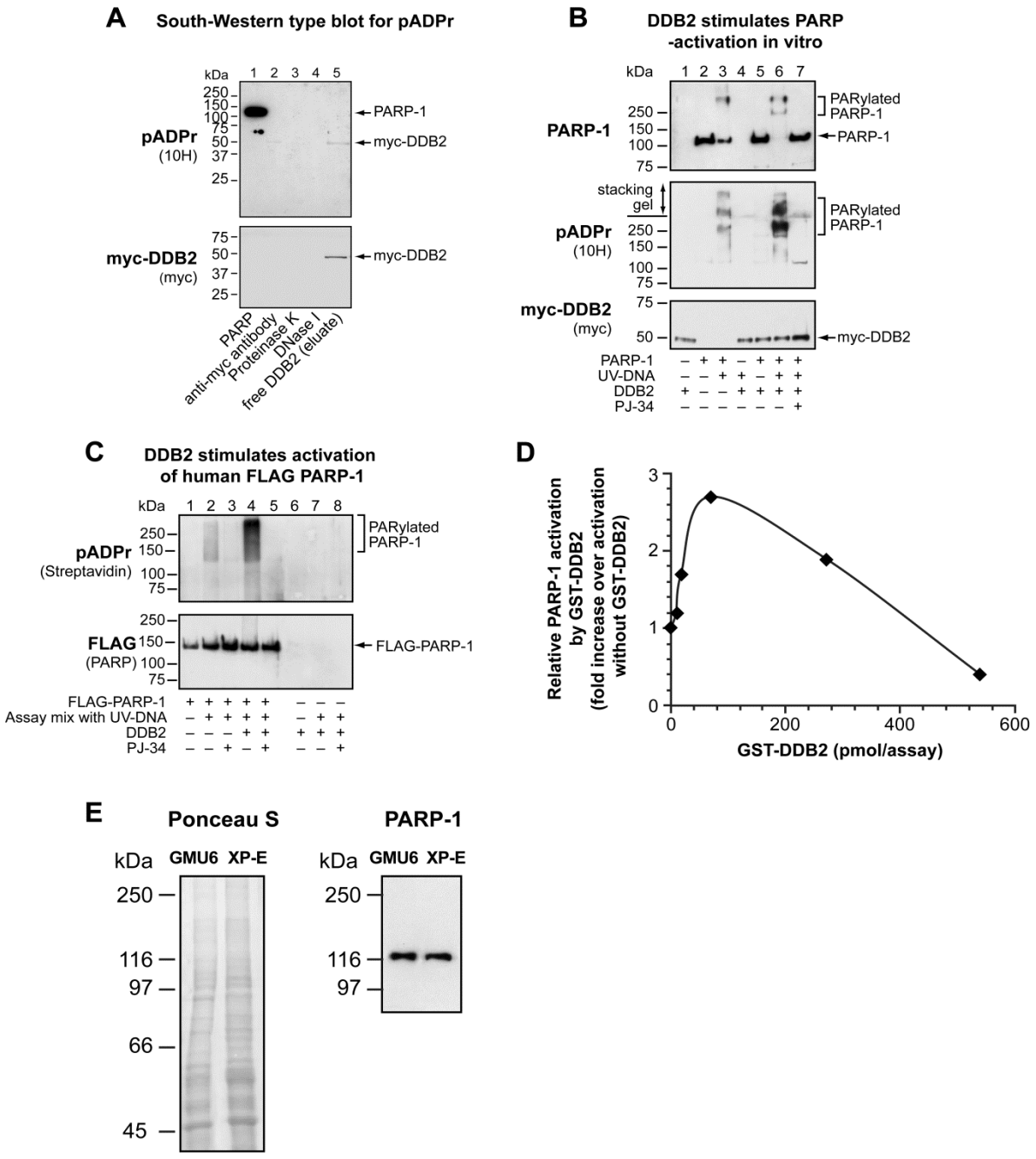

Figure S3.3 Additional evidence and controls for PARP-1 activation assays and PARP-1 levels in XP-E cells.

(**A**) DDB2 binds to free pADPr. The immunopurified mycDDB2, purified bovine PARP-1, proteinase K and DNase1 were resolved on SDS-PAGE, blotted and reacted with polymer followed by immunoprobing for bound pADPr and myc. The results are representative of

two experiments with similar results. (**B-C**) DDB2 stimulates catalytic activity of PARP-1 in response to UVC-damaged DNA. *In vitro* PARP-1 activation assays were performed with purified bovine PARP-1 (panel B) or immunopurified FLAG-PARP-1 (panel C), in presence or absence of immunopurified mycDDB2 and UV-irradiated covalently closed circular DNA, untagged or biotinylated NAD and PJ-34, as specified. Aliquots were immunoblotted for PARP-1, pADPr (10H or streptavidin) and DDB2 (myc or DDB2). The results are representative of 3-4 experiments with similar results. (**D**) Dose-response curve for GST-DDB2 in PARP-1 activation assay: In an assay containing 860 pmol PARP-1, specified amounts of GST-DDB2 were added to observe pADPr-modification of PARP-1 as a measure of PARP-1 activation. In the 10H immunoblot shown in Fig. 3D, the total pixels in the defined area of signal for pADPr-modified PARP-1 were quantified using ChemiGenius2 BioImaging System using GeneTools software version 4.00.00. The results are representative of 2 experiments with similar results. (**E**) PARP-1 levels in XP-E and GMU6 cells. The whole cell extracts from 200,000 GMU6 and XP-E cells were immunoblotted for PARP-1, and the Ponceau staining served as a loading control.

3.8 Materials and Methods

Full details are provided in the supplementary information.

Cells, clones, transient transfections and mice: SV-40 immortalized GM637 and XP-C (GM15983) human skin fibroblasts, and untransformed XP-E (GM01389) cells were obtained from Coriell. The hTert-immortalized human skin fibroblasts were a gift of W. Hahn. PARP-1 replete GMU6 and PARP-1 depleted GMSiP cells have been reported [372]. Details for FLAG-hPARP-1 expressing GMRSiP or mycDDB2 and FLAG-XPA expressing GMU6 derived clones are in supplemental section. XP-E cells were transfected with pcDNA3-mycDDB2 plasmid for 24h before irradiation. Four weeks old female SKH-1 hairless mice were from Charles River.

UV irradiation, analyses of DNA repair and recruitment of NER factors: Global and local UVC irradiation of cells has been reported [338]. The repair kinetics assays for T-T and 6-4PP in cellular genomic DNA by flow cytometry and immunofluorescence microscopy, and detection of NER proteins after local irradiation are detailed in supplementary information. SKH-1 hairless mice were irradiated with 1600 J/m^2 of UVB and immunohistological analysis was performed on paraffin sections of skin.

Immunopurification, cell fractionation and co-IP: FLAG-hPARP-1, mycDDB2 and FLAG-XPA were expressed in cells and immunopurified from whole cell extracts using suitable antibodies and beads. Purified human GST-DDB2 was purchased from Abnova. Cell fractionation protocol to extract chromatin-bound proteins (Ch-fraction) is detailed in supplementary information. IP was carried out with 100-300 µg protein of Ch-fractions.

***In vitro* PARP-1 activation reactions, pADPr Dot-blot and SouthWestern blot:** The pADPr immunodot-blot [376] and *in vitro* PARP-1 activation reaction [373] were performed as described. SouthWestern blot method was derived from Activity-Western blot of PARP-1 [373].

Extended Experimental Procedures

Materials

Cells: The SV-40 immortalized human skin fibroblasts GM00637 or GM637 (NER-proficient) and GM15983 (NER-deficient XP-C), as well as untransformed GM01389 (XP-E) cells were obtained from Coriell Cell Repository. The hTert immortalized BJ-EH2 human foreskin fibroblasts were a kind gift from W. Hahn. The cells were grown in a humidified incubator (37°C, 5% CO_2) in a medium containing 10% FBS (15% FBS for XP-E) and penicillin and streptomycin. GM cells were grown in α-MEM and the clones were selected using hygromycin (Calbiochem, 200 µg/ml). The BJ cells were grown in a medium containing 4 parts of DMEM-high glucose medium and 1 part of 199 medium, supplemented with 4 mM L-glutamine.

The stable PARP-1 depleted GMSiP clones were derived from GM637 human skin fibroblasts [372]. The RNAi-resistant FLAG-PARP-1 cDNA was created by inserting silent base mutations in the RNAi-target sequence of cDNA using QuickChange XL Site directed Mutagenesis kit (Stratagene). GMRSiP clones were generated by expression of RNAi-resistant FLAG-tagged hPARP-1 in GMSiP cells (Fig. S1B). GMU6-mycDDB2 clones were created after transfection of GMU6 cells with pcDNA3-mycDDB2 (Addgene), and selected with G418 (800 µg/ ml) (Fig. S2A-C).

Chemicals and other reagents: The chemicals used in preparing the buffers and other fine chemicals were purchased from Sigma. The Dynabeads protein G were obtained from Invitrogen, nitrocellulose ECL membrane was from Amersham, PJ-34 was from Alexis, G418 was from Bioshop, hygromycin was from Calbiochem, the chemiluminescent HRP reagent was from Millipore, the protease inhibitor tablets were from Roche, the secondary HRP conjugated antibodies for Western blots and mouse and rabbit IgGs were from Jackson Immunoresearch Laboratories, the secondary fluorescent antibodies for the FACS and immunocytochemistry were from Molecular Probes and the Streptavidin was from Sigma. All the cell culture media and related products were from GIBCO. Purified bovine PARP

was obtained from Aparptosis (1.431 U/ µg protein, 0.6 U/ µl), GST-DDB2 were obtained from Abnova and 6-Biotin-17-NAD was obtained from Trevigen.

Antibodies for DNA damage: 6-4PP and T-T antibodies were obtained from Kamiya Biochemical Company (KTM50 and KTM53). The dilutions used for 6-4PP were 1: 1,000 and 1: 5,000 for FACS and Western blot analysis, respectively. The T-T antibody dilutions were 1: 500 for FACS, 1: 2,000 for immunocytochemistry, 1: 200 for immunohistochemistry and 1: 5,000 for Western Blot. Anti-rabbit myc antibody (Abcam) was used at 1: 2,000 for immunocytochemistry. Anti-rabbit XPC (GeneTex) was used at 1: 500 for immunocytochemistry.

Antibodies for co-IP studies: FLAG-monoclonal antibody tagged beads were obtained from Sigma. Polyclonal PARP-1 antibody (1:500) was from Alexis Biochemicals. For myc-IP, rabbit anti-myc antibody from Abcam was used at 1: 250 dilution. Anti-pADPr polyclonal LP-96-10 was from Aparptosis, and used at 1: 500 dilution. The following antibodies were used for IP at 1 µg /100 µg of chromatin protein in 1 ml volume: rabbit anti-DDB2 and rabbit anti-ubiquitin from Santacruz, XPC polyclonal from GeneTex, goat antiDDB2 from R&D Systems, IgG anti-mouse, anti-rabbit and goat serum from Jackson Laboratories.

Antibodies for detection of proteins on Western blot: FLAG monoclonal antibody (Sigma, 1: 5,000), polyclonal PARP-1 antibody (Alexis Biochemicals, 1: 5,000), XPA monoclonal (Medicorp, 1: 500), XPC polyclonal (GeneTex, 1: 2,500), Histone H3 polyclonal (Abcam, 1: 40,000), PARP-1 monoclonal (F2, Santacruz, 1: 500), DDB2 monoclonal (Abcam, 1: 50), Myc monoclonal (9-E-10, Biolegend, 1: 500), Beclin-1 polyclonal (Cell Signaling, 1: 1,000), and ubiquitin monoclonal (Santacruz, 1: 500), β-actin (Sigma, 1: 20,000). The anti-pADPr monoclonal 10H was purified from the culture medium of 10H hybridoma obtained from Dr Miwa through the Riken cell bank, and used at 1: 500.

Methods

Animal Studies:

Mice and UVB irradiation: The animal experiment protocols were approved by the CPA-CHUQ ethical committee and performed in accordance with the Canadian Council on Animal Care (CCAC) Guide for Care and Use of Experimental Animals. Three-week old female SHK-hairless mice were obtained from Charles River, and housed in standard cages, with controlled humidity and temperature, with alternating 12h light and dark cycles. The mouse were fed commercial diet and given water ad libitum. Three to seven mice were used per time point. A dose of 100 µmoles of 1,5-dihydroxyisoquinoline (DHQ) diluted in 200 µl of acetone was applied on the dorsal skin of mice 1h before irradiation, and repeated every 3h until 12h. The solvent acetone was applied on the skin of control group. The mice in standard cages (4 mice/cage) covered with a UVC filter (Kodacel K6805 0.0127 cm thick) were exposed to 1600 J/m^2 of UVB from a bank of 6 Phillips FS20T12 UVB lamps (Spectronics) placed 30 cm above the cage. Mice were sacrificed up to 48h by CO_2 inhalation followed by cervical dislocation.

Immunohistochemistry of T-T in mouse skin: Within two min of sacrifice, dorsal skin was removed and frozen on glass plate cooled over ice. Subdermal fat was removed and pieces of skin (dermis plus epidermis) were fixed in 4% PBS-buffered formaldehyde and embedded in paraffin. The sections were deparaffinized in toluene and rehydrated in graded ethanol baths (100%, 95%, 70%). Endogenous peroxidase activity was blocked with 1.5% H_2O_2 in methanol. Antigen retrieval was performed by boiling for 15 min in citrate buffer (0.1M, pH 6.0) at 20% power of a 700W microwave [382]. Samples were then permeabilized in trypsin (0.1% in Tris-HCl buffer, pH 7.5) for 10 min at room temperature. After blocking in PBS buffer containing 5% non-fat milk powder and 0.01% Tween20, the sections were incubated with monoclonal T-T antibody overnight at 4ºC in a humidified chamber, followed by washes and reaction with secondary peroxidase-coupled antimouse IgG for 3h at ambient temperature. Revelation was performed in 0.2mg/ml 3,3-diaminobenzidine (DAB) and slides were counterstained in Harris modified Hematoxylin (Sigma), dehydrated in graded alcohol baths and mounted with Permount (Fisher). Images were taken with a Nikon Eclipse E800

microscope at 600X using a color digital camera (Optronics) and data are representative of results obtained from skin of 3-6 animals per point.

Cellular Studies

Immunocytochemistry of DNA damage and NER proteins after global and local UVC irradiation: Global or local UVC irradiations were carried out as described [338]. GM637 derived clones were cultured on circular coverslips in 35 mm dishes. At the designed time, the globally irradiated cells were probed for T-T as per the protocol provided by the supplier of the antibody (MBL). At least 100 nuclei from three different coverslips per time point were analyzed by Axiovert 200 (Zeiss) for fluorescence imaging using the program "AutoMeasure Plus" of the software Axiovision version 4.7 and expressed as pixel/area. Results are expressed as mean ± SE. The locally irradiated cells were probed for T-T dimers and other NER proteins as per the protocol described [383]. XP-E cells, seeded on coverslips in 35 mm dishes 48h before, were transiently transfected with 4 µg DNA of pcDNA3-mycDDB2 expression vector and 16 µl Lipofectamine in a total volume of 400 µl made with Opti-MEM medium (per dish). The 400 µl mix was added to the dish containing 1.6 ml of Opti-MEM, and incubated in the cell culture incubator for 4h. The medium was removed, and replaced by α-MEM, containing 15% FBS. After 24h, cells were treated with PJ-34 (10 µM, 30 min or control) and irradiated with 10 J/m^2 UVC. After 5 min, the cells were fixed and permeabilized with methanol: acetone (1: 1) for 30 min on ice, blocked in PBS containing 3% non-fat milk and 0.1% Tween 20 (PBS-MT) for 30 min, and reacted with LP-96-10 (1: 1500, polyclonal antibody for polymer) and anti-myc (1: 100, monoclonal antibody for mycDDB2) for 3h at ambient temperature. The fluorescent secondary antibodies (1:500) were reacted for 45 min. Images were taken with Axiovert 200 at 40X or 63X and photos were taken with AxioCam MRm.

Flow cytometry analyses of DNA damage: The flow cytometry analyses of T-T and 6-4PP were carried out as described earlier [384]. The cells were synchronized in G1 phase by treating with 0.5 µM freshly prepared L-mimosine for 24h in complete medium. FACS analyses were carried out with BD FACSCalibur flow cytometer and the data were analysed with BD FACSDiva software. The superimposition of histograms were generated using FlowJo 7.6.1 software from Tree Star, Inc. Statistical analyses were done by Student's t-test.

Immunopurification of mycDDB2, FLAG-PARP-1 and FLAG-XPA: For mycDDB2, the GMU6-mycDDB2 cells were lysed in 50 mM Tris-HCl pH 7.5, 5 mM EDTA, 0.2 % IGEPAL, 150 mM NaCl, 0.5 mM PMSF and protease inhibitors. The mycDDB2 was purified from this lysate using myc-polyclonal antibody (Abcam), and Protein G-coated magnetic beads. The beads with the DDB2 were washed 5x10 min each with 50 volumes of PBS-T (PBS containing 0.05 % Tween-20), suspended in PBS containing 10 % glycerol and either stored frozen at -30 °C or mycDDB2 eluted with 50 mM glycine, pH 3.0 followed by neutralization with 1 M Tris HCl, pH 8.0, and frozen at -30 °C.

The FLAG-PARP-1 was prepared from the lysates of GMRSiP cells expressing RNAi-resistant FLAG-PARP-1 using the FLAG-magnetic beads. The bead-bound FLAG-PARP-1 was washed 3 times with PBS-T (as described above), followed by three additional washes of 15 min each (at 4 °C) with 25 mM Tris-HCl pH 7.9, 150 mM NaCl, 0.1 % EDTA, 10 % glycerol, 1 % IGEPAL, protease inhibitor [385] to remove proteins interacting with PARP-1. The IGEPAL was removed by washing with 10mM Tris-HCl pH 8.0, 150 mM NaCl, and suspended in the same buffer containing 10 % glycerol and protease inhibitor. The beads were stored at -30 °C.

The FLAG -XPA was purified from FLAG -XPA expressing GM637 cells. The soluble lysate was prepared as described for the purification of DDB2. The XPA was purified using the FLAG beads and eluted using FLAG peptides as described in the instructions provided by Sigma.

In vitro PARP-1 activation assay: The PARP-1 activation assays were performed in 20 µl at 30°C, for 30 min [373]. The reaction mixture contained 100 mM Tris-HCl, pH 8.0; 10 mM $MgCl_2$; 10 % glycerol; 1.5 mM DTT as the basic components. The unlabeled NAD was generally used at 500 µM for most experiments except that 30 µM was used for GST-DDB2 studies. The biotinylated NAD was used at 100 µM. The DNA used was either un-irradiated covalently closed circular pBS-U6 plasmid (3.2 kb) or the same plasmid irradiated with UVC (500 J/m^2) to acquire UV-induced DNA lesions without having strand breaks, as described earlier [338]. The final concentration of the DNA was 100 µg/ ml of the reaction or 2 µg in 20 µl. When specified, 200 µM PJ-34 was added prior to addition of the enzyme. Immunopurified eluted or bead-bound mycDDB2 and highly purified GST-DDB2 (Abnova)

were used as specified. For PARP-1, we used either purified bovine PARP-1 or immunopurified bead-bound FLAG-hPARP-1, as specified. The amount of mycDDB2 used in the in-vitro assays (either eluted or bead-bound) was equivalent to that purified from approximately $1x10^6$ cells and the GST-DDB2 is expressed in molar concentration. The FLAG-hPARP-1 used in the in-vitro assay corresponded to that purified from 2×10^6 cells. Bovine PARP-1 added in the assay was 200 ng (258 mUnits). Reaction was terminated by magnetically dissociating the beads from the supernatant. Equal amount of 2X loading buffer for Western blot analysis was added to the supernatant. The separated magnetic beads were washed 5 times with 100 volumes of PBS-T (0.05 % Tween20), and then suspended in loading buffer for Western blot analysis. The beads were heated for 10 min at 95 °C with intermittent vortexing during elution. Bead extracts and supernatant were resolved on SDS-PAGE, blotted to a nitrocellulose membrane and probed for polymer (either by 10H or streptavidin), PARP-1 and myc or DDB2.

pADPr Dot-blot and SouthWestern blot: The free polymer was synthesized in a PARP-1 activation assay using non-isotopic NAD and purified on DHBB column, as described [373]. Polymer binding immunodot-blot assay was performed, as described [376]. Briefly, for pADPr immunodot-blot, specified proteins were spotted on nitrocellulose membrane using Dot blot apparatus. The membrane was washed thrice with TBS-T (10 mM Tris, 150 mM NaCl, 0.05 % Tween-20), and incubated for 1h at room temperature with 10 ml of TBS-T containing approximately 500 pmoles of polymer. The membrane was washed three times with TBS-T (10 min each), followed by three washes with TBS-T containing 1 M NaCl. The membrane was blocked with TBS-T containing 5 % milk, and probed with 10H antibody. For SouthWestern blots, PARP-1 (120 ng), proteinase K (400 ng), immunopurified mycDDB2 (purified from ~$2x10^6$ cells), purified GST-DDB2 (500 ng, Abnova) and DNaseI (4 Units, Fermentas) were resolved on a 10 % SDS-PAGE gel. The proteins were renatured by soaking the gel in 20-30 ml of running buffer containing 5 % β-mercaptoethanol, for 1h at 37°C. Proteins were transferred on nitrocellulose, and membrane was processed as described above for immunodot-blot.

Cell Fractionation protocol to isolate Chromatin-bound protein (Ch)-fraction: The cellular fractionation protocol to derive Ch-fraction was derived from an earlier protocol to isolate the nuclear fraction [386]. In brief, cells were harvested, washed in PBS and suspended in cell lysis buffer (10 mM HEPES (pH 7.8), 0.34M sucrose, 10% glycerol, 10 mM KCl, 1.5 mM $MgCl_2$, 1mM PMSF, protease and phosphatase inhibitors and 0.1 % Triton-X-100). Cells were lysed by repeated pipetting and kept on ice for 7 min to generate the whole cell extract (WCE fraction). WCE was centrifuged at 1,000*g* for 5 min at 4°C to separate the nuclear pellet (Np fraction) from cytoplasm (C fraction).

To extract the chromatin-bound protein fraction from nuclear fraction, we developed a protocol based on a previously described procedure [84]. The nuclear pellet (Np fraction) was washed once with cell lysis buffer and suspended in nuclear lysis buffer (50 mM Tris-Cl, pH 7.8, 420 mM NaCl, 0.5 % IGEPAL, 0.34M sucrose along with protease and phosphatase inhibitors). The nuclei were kept on ice for 30 min, and then spun at 16,000*g* for 30 min at 4°C to separate nucleoplasm (Np fraction) suspension from the pellet. This chromatin pellet was suspended in 20 mM Tris-Cl (pH 7.5) containing 100 mM KCl, 2 mM $MgCl_2$, 1 mM $CaCl_2$, 0.3M sucrose, 0.1% Triton-X-100, 1 mM PMSF, and protease and phosphatase inhibitors. To obtain a uniform suspension of chromatin, suspension was briefly sonicated at a low setting (level 11) with a microtip using Ultrasonic Dismembrator (Fisher model 500) and repeatedly pipetted through a small-bore (P200) tips (dounce homogenization in place of sonication also gave similar results). The chromatin proteins were extracted by incubation with micrococcal nuclease (25 U/mL) at ambient temperature for 40 min. The reaction was terminated by addition of 5 mM each of EDTA and EGTA, and spun at 13,000 rpm for 10 min to separate the insoluble chromatin pellet from supernatant designated as chromatin-bound protein fraction (Ch).

IP of chromatin bound proteins after cell fractionation. Ch-fraction prepared as described above was used for IP or co-IP. Generally, 100-300 µg proteins were suspended in 500-1,000 µl of chromatin buffer, as described above, NaCl concentration was adjusted to 200 mM prior to reaction with the specific antibody overnight at 4 °C. For some co-IP, Ch-fractions were incubated with 200 µg/ ml of ethidium bromide for 1h at 4ºC before addition of antibody. The same concentration of ethidium bromide was added to PBS-containing 0.05% Tween20n

(PBS-T) during the washing of the beads. The Dynabeads Protein G, washed with PBS-T, were added (30µl/100 µg protein) to the IP mixture and incubated for 1h. The beads were separated on magnetic stand, and washed 4x5 min with PBS containing 0.05% Tween20 and protease inhibitors. Proteins were extracted from the beads with SDS-PAGE gel loading buffer at 95°C for 10 min, resolved on SDS-PAGE, blotted to nitrocellulose, and probed for proteins.

Acknowledgments

We thank W. Hahn and P. Lee for BJ-hTert cells, E. Drobetksy, H. Naegeli and M Ghodgaonkar for helpful suggestions. Scholarship supports were received from NSERC (MR, NP and FKK), Laval University (MR), and FRSQ (NP). This work was supported by NCIC/CCS grant #16407 to GMS.

3.9 References

1. Krishnakumar R & Kraus WL (2010) The PARP Side of the Nucleus: Molecular Actions, Physiological Outcomes, and Clinical Targets. *Mol. Cell* 39(1):8-24.

2. De Vos M, Schreiber V, & Dantzer F (2012) The diverse roles and clinical relevance of PARPs in DNA damage repair: current state of the art. *Biochem Pharmacol* 84(2):137-146.

3. Yélamos J, Farrés J, Llacuna L, Ampurdanés C, & Martin-Cabllero J (2011) PARP-1 and PARP-2: New players in tumor development. *Am. J. Cancer Res.* 1(3):328-346.

4. Cleaver JE, Lam ET, & Revet I (2009) Disorders of nucleotide excision repair: the genetic and molecular basis of heterogeneity. *Nat Rev Genet* 10(11):756-768.

5. Sugasawa K, *et al.* (2005) UV-induced ubiquitylation of XPC protein mediated by UV-DDB-ubiquitin ligase complex. *Cell* 121(3):387-400.

6. Fei J, *et al.* (2011) Regulation of nucleotide excision repair by UV-DDB: prioritization of damage recognition to internucleosomal DNA. *PLoS Biol.* 9(10):e1001183.

7. Luijsterburg MS, *et al.* (2012) DDB2 promotes chromatin decondensation at UV-induced DNA damage. *J Cell Biol* 197(2):267-281.

8. Ciccia A & Elledge SJ (2010) The DNA damage response: making it safe to play with knives. *Mol. Cell* 40(2):179-204.

9. Vodenicharov MD, Ghodgaonkar MM, Halappanavar SS, Shah RG, & Shah GM (2005) Mechanism of early biphasic activation of poly(ADP-ribose) polymerase-1 in response to ultraviolet B radiation. *J Cell Sci* 118(Pt 3):589-599.

10. Stevnsner T, Ding R, Smulson M, & Bohr VA (1994) Inhibition of gene-specific repair of alkylation damage in cells depleted of poly(ADP-ribose) polymerase. *Nucl. Acids Res.* 22(22):4620-4624.

11. Flohr C, Burkle A, Radicella JP, & Epe B (2003) Poly(ADP-ribosyl)ation accelerates DNA repair in a pathway dependent on Cockayne syndrome B protein. *Nucl. Acids Res.* 31(18):5332-5337.

12. Hastak K, Alli E, & Ford JM (2010) Synergistic chemosensitivity of triple-negative breast cancer cell lines to poly(ADP-Ribose) polymerase inhibition, gemcitabine, and cisplatin. *Cancer Res* 70(20):7970-7980.

13. Auclair Y, Rouget R, Affar el B, & Drobetsky EA (2008) ATR kinase is required for global genomic nucleotide excision repair exclusively during S phase in human cells. *Proc Natl Acad Sci U S A* 105(46):17896-17901.

14. Shah RG, Ghodgaonkar MM, Affar EB, & Shah GM (2005) DNA vector-based RNAi approach for stable depletion of poly(ADP-ribose) polymerase-1. *Biochem Biophys Res Commun* 331(1):167-174.

15. Shah GM, *et al.* (2011) Approaches to detect PARP-1 activation in vivo, in situ, and *in vitro*. *Methods Molec Biol* 780:3-34.

16. Fitch ME, Cross IV, & Ford JM (2003) p53 responsive nucleotide excision repair gene products p48 and XPC, but not p53, localize to sites of UV-irradiation-induced DNA damage, in vivo. *Carcinogenesis* 24(5):843-850.

17. Luijsterburg MS, *et al.* (2007) Dynamic in vivo interaction of DDB2 E3 ubiquitin ligase with UV-damaged DNA is independent of damage-recognition protein XPC. *J. Cell Sci.* 120(Pt 15):2706-2716.

18. Pleschke JM, Kleczkowska HE, Strohm M, & Althaus FR (2000) Poly(ADP-ribose) binds to specific domains in DNA checkpoint proteins. *J. Biol. Chem.* 275(52):40974-40980.

19. Epstein JH & Cleaver JE (1992) 3-Aminobenzamide can act as a cocarcinogen for ultraviolet light-induced carcinogenesis in mouse skin. *Cancer Res.* 52(14):4053-4054.

20. Ghodgaonkar MM, Zacal NJ, Kassam SN, Rainbow AJ, & Shah GM (2008) Depletion of poly(ADP-ribose)polymerase-1 reduces host cell reactivation for UV-treated adenovirus in human dermal fibroblasts. *DNA Repair (Amst)* 7:617-632.

21. Gibson BA & Kraus WL (2012) New insights into the molecular and cellular functions of poly(ADP-ribose) and PARPs. *Nature Reviews: Molec. Cell Biol.* 13(7):411-424.

22. Lan L, *et al.* (2012) Monoubiquitinated histone H2A destabilizes photolesion-containing nucleosomes with concomitant release of UV-damaged DNA-binding protein E3 ligase. *J Biol Chem* 287(15):12036-12049.

23. Lukas J, Lukas C, & Bartek J (2011) More than just a focus: The chromatin response to DNA damage and its role in genome integrity maintenance. *Nat. Cell Biol.* 13(10):1161-1169.

24. Sugasawa K (2010) Regulation of damage recognition in mammalian global genomic nucleotide excision repair. *Mutat Res* 685(1-2):29-37.

References for Supplementary Information

1. Shah RG, Ghodgaonkar MM, Affar EB, & Shah GM (2005) DNA vector-based RNAi approach for stable depletion of poly(ADP-ribose) polymerase-1. *Biochem Biophys Res Commun* 331(1):167-174.

2. Midgley CA, *et al.* (1995) Coupling between gamma irradiation, p53 induction and the apoptotic response depends upon cell type in vivo. *J Cell Sci* 108 (Pt 5):1843-1848.

3. Vodenicharov MD, Ghodgaonkar MM, Halappanavar SS, Shah RG, & Shah GM (2005) Mechanism of early biphasic activation of poly(ADP-ribose) polymerase-1 in response to ultraviolet B radiation. *J Cell Sci* 118(Pt 3):589-599.

4. Zhu Q, *et al.* (2009) Chromatin restoration following nucleotide excision repair involves the incorporation of ubiquitinated H2A at damaged genomic sites. *DNA Repair* 8(2):262-273.

5. Rouget R, Auclair Y, Loignon M, Affar el B, & Drobetsky EA (2008) A sensitive flow cytometry-based nucleotide excision repair assay unexpectedly reveals that mitogen-activated protein kinase signaling does not regulate the removal of UV-induced DNA damage in human cells. *J Biol Chem* 283(9):5533-5541.

6. Krishnakumar R & Kraus WL (2010) PARP-1 regulates chromatin structure and transcription through a KDM5B-dependent pathway. *Molecular Cell* 39(5):736-749.

7. Shah GM, *et al.* (2011) Approaches to detect PARP-1 activation in vivo, in situ, and *in vitro*. *Methods Molec Biol* 780:3-34.

8. Pleschke JM, Kleczkowska HE, Strohm M, & Althaus FR (2000) Poly(ADP-ribose) binds to specific domains in DNA checkpoint proteins. *J. Biol. Chem.* 275(52):40974-40980.

9. Wu X, Shell SM, Liu Y, & Zou Y (2007) ATR-dependent checkpoint modulates XPA nuclear import in response to UV irradiation. *Oncogene* 26(5):757-764.

10. Fousteri M, Vermeulen W, van Zeeland AA, & Mullenders LH (2006) Cockayne syndrome A and B proteins differentially regulate recruitment of chromatin remodeling and repair factors to stalled RNA polymerase II in vivo. *Mol Cell* 23(4):471-482.

Chapitre 4

Characterization of the interactions of PARP-1 with UV-damaged DNA in vivo and in vitro

Nupur K. Purohit[1#], Mihaela Robu[1#], Rashmi G. Shah[1#], Nicholas E. Geacintov[2] and Girish M. Shah[1*]

[1]: Laboratory for Skin Cancer Research, CHU-Q (CHUL) Quebec University Hospital Research Centre & Laval University, 2705, Laurier Boulevard, Québec (QC) Canada G1V 4G2; [2]: New York University, Department of Chemistry, New York, NY, USA

*To whom correspondence should be addressed.

Tel: [1-418-525-4444/ext. 48259]; Fax: [1-418-654-2739]; Email: [girish.shah@crchul.ulaval.ca]

The authors wish it to be known that, in their opinion, the first 3 authors should be regarded as joint First Authors".

4.1 Avant-propos

Des études de cristallographie avaient démontré la liaison directe du facteur « DNA damage binding protein 2 » (DDB2) aux dommages de type CPD et 6-4PP. Nos résultats précédents montraient que la PARP1 interagissait avec le DDB2 sur le même brin d'ADN, le brin contenant le dommage. Afin de comprendre comment ces deux facteurs pouvaient se lier à l'ADN simultanément, nos travaux se sont orientés vers la caractérisation de la liaison de la PARP1 à un dommage de type UV. Nos résultats ont mené, en janvier 2015, à la publication d'un article dans la revue *Scientific Report*, disponible en version PDF à l'annexe 2.

Pour cette étude, j'ai développé une nouvelle technique de fractionnement in situ, qui couple le fractionnement cellulaire à l'immunofluorescence. La PARP1 est une des plus abondantes protéine nucléaire. Par conséquent, la visualisation du recrutement de la PARP1 endogène aux dommages n'était pas possible en utilisant les techniques connues (Figure 4.1A). Pour cela, dans leur grande majorité, les études utilisent la formation des PAR comme preuve de la présence de la PARP1 aux lésions. Cependant, d'autres PARP forment également des PAR et PARP1 pourrait aussi avoir des rôles dans la réparation de l'ADN après la dégradation des PAR. Cette technique m'a permis de montrer l'accumulation de la PARP1 endogène (Figure 4.1E) et exogène (Figure 4.2A) au niveau du site local d'irradiation marqué avec un anticorps contre DDB2 ou contre le dommage de type thymine-thymine. De plus, j'ai démontré que le domaine N terminal de la PARP1 contenant les deux doigts à zinc est suffisant pour son recrutement (Figure 4.2B). La caractérisation de la liaison de la PARP1 *in vitro* à un dommage CPD, a été réalisée par mes collègues Nupur Pourohit et Rashmi Shah, ce qui inclut la création d'un oligonucléotide avec un dommage défini et la description de l'empreinte de la PARP1 autour d'un dommage UV (Figures 4.3, 4.4 et 4.5). L'ADN avec un seul dommage synthétisé chimiquement utilisé dans la Figure 4.5A a été fourni par Dr Nicholas Geacintov. En tant que première co-auteure, j'ai également pris part à la rédaction du manuscrit, à sa révision et au montage des figures.

4.2 Résumé

Les méthodologies existantes pour étudier les réponses robustes de la poly (ADP-ribose) polymérase-1 (PARP-1) aux lésions de l'ADN avec cassures de brin sont souvent inappropriées pour examiner ses réponses subtiles à l'ADN altéré mais sans cassure de brin. Ici, nous décrivons deux nouveaux essais avec lesquels nous avons caractérisé l'interaction de la PARP-1 avec l'ADN endommagé par les UV in vivo et in vitro. En utilisant la technique de fractionnement in situ qui élimine sélectivement la PARP-1 libre tout en conservant la PARP-1 liée à l'ADN, nous démontrons le recrutement direct de la PARP-1 endogène ou exogène sur le site de lésions induites par les UV in vivo après irradiation locale. De plus, en utilisant un modèle d'oligonucléotide avec une seule lésion de type UV entourée de sites de reconnaissance multiples pour des enzymes de restriction, nous avons démontré in vitro que le facteur DDB2 et la PARP-1 peuvent se lier simultanément à l'ADN endommagé par les UV et que la PARP-1 a une empreinte bilatérale asymétrique de -12 à +9 nucléotides de chaque côté du dommage UV. Ces techniques permettront de caractériser les différents rôles de la PARP-1 dans la réparation de l'ADN endommagé par les UV et ses rôles constitutifs impliquant l'ADN non endommagé.

4.3 Abstract

The existing methodologies for studying robust responses of poly(ADP-ribose) polymerase-1 (PARP-1) to DNA damage with strand breaks are often not suitable for examining its subtle responses to altered DNA without strand breaks, such as UV-damaged DNA. Here we describe two novel assays with which we characterized the interaction of PARP-1 with UV-damaged DNA in vivo and in vitro. Using an in situ fractionation technique to selectively remove free PARP-1 while retaining the DNA-bound PARP-1, we demonstrate a direct recruitment of the endogenous or exogenous PARP-1 to the UV-lesion site in vivo after local irradiation. In addition, using the model oligonucleotides with single UV lesion surrounded by multiple restriction enzyme sites, we demonstrate in vitro that DDB2 and PARP-1 can simultaneously bind to UV-damaged DNA and that PARP-1 casts a bilateral asymmetric footprint from -12 to +9 nucleotides on either side of the UV-lesion. These techniques will permit characterization of different roles of PARP-1 in the repair of UV-damaged DNA and also allow the study of normal housekeeping roles of PARP-1 with undamaged DNA.

4.4 Introduction

The abundance of poly(ADP-ribose) polymerase-1 (PARP-1) in mammalian cells and its rapid catalytic activation to form polymers of ADP-ribose (PAR) in the presence of various types of DNA damages with or without strand breaks has made it an ideal first responder at the lesion site to influence downstream events [387, 388]. Apart from DNA damages, PARP-1 is also recruited to DNA during normal physiological processes such as transcription and chromatin remodeling [389], which do not involve overt DNA damage but just altered DNA structures. While we know much more about how PARP-1 rapidly recognizes and binds to single or double strand breaks in DNA, we know very little about how PARP-1 interacts with DNA damages or altered DNA structures without strand breaks. The key reason is that the existing methodologies that readily identify interactions of PARP-1 with DNA strand breaks are not sufficiently sensitive to study the relatively weaker responses of PARP-1 to DNA damage without strand breaks. The response of PARP-1 to UVC-induced direct photolesions, such as cyclobutane pyrimidine dimers (CPD) that are formed without any DNA strand breaks exemplifies this problem.

Recent studies from others and our team have shown the involvement of PARP-1 in the host cell reactivation [378] and specifically in the nucleotide excision repair (NER) of UV-damaged DNA through its interaction with early NER protein DDB2 [390-392]. Additional studies have shown that downstream NER proteins XPA [393, 394] and XPC [395] are PARylated. Thus, PARP-1 possibly has multiple roles in NER, but we do not yet fully understand its interactions with UV-damaged DNA or other NER proteins due to two major challenges. The first challenge is that unlike for many NER proteins, the abundance of endogenous PARP-1 in the nucleus makes it nearly impossible to visualize its dynamics of recruitment to UV-damaged DNA in situ using conventional immunocytological methods. To circumvent this challenge, the detection of its activation product PAR has been used as a proxy for PARP-1 recruitment at UV-lesion [390, 396]. However, PAR may underestimate the role of PARP-1 in response to UV-damage due to weak activation of PARP-1 by UV [378, 397], short half-life of PAR [388], and technical limitations in combining the detection of PAR with other proteins [398, 399]. PAR detection will also not reveal participation of

PARP-1 in protein-protein interactions without formation of PAR. Thus, there is a need for methods that permit direct visualization of recruitment of PARP-1 to UV-induced DNA lesions.

The second major challenge is that we do not know the exact footprint of PARP-1 at the UV-lesion site that could explain its interaction with different NER proteins. We have earlier shown that PARP-1 binds to UV-damaged large oligonucleotide *in vitro* or to chromatin fragments containing T-T lesions in vivo [396]. We also showed that PARP-1 and DDB2 associate with each other on the chromatin of UV-irradiated cells and that DDB2 stimulates catalytic activity of PARP-1 in the presence of UV-damaged DNA [392]. However, these assays lack the nucleotide level resolution to reveal whether PARP-1 was bound directly to the UV-damaged bases or to any other base in those long pieces of DNA and whether PARP-1 and DDB2 have sufficient space to co-exist around UV-induced DNA lesion. To address these challenges, here, we describe two novel assays. The first assay is an in situ fractionation technique that allows a direct visualization of PARP-1 recruited to UV-damaged DNA in vivo. The second assay involves use of model oligonucleotides with a defined UV-damage surrounded by multiple restriction enzyme sites that reveals a bilateral asymmetric footprint of PARP-1 around the UV-lesion.

4.5 Results and discussion

Novel in situ fractionation protocol to reveal recruitment of endogenous PARP-1 to UV-induced DNA lesion

We first determined whether different permeabilization-fixation protocols conventionally used for PARP-1 could reveal a direct recruitment of PARP-1 to UVC-induced DNA photolesions in situ. There was no change in the pattern of abundant PARP-1 signal before or after global UVC-irradiation using formaldehyde-methanol protocol despite using three different antibodies to PARP-1 (Fig. 4.1a, left panel). Unlike global irradiation, local UVC-irradiation produces defined size subnuclear spots of UV-damaged DNA that could be identified either by immunodetection of T-T lesions or DDB2 that is recruited very

rapidly to these lesions (Supplementary Fig. S4.1a). Therefore, we examined whether the formaldehyde-methanol protocol could reveal localization of PARP-1 to subnuclear UV-damaged DNA spots after local irradiation. Once again, we could not observe colocalization of PARP-1 with the subnuclear spots of DDB2 (Fig. 4.1a, right panel). Next, we tried previously described formaldehyde-Triton protocol [393] which was shown to display a punctate pattern of PARP-1. However, we noted that this pattern did not correlate with recruitment of PARP-1 to UV-damaged DNA, because it was observed in both the unirradiated control and globally UVC-irradiated cells; and none of the spots of PARP-1 were co-incident with DDB2, i.e., UV-damaged DNA in the cells after local UVC-irradiation (Supplementary Fig. S4.1b).

In view of these challenge in the immunocytological detection of PARP-1 bound to UV-damaged DNA due to the background "noise" created by rest of the nuclear PARP-1, we designed a novel in situ fractionation technique to selectively deplete unbound or "free" PARP-1 from the nuclei while leaving behind the PARP-1 that is bound and cross-linked to the UV-damaged DNA. We used CSK buffer (C) with Triton (C+T) as the basic conditions, which have been used earlier to extract majority of the cellular proteins without destroying the cellular architecture and permit visualization of NER and other repair proteins recruited to the damaged DNA [383, 400-402]. To this buffer, we added 0.42 M NaCl (C+T+S), since we had earlier seen that 0.42 M NaCl retained chromatin-bound PARP-1 during cell fractionation *in vitro* [392] whereas 1.6 M NaCl was shown to strip almost all PARP-1 from cells [403]. We first compared the efficiency of these three protocols (i.e., C, C+T and C+T+S) for the extraction of PARP-1 and DDB2 from unirradiated control cells. The immunoblotting of cell pellet and supernatant from each protocol revealed that while C+T protocol could efficiently remove majority of the free DDB2, a significant extraction of the free PARP-1 from cell pellet required C+T+S protocol (Fig. 4.1c). Next, we compared the capacity of these three protocols for the in situ extraction of PARP-1 from control and global UVC-irradiated cells. The immunocytological visualization confirmed that C+T+S buffer extracted most of the "free" PARP-1 from the control and UVC-irradiated cells, while leaving behind residual PARP-1 that would be interacting with DNA for normal

physiological functions in control cells and relatively stronger punctate pattern of PARP-1 in UV-irradiated nuclei (Fig. 4.1d).

When the three protocols were compared after local irradiation, we observed that the C+T+S protocol offered the best extraction condition for visualization of the recruitment of PARP-1 to the subnuclear spots of DDB2 (Fig. 4.1e, left panel). The pooled data from at least 100 subnuclear spots revealed that each additional step of extraction with detergent and salt improved our ability to discern colocalization of PARP-1 with DDB2 (Fig. 4.1e, left chart). Since the initial irradiation conditions were identical prior to extraction with each of the protocols, the improved detection of colocalization of PARP-1 with DDB2 could only be due to a more efficient removal of rest of the nuclear "free PARP-1" by the C+T+S protocol. This was evident when PARP-1 signal at the irradiated site was corrected for the background signal from an equivalent area of the unirradiated part of the same nucleus for all techniques (Fig. 4.1e, right chart).

Validation of the in situ fractionation protocol with GFP-tagged exogenous PARP-1 or its N-terminal DNA binding domain

We compared the efficiency of each of the three protocols in revealing the recruitment of exogenous GFP-tagged PARP-1 to UV-induced T-T lesion in locally UV-irradiated cells (Fig. 4.2a). The C protocol was inefficient in revealing the co-localization of GFP signal with T-T spots especially in the cells expressing higher levels of exogenous PARP-1. The C+T and C+T+S protocols increasingly resolved this problem by removing "free" PARP-1; thus giving a background-corrected signal for GFP-PARP-1 at T-T lesion that was 1.9 and 2.7 times better than the C protocol, respectively (Fig. 4.2a, chart). The additional advantage was that this co-localization could be readily observed whether these cells initially expressed high or low levels of GFP-PARP-1.

The N-terminal DNA binding domain (DBD) of PARP-1 containing first two zinc fingers was shown to be sufficient for its recruitment to different types of DNA damages caused by laser irradiation of cells [404, 405]. In the cells transiently transfected with GFP-

DBD, the colocalization of DBD with T-T was evident only in low DBD-expressers, as shown in low and high exposure panels of C-protocol (Fig. 4.2b). The ability to discern co-localization of GFP-DBD to T-T lesion sites was significantly improved by 1.5 and 2.1 times with C+T protocol and C+T+S protocol, respectively (Fig. 4.2b, chart). Immunoblotting for GFP-DBD and endogenous untagged PARP-1 in control cell pellets in these extraction protocols revealed that the extent of removal of exogenous GFP- DBD at each step was similar to that of the endogenous cellular PARP-1 (Supplementary Fig. S4.1c). Our results show that the N-terminal DBD of PARP-1 is sufficient to recognize and bind to UVC-induced DNA damage.

To assess the specificity of the new protocol, we examined the status of UV-induced colocalization of unrelated proteins, such as the exogenous tag protein GFP (Fig. 4.2c) or the cellular DNA double strand break-repair protein Rad51 (Fig. 4.2d) at UV-lesion spots after processing with all three protocols. Although C+T and C+T+S protocols progressively removed both of these proteins from the cells, neither GFP nor Rad51 colocalized with UV-induced T-T lesions. Thus, our results show that the C+T+S protocol does not cause an artifact of random colocalization of unrelated proteins with UV-damaged DNA. This simple yet selective in situ fractionation protocol to reveal PARP-1 at UV-lesion site would be useful in studying other NER-related roles of PARP-1 with or without its catalytic activation at the site of UV-damaged DNA.

An oligo with defined UV-lesion for restriction mapping of PARP-1

To determine the exact footprint of PARP-1 at the UV-lesion site, we created biotin-tagged 40mer oligonucleotides with or without a single defined UV-lesion surrounded by multiple unique restriction enzyme sites (Supplementary Fig. S 4.2a). The UVC-irradiation of the top strand of the oligo, which has only one pair of adjacent Ts and no other adjacent pyrimidines (T or C), resulted largely in the formation of T-T rather than 6-4PP lesions (Supplementary Fig. S 4.2b). The inability of restriction enzymes to digest through UV-induced CPD [406, 407] was exploited for purification of UV-DNA with VspI enzyme to remove all DNA molecules that did not form T-T at this site (Supplementary Fig. S 4.2c).

The biotin-tagged complementary strand for both control and UV-DNA allowed a common procedure for their immobilization to streptavidin beads (Fig. 4.3a). We reasoned that any protein bound at or around the UV-lesion site would prevent the restriction enzyme from digesting the DNA at that site; and thus decrease the quantity of non-biotinylated 5'-restriction fragment released from bead-bound DNA into the supernatant. This model allowed us to compare the extent of binding of proteins to control versus UV-DNA and also provide a non-isotopic method to footprint proteins on UV-DNA.

PARP-1 and DDB2 bind more to UV-DNA than control DNA

We had shown in the cells and *in vitro* that PARP-1 not only binds to UV-damaged DNA [396], but also interacts with DDB2 in the vicinity of UV-induced DNA lesions [392]. Using the model oligo described in Fig. 4.3a, we examined the extent of binding of PARP-1 and DDB2 to control and UV-DNA at two different molar ratios of protein : DNA (Fig. 4.3b). The 2.1-2.2x fold higher binding of DDB2 to UV-DNA than the control-DNA at these two molar ratios is in agreement with a previous report [408]. The binding of PARP-1 to UV-DNA was also 1.5-1.7x fold more than the control-DNA (Fig. 4.3b). We confirmed that PARP-1 did not bind to the beads per se unless DNA was attached to it (Supplementary Fig. S 4.3a: left panel). To determine the site of PARP-1 binding to the control DNA without UV-lesion, we digested PARP-1-bound control DNA with VspI or NspI and noted that PARP-1 was attached more to the bead-bound 3'-end than to the 5'-end that is released after the restriction digestion (Supplementary Fig. S 4.3a: right panel). This could be due to the linker attached biotin providing a pseudo-overhang at the 3'-end unlike blunt 5'-end, because PARP-1 has higher affinity for overhangs as compared to the blunt ends of DNA [409]. However, since the same 3' and 5'-ends exist in both control and UV-DNA, any increase in PARP-1 binding to UV-DNA as compared to control-DNA must be due to the interaction of PARP-1 with UV-lesion, which we footprinted using a series of restriction enzymes that digest on either side of the lesion.

Restriction protection profile of PARP-1 is distinct from that of DDB2 on either side of the T-T lesion

We established the optimal amount of DNA required in the assay for detection of DNA fragments released after digestion with restriction enzyme (Supplementary Fig. S 4.3b) and also confirmed that both the control and UV-DNA without bound protein could be digested by all the restriction enzymes used in our footprinting assays (Supplementary Fig. S 4.3c-d). Thus, any restriction protection offered to DNA after reaction with protein could be attributed to the footprint of the protein. During the restriction digestion by NspI and MslI that recognize sequences from -2 to -12nt on the 5'-side of the T-T lesion, PARP-1 offered more protection to UV-DNA than control DNA, as seen from a significant PARP-1 dose-dependent decrease in the corresponding 5'-fragments released by these enzymes (Fig. 4.4a). Thus, the footprint of PARP-1 on UV-DNA extended from 2-12nt upstream of the lesion site. In contrast, DDB2 failed to protect UV-DNA against NspI (-2 to -7 nt), indicating that its footprint stays within 2nt on the 5'-side of T-T, as reported earlier [77].

PARP-1 has been shown to have a bilateral footprint of 7nt on either side of DNA single strand breaks [410]. Therefore, we compared the protections offered by PARP-1 and DDB2 against the restriction enzymes ApalI and Bsp1286I that target from 3 to 9nt on the 3'-side of the T-T lesion. The DDB2 did not offer any protection to control or UV-DNA against ApalI (Fig. 4.4b), indicating that its footprint does not exceed beyond 3nt on 3'-side of T-T, as reported earlier [77]. In contrast, PARP-1 offered a strong but equal protection to both UV and control oligos against both the enzymes, possibly due to PARP-1 bound to 3'-ends of both types of DNA, as noted earlier (Supplementary Fig. S 4.3a: right panel). Thus using 40mer oligo, it was difficult to discern additional protection, if any, offered by PARP-1 that is bound at or near T-T site from the protection offered by PARP-1 that is bound to the 3'-end of the oligo.

To resolve this issue, we extended the size of 40mer oligo on either ends to create a 60mer, in which 3'-end was significantly separated from these two restriction sites and added a new RsaI restriction site at +11 nt from T-T (Fig. 4.4c, top panel). PARP-1 significantly

protected 60mer UV-DNA against digestion by Bsp1286I as compared to control DNA, confirming its footprint up to +9nt from T-T lesion. Moreover, the lack of any additional protection by PARP-1 to UV-DNA against digestion by RsaI defined that PARP-1 footprint does not reach up to +11nt from T-T site (Fig. 4.4c). Thus using restriction-mapping technique on our model oligo, we show that PARP-1 bound at or near the T-T lesion extends asymmetric bilateral protection against restriction digestion from -12 to +9nt around the lesion.

Next, we examined whether PARP-1 and DDB2 can simultaneously bind to UV-DNA and whether DDB2 bound at the T-T lesion would alter the footprint of PARP-1 around the lesion. Using 60mer oligo, we noted that when incubated together, both DDB2 and PARP-1 could bind to UV-DNA (Fig. 4.4d, left panel). We observed in two independent experiments that the presence of PARP-1 increased the binding of DDB2 to UV-DNA, whereas that of DDB2 reduced the binding of PARP-1. However, the presence of DDB2 did not affect the restriction footprint of PARP-1 on UV-DNA, because PARP-1 offered identical protection to UV-DNA against restriction digestion on either side of the lesion site by MslI and Bsp1286I in the absence or the presence of DDB2 (Fig. 4.4d, right panel). Thus, the footprint of PARP-1 around the lesion was not compromised in the presence of DDB2 whereas DDB2 was more stabilized in the presence of PARP-1.

<u>No effect of PARP-1 and DDB2 binding on CPD-photolyase mediated repair of T-T in UV-DNA</u>

Unlike restriction enzymes that cleave the DNA in the sugar phosphate backbone, the CPD photolyase directly removes the cross-linking of adjacent pyrimidines in the CPD photolesions such as T-T [411]. Structural studies have revealed that DDB2 has a protein fold that flips out and maintains contact with T-T [77], and our results indicate that PARP-1 also remains in the vicinity of T-T lesion. Hence, we examined whether binding of DDB2 or PARP-1 to UV-DNA could influence the repair of T-T by CPD photolyase (Fig. 4.4e). The immunodot-blot of DNA with or without photolyase treatment revealed that binding of DDB2 or PARP-1 to DNA could not inhibit the ability of photolyase to repair the T-T lesions,

indicating that these two proteins do not exclude other repair proteins from accessing the lesion. This is also in agreement with a previous report that binding of DDB2 to UV-DNA does not prevent CPD photolyase from repairing the UV-lesion [412].

Catalytic activation of PARP-1 is stronger with 6-4PP than T-T lesion

We used the model oligos for further characterization of the interaction of PARP-1 with UV-damaged DNA. Since the catalytic activation of PARP-1 is more with damaged DNA than with undamaged DNA [399], we examined the extent of activation of PARP-1 with 40mer control or UV-oligo *in vitro* as an additional indicator of the extent of binding of PARP-1 to these DNA. A stronger PARP-1 activation with UV-DNA was observed as compared to control-DNA at two different molar ratios of PARP-1 to DNA (Fig. 4.5a, left panel). Thus the binding of PARP-1 to UV-lesion caused stronger stimulation of its catalytic activity as compared to its binding to either the 3' or 5'-ends of both the control and UV-DNA. To compare the capacity of different UV-induced direct damages for activation of PARP-1, we assessed the efficacy of 24mer oligo containing a single chemically synthesized T-T or 6-4PP lesion [413] in the PARP-1 activation assay *in vitro* (Fig. 4.5a, right panel). Both the DNA containing defined UV-lesions were stronger activator of PARP-1 than the 24mer control-DNA at two different molar ratios of PARP-1 to DNA. Moreover, 6-4PP, which is known to cause a higher degree of helical distortion, was a stronger stimulator of the catalytic activity of PARP-1 than T-T.

Model for the interaction of PARP-1 and DDB2 with UV-damaged DNA.

Based on the current results of in situ visualization and footprinting of PARP-1 and DDB2 at UV-induced DNA lesion site, we propose that DDB2 attaches directly at the UV-lesion site whereas PARP-1 makes an asymmetric bilateral contact from -12 to +9nt around the lesion (Fig. 5b). This footprint is compatible with either one or two PARP-1 molecules enveloping around the UV-lesion, similar to the reported binding of either one [414] or two [405] PARP-1 molecules binding at the site of DNA strand breaks. The N-terminal DNA binding domain of PARP-1 that is known to be recruited to DNA strand breaks [404] was

also recruited to UV-lesions without strand breaks, indicating more general property of this domain of PARP-1 to bind to different types of DNA damages. Our model is also consistent with previously reported interactions of DDB2 and PARP-1 at the UV-lesion site [390, 392]. We have earlier shown that PARP-1 and DDB2 co-immunoprecipitate at the UV-damaged chromatin in the presence of ethidium bromide, indicating their direct interaction on the same DNA strand [392]. Here, we confirm that PARP-1 and DDB2 can co-exist at the UV-lesion site and the presence of DDB2 does not alter the footprint of PARP-1 around the lesion. Our results do not exclude the possibility that PARP-1 footprint may vary when the damaged DNA is in the context of chromatin or when there are multiple UV-lesions in close proximity. We had earlier shown that PARP-1 is weakly activated by UV in the DDB2-deficient XP-E cells, but introduction of DDB2 in these cells strongly stimulates PARP-1 catalytic activity in response to UV [392]. Moreover, we had also observed that DDB2 stimulates catalytic activity of PARP-1 *in vitro* with UV-damaged DNA that largely contains T-T lesions [392], and here we show that PARP-1 activation was much stronger with 6-4PP than with T-T. Since the 6-4PP by itself causes larger distortion of DNA as compared to T-T, whereas the binding of DDB2 to T-T increases the distortion of DNA [77], collectively these results indicate that the extent of DNA distortion could be the determinant for PARP-1 activation with UV-damaged DNA. Our results show that PARP-1 and DDB2 do not prevent access to the lesion site by other repair proteins such as CPD photolyase, and may even be more flexible and accommodating in vivo conditions as compared to our *in vitro* condition in which damaged DNA is anchored to beads and interacting proteins are cross-linked to the DNA. Together, these two novel assays will open new avenues to study the ever-expanding roles of PARP-1 in NER and housekeeping functions in which PARP-1 shows subtle interactions with DNA without strand breaks.

4.6 Figures and legends

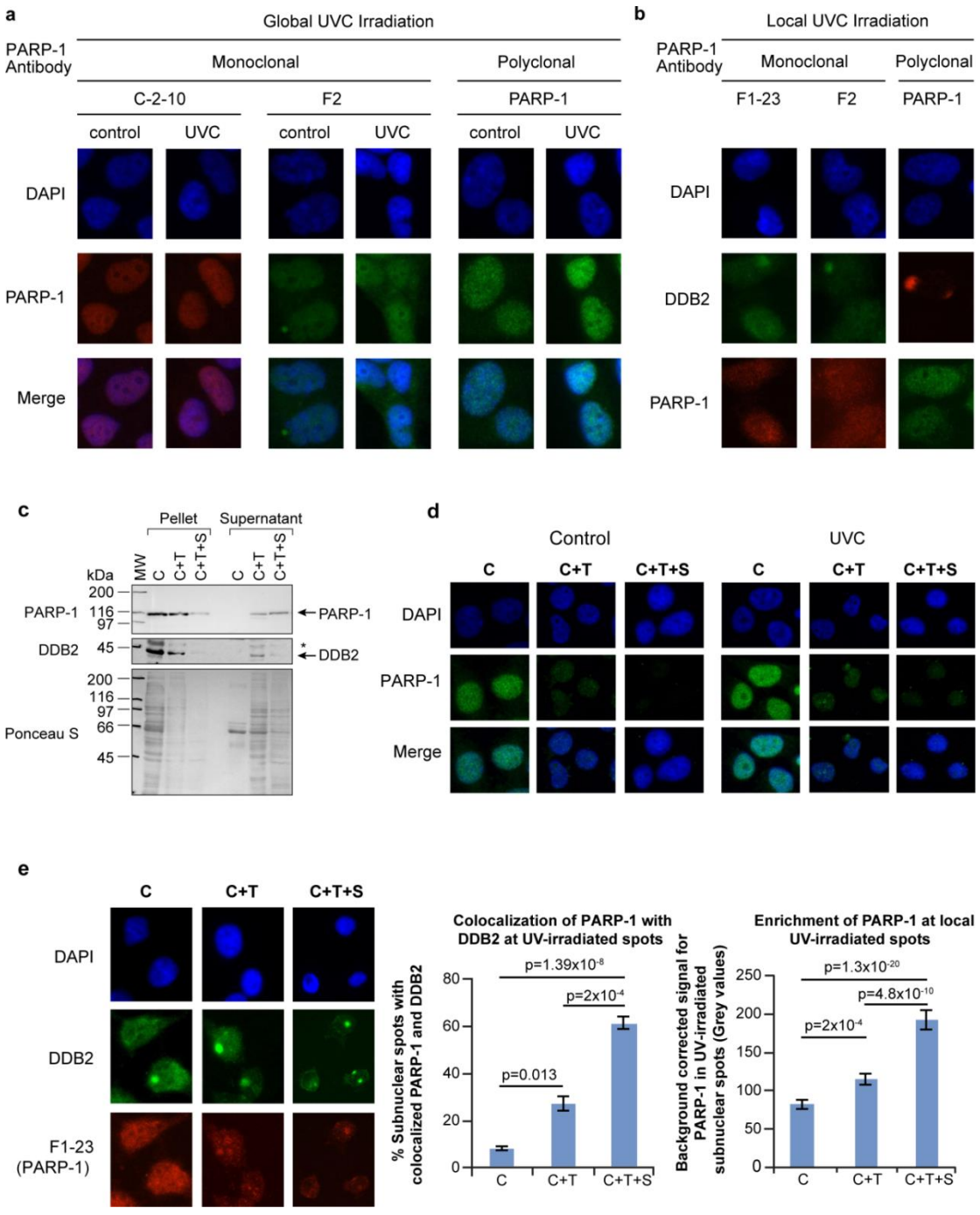

Figure 4.1 In situ fractionation to reveal the recruitment of endogenous PARP-1 to UV-induced DNA lesion site.

(a-b) Unchanged pattern of nuclear staining for PARP-1 after global or local UVC-irradiation of cells processed with conventional immunocytological techniques. Human skin fibroblasts were exposed either to global (panel a) or local (panel b) irradiation with UVC, fixed with formaldehyde-methanol and probed for PARP-1 (global and local UVC) and DDB2 (local UVC) using specified antibodies. DAPI staining was carried out to define nuclei. **(c)** Efficiency of extraction of free PARP-1 and DDB2 from adherent control GMU6 cells. The pellets and supernatants obtained from equivalent cell numbers after extraction with CSK buffer (C), CSK+0.5 % Triton (C+T) or CSK + 0.5 % Triton + 0.42 M NaCl (C+T+S) were immunoblotted for PARP-1 and DDB2. The * refers to non-specific signal in DDB2 probing and Ponceau S staining reflected the residual protein content in cell pellets and supernatant at the end of each protocol. **(d)** Comparison of the efficiency of three protocols for extraction of the endogenous PARP-1 from adherent control and UV-irradiated cells. The GMU6 human skin fibroblasts were globally irradiated with 10 J/m^2 UVC (or control), extracted 10 min later with the three protocols and probed for PARP-1 using polyclonal PARP-1 antibody. **(e)** Colocalization of endogenous PARP-1 with DDB2 at local UVC-induced DNA damage. GMU6 cells were irradiated locally with 100 J/m^2 and after 10 min subjected to the three protocols (C, C+T and C+T+S) followed by visualization of PARP-1 (F1-23, red) and DDB2 (green). The left chart represents the percent of subnuclear PARP-1 spots that colocalize with DDB2. The right chart represents the quantification of the PARP-1 intensity at the DDB2 spots after subtraction of background signal intensity for PARP-1 from an equivalent area of unirradiated part of the same nucleus. Data of the charts are pooled from three experiments (n = 120 -150 spots, data points are mean ± s.e.).

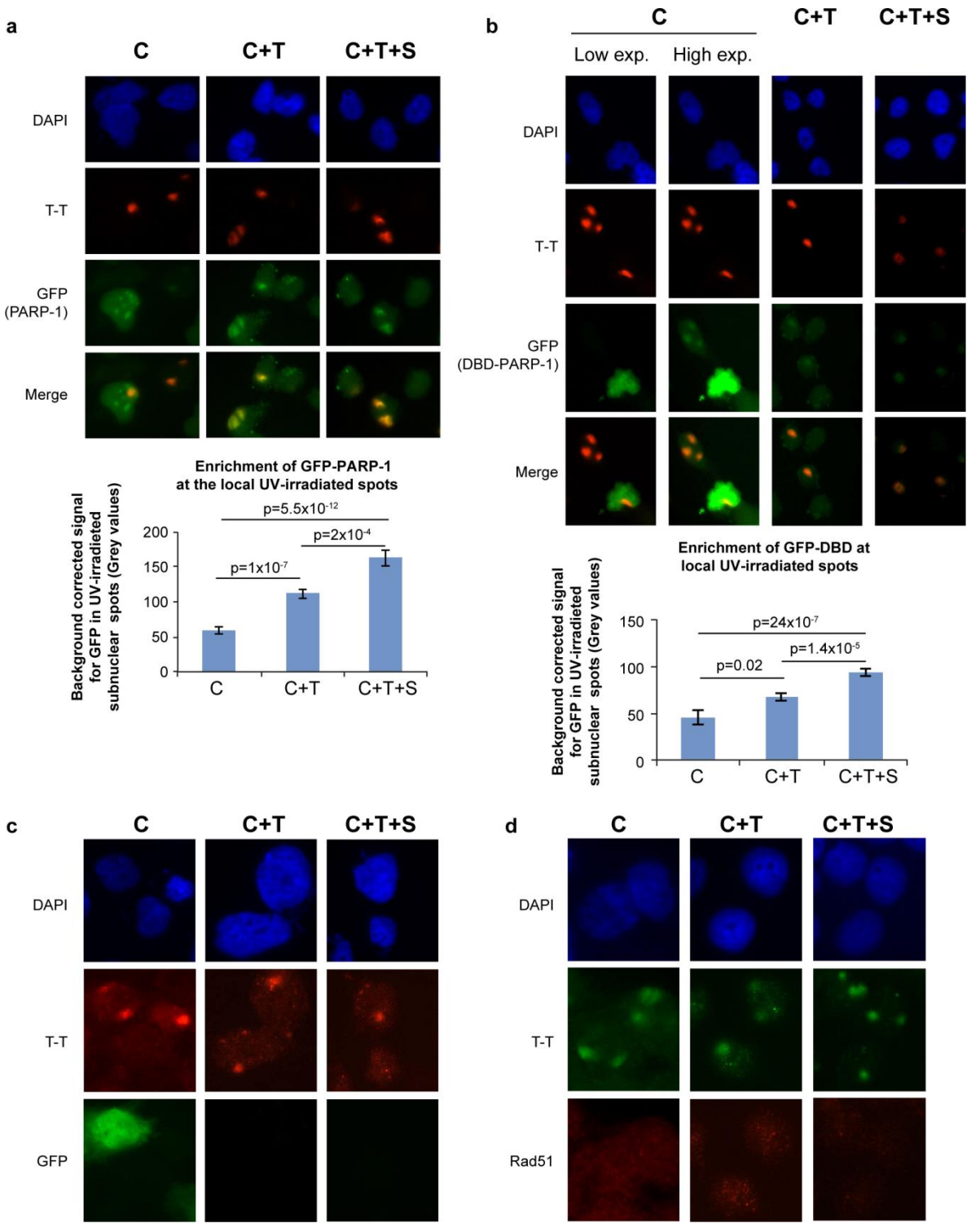

Figure 4.2 In situ fractionation improves detection of exogenous GFP-PARP-1 or its DNA binding domain at local UV-irradiated spots.

(a-b) Recruitment of GFP-PARP-1 or its DBD to UV-induced T-T lesions. GMU6 cells were transfected with GFP- PARP-1 or GFP-DBD of PARP-1 for 24 h. The cells were locally irradiated and processed by C, C+T or C+T+S protocols. GFP-PARP-1 or GFP-DBD (green) and T-T (red) were visualized in DAPI-stained nuclei by immunofluorescence microscopy. The charts represent the quantification of GFP intensity for GFP- PARP-1 or GFP-DBD of PARP-1 at the T-T spots after background correction. (n = 80–150 spots, data points are mean ± s.e.). **(c-d)** Specificity of in situ extraction protocol: unrelated nuclear proteins (GFP and Rad51) do not colocalize with UV-damaged DNA. GMU6 cells were locally irradiated with 100 J/m^2 UVC and subjected 10 min later to in situ fractionation using the three protocols. For panel-c, the cells were transfected with GFP expressing plasmid 24 h before irradiation and protein extraction. The cells were processed for immunofluorescence detection of GFP, Rad51 (green) and T-T (red). DAPI staining was carried out to define nuclei.

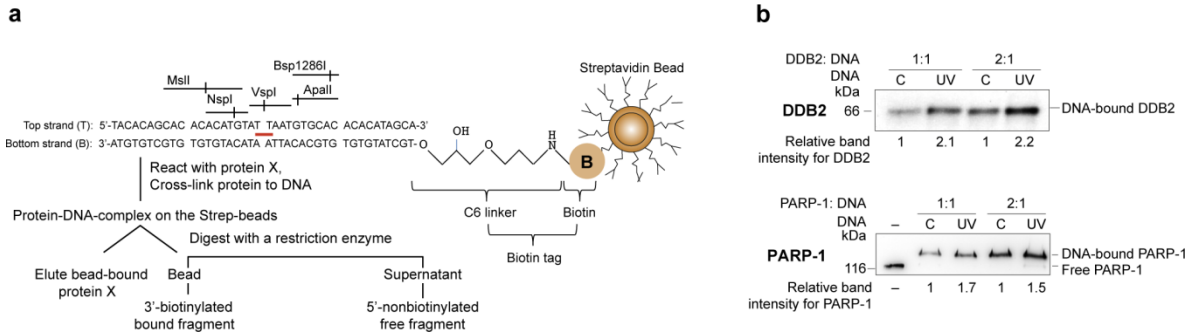

Figure 4.3 Strategy to study binding and footprint of proteins on UV-DNA.

(a) The experimental design for determining the extent of binding of proteins to UV-DNA and analyses of protection of DNA during restriction digestion. The control and UV-DNA were immobilized on streptavidin beads via their biotin tag and reacted with purified PARP-1 or DDB2. The unreacted proteins were removed and bound proteins were cross-linked. The beads were then either analysed for bound-proteins by eluting the protein in Laemmli buffer, followed by SDS-PAGE, transfer and probe with specific antibodies or they were subjected to restriction digestion followed by analyses of the released DNA fragments on 10-15 % native PAGE stained with gel red. **(b)** DDB2 and PARP-1 bind more to UV-DNA than control DNA. PARP-1 and DDB2 were reacted with 50 ng of control or UV-DNA at 1:1 or 1:2 (DNA:protein) molar ratios. The proteins were eluted from the beads, resolved on SDS-PAGE and analyzed by immunoblotting as shown in Fig. 3a. The band intensities of protein bound to UV-DNA are shown as relative to signal for protein bound to control DNA.

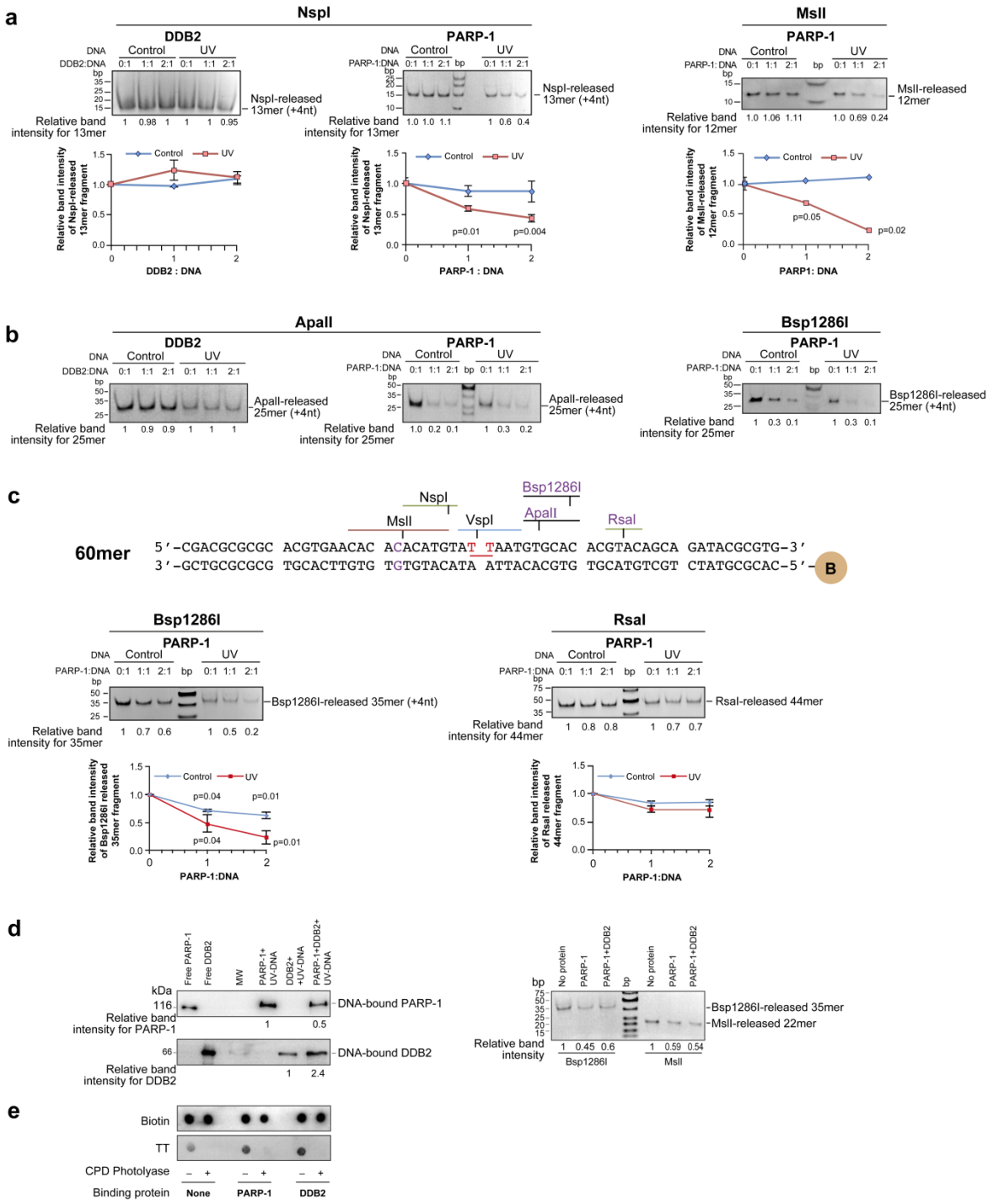

Figure 4.4 Footprinting of PARP-1 and DDB2 at UV-lesion site.

(a) Restriction mapping of proteins on the 5'of the UV-lesion on 40mer DNA. 100 ng of bead-bound control or UV-DNA were reacted with DDB2 or PARP-1 at different DNA: protein ratios and digested at 37° C with NspI (30 min) or MslI (15 min). The released 5'-

fragments were resolved on 15 % native PAGE and band intensities were measured. Each data point derived from three independent experiments represents mean ± s.d. for relative band intensity from three experiments for the fragment released from protein-bound versus protein-free DNA, with *P* values shown in the chart. **(b)** Mapping of proteins on the 3'-side of the UV-lesion on 40mer DNA. The protein-bound DNA was digested with ApalI (60 min) and Bsp1286I (20 min), and released 5'-fragments were resolved on 12% native PAGE. The data derived from two independent experiments is represented in the chart as described in panel-a. **(c)** *Top panel*-Structure of 60mer oligo with defined UV-damage. The 60mer oligo sequence was based on 40mer oligo but with a new RsaI site near 3'-end. *Bottom panels*-Restriction mapping of proteins on the 3'-side of the UV-lesion on 60mer DNA. The protein-bound DNA was digested with Bsp1286I (20 min) and RsaI (30 min) and released 5'-fragments were analysed by 12 % native PAGE. The data derived from three independent experiments is represented in the chart as described in panel-a. **(d)** Simultaneous binding and footprint of DDB2 and PARP-1 on 60mer UV-DNA. PARP-1 and DDB2 were reacted either separately or together with bead-bound UV-DNA (50 ng), at 2:1 molar ratio of protein:DNA. The proteins bound to the beads were detected by immunoblotting (left panels), and footprint of proteins on DNA was examined by restriction digestion with Bsp1286I and MsII (right panels). **(e)** Repair of T-T by CPD photolyase despite binding of DDB2 or PARP-1 to UV-DNA. Bead-bound 40mer UV-DNA was reacted (or not) with DDB2 or PARP-1, and subjected to repair (or not) by CPD photolyase. The DNA was eluted and immunodot-blotted for T-T. The data represents identical results obtained in three independent experiments.

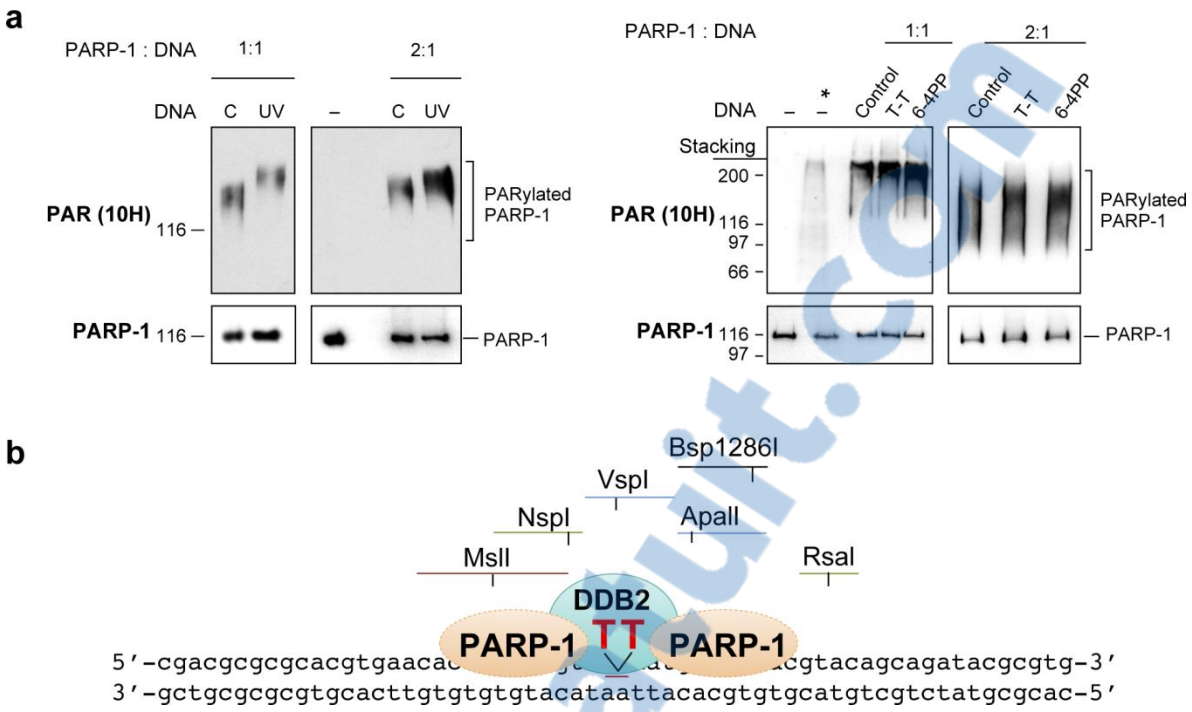

Figure 4.5 Catalytic activation of PARP-1 with defined UV-damaged DNA and a model for footprint of PARP-1 and DDB2 on UV-lesion site.

(a) Stimulation of catalytic activity of PARP-1 by various defined UV-damaged DNA *in vitro*. PARP-1 activation assay was performed using 40mer control or UV-DNA (left panel) or using 24mer DNA with no damage (control) or with a single defined T-T and 6-4PP (right panel) at 1:1 or 1:2 molar ratio of DNA:protein. After resolution on SDS-PAGE, immunoprobing for PARP-1 and PARylated PARP-1 (10H antibody) was carried out. The * refers to the cell extract containing H_2O_2-activated PARP-1. Panel represents one of three identical experiments. **(b)** Model for binding of PARP-1 and DDB2 to the UV-lesion site on 60mer oligo (see Results and Discussion section for details).

Supplementary Figures

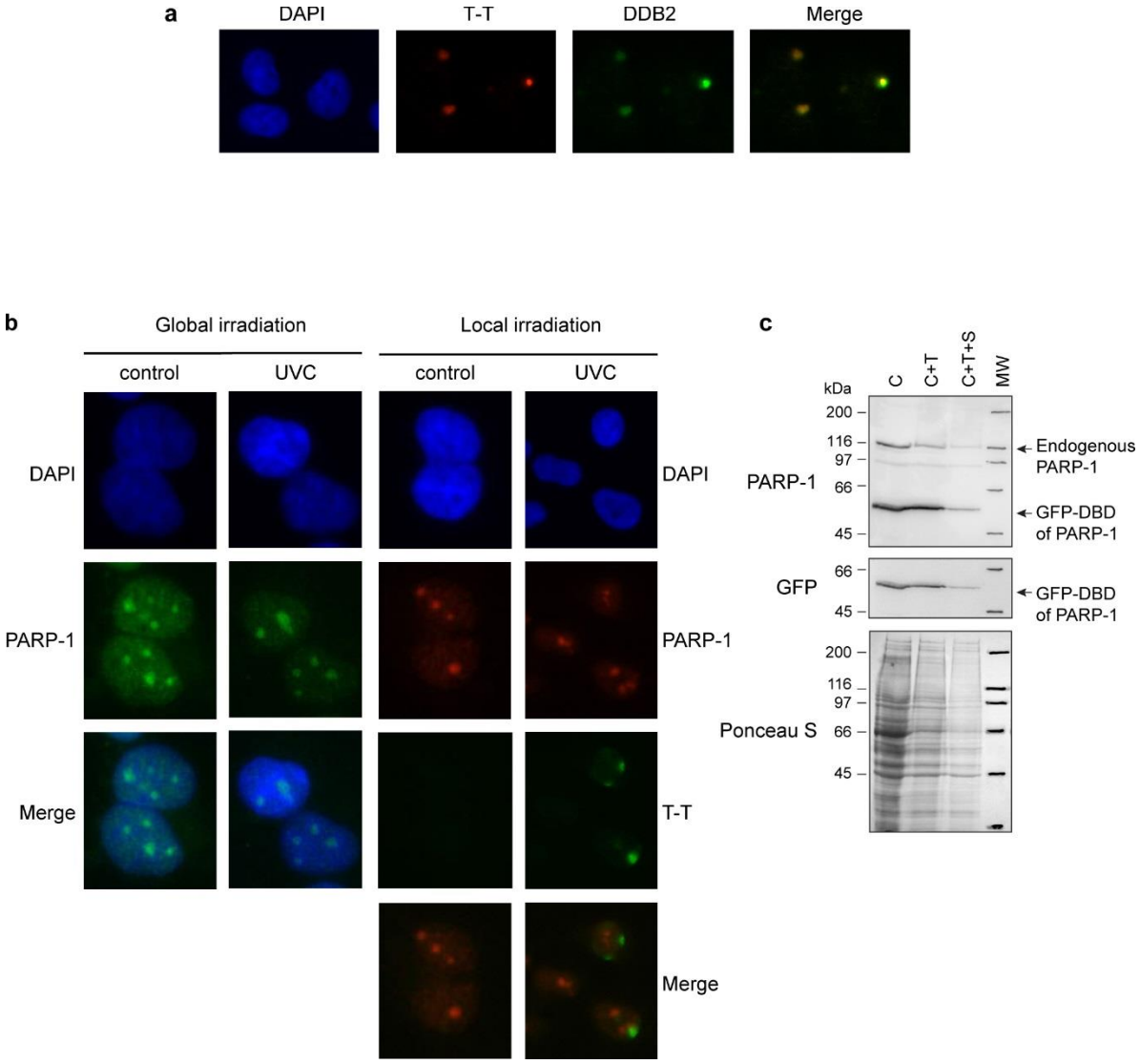

Figure S4.1 Controls for in situ fractionation protocol.

(a) DDB2 colocalizes with T-T spots. GMU6 cells locally irradiated with 100 J/m^2 UVC were probed after 10 min for DDB2 (green) and T-T (red) in DAPI stained cells. **(b)** PARP-1 spots after formaldehyde-Triton protocol do not colocalize with T-T. Human skin fibroblasts growing on coverslips were exposed either to global (10 J/m^2) or local (100 J/m^2) irradiation with UVC and 10 min later fixed with formaldehyde for 10 min followed by 5 min permeabilization with 0.5 % Triton. The globally irradiated cells were probed for PARP-

1 (green) and the locally irradiated cells for PARP-1 (red) and T-T (green). The nuclear DNA was stained with DAPI. **(c)** Verification of the in situ protocol for extraction of GFP-DBD and endogenous PARP-1 in control cells by Western blot. The GMU6 cells were transfected with GFP-DBD of PARP-1 and 24 h later extracted with C, C+T and C+T+S buffers. The cell pellets from equivalent number of cells for each of the three protocols were immunoblotted for GFP and PARP-1. Ponceau S staining reflected the residual protein content in cell pellets at the end of each protocol.

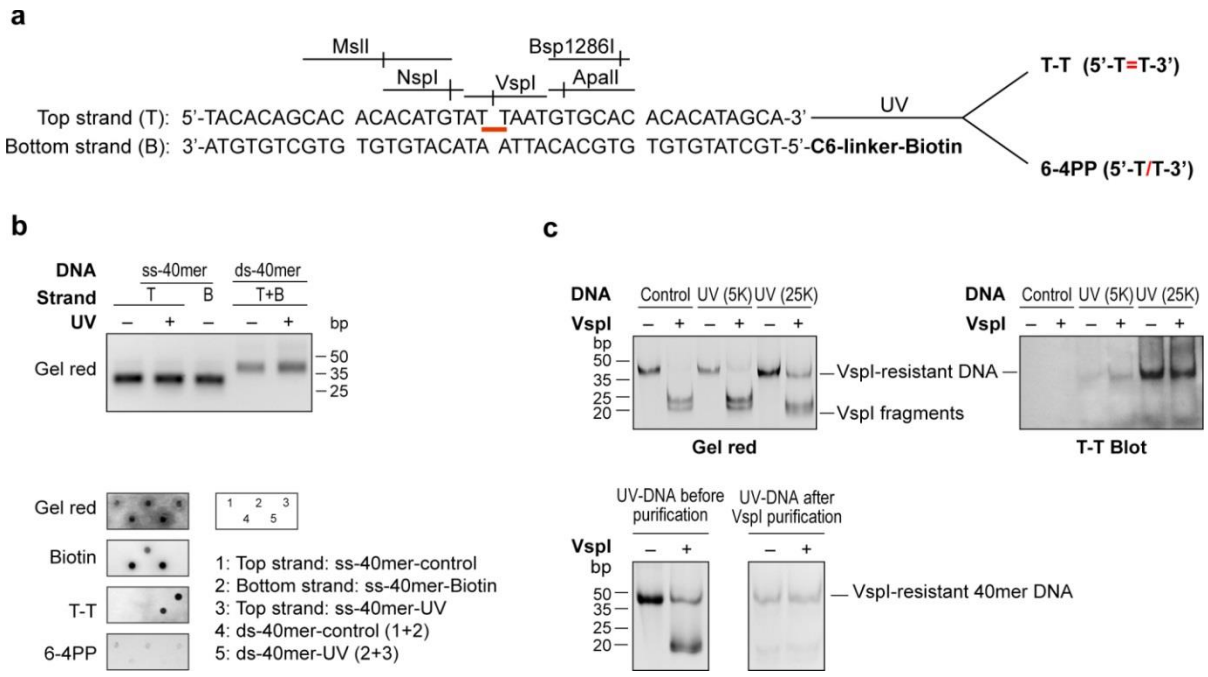

Figure S4.2 Preparation and characterization of double stranded (ds) 40mer DNA.

(a) Construction of biotinylated ds 40mer with and without defined T-T. The top single strand (ss) 40mer sequence was designed to carry only one adjacent pair of Ts, and no other pair of pyrimidines, i.e., T or C. The complementary bottom ss 40mer contained a biotin tag at its 5'-end attached via a 6-carbon linker chain. For UV-DNA with defined T-T, the top strand was irradiated in TE at 25,000 J/m^2 UVC at the fluence rate of 51.2 J/m^2/sec in Spectrolinker XL1000. Where specified, top strand was also irradiated with lower UVC-dose (5,000 J/m^2) at the fluence rate of 10 J/m^2/sec. The control and UV-irradiated top ss oligos were annealed with biotin tagged complementary bottom strand to form control and UV ds 40mer oligos, respectively. **(b)** *Top panel*-The ss 40mer and ds 40mer were verified on agarose gel. *Bottom panel*- 25 ng of the individual ss and the resulting ds 40mer were spotted on charged nylon membrane, and probed for T-T, 6-4PP, biotin and stained with gel red (to indicate the loading of DNA). **(c)** Enrichment of 40mer UV-DNA using VspI. Top left panel- Control, 5,000 and 25,000 J/m^2 UVC irradiated DNA were digested (37° C for 1 hr) with VspI (or undigested) and resolved on 12 % native PAGE. Top right panel- Same as top left, but the native PAGE

resolved DNA was transferred on charged nylon membrane for 75 min at 0.2 A (45-60V) and probed for T-T. *Bottom left and right panel*-Purification of T-T containing DNA using VspI digestion. The undigested and VspI-digested 25,000 J/m^2 UV-DNA were run on 12 % native PAGE before (bottom left) and after purification (bottom right).

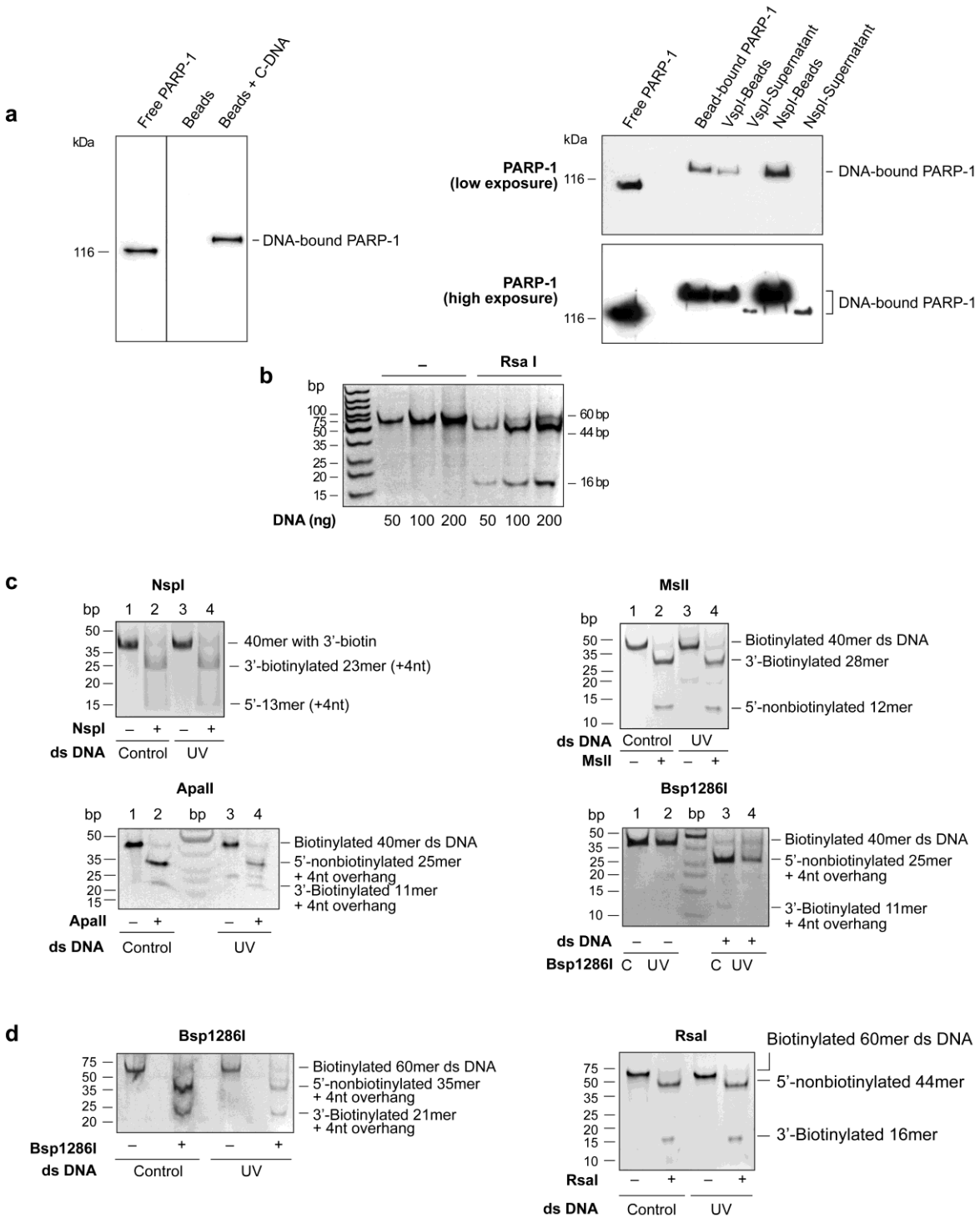

Figure S4.3 Optimization of protein binding and restriction assays with control and UV-DNA.

(a) PARP-1 binds to bead-bound 40mer control DNA mainly at 3'-end of oligo and does not bind to streptavidin beads per se. *Left panel*- PARP-1 was reacted with either free streptavidin beads or beads bound to control DNA. The bound-protein was immunoblotted for PARP-1. *Right panel*- Bead-bound control DNA was reacted with PARP-1 and the reaction mixture divided in three equal aliquots. One aliquot was not reacted with any restriction enzyme (bead-bound PARP-1) and other two aliquots were digested with VspI or NspI. Immunoblotting was carried out to detect PARP-1 that was attached to the bead-bound undigested 40mer, the 5'-restriction fragment of DNA released in the supernatant and 3'-restriction fragment of DNA bound to the beads. **(b)** Optimization of DNA concentration in restriction digestion assay. The 50-200 ng control 60mer DNA were digested with RsaI and the resulting 3' and 5' DNA fragments were resolved on 15 % native PAGE and visualized using gel red. **(c)** Digestion of protein-free 40mer control or UV-DNA with different restriction enzymes. Both DNA were digested at 37˚ C with NspI for 30 min (top left panel), MslI for 15 min (top right panel), ApalI for 1h (bottom left panel) and Bsp1286I for 20 min (bottom right panel). The DNA or its fragments recovered from undigested and enzyme digested samples were resolved on native PAGE prior to detection with gel red. **(d)** Digestion of protein-free 60mer control or UV-DNA with different restriction enzymes. Both the DNA were digested at 37˚ C with Bsp1286I for 20 min (left panel) or RsaI for 30 min (right panel), followed by detection of DNA or its fragments as described above.

4.7 Material and methods

Antibodies: For Western blotting: Monoclonal 6-4PP (KTM50) and T-T (KTM53) (1:5,000), polyclonal PARP-1 (1:5,000), PARP-1 monoclonal (F2, 1:500), GFP monoclonal (1:5,000), DDB2 anti goat (1:500), PAR monoclonal (10H, 1:1,000), HRP-conjugated secondary antibodies (1:2,500). For immunocytology: T-T (KTM53, 1:2,000), polyclonal PARP-1 (1:5,000), PARP-1 monoclonal F2 (1:500), PARP-1 monoclonal C2-10 (1:500), F1-23 monoclonal (1:500), DDB2 anti goat (1:200), Rad51 polyclonal (1:500) and secondary fluorescent antibodies (1:500).

Cell culture: Cells were grown in 5 % humidified incubator at 37º C in □MEM medium supplemented with 10 % FBS, penicillin and streptomycin and 200 µg/ml hygromycin. The creation of GM637-derived PARP-1 replete GMU6 cells were described earlier [415].

Expression Plasmids: The pGFP-hPARP-1 was a gift from V. Schreiber, pGFP-DBD of PARP-1 was generated by subcloning the 0.7 kb SacI (blunted) and HindIII-fragment of PARP31 cDNA into NheI (blunt)/HindIII sites of pEGFP-N1 plasmid.

Transfection and UVC-irradiation: GMU6 cells were transfected with pEGFP-hPARP-1, pEGFP-DBD-PARP-1 and pEGFP-N1 plasmid using Turbofect reagent**.** After 24 h, cells were irradiated for global UVC (10 J/m^2) or through polycarbonate filter with 5 µm pores for local (100 J/m^2) UVC [396].

Indirect immunofluorescence detection in situ: The cells adherent on the coverslip were processed by one of the three protocols: *C protocol:* After washing with CSK buffer (100 mM NaCl, 300 mM sucrose, 10 mM PIPES pH 6.8, 3 mM $MgCl_2$, 1 mM EGTA), cells were fixed with 3 % formaldehyde (10 min, ambient temperature), rinsed with PBS, permeabilized with 100 % methanol (-30º C, 10 min), rinsed with PBS, blocked for 30 min with 5 % BSA in PBS-0.1 % Triton-X-100 followed by reaction with primary antibodies given below. *C+T protocol:* Cells were washed twice with CSK buffer, extracted with 0.5 % Triton in CSK buffer for 8 min at ambient temperature, fixed and blocked as in C protocol. *C+T+S protocol:*

After C+T protocol fixation step, cells were washed and extracted with 0.5 % Triton in high salt CSK buffer (420 mM NaCl, 300 mM sucrose, 10 mM PIPES pH 6.8, 3 mM $MgCl_2$, 1 mM EGTA) for 20 min on ice. After DNA denaturation in 0.07 N NaOH for 8 min at ambient temperature, immunoprobing was carried out for all three protocols as follows: The cells were incubated for 1 h with primary antibodies in the blocking buffer, washed with PBS containing 0.1 % Tween 20 and incubated for 30 min with Alexa 488 or 594-linked secondary antibodies. After washing with PBS-0.1 % Tween 20, coverslips were incubated in PBS-0.25 µg/ml DAPI for 5 min and mounted with ProLong Gold Antifade. Images were captured with Zeiss Axiovert 200 and AxioCam MRm and the brightness and contrast were uniformly adjusted across the panels with Photoshop CS5.5. The fluorescent intensity of PARP-1 at the irradiated spots was analyzed with AxioVision 4.7 and corrected for background signal for similar area in the unirradiated zone of nucleus, where specified.

Statistical analyses for immunocytology: Data for intensity of at least 100 foci from three independent experiments were pooled to create mean $\pm$ s.e., and subjected to the unpaired two-tailed t-tests to determine the significance of difference. The significant *P*-values <0.05 are stated in the charts.

Oligos: The ss-24mer oligos with T-T or 6-4PP were chemically synthesized and hybridized with the complementary ss-24mer to get 24mer ds oligo with T-T or 6-4PP lesions. The creation of 40 or 60mer oligos are described in Figs. 3a, 4c, and Supplementary Fig. S2a.

VspI-purification of 25 kJ/m^2 UVC irradiated oligo. The UVC irradiated 40mer or 60mer ds oligos were digested with VspI for 1 h at 37° C, followed by VspI-inactivation at 65° C for 5 min. The VspI-resistant 40 or 60mer UV-DNA were separated on 12 % PAGE from the digested fragments of DNA without UV-damage, cut from the gel and eluted with PAGE elution buffer (0.5 M ammonium acetate, 10 mM magnesium acetate and 1 mM EDTA) overnight at 37° C. The eluted UV-DNA were cleaned by passage through ULTRAFREE–DA filter units, concentrated in Microcon YM-10 followed by purification in Zymo Research oligo clean and concentrator columns.

The protein-DNA interactions, restriction mapping and CPD photolyase assays for bead-bound oligos with proteins: The control or UV-DNA with biotin tag was immobilized on Dynabeads MyOne streptavidin T1.

(i) The binding of PARP-1 or DDB2 to control or UV-oligos immobilized on the magnetic streptavidin beads: The bead-bound oligos (50-100 ng) were reacted with PARP-1 or DDB2 at 1:1 or 1:2 molar ratio. PARP-1 was reacted at 25° C for 15 min in 10 µL of Na-PO_4 reaction mixture (20 mM of Na-PO_4 buffer pH 7.4, 5 mM $MgCl_2$, 150 mM NaCl, 5 % glycerol, 1 mM DTT, 0.01 % Triton, 20 µM Zn-acetate and 1X protease inhibitor). DDB2 was reacted at 25˚ C for 30 min in Tris reaction mixture (100 mM Tris buffer pH 8.0, 10 mM $MgCl_2$, 10 % glycerol, 150 mM NaCl, 1.5 mM DTT and 1X protease inhibitor). The simultaneous binding of PARP-1 and DDB2 was carried out in Tris reaction mixture for 15 min at 25˚ C. The unbound proteins were removed and the bound proteins were crosslinked to oligo with 1 % formalin in Na-PO_4 reaction mixture for 10 min at ambient temperature. After quenching formalin with 250 mM Tris-HCl pH 8.0, the beads were washed twice with Tris-reaction mixture and subjected to following steps.

(ii) Assessment of binding of proteins with DNA: The proteins that were attached to bead-bound DNA were extracted with Laemmli buffer at 95° C for 10 min. The eluted proteins were resolved on SDS-PAGE for immunoblotting of the protein. The band quantification for immunoblots was carried out with ChemiGenius 2 using SynGene software.

(iii) Restriction protection assay of protein-bound oligos: For the restriction protection assay, the magnetic streptavidin beads bound control or UV-DNA with or without bound protein were digested with the specified Fast-digest or CutSmart restriction enzyme in 10 µL reaction buffer at 37° C for specified time. The DNA fragments released in the supernatant were resolved on 10-15 % native PAGE and stained with gel red for identification and quantification with ChemiGenius2 using SynGene software. The relative band intensities were derived by comparing the intensities of the fragments released from the protein-bound DNA with that from protein-free DNA. The significance was calculated by unpaired two-tailed t-test and the *P* values <0.05 were considered significant.

(iv) CPD photolyase repair assays: The bead-bound UV-DNA with or without attached proteins was split into two aliquots; one subjected to repair by CPD photolyase and the other was mock-treated. The CPD repair was carried out in 20 µL CPD photolyase binding mix (20 mM Tris buffer pH 7.5, 1 mM DTT, 0.2 mg/ml BSA, 125 mM NaCl) with 0.2 µL Oryza sativa CPD photolyase and incubated for 15 min in dark at ambient temperature, followed by exposure for 15 min to UVA (Spectrolinker XL-1500, 363 nm, 15 watts). DNA was eluted with 95 % formamide, 10 mM EDTA pH 8.0 for 5 min at 95° C, dot-blotted on the Hybond N^+ and probed for T-T.

PARP-1 activation assay *in vitro*. In a 10 µL reaction mixture containing 100 mM Tris-HCl pH 8.0, 10 mM $MgCl_2$, 10 % glycerol, 1.5 mM DTT, 1X protease inhibitor and 10 µM NAD, purified PARP-1 was reacted at 25° C for 30 min with specified DNA for each reaction. After adding an equal volume of 2X Laemmli buffer, samples were resolved on SDS-PAGE and immunoblotted for PAR (10H) and PARP-1 [399].

Immuno-Dot-blot. DNA samples were heated at 95° C for 5 min, chilled on ice for 5 min and adjusted to final concentration of 6X SSC. Samples were dot-blotted on Hybond N+ membrane, baked at 80° C for 1-2 h and processed for antibody probing.

4.8 References

1. Robert, I., Karicheva, O., Reina San Martin, B., Schreiber, V., and Dantzer, F. Functional aspects of PARylation in induced and programmed DNA repair processes: Preserving genome integrity and modulating physiological events. *Mol. Aspects Med.* **34**, 1138-1152 (2013).

2. Pascal, J. M., and Ellenberger, T. The rise and fall of poly(ADP-ribose): An enzymatic perspective. *DNA Repair (Amst)* **32**, 10-16 (2015).

3. Kim, M. Y., Mauro, S., Gevry, N., Lis, J. T., and Kraus, W. L. NAD+-dependent modulation of chromatin structure and transcription by nucleosome binding properties of PARP-1. *Cell* **119**, 803-814 (2004).

4. Ghodgaonkar, M. M., Zacal, N. J., Kassam, S. N., Rainbow, A. J., and Shah, G. M. Depletion of poly(ADP-ribose)polymerase-1 reduces host cell reactivation for UV-treated adenovirus in human dermal fibroblasts. *DNA Repair (Amst)* **7**, 617-632 (2008).

5. Pines, A., *et al.* PARP1 promotes nucleotide excision repair through DDB2 stabilization and recruitment of ALC1. *J. Cell Biol.* **199**, 235-249 (2012).

6. Luijsterburg, M. S., *et al.* DDB2 promotes chromatin decondensation at UV-induced DNA damage. *J. Cell Biol.* **197**, 267-281 (2012).

7. Robu, M., *et al.* Role of poly(ADP-ribose) polymerase-1 in the removal of UV-induced DNA lesions by nucleotide excision repair. *Proc. Natl. Acad. Sci. U.S.A.* **110**, 1658-1663 (2013).

8. King, B. S., Cooper, K. L., Liu, K. J., and Hudson, L. G. Poly(ADP-ribose) contributes to an association between Poly(ADP-ribose)polymerase-1 and Xeroderma pigmentosum complementation group A in nucleotide excision repair. *J. Biol. Chem.* **287**, 39824-39833 (2012).

9. Fischer, J. M., *et al.* Poly(ADP-ribose)-mediated interplay of XPA and PARP1 leads to reciprocal regulation of protein function. *FEBS J.* **281**, 3625-3641 (2014).

10. Maltseva, E. A., Rechkunova, N. I., Sukhanova, M. V., and Lavrik, O. I. Poly(ADP-ribose)polymerase 1 Modulates Interaction of the Nucleotide Excision Repair Factor XPC-RAD23B with DNA via Poly(ADP-ribosyl)ation. *J. Biol. Chem.* **290**, 21811-21820 (2015).

11. Vodenicharov, M. D., Ghodgaonkar, M. M., Halappanavar, S. S., Shah, R. G., and Shah, G. M. Mechanism of early biphasic activation of poly(ADP-ribose) polymerase-1 in response to ultraviolet B radiation. *J. Cell Sci.* **118**, 589-599 (2005).

12. Berger, N. A., and Sikorski, G. W. Poly(adenosine diphosphoribose) synthesis in ultraviolet-irradiated xeroderma pigmentosum cells reconstituted with Micrococcus luteus UV endonuclease. *Biochemistry* **20**, 3610-3614 (1981).

13. Kawamitsu, H., *et al.* Monoclonal antibodies to poly(adenosine diphosphate ribose) recognize different structures. *Biochemistry* **23**, 3771-3777 (1984).

14. Shah, G. M., *et al.* Approaches to detect PARP-1 activation *in vivo*, in situ, and *in vitro*. *Methods Mol. Biol.* **780**, 3-34 (2011).

15. Mirzoeva, O. K., and Petrini, J. H. DNA damage-dependent nuclear dynamics of the Mre11 complex. *Mol. Cell. Biol.* **21**, 281-288 (2001).

16. Balajee, A. S., and Geard, C. R. Chromatin-bound PCNA complex formation triggered by DNA damage occurs independent of the ATM gene product in human cells. *Nucleic Acids Res.* **29**, 1341-1351 (2001).

17. Zhu, Q., *et al.* Chromatin restoration following nucleotide excision repair involves the incorporation of ubiquitinated H2A at damaged genomic sites. *DNA Repair* **8**, 262-273 (2009).

18. Fey, E. G., Wan, K. M., and Penman, S. Epithelial cytoskeletal framework and nuclear matrix-intermediate filament scaffold: three-dimensional organization and protein composition. *J. Cell Biol.* **98**, 1973-1984 (1984).

19. Kaufmann, S. H., *et al.* Association of poly(ADP-ribose) polymerase with the nuclear matrix: the role of intermolecular disulfide bond formation, RNA retention, and cell type. *Exp. Cell Res.* **192**, 524-535 (1991).

20. Mortusewicz, O., Ame, J. C., Schreiber, V., and Leonhardt, H. Feedback-regulated poly(ADP-ribosyl)ation by PARP-1 is required for rapid response to DNA damage in living cells. *Nucleic Acids Res.* **35**, 7665-7675 (2007).

21. Ali, A. A., *et al.* The zinc-finger domains of PARP1 cooperate to recognize DNA strand breaks. *Nat. Struct. Mol. Biol.* **19**, 685-692 (2012).

22. Hall, R. K., and Larcom, L. L. Blockage of restriction endonuclease cleavage by thymine dimers. *Photochem. Photobiol.* **36**, 429-432 (1982).

23. Cleaver, J. E. Restriction enzyme cleavage of ultraviolet-damaged simian virus 40 and pBR322 DNA. *J. Mol. Biol.* **170**, 305-317 (1983).

24. Wittschieben, B. O., Iwai, S., and Wood, R. D. DDB1-DDB2 (xeroderma pigmentosum group E) protein complex recognizes a cyclobutane pyrimidine dimer, mismatches, apurinic/apyrimidinic sites, and compound lesions in DNA. *J. Biol. Chem.* **280**, 39982-39989 (2005).

25. Clark, N. J., Kramer, M., Muthurajan, U. M., and Luger, K. Alternative modes of binding of poly(ADP-ribose) polymerase 1 to free DNA and nucleosomes. *J. Biol. Chem.* **287**, 32430-32439 (2012).

26. Fischer, E. S., *et al.* The molecular basis of CRL4DDB2/CSA ubiquitin ligase architecture, targeting, and activation. *Cell* **147**, 1024-1039 (2011).

27. Menissier-de Murcia, J., Molinete, M., Gradwohl, G., Simonin, F., and de Murcia, G. Zinc-binding domain of poly(ADP-ribose)polymerase participates in the recognition of single strand breaks on DNA. *J. Mol. Biol.* **210**, 229-233 (1989).

28. Sancar, A., and Sancar, G. B. DNA repair enzymes. *Annu. Rev. Biochem.* **57**, 29-67 (1988).

29. Fitch, M. E., Nakajima, S., Yasui, A., and Ford, J. M. In vivo recruitment of XPC to UV-induced cyclobutane pyrimidine dimers by the DDB2 gene product. *J. Biol. Chem.* **278**, 46906-46910 (2003).

30. Hendel, A., Ziv, O., Gueranger, Q., Geacintov, N., and Livneh, Z. Reduced efficiency and increased mutagenicity of translesion DNA synthesis across a TT cyclobutane pyrimidine dimer, but not a TT 6-4 photoproduct, in human cells lacking DNA polymerase eta. *DNA Repair (Amst)* **7**, 1636-1646 (2008).

31. Langelier, M. F., and Pascal, J. M. PARP-1 mechanism for coupling DNA damage detection to poly(ADP-ribose) synthesis. *Curr. Opin. Struct. Biol.* **23**, 134-143 (2013).

32. Shah, R. G., Ghodgaonkar, M. M., Affar el, B., and Shah, G. M. DNA vector-based RNAi approach for stable depletion of poly(ADP-ribose) polymerase-1. *Biochem Biophys Res Commun* **331**, 167-174 (2005).

ACKNOWLEDGEMENT

We are thankful to V. Schreiber for GFP-PARP-1, K. Hitomi for the CPD photolyase and J. Brind'Amour for creating cDNA for GFP-DBD. We thank M. Miwa, National Cancer Center Research Institute, Tokyo, for permission to receive 10H hybridoma through the Riken cell bank. This work was supported equally by the two grants to GMS: Discovery Grant 155257-2011 from NSERC, Canada and Grant IMH-131569 from the Canadian Institutes of Health Research: Priority Announcement of Musculoskeletal Health, Arthritis, Skin and Oral Health. The work related to the site-specifically modified oligonucleotides was supported by the National Institutes of Health Grant CA-168469 to NEG. NP received the scholarship support from Quebec Government and Shastri Indo-Canadian Institute from foreign student fee waiver program and MR received graduate scholarship from the Fonds de recherche du Québec-Santé.

Author Contributions Statement

The first three authors (NKP, MR and RGS) contributed equally to performing all the experiments and preparing the figures. NEG provided material support and guidance in planning the experiments with synthetically defined UV-damaged oligo. All authors contributed towards writing and reviewing the manuscript.

Additional Information

Competing Financial Interest Statement: The authors declare no competing financial interests.

Chapitre 5

Poly(ADP-ribose) polymerase 1 escorts XPC to UV-induced DNA lesions during nucleotide excision repair

Mihaela Robu[#1], Rashmi G. Shah[#1], Nupur K. Purohit[1], Pengbo Zhou[2], Hanspeter Naegeli[3] and Girish M. Shah[*1]

[1]Laboratory for Skin Cancer Research, CHU-Q (CHUL) Quebec University Hospital Research Centre & Laval University, 2705, Laurier Boulevard, Québec (QC), Canada G1V 4G2. [2]Weill Cornell Medical College, Department of Pathology and Molecular Medicine, New York (NY) USA. [3] Institute of Pharmacology and Toxicology, University of Zurich, Zurich, Switzerland.

[#] indicates co-first authorship

*To whom correspondence should be addressed.

Tel: [1-418-525-4444/ext. 48259]; Fax: [1-418-654-2739]; Email: [girish.shah@crchul.ulaval.ca]

Classification: Biological Sciences / Cellular Biology

Keywords: PARP1, XPC, NER, DDB2, UV

5.1 Avant-propos

Lorsque nous avons cherché les partenaires de la PARP1 dans la NER, nous avons également trouvé la protéine XPC. Après avoir caractérisé l'interaction entre la PARP1 et le facteur DDB2 après irradiation aux UVC nous avons voulu déterminer si cette interaction expliquait en totalité l'influence de la PARP1 sur les fonctions de la XPC. Nos travaux se sont donc orientés vers cette protéine, dans le but d'en apprendre davantage sur les fonctions de la PARP1 dans la phase de reconnaissance des dommages de la NER. Nos résultats ont fait l'objet d'un manuscrit qui a été soumis à la revue *Proceeding of the National Academy of Sciences of the United States of America* pour publication.

Avant de m'impliquer dans ce projet, Rashmi Shah avait démontré que l'interaction entre PARP1 et XPC dans le nucléoplasme, avant irradiation, était indépendante de la présence du DDB2. De plus, elle a aussi observée que ces deux protéines, la PARP1 et la XPC, interagissent au niveau de la chromatine après irradiation (Figures 5.1 et S5.2A). Par des essais *in vivo* et *in vitro*, Rashmi a identifié les domaines de la XPC et de la PARP1 impliqués dans cette interaction (Figures 5.2B-D) et caractérisé les conditions nécessaires au transfert de la XPC du complexe formé avec PARP1 vers la lésion (Figures 5.5B-D). Nupur Purohit a démontré l'effet positif de l'activité catalytique de la PARP1 sur le recrutement de la XPC aux sites des dommages, ainsi que sur la réparation de dommages à l'ADN dans les cellules déficientes en DDB2 (Figures 5.4A et B).

Dans cette étude, j'ai suis l'auteure des expériences d'immunofluorescence montrant l'effet de l'inhibition de la PARP1 sur la cinétique d'accumulation de la XPC (Figure 5.3B) et de la PARP1 (Figures 5.3C-D et S5.3) dans les cellules normales pour la NER. J'ai aussi mis en évidence que le recrutement de la PARP1 ne dépend pas de la présence de la XPC aux dommages (Figure 5.3E) et que la PARP1 et le DDB2 ont un effet additif sur le recrutement de la XPC (Figures 5.4C-D) et de la XPA (Figure 5.4E) aux lésions. Par immunoprécipitation, j'ai montré que l'interaction dans le nucléoplasme entre PARP1 et la XPC est indépendante de l'ADN (Figure 5.2A et S5.1) et j'ai suivi la cinétique de séparation du complexe PARP1-XPC une fois recruté à la chromatine (Figure 5.5A). Avec Rashmi, nous avons créé un nouvel outil, un plasmide qui code pour la PARP1

couplée à la biotine ligase promiscue BirA. Cette construction nous a permis de suivre le mouvement du complexe PARP1-XPC du nucléoplasme à la chromatine grâce à la modification des partenaires de la PARP1 avec de la biotine (Figures 5.3A et S5.2). En tant que première co-auteure, j'ai participé à la rédaction, à la correction et à la révision du manuscrit et au montage des figures.

5.2 Résumé

La protéine Xeroderma pigmentosum C (XPC) initie la voie de réparation globale du génome par excision de nucléotides (GG-NER) pour éliminer les photolésions de l'ADN génomique. La XPC a la capacité inhérente de reconnaître les lésions d'ADN et de s'y stabiliser. Cette fonction est facilitée dans le contexte génomique par la protéine « UV-damaged DNA binding protein 2» (DDB2), qui fait partie du complexe ubiquitine ligase UV-DDB. Il a été démontré que l'enzyme nucléaire poly(ADP-ribose) polymerase 1 (PARP1), par son interaction avec DDB2 au site de la lésion, facilite l'étape de reconnaissance des dommages de la GG-NER. Ici, nous montrons que PARP1 joue un nouveau rôle, indépendant de DDB2, dans le recrutement et la stabilisation de la XPC au niveau des lésions induites par les UV pour promouvoir la réparation globale du génome. La PARP1 forme avant l'irradiation un complexe stable avec la XPC dans le nucléoplasme et l'escorte rapidement après irradiation à l'ADN endommagé d'une manière indépendante de DDB2. L'activité catalytique de PARP1 n'est pas nécessaire pour la formation initiale du complexe avec la XPC, mais elle améliore le recrutement de la XPC aux lésions d'ADN après irradiation. En utilisant des protéines purifiées, nous montrons également que le complexe PARP1-XPC facilite le transfert de la XPC sur les lésions induites par les UV en présence du complexe ubiquitine ligase UV-DDB. Ainsi, dans le contexte génomique, la fonction de recherche de lésions de la XPC est contrôlée par la XPC elle-même, le DDB2 et la PARP1. Nos résultats révèlent un nouveau paradigme selon lequel l'interaction connue de nombreuses protéines avec la PARP1 en conditions de croissance favorable, *e.g* en absence des dommages à l'ADN, pourrait avoir une importance fonctionnelle pour ces protéines.

5.3 Abstract

Xeroderma pigmentosum C (XPC) protein initiates the global genomic sub-pathway of nucleotide excision repair (GG-NER) for removal of UV-induced direct photolesions from genomic DNA. The XPC has an inherent capacity to identify and stabilize at the DNA lesion sites, and this function is facilitated in the genomic context by UV-damaged DNA binding protein 2 (DDB2), which is part of a multi-protein UV-DDB ubiquitin ligase complex. The nuclear enzyme poly(ADP-ribose) polymerase 1 (PARP1) has been shown to facilitate the lesion recognition step of GG-NER via its interaction with DDB2 at the lesion site. Here, we show that PARP1 plays an additional DDB2-independent direct role in recruitment and stabilization of XPC at the UV-induced DNA lesions to promote GG-NER. It forms a stable complex with XPC in the nucleoplasm under steady-state conditions prior to irradiation and rapidly escorts it to the damaged DNA after UV-irradiation in a DDB2-independent manner. The catalytic activity of PARP1 is not required for the initial complex formation with XPC but it enhances the recruitment of XPC to DNA lesion site after irradiation. Using purified proteins, we also show that PARP1-XPC complex facilitates the handover of XPC to the UV-lesion site in the presence of UV-DDB ligase complex. Thus the lesion search function of XPC in the genomic context is controlled by XPC itself, DDB2 and PARP1. Our results reveal a novel paradigm that the known interaction of many proteins with PARP1 under steady-state conditions without DNA damage could have functional significance for these proteins.

5.4 Significance Statement

The repair of majority of UV-induced DNA damage in mammalian cells by NER pathway starts with rapid recruitment of XPC protein to the lesion. However, the rapidity of XPC recruitment to the lesion site in genomic context could not be fully explained by the known properties of XPC or its partner protein DDB2. Here, we show that the DNA damage-detecting nuclear protein PARP1 forms a stable complex with XPC prior to DNA damage and transfers it very rapidly to the DNA lesion site if other repair conditions are present. Since PARP1 is known to interact with many proteins under steady-state conditions, our results reveal a novel paradigm that an association with PARP1 could confer a functional advantage to these proteins.

5.5 Introduction

The nucleotide excision repair (NER) is a versatile pathway that removes a wide variety of DNA lesions including ultraviolet radiation (UV)-induced cyclobutane pyrimidine dimers (CPD) and 6-4 pyrimidine-pyrimidone photoproducts (6-4PP). There are two sub-pathways of NER: the global-genomic NER (GG-NER) that removes majority of the lesions from the entire genome and the transcription-coupled NER (TC-NER) that repairs the minority of total lesions that occur on the transcribed strand [416]. The GG-NER process is dependent on Xeroderma pigmentosum C (XPC) protein whose arrival and stabilization at the lesion site, followed by its timely departure are crucial for permitting the downstream NER events [417]. XPC accomplishes some of these tasks on its own or with the help of processes initiated by two proteins that independently reach very rapidly at the lesion site, namely UV-damaged DNA binding protein 2 (DDB2) and poly(ADP-ribose) polymerase 1 (PARP1). It is known that once XPC reaches the vicinity of DNA lesion site, the UV-DDB ubiquitin ligase complex containing DDB1, DDB2, Cul4A and Rbx1 regulate its specific binding and stabilization at the site [164]. However, we have the least understanding of the ability of XPC to rapidly search for and arrive at the very few lesions surrounded by a vast majority of undamaged bases in the chromatin structure [90].

There are three proposed mechanisms by which XPC could be rapidly recruited to the lesion site in the genomic context. The first mechanism is based on its inherent capacity to interrogate the DNA for verifying the presence or absence of a lesion. It has been suggested that XPC searches for the lesion-induced helical distortion in the genome [69] by association and quick dissociation until it encounters the lesion site where it stabilizes due to a stronger association [140]. As the yeast orthologue of XPC forms identical crystal structures with normal and UV-damaged DNA [139], it is proposed that the discrimination between normal and damaged DNA depends on the difference in the kinetics of twisting and opening of the helix by XPC at these two sites [139, 143]. While this physical verification mechanism could work rapidly in vitro with small and naked DNA, it would be too slow to explain the rapid recruitment of XPC that is known to occur within minutes at UV-lesion sites in a complex eukaryotic chromatin. Therefore, the second proposed mechanism is that DDB2 helps XPC

in finding the UV-lesions in the genomic context. This is based on the observation that the XP-E cells, which are deficient in DDB2 but proficient in XPC, can slowly repair 6-4PP lesions but fail to remove CPD lesions, which constitute majority of the lesions formed by UV [418, 419]. Based on the phenotype of XP-E cell and the biochemical studies of XPC with these two types of lesions [164], it is proposed that while XPC can directly recognize the greater degree of helical distortion in DNA induced of 6-4PP lesions, it cannot recognize the smaller degree of distortion caused by CPD lesions until DDB2 binds to these lesions and increases the degree of helical distortion at the site [90]. Finally, the third proposed mechanism is that XPC recognizes the remodeled chromatin at the lesion site, which is the result of events initiated by ubiquitination of histones by UV-DDB complex [375]. This is supported by the observations that decreased histone ubiquitination impairs the eviction of UV-DDB [177] and recruitment of XPC to the lesions site [176]. Thus, apart from the direct recognition of the DNA damage by XPC, all other mechanisms to explain XPC's ability to rapidly reach most of the UV-lesions in the genomic context depend on DDB2. However, XPC must have some DDB2-independent mechanism of recruitment to lesions other than 6-4PP. For example, CPD are recognized and repaired even after DDB2 is degraded [165] or when the number of lesion sites exceed the number of DDB2 molecules in the cell [160]. In addition, XPC recognizes and starts NER at other types of DNA damages, such as bulky adducts and crosslinks that are not likely to be recognized by DDB2, because these lesions could not be accommodated in its recognition pocket [91, 135, 420].

Earlier, we have shown that poly(ADP-ribose) polymerase 1 (PARP1), an abundant nuclear enzyme in higher eukaryotes, is recruited very early to the UV-lesion site and catalytically activated to form polymers of ADP-ribose (PAR) [392, 396]. It has been shown by others and our team that PARP1 and DDB2 reach the lesion site in the same time frame and cooperate with each other to increase the efficiency of GG-NER. More specifically, DDB2 has been shown to stimulate catalytic activity of PARP1, which in turn PARylates DDB2 and DDB1 [390, 392]. The inhibition of PARylation has been shown to block the turnover of DDB2 at UV-damaged chromatin [392] and decrease total cellular levels of DDB2 [390]. Additionally, the activated PARP1 promotes chromatin relaxation via recruitment of the remodeler protein ALC1 at the UV-lesion site [390]. Together these

studies suggest that the interplay of PARP1 and DDB2 at UV-damaged DNA could be a mechanism for recruitment and stabilization of XPC at UV-damaged chromatin [391, 392]. Recent studies have shown PARylation of XPC in vitro (24) and in the cells responding to oxidative DNA damage (25). However, the significance of PARylation of XPC in NER of UV-induced DNA damage is not clear, since, the higher affinity of XPC for larger PAR chains shown in vitro (24) would repel XPC from DNA, and in vivo PARylation of XPC was not observed in UV-irradiated cells (25). Thus, studies to date have not shown an unequivocal direct DDB2-independent role for PARP1 and PARylation in recruitment of XPC in GG-NER.

Here, we show that PARP1 stably interacts with XPC in the nucleoplasm under unchallenged conditions, i.e., in the absence of any type of exogenously induced DNA damage. The functionally important DNA-binding region of XPC is involved in its interaction with PARP1. Using various cellular models and in vitro assays with purified proteins, we show that after UV-irradiation, PARP1 rapidly escorts XPC to the UV-lesion site and facilitates its handover to the damaged DNA in the presence of UV-DDB ligase complex. We also show that although the PARP1 catalytic function does not influence the initial interaction between these two proteins in the nucleoplasm, it is required for efficient recruitment of their complex to the lesion site. Our results reveal that the interaction of XPC with PARP1 in nucleoplasm under steady-state conditions facilitates the search function of XPC for DNA damage in the genomic context.

5.6 Results

DDB2-independent nucleoplasmic interaction of PARP1 with XPC before and after DNA damage

Within minutes after UV-irradiation, XPC, DDB2 and PARP1 are present at the UV-induced DNA lesions in cells. While independent interactions of DDB2 with XPC [367, 392] or PARP1 [390, 392] at the lesion site are known, here we examined whether XPC interacts directly with PARP1 on the UV-damaged chromatin. The FLAG-PARP1 expressing

human skin fibroblasts (GMRSiP) were fractionated before and after UV-irradiation to prepare cytoplasm, nucleoplasm and chromatin-bound protein fractions (Fig. 5.1A), as described earlier [392]. In this protocol, the chromatin proteins such as histone H3 do not leak in the nucleoplasmic fraction but are extracted in the chromatin-bound protein fraction. Moreover, we confirmed our earlier observation [392] about UV-induced accumulation of DDB2 in the chromatin fraction (Fig. 5.1A), further validating this fractionation protocol. The XPC-immunoprecipitation (IP) of chromatin extracts with equal protein content from control and UV-irradiated cells revealed a significant increase in UV-induced association of PARP1 with XPC on the chromatin (Fig. 5.1B, left panel). We also observed UV-induced increase in the interaction of DDB2 with XPC at the chromatin, which is in agreement with our previous observation of this interaction identified by DDB2-IP [392]. The reciprocal PARP1-IP using FLAG antibody revealed a strong UV-induced association of XPC with PARP1 in the chromatin-bound fraction (Fig. 5.1B, right panel). Since PARP1 and XPC are present in the nucleoplasm before and after irradiation (Fig. 5.1A), we examined whether they also interact with each other in this subnuclear fraction. The reciprocal IP for XPC and PARP1 in the nucleoplasmic fraction revealed a strong association of these two proteins not just after UV-irradiation but also under control conditions prior to irradiation (Fig. 5.1C). Both the IPs failed to pull down DDB2 from control nucleoplasm, indicating a DDB2-independent nature of PARP1-XPC nucleoplasmic interaction before irradiation. Even after UV-irradiation, XPC-IP confirmed its lack of interaction with DDB2 in nucleoplasm, whereas PARP1-IP revealed a feeble interaction of PARP1 with DDB2 (Fig. 5.1C), reflecting some turnover of PARP1-DDB2 complex from post-irradiation chromatin to nucleoplasm.

The interaction between PARP1 and XPC in UV-irradiated chromatin was expected, as both are known to bind to UV-damaged DNA. However their interaction in nucleoplasm under steady-state conditions prior to UV-challenge was unexpected; therefore we examined this interaction in further details using multiple cellular and in vitro models. To exclude the possibility that this could be an artifact of the expression of exogenous FLAG-tagged PARP1 in the above model, we examined this interaction in HEK293 cells that express endogenous XPC, PARP1 and DDB2. The mass spectrometry of the proteins that co-IP with XPC from the lysates of unirradiated HEK cells confirmed the presence of PARP1 as well as two known

partners of XPC, namely HR23B and Centrin2 (Fig. 5.1D). The reciprocal IP for PARP1 and XPC validated the interaction of even the endogenous PARP1 with XPC in this fraction (Fig. 5.1E). Interestingly, the mass spectrometry of XPC-eluate did not reveal the presence of DDB2, confirming its lack of interaction with XPC under control conditions. The DDB2-independent interaction between endogenous PARP1 and endogenous XPC was further confirmed in the nucleoplasm of DDB2-deficient XP-E cells (Fig. 5.1F). Thus, using different cellular models expressing endogenous or exogenous PARP1, and variable status of DDB2, we consistently observed a DDB2-independent interaction between XPC and PARP1 in the nucleoplasm before and after irradiation and an increased interaction at the chromatin after irradiation.

Direct interaction of XPC and PARP1

PARP1 and XPC are DNA binding proteins, therefore we examined the possibility that DNA could be mediating their interaction in the nucleoplasm. Unlike chromatin fraction, the nucleoplasmic fraction of the unirradiated HEK cells contained undetectable levels of DNA (Fig. S5.1). Very high dose of micrococcal nuclease (MNase) or benzonase are often used for digesting DNA from chromatin preparations to demonstrate direct interactions of proteins. In our IP studies, we prepared chromatin-bound protein fraction after treatment of chromatin pellets with very low dose MNase (25 U/mL). Since treatment of HeLa cell extracts with high dose MNase was shown to digest the DNA to mono-nucleosomes [367], we treated the chromatin fraction of HEK cells with different doses of MNase up to 4,000 U/mL or benzonase up to 50 U/mL to digest it down to mono-nucleosomal DNA at 147 bp (Fig. S5.1). Although there was no detectable DNA in the nucleoplasmic fraction, we still treated this fraction from control or UV-treated HEK cells with 4,000 U/mL MNase prior to subjecting it to XPC-IP, and observed that MNase did not break the association of XPC with PARP1 (Fig. 5.2A), confirming DNA-independent interaction of these two proteins in the nucleoplasm.

To identify the domains of XPC involved in interaction with PARP1, we expressed GFP-tagged XPC and its five different partially overlapping fragments in HEK cells (Fig.

5.2B, top panel). The nucleoplasmic fractions from these cells under control conditions were subjected to PARP1-IP followed by immunoblotting for GFP. Since the expression levels of full length XPC and its fragments varied greatly after transfection (Fig. 5.2B, input lanes), the strength of interaction of each XPC fragment with PARP1 was measured as a fraction of total input protein that co-immunoprecipitated with PARP1 and expressed relative to the interaction of full length XPC with PARP1 (Fig. 5.2B, lower panel). While control GFP protein did not interact with PARP1, the XPC fragments that span from 427 to 940aa showed an interaction with PARP1 similar to that seen with full length XPC, whereas a comparatively weaker interaction was observed with N-terminal fragment (1-495aa).

The interaction observed above between XPC or its fragments and PARP1 after PARP1-IP could not exclude the possibility that a PARP1 interacting proteins may be indirectly mediating their interaction. Therefore, we examined the interaction of purified PARP1 in vitro with equimolar amount of three purified fragments of XPC, namely GST-tagged 141-250aa (XPC-N), His-tagged 496-734aa (XPC-C1) and His-tagged 734-933aa (XPC-C2) (Fig. 5.2C, top panel). The PARP1-IP of above reaction mixtures revealed a strong interaction of PARP1 with XPC-C1 fragment and a weak interaction with XPC-C2 fragment indicating that the central portion of XPC protein spanning 496-734aa is key region for its direct interaction with PARP1 (Fig. 5.2C, lower panel). The purified XPC-N fragment revealed no interaction with PARP1. The results with purified proteins strongly indicated an interaction of the central portion of XPC protein spanning 496-734aa with PARP1 without intervention of other proteins or DNA.

To identify the domains of PARP1 implicated in this interaction, its N-terminal (1-232aa) fragment was expressed in GMSiP cells in which endogenous PARP1 was depleted by shRNA, whereas the C-terminal (232-1014aa) fragment of PARP1 was expressed in $PARP1^{-/-}$ A1 cells. For control, we used GMRSiP cells that express FLAG-tagged full length PARP1 in the GMSiP cells (Fig. 5.2D, top panel). The XPC-IP in the nucleoplasmic fraction of these cells revealed that the C-terminal fragment of PARP1 is implicated in its interaction with XPC (Fig. 5.2D, lower panel). Our results demonstrate that the region of XPC that is

involved in its interaction with DNA, DDB2 and HR23B is also involved in its interaction with PARP1.

Roles of PARP1-XPC complex and catalytic activity of PARP1 in recruitment of XPC to UV-damaged DNA

PARP1 is known to rapidly reach damaged DNA in the chromatin context; hence the PARP1-XPC complex formed in the nucleoplasm prior to irradiation could have a potential role of rapidly escorting XPC to the UV-damaged DNA after irradiation. Therefore, to trace the intranuclear movement of PARP1-bound XPC, we used proximity-dependent biotin identification (Bio-ID) technique [421]. The FLAG-PARP1 was cloned in the myc-tagged biotin ligase BirA vector to create a new Bio-ID-PARP1 vector. The expression of Bio-ID-PARP1 in GMSiP cells depleted of endogenous PARP1 in the nuclear fraction (Fig. S5.2A) ensured that any nuclear protein that stably associates with or stays within 10 nm of the cloned PARP1 would be stably biotinylated. The absence of the endogenous PARP1 in these cells eliminated the possibility that any PARP1 associated protein would not be biotinylated. In these cells, we confirmed biotinylation of XPC and auto-biotinylation of PARP1 by streptavidin probing of XPC-IP eluates of the nucleoplasm of control and UV-irradiated cells (Fig. S5.2B). To examine the role of catalytic activity of PARP1 in this interaction, we also treated the cells with PARPi PJ34 under conditions that abolished the signal for PAR-modified proteins in control or UV-irradiated cells (Fig. S5.2C). Interestingly, the presence of PARPi did not abolish the interaction between XPC and PARP1, indicating that catalytic function of PARP1 is not required for this interaction in the nucleoplasm (Fig. S5.2B). Using this model, we tracked UV-induced movement of biotinylated XPC and PARP1 from the nucleoplasmic to chromatin fractions of control or UV-treated cells (Fig. 5.3A). In the streptavidin-IP of nucleoplasm, both PARP1 and XPC were detectable before and after irradiation, confirming biotinylation of XPC and auto-biotinylation of Bio-ID-PARP1 (Fig. 5.3A, left panel and Fig. S5.2D). The decrease in signal for biotinylated XPC after UV irradiation indicated a movement of XPC away from this fraction. Interestingly, PARPi blocked the reduction in the signal for XPC after UV-irradiation, indicating a potential role of catalytic activity of PARP1 in the movement of XPC

from the nucleoplasmic fraction to damaged DNA. The absence of biotinylated DDB2 in streptavidin-IP (Fig. 5.3A, left panel), once again confirmed that DDB2 did not interact with Bio-ID-PARP1 or its complex with XPC in the nucleoplasm.

In order to examine whether the biotinylated nucleoplasmic XPC reaches the UV-damaged DNA, we performed the streptavidin-IP of corresponding chromatin fractions from these cells (Fig. 5.3A, right panel). As compared to unirradiated cells, there was an increase in the signal for biotinylated XPC in UV-treated cells, which was suppressed by PARPi (Fig. 5.3A, right panel). The signal for biotinylated XPC in control condition indicated either a basal level of interrogation of DNA at all times by PARP1-XPC complex or other DNA related functions of these two multifunctional proteins. The UV-mediated increase in biotinylated XPC at chromatin with a corresponding decrease in nucleoplasm suggests that either PARP1-bound XPC moved from nucleoplasm to UV-damaged chromatin or a completely independent XPC arrived at the lesion site, and was biotinylated by PARP1 within 30 min after irradiation when the samples were harvested. However, within the same time period of 30 min post-irradiation, DDB2 that is known to closely interact with PARP1 at the chromatin immediately after UV-irradiation [390, 392] was not strongly biotinylated by Bio-ID-PARP1 (Fig. 5.3A, right panel). Thus, the biotinylated XPC that is deposited on the UV-damaged chromatin must have originated from nucleoplasmic PARP1-XPC complexes formed prior to UV-damage, and PARPi suppressed this movement.

To validate the inhibitory effect of PARPi on the movement of XPC from nucleoplasm to chromatin, we used immunocytological methods to visualize XPC at the site of local UVC-irradiation up to 3h in the NER proficient GMU6 human skin fibroblasts with or without treatment with PARPi (Fig. 5.3B). We confirmed that PARPi treatment was sufficient to abolish the signal for PAR-modified proteins in control and UV-irradiated cells (Fig. S5.2E). The GMU6 fibroblasts were locally irradiated with UVC through 5µm pores in polycarbonate filter, which produces distinct subnuclear areas of irradiation that are surrounded by unirradiated zones in the nucleus [422]. In the subnuclear irradiated zones identified by staining with thymine dimer (T-T) CPD-specific antibody, the endogenous XPC followed a normal kinetics, i.e., initial strong accumulation at 10 min followed by a steady

decline to 40% of initial levels in 90 min. The treatment of cells with PARPi suppressed the initial recruitment of XPC at 10 min by 50%. Moreover, PARPi slowed down the departure of XPC from the lesion site in the first 90 min, as compared to the rapid turnover of XPC in cells not treated with PARPi (Fig. 5.3B, chart). Thus, the major impact of PARPi was in partially suppressing the initial recruitment of XPC to UV-lesion sites.

Since XPC is in a complex with PARP1 in the nucleoplasm, we reasoned that PARPi would also be partially suppressing the recruitment of PARP1 to UV-damaged chromatin. Using cells expressing GFP-PARP1 and recently developed in situ extraction technique that can selectively identify DNA-bound PARP1 [423], we examined the effect of PARPi PJ-34 on the recruitment of PARP1 to local UVC-induced DNA damage. We observed that PARPi suppressed by 50% the initial recruitment of GFP-PARP1 to local UV-irradiated subnuclear zones, which were identified by immunostaining for T-T (Fig. 5.3C and chart). The Z-stack images (Fig. S5.3A) and their orthogonal view (Fig. S5.3B) of the locally irradiated GMU6 cells confirmed the spatial colocalization of the GFP-PARP1 with T-T (Fig. 5.3C). The immunofluorescence image with multiple locally irradiated cells presented in 2D and 2.5D format revealed that PARPi treatment significantly reduced the intensity of colocalized signal for GFP-PARP1 at the site of DNA damage (Fig. 5.3D). Interestingly, the recruitment of PARP1 itself to UV-lesion site is not dependent on XPC, because it occurs to an identical extent in both XPC-proficient (GMU6) and deficient (XP-C) cells (Fig. 5.3E and chart). Collectively, our results indicate that the initial phase of basal level of recruitment of PARP1 and XPC to UV-damaged DNA does not require catalytic activity of PARP1, whereas the second phase occurs in response to PARP1 activation. A similar two-stage recruitment of PARP1 to laser micro-irradiation site of DNA damage has been demonstrated using two different PARP inhibitors: PJ-34 [424] and NU-1025 [404].

PARP1-mediated recruitment of XPC to UV-lesions site is independent of DDB2

DDB2 is known to recruit XPC to the UV-lesion site, and since DDB2 and PARP1 interact with each other to facilitate NER [320], our results of suppression of XPC recruitment to UV-lesion site could also be an indirect effect of PARPi on suppression of the

role of DDB2 in recruitment of XPC. To exclude this possibility, we used DDB2-deficient XP-E cells to examine the effect of PARPi on colocalization of XPC with 6-4PP lesions after local UV-irradiation. At the lesion sites, the signal for XPC declined rapidly by 50-60% from 10 to 60 min (Fig. 5.4A and chart). In contrast, PARPi-treatment not only reduced the initial recruitment of XPC at lesion site by 50%, but also slowed down XPC turnover up to 60 min, a trend that was also observed in DDB2-proficient GM cells (Fig. 5.3B). An identical profile of suppression of XPC recruitment and turnover in DDB2 proficient and deficient cells indicate that the suppression of XPC recruitment by PARPi is not mediated via DDB2. The biological end-point of XPC recruitment to the lesion site is the repair of UV-damaged DNA. Therefore, we measured the kinetics of removal of 6-4PP lesions up to 8h following global UV-irradiation in XP-E cells. As expected, almost all 6-4PP lesions were removed in XP-E cells by 8h, but the treatment with PARPi significantly slowed down this repair process (Fig. 5.4B and chart). Since the depletion of PARP1 completely suppressed any PAR formation in response to UV-irradiation without affecting PARP2 expression [378, 392, 425], these results indicate that XPC recruitment is partially controlled by the catalytic activity of PARP1 in a DDB2-independent manner. Collectively, our findings demonstrate that the inhibition of PARP1 activity reduces recruitment of XPC to UV damage with a direct negative consequence on the repair of UV-induced lesions.

To determine the extent of contribution of DDB2 and PARP1 in the recruitment of XPC to DNA lesions, we used four different cell lines described earlier [425] (Fig. 5.4C): CHOSiP cells (deficient in both PARP1 and DDB2); CHOU6 cells (deficient only in DDB2); GMSiP cells (deficient only in PARP1) and GMU6 (proficient in both DDB2 and PARP1). In each cell type, we examined the early accumulation of XPC at local UV-lesion site (Fig. 5.4C and chart). The CHOSiP cells displayed a basal level of accumulation of XPC at UV-lesion site, which represents the inherent capacity of XPC to reach the lesions without the help of DDB2 or PARP1. Relative to this basal level, the presence of only PARP1 (CHOU6) or only DDB2 (GMSiP) increased XPC recruitment by about 40%. However, the presence of both DDB2 and PARP1 in GMU6 cells nearly doubled the XPC accumulation as compared to the CHOSiP model, strongly supporting independent roles of DDB2 and PARP1 in this process.

Since the cellular levels of XPC in PARP1-depleted GMSiP and CHOSiP cell lines were similar to PARP1-proficient GMU6 and CHOU6 cells (Fig. 5.4D), the suppression of recruitment of XPC to the damaged site in PARP1-depleted cells was not an artifact of reduced XPC expression in these cells. Since the recruitment of the downstream NER proteins depend on XPC loading and stabilization at the damage site [426], we measured the accumulation of XPA on the chromatin of these cells, up to 4 hr after damage (Fig. 5.4E). In each of these cellular models, the kinetics of XPA recruitment reflected the status of XPC at the UV-damaged chromatin. The XPA accumulation was robust in GMU6 cells and it was reduced in the absence of PARP1 (GMSiP cells) or DDB2 (CHO cells), whereas the weakest accumulation and a rapid turnover of XPA were seen in the CHOSiP cells devoid of both DDB2 and PARP1.

Our results show that XPC has an inherent basal capacity to recognize and stabilize at DNA lesion site, which promotes recruitment of the downstream XPA protein. This process becomes more efficient in the presence of DDB2 or PARP1. Interestingly, two proteins together give an additive effect strongly supporting the argument that PARP1 has a DDB2-independent mechanism to facilitate XPC recruitment and stabilization at DNA lesions. Finally, since PARPi suppressed XPC recruitment to the lesion site in DDB2-proficient as well as DDB2-deficient cells (Figs. 5.3B and 5.4A), there is an additional component of recruitment of XPC that depends on catalytic activity of PARP1. Collectively our results suggest that there are three components of recruitment of XPC to DNA lesion site: the first is a basal level of recruitment by XPC, the second is dependent on PARP1 or DDB2 proteins and the last component depends on the catalytic activation of PARP1.

Characterization of the handover of XPC from its complex with PARP1 to UV-damaged DNA

Our results show that PARP1 and XPC are together as a complex in the nucleoplasm, and the biotin tag on XPC at the UV-lesion site, indicates a physical handover of XPC from its complex with PARP1 to UV-damaged DNA. To explore the mechanistic aspect of this transfer in vivo, we carried out XPC-IP of chromatin fraction from HEK cells

expressing GFP-tagged XPC up to 3h after irradiation and examined the state of association of PARP1 with XPC (Fig. 5.5A, left panel). The GFP (XPC)-IP revealed a normal kinetics of recruitment and departure of XPC at the UV-damaged chromatin with a strong accumulation at 30 min and a significant reduction by 3h. In contrast, the amount of PARP1 that is associated with GFP-XPC decreased rapidly from 30 to 90 min and no signal was detected at 180 min. It is noteworthy that although a significant amount of PARP1 was still present in the chromatin fraction from 30-180 min (as seen in the input samples), it was not associated with XPC after the peak period of recruitment of XPC to the lesion. A similar kinetics of association and dissociation of XPC and PARP1 was observed at chromatin over 3h period after exposure to $30J/m^2$ UVC in GM cells that express endogenous XPC and PARP1 (Fig. 5.5A, middle panel), demonstrating a general nature of this observation. Moreover, XPC-IP of chromatin bound fraction of the same GM cells 10 min after exposure to various doses up to 100 J/m2, revealed a dose-dependent increase in the interaction between XPC and PARP1 at the chromatin (Fig. 5.5A, right panel). Interestingly, despite an abundance of DDB2 in the input chromatin fraction at all doses, the association of DDB2 and XPC at 10 and 30 J/m2 was no longer detectable at 100 J/m2 (Fig. 5.5A, right panel). The dose-dependent increase in association of XPC and PARP1 at early time point and their dissociation at later time support a model that early recruitment of XPC occurs as a complex with PARP1, but having reached the lesion site, XPC gradually dissociates from PARP1 to continue with its functions in NER.

To explore the conditions required for XPC to dissociate from its complex with PARP1 and bind to UV-damaged DNA, we designed in vitro assays using the factors prevalent at the lesion site in vivo, namely UV-damaged DNA, DDB2, PARP1 and XPC represented by its key fragment 496-734aa (ΔXPC) that interacts with PARP1 (Figs. 5.5B-D). To examine the endogenous properties of each of these three proteins to bind to UV-damaged DNA, we reacted each of them with UVC-irradiated plasmid DNA, which was immobilized on the magnetic beads via T-T antibody (Fig. S5.4). All the proteins could bind to UV-damaged DNA on their own and even in combination with other proteins (Fig. 5.5B). While this assay confirms the inherent capacity of XPC, DDB2 and PARP1 to bind to UV-

damaged DNA, it does not reveal how DDB2 or PARP1, which are recruited prior to XPC at UV-damaged DNA, could participate in the loading of XPC to UV-damaged DNA.

Since XPC exists as a complex with PARP1 in the nucleoplasm prior to reaching UV-damaged DNA, we examined whether this PARP1-XPC complex would simulate conditions for in vivo loading of XPC to UV-damaged DNA. We immobilized the PARP1-ΔXPC complex on the agarose beads with PARP1 antibody (A beads), and reacted it with the above described UV-damaged DNA bound to magnetic beads (M1), in the presence of either PARP1 (M2 beads) or DDB2 (M3-beads) or both PARP1 and DDB2 (M4) (Fig. 5.5C, top panel). After each reaction, the agarose (A beads) and magnetic beads (M1 to M4) were separated, washed and the proteins present in each of these beads were examined by immunoblotting of bead-eluates. The immunoprobing for ΔXPC in the agarose and magnetic beads after the reaction revealed none of the above conditions could dissociate ΔXPC from its complex with PARP1 (Fig. 5.5C).

At the UV-lesion site on DNA, DDB2 is not recruited alone but as a UV-DDB-ligase complex containing DDB2, DDB1, Cullin4A and Rbx1, and PARP1 also interacts with DDB2 at the lesion site. Therefore, we examined whether the entire UV-DDB complex as well as PARP1 are required for loading of XPC to UV-DNA (Fig. 5.5D, top panel). We recreated this complex by loading purified Cul4A-Rbx1 on agarose beads and reacted it with purified DDB1, DDB2 and UV-DNA in absence (A1) or presence of PARP1 (A2). On the other hand, the PARP1-ΔXPC complex was immobilized via PARP1 antibody on the magnetic beads (M). The immunoblotting confirmed the presence or absence of each of the six designated proteins in the input beads M, A1 and A2 (Fig. 5.5D, input lanes). The PARP1-ΔXPC (M) beads were reacted with A1 or A2 agarose beads, the beads were separated and washed followed by immunoblotting of each of these beads for detection of these six proteins. The immunoprobing for his ΔXPC in the magnetic and agarose beads revealed that the UV-DDB ligase complex with UV-DNA provided favorable conditions for promoting the dissociation of ΔXPC from its complex with PARP1 on magnetic beads (Fig. 5.5D, lanes 1 versus 5) as well as loading of ΔXPC onto the UV-DNA on A1 agarose beads (Fig. 5.5D, lanes 2 versus 6). Addition of PARP1 to UV-DDB complex on agarose beads A2 in the above

reaction did not confer any additional movement of ΔXPC to UV-DNA on agarose beads (Fig. 5.5D, lanes 6 versus 8). Collectively, these in vitro assays with purified proteins reveal that while free XPC has an inherent capacity to efficiently bind to UV-DNA, its presence as a complex with PARP1 prior to irradiation ensures that XPC is preferably deposited at the UV-damaged sites, which contain UV-DDB ligase complex.

5.7 Discussion

The GG-NER of UV-damaged DNA starts with recognition of the damaged bases by the Xeroderma pigmentosum C protein. For the last 15 years, focused efforts have been made to understand how XPC with or without help of other proteins rapidly searches for its target lesions scattered across the entire genome in higher order chromatin structure. Many studies indicated a role for DDB2 in the proper functioning of XPC with an indirect role for PARP1 via its ability to participate in chromatin remodeling [320]. The present study reveals a novel paradigm for the functional role of physical interaction of PARP1 with XPC prior to DNA damage in the initial recruitment, hand-over and subsequent NER functions of XPC at UV-induced DNA lesions. Using various cell lines with exogenous or endogenous PARP1 and XPC, we show that the PARP1 and XPC interact in the nucleoplasmic fraction of the cells even in the absence of DNA damage and that this interaction is independent of DDB2 and catalytic activation of PARP1. By using the PARP1 proximity-mediated biotinylation model in vivo, we also show that XPC from the nucleoplasmic XPC-PARP1 complex is deposited at the DNA lesion site after UV irradiation. Using PJ-34 as PARPi, we observed that PARP inhibition partially suppresses the initial recruitment of XPC and PARP1 to the UV-lesion site, which is in agreement with earlier reports showing decreased recruitment of PARP1 to the site of micro-irradiation induced DNA damage in the presence of PARPi such as PJ-34 [424] and NU-1025 [404]. Another study reported an increased signal for PARP1 at damaged DNA after treatment with the PARPi 4-amino-1,8-naphthalimide [427]. This difference in the end-results among these studies could be attributed to the time of harvesting of the samples after treatment and the capacity of different PARPi to immobilize PARP1 on the DNA lesion sites [424, 428]. Since, PARP1-depletion reduces XPC recruitment to the lesion site, and PARPi reduces the rapid colocalization of PARP1 and XPC to the lesion site

in vivo, our results indicate that both PARP1 and its catalytic function determine the movement of PARP1-XPC complex from nucleoplasm to chromatin after irradiation.

In XP-E cells deficient in DDB2 function, the repair of 6-4PP is attributed to the inherent property of XPC to recognize 6-4PP lesions. Nonetheless, some studies demonstrated a reduced level of recruitment of XPC to UV-damage in these cells as compared to DDB2 proficient cells [412, 418, 419]. Additionally, we show that PARPi not only causes further reduction in initial recruitment of XPC to local spots of UV-induced DNA lesions but also significantly hampers the repair of 6-4PP lesions in these cells. Thus, in the XP-E model, our results clearly reveal a DDB2-independent role of PARP1 in facilitating XPC recruitment to the UV-lesions and repair of 6-4PP by NER. It has been shown that XP-E cells have very low levels of PAR and both ubiquitination and ALC1 mediated chromatin remodeling are absent in these cells [390]. Hence, the decrease in recruitment of XPC by PARPi could not be related to ubiquitination or chromatin remodeling at the damaged site but mainly due to the suppression of movement of XPC-PARP1 complex from nucleoplasm to the lesion site on chromatin in XP-E cells. Using cells which are DDB2-deficient, PARP1-depleted or treated with PARPi, we identified that the recruitment of XPC to the UV-lesion site in the genomic context is the sum of efforts by multiple factors including XPC itself, DDB2, PARP1 and the catalytic activity of PARP1. In a cell line that is devoid of functional DDB2 and PARP1 (CHO-SiP) there is a basal level of recruitment of XPC to the lesion site, indicating that XPC has some inherent capacity to reach DNA lesion site that is not dependent on DDB2 or PARP1 or its activation. The reduced level of XPC translates to an impaired accumulation of XPA at the lesion site. Nonetheless, adding PARP1 alone in this DDB2 deficient background (CHOU6 cells) or DDB2 alone in PARP1-deficient background (GMSiP) improves the recruitment of XPC above the basal level, indicating that each of these two proteins independently participates in XPC recruitment and stabilization. Finally, in the cells with PARP1 and DDB2, it is the DDB2-stimulated catalytic activation of PARP1 [392] that would provide the last boost for recruitment of XPC to the lesion.

PARP1 has many characteristics that would facilitate the search function of XPC in NER: (a) PARP1 is an abundant protein in mammalian nucleus, which is rapidly recruited to

all types of DNA damages [429] including UV-induced DNA lesions [423]. Thus, PARP1-associated XPC could be rapidly recruited to lesions anywhere in the genome; (b) Since PAR formed by activated PARP1 create a protein-recruiting platform [388], detection of lesion by a single PARP1 and its activation to form PAR at the site can bring in more PARP1 with XPC and other PAR-seeking proteins to the site; (c) Like XPC, the binding of PARP1 to damaged DNA is independent of the sequence or the chemical nature of DNA damage [414, 416]. Moreover, both XPC and PARP1 have affinity for unusual DNA structures with non-hydrogen bonded bases, such as hairpins, stem loops, bubbles and over-hangs [228, 416]. Thus PARP1 could rapidly recruit XPC to all types of damages that are repaired by NER irrespective of their recognition by DDB2 [146]; (d) PARP1 is a part of chromatin structure with preference for binding to the internucleosomal linker region [409], which is also the site where 6-4PP lesions are prioritized for repair [367]. Thus, the chromatin-bound PARP1 could rapidly bind to these lesions in the linker region and recruit nucleoplasmic PARP1-XPC complex. Since UV-DDB ligase complex is also promptly recruited to the linker region [367], presence of UV-DDB ligase complex would allow handover and stabilization of XPC at the lesion site; (e) Finally, PARP1 activation at the lesion site remodels chromatin via recruitment of ALC1 [390] and PARylation of histones [429], which would subsequently permit XPC to repair less accessible intranucleosomal lesions.

Interaction of PARP1 and XPC in the nucleoplasm offers an interesting contrast with the interaction of PARP1 with DDB2. Unlike XPC, DDB2 does not interact with PARP1 in the nucleoplasm under control conditions. However, both the proteins interact with PARP1 at the chromatin immediately after irradiation. We have already shown that the PARP1 interacts with DDB2 on the chromatin [392], and here we show a similar direct interaction between PARP1 and XPC. The formation of a complex with PARP1 in nucleoplasm confers two advantages to XPC that it would not have as a free protein in its search for the DNA lesion to start NER. First, PARP1's known capacity to rapidly zoom in on UV-lesion site allows XPC to be escorted rapidly to the lesion site. Secondly, our in vitro results with purified proteins and UV-DNA reveal that XPC is dissociated from its complex with PARP1 when UV-DDB ligase complex is present with UV-DNA. The requirement of UV-DNA with UV-DDB ligase complex for successful transfer of XPC from its complex with PARP1 to

UV-DNA replicates the physiological conditions that exist at the lesion site in DDB2 competent cells, because DDB2 is recruited to the UV-lesion site as UV-DDB ligase complex. Moreover, it has been shown that the handover of UV-damaged DNA site from UV-DDB to XPC requires a transient physical interaction between DDB2 and the central region of XPC (496-679aa) containing the domains required for its interaction with DNA [367]. Interestingly, our in vitro studies have identified that the same central domain of XPC (496-734aa) mediates its interaction with PARP1 (Fig. 2C). This indicates a dynamic process where PARP1 and UV-DDB complex could cooperate in the hand-over XPC to the lesion site. Thus, our in vitro model faithfully replicates the sequence of events surrounding efficient stabilization of XPC to the lesion site which start with its dissociation from the complex formed with PARP1, followed by the formation of a new complex with UV-DDB. The presence of UV-DDB complex not only positions XPC onto the lesion site, but also prioritizes the repair of 6-4PP lesions from the linker DNA. Nonetheless, our model does not exclude additional roles for PARylation status of PARP1, XPC and other proteins as well as changes in the structure of DNA at the lesion site towards dissociation of PARP1-XPC complex and stabilization of XPC, as it has been shown for the interaction between PARP1 and XRCC1 or APE1 during base excision repair [48, 430]. These additional factors could play a key role in the sub-optimal delivery of XPC from its complex with PARP1 to UV-lesion site in the absence of DDB2, such as in XP-E cells in our cellular studies.

We propose a model for the roles of PARP1 in the lesion recognition function of XPC (Fig. 5.6). Prior to UV-irradiation, PARP1 and XPC co-exist as a complex in the nucleoplasm, and DDB2 is not part of this complex. Since PARP1 is more abundant protein as compared to XPC [375, 431], there will still be sufficient free PARP1 molecules to separately interact with DDB2 at the lesion site. The free PARP1 molecules as well as PARP1-XPC complex will scan the intact DNA due to the affinity of PARP1 and XPC for DNA, which explains the presence of basal levels of biotinylated XPC and PARP1 in chromatin bound protein fractions from control cells. However, the transient binding of the complex to control DNA will not result in separation of XPC from PARP1 because UV-DDB ligase complex is not recruited to chromatin until DNA damage occurs. Upon UV-irradiation, free PARP1 as well as XPC-bound PARP1 molecules will reach the lesion site, and may

deposit XPC from the complex to the lesion site with the help of other factors. However, the optimum deposition of XPC from its complex with PARP1 to the UV-lesion site would occur when UV-DDB ligase complex is present at the lesion site, a condition that would be observed in normal DDB2-competent cells. That PARP1 and DDB2 can co-exist at the UV-induced CPD lesion [423] allows DDB2 to further stimulate catalytic activation of PARP1 and formation of more PAR in the vicinity of the lesion [392]. This catalytic activation of PARP1 provides a platform for additional PAR-seeking molecules to accumulate at the damaged site, including more of the nucleoplasmic PARP1-XPC complex. Thus catalytic activation of PARP1 at the site of DNA lesion provides an additional boost for accumulation of XPC and more efficient NER at the lesion site. Moreover, the presence of UV-DDB complex at the lesion site in the linker region [367] or in the core region [432] would facilitate prioritization of these site for initial recruitment of XPC and the repair. Additionally, the PARylation, DDB2 and UV-DDB ubiquitin ligase complex-mediated chromatin remodeling events will open the nucleosomal structure to allow the arrival of downstream proteins to complete the process of NER at all the remaining lesions in the genome.

While a lot of efforts have gone in understanding the interaction of PAR and PARP1 with different proteins in the cells after DNA damage, not much is known about the importance of interaction of PARP1 with multiple cellular proteins in steady-state conditions prior to DNA damage, which has been reported in the proteomics study [433]. Here, we clearly show that the interaction of PARP1 with XPC prior to DNA damage is not a random phenomenon, but serves a definitive purpose of delivering XPC to the site of DNA damage within seconds after irradiation for efficient NER-mediated repair by XPC. We suggest that similar functional roles are possible for the steady-state interaction of other proteins with PARP1. Our study also highlights the fact that proteins move from one subnuclear compartment to another and thus they may carry old partners into new compartment or make new partners in the new location. Hence the proteomic studies of PARP1 interactors would be much more informative if one were to perform these analyses before and after DNA damage and in different subnuclear compartments.

5.8 Figures and legends

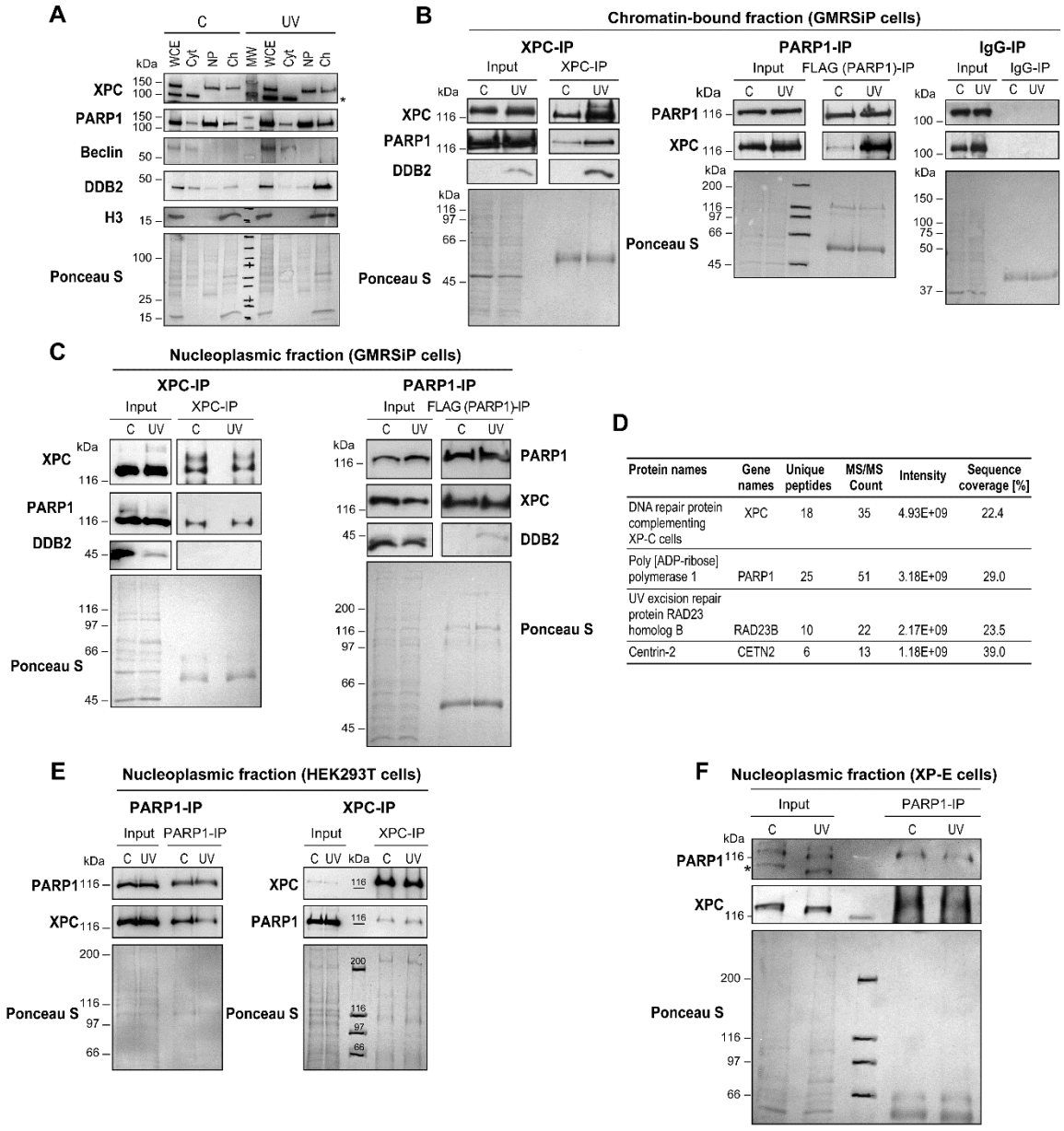

Figure 5.1 PARP1 interacts with XPC in the nucleoplasmic and chromatin fractions.

(A) The GMRSiP cells expressing FLAG tagged PARP1 were irradiated with 30J/m2 UVC (or control) and the whole cells extracts (WCE) were fractionated to obtain cytoplasm (Cyt), nucleoplasm (Np) and chromatin-bound (Ch) fractions. The proteins from each fraction were immunoblotted for XPC, PARP1 and DDB2. Beclin and histone H3 were used as cytoplasmic

and chromatin marker respectively. * indicates a non-specific band in XPC probing. The Ponceau S staining reflects the protein content at the end of each fractionation step. **(B-C)** The chromatin (B) and nucleoplasm fractions (C) of GMRSiP cells prepared as described above were subjected to IP for XPC, FLAG (PARP1) and mouse IgG (negative control), followed by the detection of PARP1, XPC and DDB2. **(D)** Table showing the XPC interacting proteins identified after XPC-IP of HEK293T cells followed by mass spectrometry analysis. **(E)** PARP1-IP and XPC-IP was performed in the Np fraction of control and UVC treated HEK293T cells as shown in panels B and C. The input and IP-eluates were probed for XPC and PARP1. **(F)** PARP1-IP was performed in the Np fraction of control and UVC treated XP-E cells treated as above. The input and IP-eluates were probed for XPC and PARP1. For the panels B, C, E and F the Ponceau S staining was used as loading control and results shown here are representative of results from 2-4 experiments.

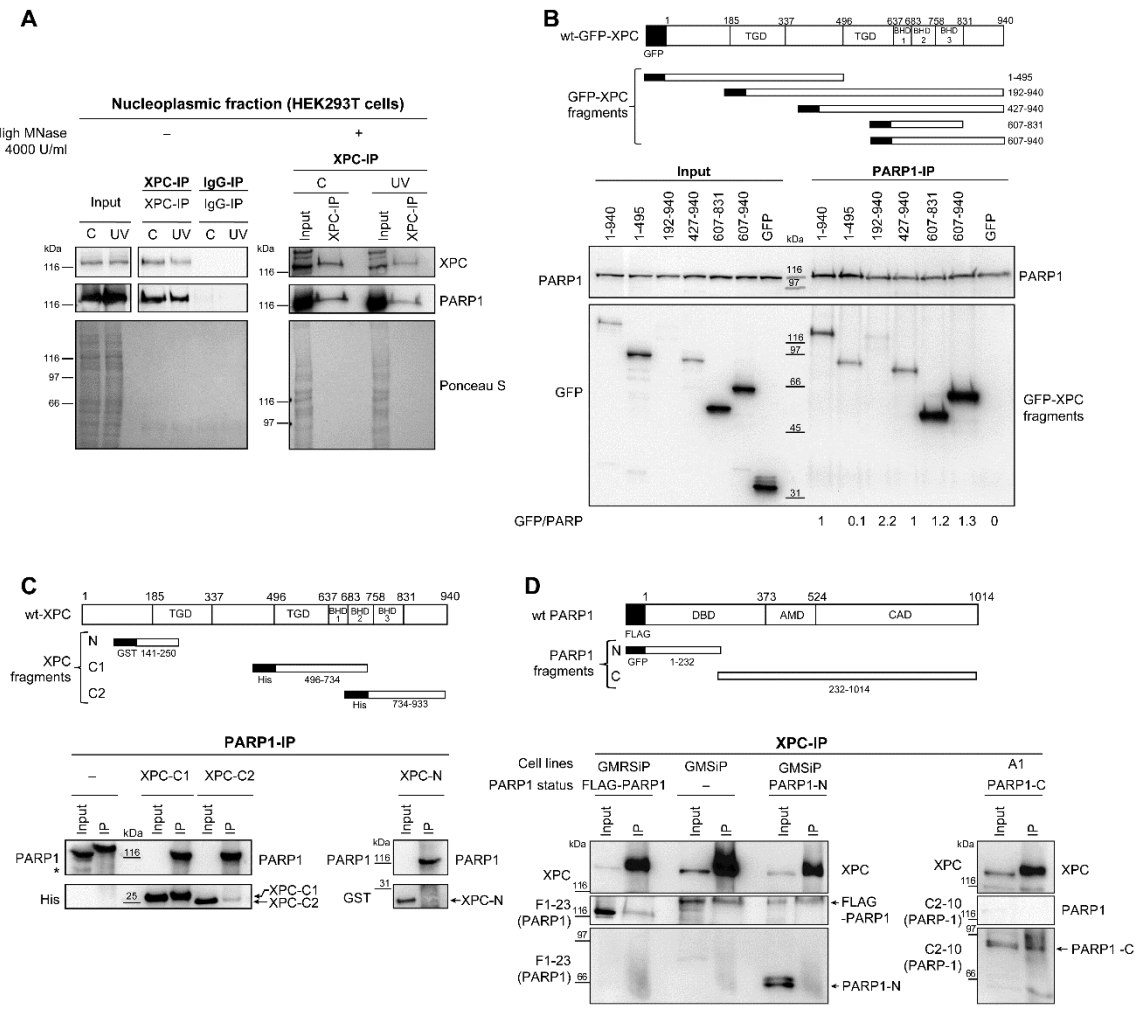

Figure 5.2 Identification of the domains implicated in the interaction between PARP1 and XPC.

(A) Left Panel: IP for XPC and rabbit IgG were performed in the nucleoplasm of HEK cells prepared as described in Fig. 1E. Right Panel: Nucleoplasmic extracts were also treated with 4000U/mL MNase and subjected to XPC-IP. The input and eluates were probed for XPC and PARP1. Ponceau S was used as loading control. **(B)** Top panel: Pictogram of GFP-tagged full length XPC and its five fragments used in the study. The domains marked as TGD and BHD1-3 represent transglutaminase homology domain and β hairpin domains 1 to 3. Bottom panel: The HEK293 cells were transiently transfected with GFP tagged full length XPC or its fragments for 48h. The nucleoplasmic fractions of these cells were subjected to PARP1-

IP. The input and the IP-eluates were analyzed for GFP (XPC) and PARP1. The relative intensity of the IP-bands was measured as a fraction of the total input protein. The strength of the interaction between XPC fragments and PARP1 was expressed as relative to the interaction of full length XPC with PARP1. **(C)** Top panel: pictogram showing the domains of wt XPC and the tagged XPC fragments used in this study. Bottom panel: The XPC fragments were reacted with pure PARP1 for 30 min at 25°C, follow by PARP1-IP on magnetic beads. The bead elutes were probed for PARP1, GST (XPC-N) and histidine (XPC-C1 and XPC-C2). **(D)** Top panel: Pictogram showing the domains of wt PARP1 and different PARP1 fragments used in this study. Bottom panel: The PARP1 depleted GMSiP were transiently transfected with full length FLAG-PARP1 or its N-terminal fragment (GFP-DBD) and the $PARP1^{-/-}$ A1 cells with C-terminal fragment for 48h. The nucleoplasmic fractions were subjected to XPC-IP and the bead-eluates were analyzed for XPC, and PARP1 (F1-23 and C2-10). The data represent identical results observed in two experiments.

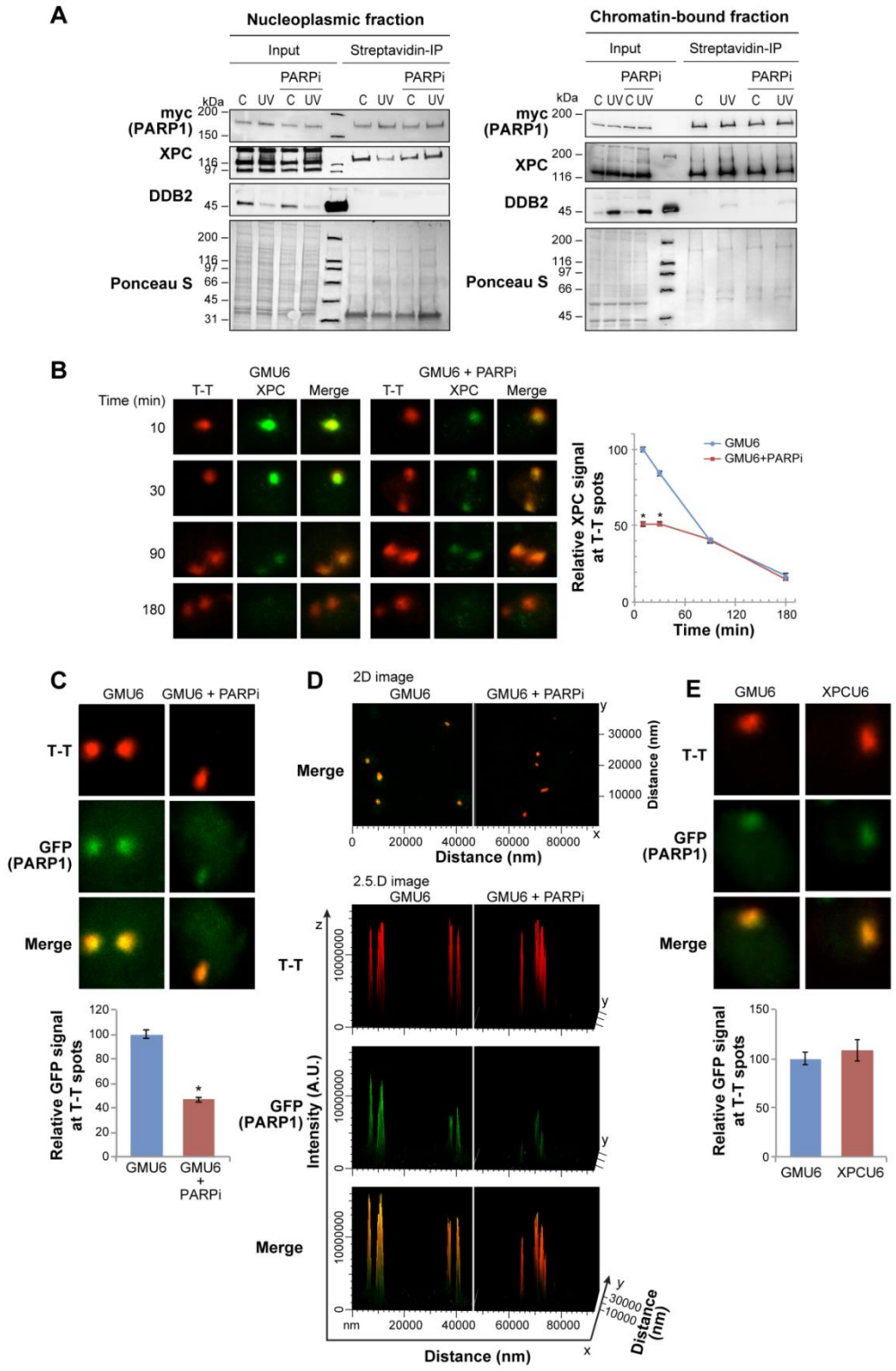

Figure 5.3 Efficient recruitment of PARP1 and XPC to the UV-lesion requires PARP1 catalytic activity.

(A) Bio-ID-PARP1 cells expressing myc-Bio-ID-FLAG-PARP1 were irradiated (30 J/m2 UVC or control) with or without PARPi (PJ-34). The nucleoplasm (left panel) and chromatin-bound (right panel) fractions were subjected to Streptavidin IP. The eluates were analyzed for myc (PARP1), XPC and DDB2. The data represent identical results observed in 3 experiments and Ponceau-staining provides loading control. # indicates the non-specific band in XPC probing. **(B)** The XPC kinetics at the UV-lesions was monitored in GMU6 cells up to 180 min after local UVC-irradiation with 100J/m2 UVC, through 5µm pores of a polycarbonate filter with or without PARPi PJ-34. The background corrected signal for XPC (green) at T-T spots (red) relative to 10 min signal is represented as mean ± SEM (200-500 spots from three experiments). Note: In all panels of this and subsequent Figs., * denotes statistically significant difference with P value <0.05 with unpaired two-tailed t-test. **(C-D)** The GMU6 cells transiently transfected with GFP-PARP1 for 24h, were locally irradiated with 100 J/m2 UVC in absence or presence of PARPi PJ-34. Panel C: The GFP (PARP1) signal at local T-T spots (red) after background correction were pooled from 200-300 spots derived from three experiments and expressed relative to the signal observed in cells not treated with PARPi. The panel D shows a representative 2D-merged image for GFP (PARP1) and T-T (red) colocalization and the orthogonal view (2.5D image) for the same field is shown to visualize signal intensity of T-T and GFP. The X and Y-axis represent distance in nm and Z-axis represents fluorescence intensity in arbitrary units. **(E)** The accumulation of the GFP (PARP1) at T-T lesions was monitored in GMU6 and XPC cells 10 min after irradiation with UVC at 100 J/m2. The background corrected GFP signal at lesion site relative to the signal observed in GMU6 cells is expressed as mean ± SEM derived from ≥150 spots from two experiments.

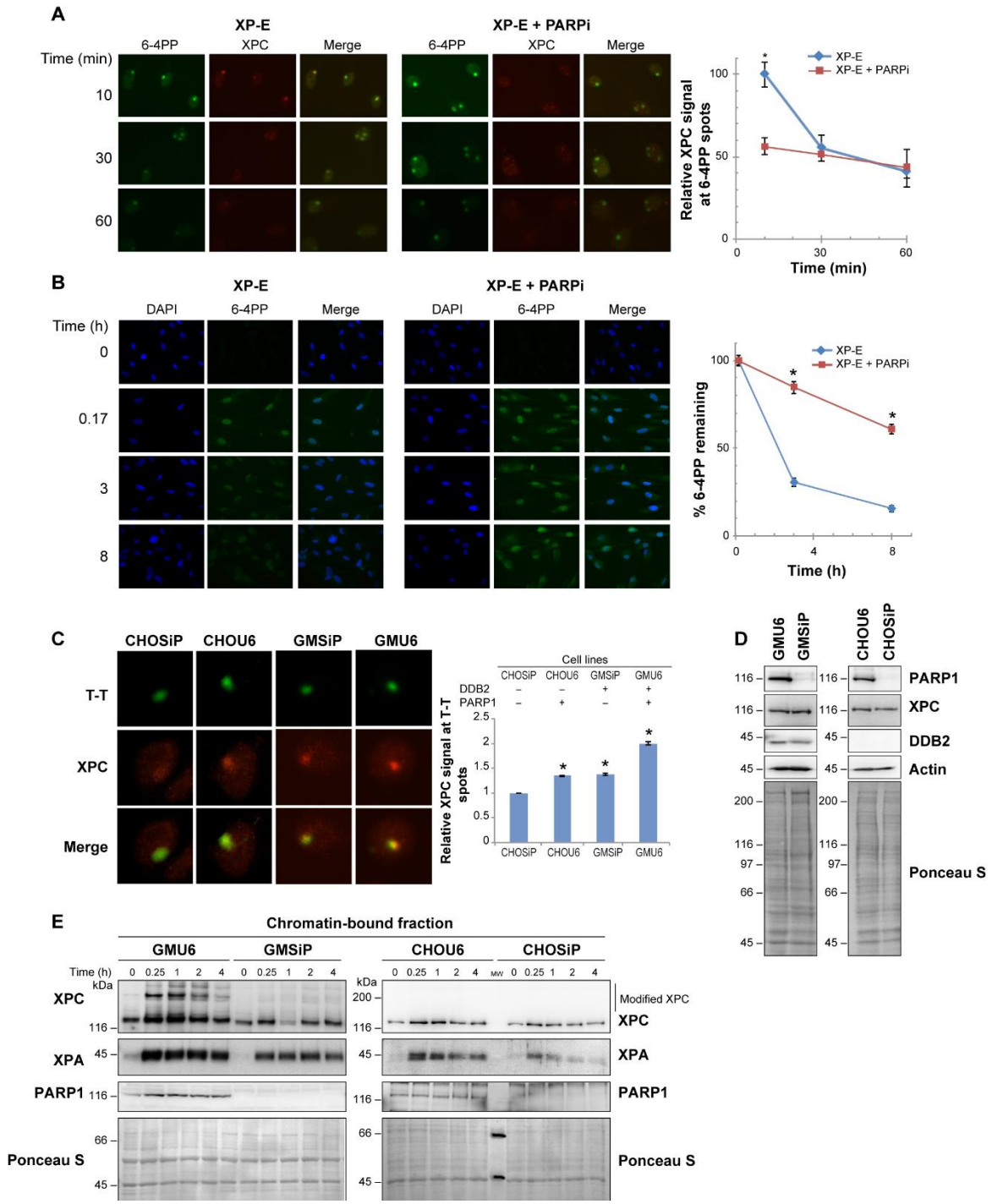

Figure 5.4 XPC recruitment to UV-lesions by PARP1 is DDB2 independent.

(A) XP-E cells with or without PARPi (ABT-888) were locally irradiated with 100J/m2 UVC and probed for XPC (red) and 6-4PP sites (green) at different times. The background corrected signal for XPC at 6-4PP spots is represented as mean ± SEM (300 spots derived

from three experiments). **(B)** The DDB2-deficient XP-E cells, with or without PARPi ABT-888, were globally irradiated with 10 J/m2 UVC and immunostained for 6-4PP lesions to determine its repair kinetics up to 8h. The data are presented as signal intensity relative to the maximum signal at 10 min (mean ± SEM, n ≥300 nuclei from 3 experiments). **(C)** The four cell lines with differing status of PARP1 and DDB2, as shown in the panel were locally irradiated with 100 J/m2 and probed for T-T and XPC at 10 min after irradiation. Background corrected signal for XPC at the T-T under identical exposure conditions was calculated as mean± SEM derived from 300-700 spots from 3 experiments. The accumulation of the XPC at T-T lesion in CHOU6, GMSiP, and GMU6 is expressed as fold increase over that observed in CHOSiP. **(D)** The total cell extracts of the four indicated cell lines, were separated on the SDS-PAGE and probed for PARP1, XPC and DDB2. Actin and Ponceau S were used as loading controls. **(E)** The four cells lines from above were globally irradiated with 30J/m2 UVC and fractionated after the time indicated. The chromatin extracts with equal proteins content were separated on SDS-PAGE and probed for XPC, XPA and PARP1. Ponceau S staining is used as loading control.

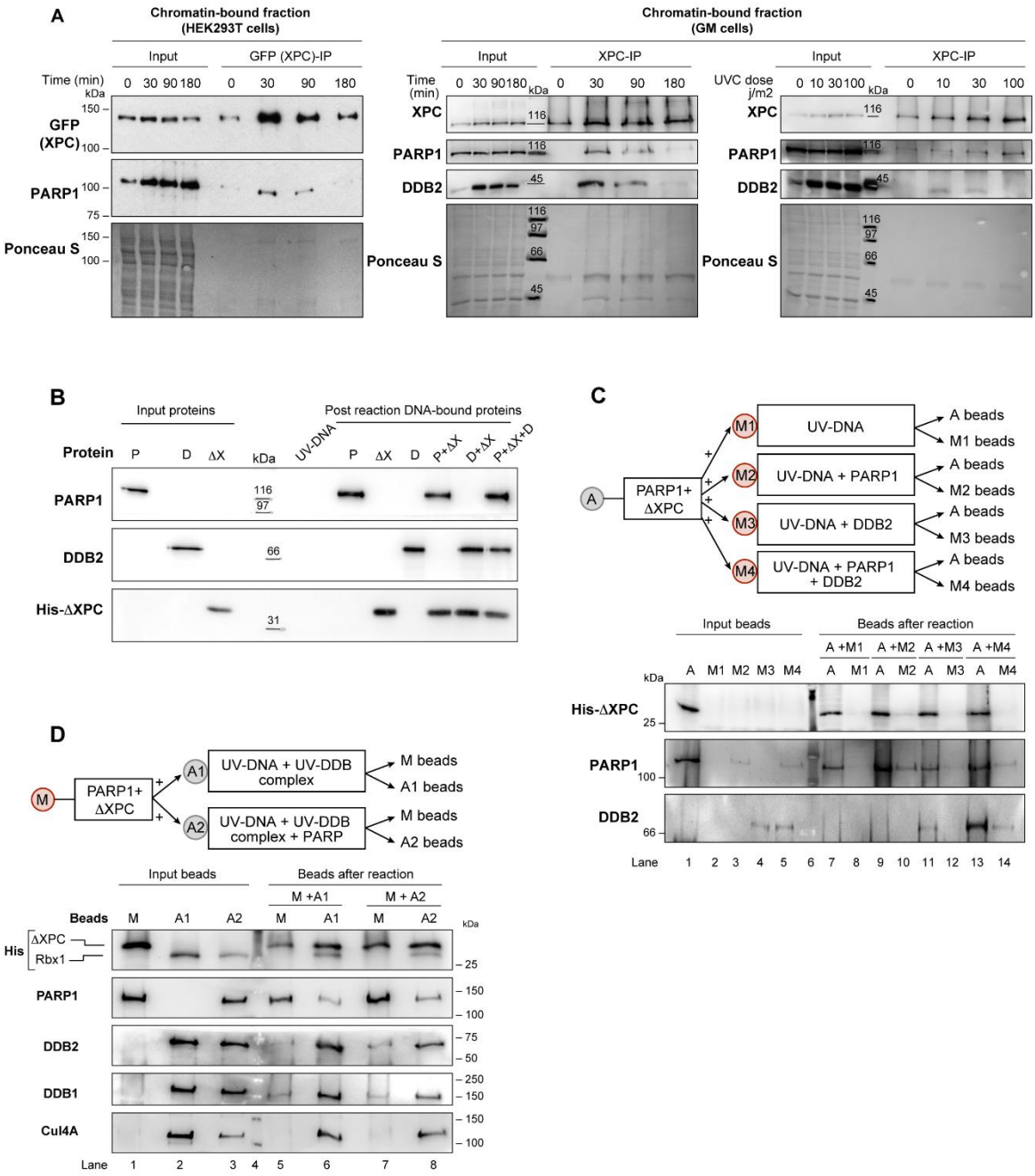

Figure 5.5 Role of PARP1 and UV-DDB ligase complex in the hand-over of XPC to the lesion site.

(A) Left panel: HEK293T cells transfected with GFP-XPC plasmid were irradiated 48h later with 30J/m2 UVC (or control) and fractionated to isolate chromatin-bound fraction, which was subjected to IP with GFP-trap beads. The eluates were probed with PARP1 and GFP

antibody. Middle and right panels: GMU6 cells were irradiated either with 30J/m2 UVC (middle panel) or different UVC doses as indicated (right panel) and fractionated after the time indicated. The chromatin bound protein fraction was used for immunoprecipitation of XPC. The IP eluates were resolved on the SDS-PAGE and probed for XPC, PARP1 and DDB2. The Ponceau S staining was used as loading control, and panel is representative of results from two experiments. **(B)** UVC-DNA was bound to magnetic beads via T-T antibody and reacted with pure proteins: PARP1 (P), XPC fragment (ΔX), DDB2 (D) and different protein combinations for 15 min at 25°C. The beads were washed, the bound proteins eluted, separated on SDS-PAGE and probed with their respective antibodies. **(C-D)** The top panels represent schematic of the different conditions used in the in vitro assays for examining the separation of XPC from PARP1-XPC complex and its hand-over to UV-DNA. The grey and red circles represent agarose and magnetic beads, respectively. Bead bound PARP1-ΔXPC complex was prepared either on magnetic or agarose beads as described in Fig. 2C. The representative results for each model from 2- 3 experiments are shown. (Panel C) PARP1-ΔXPC complex was prepared on agarose beads (A) and magnetic bead bound UV-DNA (M1) was reacted with PARP1 (M2), DDB2 (M3) or both (M4), as described for Panel B. The beads were mixed as indicated in the top panel, reacted for 15 min at 25°C in buffer, separated, washed, eluted, the elution separated on SDS-PAGE and probed for their respective antibodies. (Panel D) PARP1-ΔXPC complex was prepared on magnetic beads (M), and agarose bead bound UV-DDB-ligase complex without (A1) or with (A2) 2nd PARP1 was prepared by pre-reacting agarose bead bound Cul4-Rbx complex with free UV-DNA, DDB1 and DDB2 for 15 min at 25°C. The beads were mixed, reacted for 15 min at 25°C in buffer, separated, washed, eluted, the elution separated on SDS-PAGE and probed for their respective antibodies.

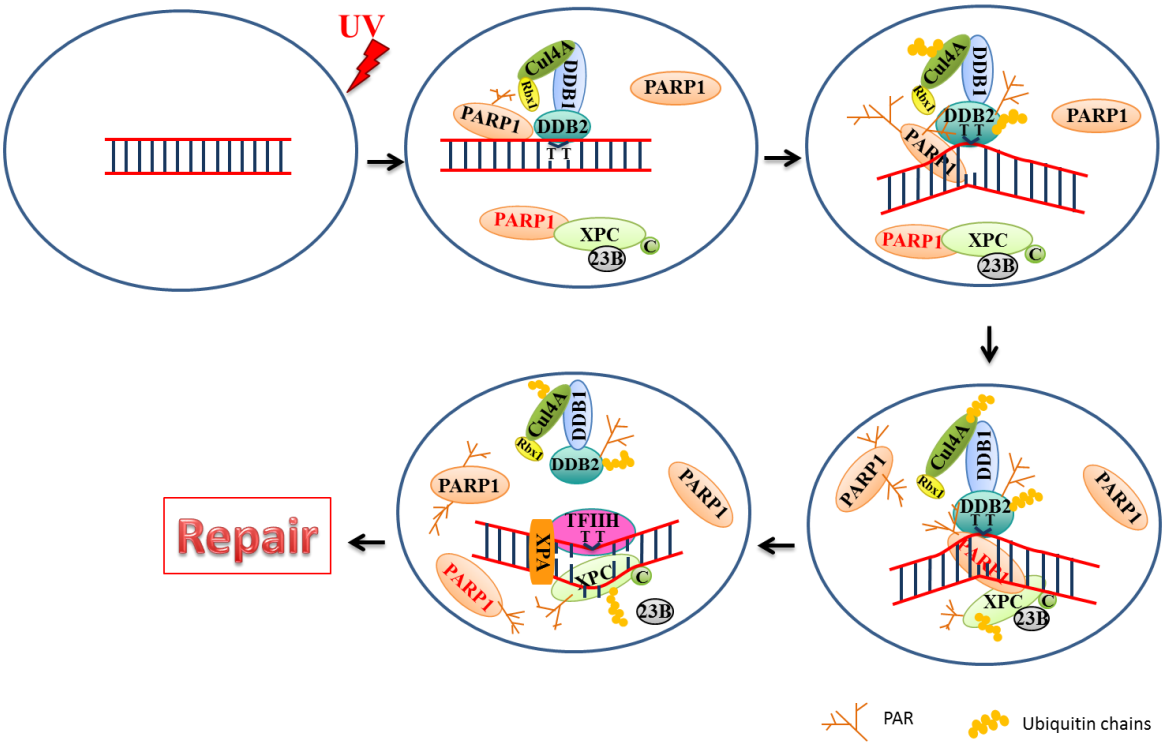

Figure 5.6 Model for the role of PARP1 in recruitment and stabilization of XPC in NER.

See details in Discussion section.

Supplementary Figures

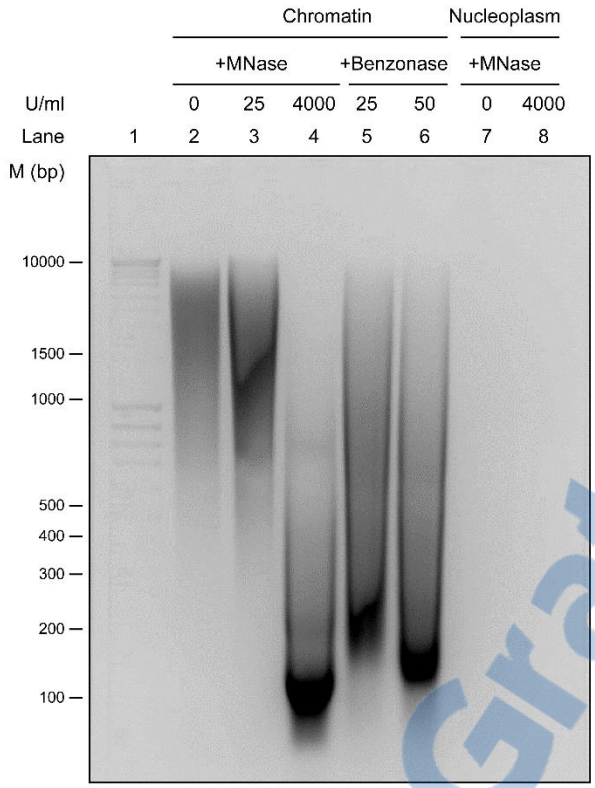

Figure S5.1 DNA profile after nucleases activity.

The chromatin and nucleoplasmic fraction of HEK293T cells were treated with increasing concentration of MNase or Benzonase, as indicated. The DNA was purified with phenol-chloroform and resolved on 2% agarose gel.

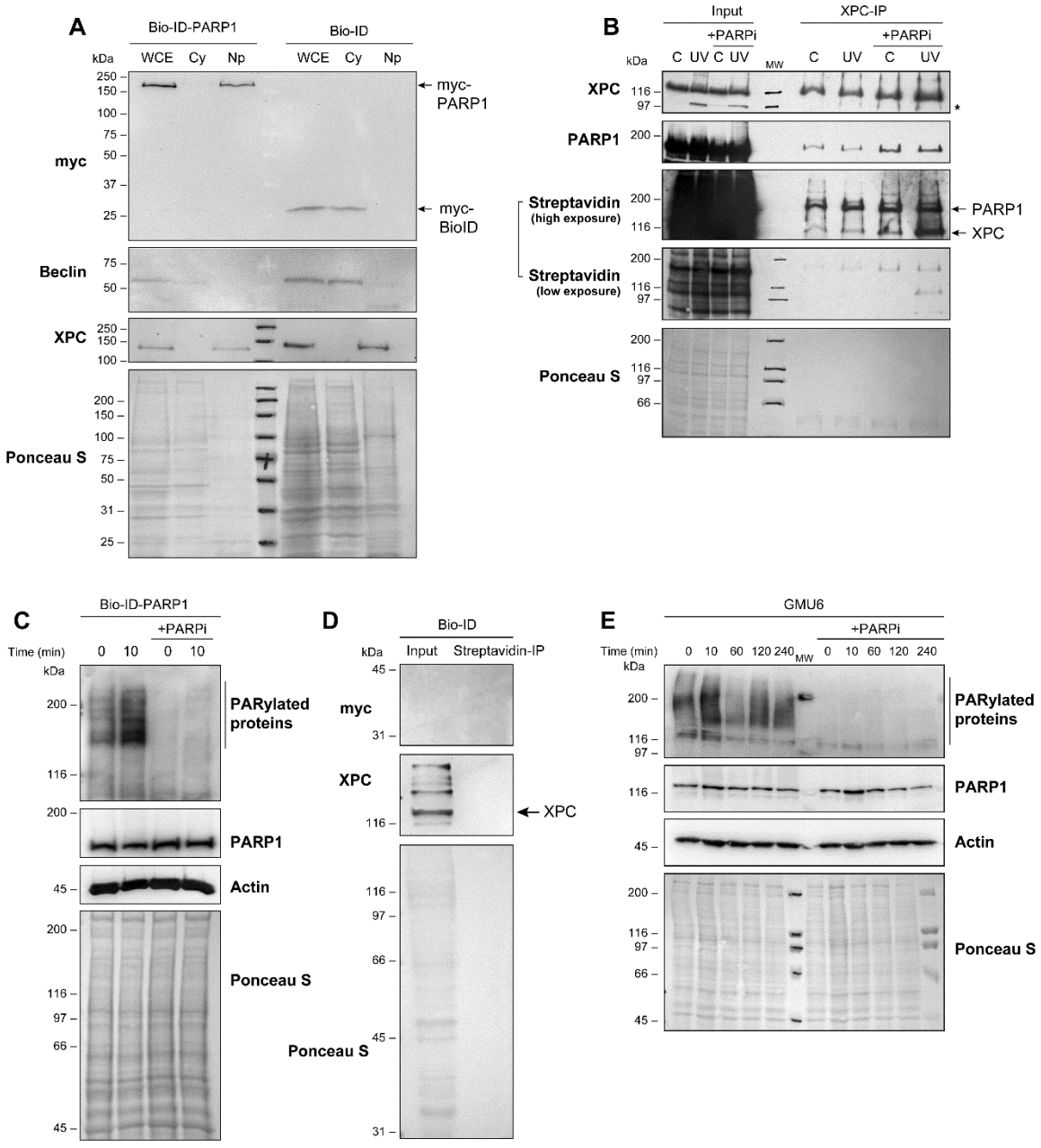

Figure S5.2 Characterization of the Bio-ID and Bio-ID-PARP1 cells.

(**A**) The control Bio-ID and Bio-ID-PARP1 whole cell extracts (WCE) were fractionated to obtain cytoplasm (Cy) and nucleoplasm (Np) fractions. The proteins in each fraction were resolved on SDS-PAGE and immunoblotted for myc. The cytoplasm and nuclear fraction were verified by probing for Beclin and XPC, respectively. (**B**) Bio-ID-PARP1 cells were treated with 50 µM biotin 16 h before irradiation with 30J/m2 UVC (or control). The PARPi, PJ-34, was used at 10 µM to inhibit PARP1 catalytic activity. Cells were

fractionated 10 minutes after irradiation to obtain nucleoplasm that was subjected to XPC-IP. The eluates were analyzed for PARP1, XPC and biotin using streptavidin. The data represent identical results observed in 2 experiments. (**C**) The Bio-ID-PARP1 cells treated with 10 µM PJ-34 (or control) were irradiated with 30J/m2 UVC. The total cells extracts prepared 10 minutes after UVC irradiation were resolved on SDS-PAGE and immunoblotted for PARylated proteins (LP-96-10), PARP1 and β-actin. (**D**) pcDNA3.1 mycBioID plasmid expressing cells were fractionated and streptavidin-IP was performed in the nucleoplasmic extract. Input and eluates were probed for myc and XPC. (**E**) The GMU6 cells were pre-treated with 10µM PJ-34 (or control) and irradiated 30 minutes after with 30J/m2 UVC. Total cells extract collected at different times after UVC irradiation as indicated were resolved on SDS-PAGE and probed for PARylated proteins (LP-96-10) PARP1 and actin. For all the panels, Ponceau S staining was used as loading control.

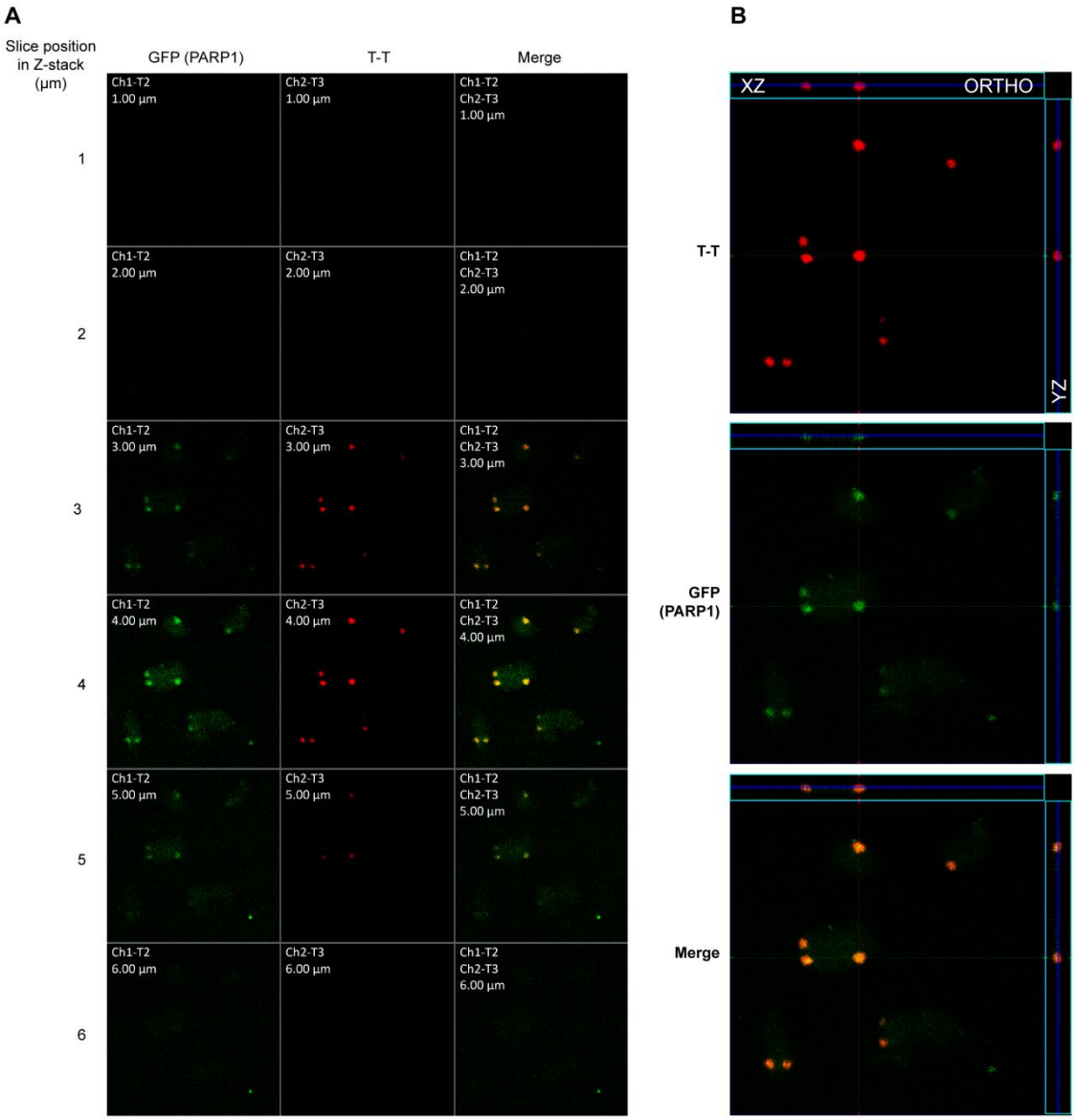

Figure S5.3 PARP1 co-localizes with UV-damaged DNA *in vivo*.

(A) The GMU6 cells were transiently transfected with GFP-PARP1 and 24h later were locally irradiated with 100J/m^2 UVC. The cells were subjected to the in situ extraction protocol, with detergent and salt as described in Methods. Representative Z-stack images collected at 1µm sections show the colocalization of the GFP (PARP1) with the T-T lesions (slices 3 to 5). **(B)** The Z-stack presented in (A) is shown in the orthogonal view to observe the GFP co-localization with T-T. The green and the red lines indicate the orthogonal planes of the X-Z and Y-Z projection, respectively and the blue lines, the Z-depth of the 4 µm optical slice.

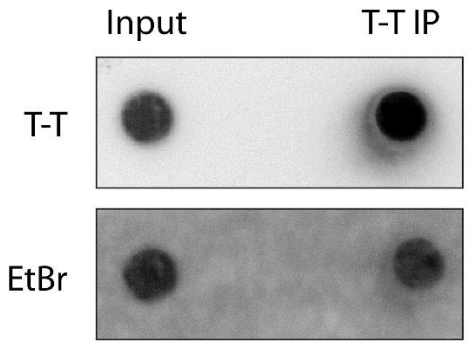

Figure S5.4 Magnetic bead bound UVC-DNA used in the in vitro assays.

The pPBS-U6 plasmid was irradiated with 5000 J/m2 UVC and bound to magnetic beads via T-T antibody. The IP was validated by Dot-blot assay using specific antibody. EtBr staining was used as loading control.

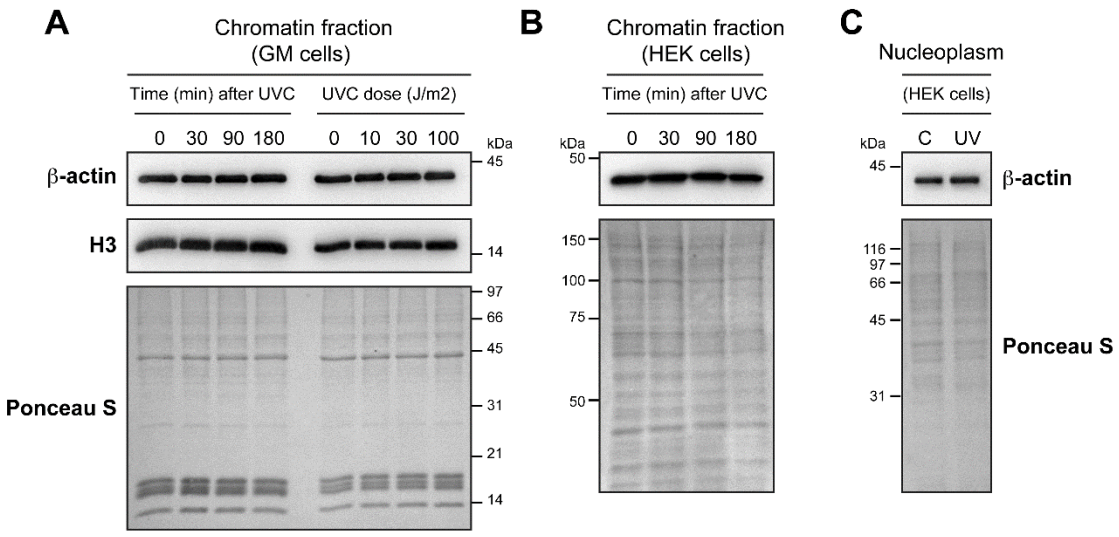

Figure S5.5 Loading controls for the nucleoplasmic and chromatin extracts of GM-U6 and HEK 293T cells.

Nucleoplasmic and chromatin extracts prepared for IP from the two cell types, were separated on SDS-PAGE, probed for β-actin and H3 to validate the equality of the proteins as estimated by Bradford. Ponceau S staining is shown as an additional loading control.

5.9 Materials and methods

Cell lines, clones and transient transfection: Parental SV-40–immortalized GM637 and primary XP-E (GM01389) human skin fibroblasts were obtained from Coriell and HEK293T and CHO cells from ATCC. The creation of the clones PARP1–replete GMU6, PARP1–depleted GMSiP, PARP1–replete CHOU6, PARP1–depleted CHOSiP and the FLAG-tagged PARP1-expressing GMRSiP clones were described [392, 425]. For the creation of the Bio-ID clones, the GMSiP cells were transfected with Bio-ID-PARP1 or mycBioID plasmids (described below) and the pooled population of cells were selected by G418 at 800µg/ml.

Plasmids and cloning: The pcDNA3.1 mycBioID plasmid expressing the promiscuous Escherichia coli biotin protein ligase BirA with N-terminal myc tag was obtained from Addgene [421]. To create the Bio-ID-PARP1 plasmid, the EcoICRI / SmaI fragment of RNAi-resistant FLAG-PARP1 from p3X FLAG-hPARP1-RSiP-CMV 7.1 plasmid [392] was ligated to the EcoRV linearized pcDNA3.1 mycBioID plasmid. The GFP-PARP1 expression vector was a gift from Dr Valerie Schreiber (Université Strasbourg 1, France). Plasmid transfection was performed using TurboFect reagent according to the manufacturer's protocol (Thermo Fisher Scientific).

UV irradiation and immunofluorescence microscopy studies: Global and local UVC irradiation though a 5 µm polycarbonate filter (Millipore) of cells were carried out with a UVC lamp (peak 254nm wavelength) in PBS or dye-free medium. For the immunofluorescence studies, cells were grown on circular coverslips in 35-mm dishes to 80% confluence. For GFP-PARP1 kinetics, cells were transfected using TurboFect reagent 24h before irradiation. The repair kinetics assays for 6-4PP and detection of the recruitment of the NER proteins to the local UVC-induced DNA damage were performed as described [392]. The in vivo recruitment of GFP-PARP1 to local UV-lesion site in the nuclei was performed by selective in situ extraction protocol, as described earlier [423]. Images of immunostained cells were taken with Axiovert 200 at 40x or 63x using the AxioCam MRm. The Z-stack images were taken using the 63x oil objective of the LSM 700 confocal laser-

scanning microscope (Zeiss), equipped with ZEN 2009 software for image acquisition. The 2.5D images were produced using ZEN 2009 software.

Cell fractionation and co-IP of proteins in the cell fractions: Cell fractionation to obtain nucleoplasm and chromatin extract and the co-IP studies were done as described [392]. The protein content in each fraction was estimated by Bradford assay; and equal amount of protein from each sample was subjected to co-IP studies, as confirmed by Ponceau S staining for all the blots. The Ponceau S staining as a measure of equal loading was validated by immunoprobing for β-actin or histone H3 in these fractions in representative blots of GM or HEK cells (Fig. S5.5). For the streptavidin-IP, 50μM biotin was added in the medium 16-18h before UV-treatment and cell fractionation, followed by IP with M280 streptavidin beads for 30 min at ambient temperature. The beads were washed as suggested in the supplier's manual (Life Technologies).

Identification of XPC interacting proteins by Mass Spectrometry: The 50-60 x 10^6 HEK cells were suspended in 2 ml of buffer containing 50 mM Tris-HCl, pH 7.5, 5 mM EDTA, 0.2% IGEPAL, 300 mM NaCl, 0.5 mM PMSF and protease inhibitors. After incubation on ice for 20 min, the cells lysate was sonicated for 20 sec at lowest amplitude (11%, Fisher Ultrasonic Dismembrator, model 500). The extract was diluted by adding equal volume of the above-mentioned buffer without NaCl to dilute the NaCl at 150mM and centrifuged at 13,000 rpm for 10 min. The IP for the relevant proteins in the supernatant was carried out overnight at 4°C by using XPC polyclonal antibody (1:500). This was followed by recovery of protein-antibody complex with magnetic Protein G beads (Life Technologies), which were extensively washed and suspended in 2x volume of TBS containing 30 % glycerol and protease inhibitors and stored at -30°C. The XPC interacting proteins were identified using LC-MS/MS and quantified on Dionex Ultimate 3000 nano HPLC system as previously described [434]. Briefly, acetonitrile/ formic acid extract of tryptic digest of the IP-beads was separated on PepMap100 C18 column and loaded on PepMap C18 nano column. The peptides were then electro sprayed on OrbiTrap QExactive mass spectrometer to obtain a survey spectra at resolution of 70,000 using 106 ions. 10 highest intensity peptides were selected for collision-induced dissociation at 35 % energy and resolution of 17,500 for 50,000

ions. Dynamic exclusion was set to retain 500 entries with a max retention time of 40s using 10 ppm mass window and an enabled lock mass option. Data acquisition was done using Xcalibur version 2.2 SP1.48. Protein identification and quantification was performed using the MaxQuant software package version 1.5.2.8 with the protein database from Uniprot (Homo sapiens, 16/07/2013, 88 354 entries). Maximum mass tolerance was set at 7 and 20 ppm for precursor and fragment ions respectively. The threshold for the false discovery rate (FDR) was 5% and protein quantification was set at minimum of two peptides identified for each protein.

In vitro studies to examine the hand-over of XPC from PARP1 to UV-damaged DNA: All the proteins used in these assay were pure, bovine PARP1 was obtained from Apartosis, XPC fragments were obtained from Antibodies online, GST-DDB1 and GST-DDB2 were obtained from Abnova. Full-length human CUL4A was co-expressed as a glutathione S-transferase (GST)-fusion protein with His6-tagged RBX1 in *E. coli*, affinity-purified by glutathione affinity chromatography, and subsequently subjected to anion exchange and gel filtration chromatography. Purified GST-CUL4A/His-Rbx1complex was concentrated by ultrafiltration and suspended in a final solution of 20 mM Tris-HCl (pH = 8.0), 200 mM NaCl, and 5 mM dithiothreitol (DTT). Antibodies were bound to magnetic beads at ambient temperature (45 min) and to agarose beads on ice (1 h) in 400-500 µl of TBS-T (50 mM Tris pH 7.5, 150 mM NaCl, 0.05 % Tween-20). The beads were washed 3 times with TBS-T, and suspended in buffer containing 100 mM Tris, pH 8.0, 10 mM MgCl2, 10 % glycerol, 1.5 mM DTT, 150 mM NaCl. UVC-DNA was prepared by irradiating 3.2 kb PBS-U6 plasmid with 5000 J/m2 UVC. Bead bound UVC-DNA was prepared by IP of the above mentioned DNA with bead bound T-T antibody at 4 °C for 2 hr. DNA bound proteins were prepared by reacting bead bound UVC-DNA with free proteins in the above buffer for 15 min at 25 °C, and washing the beads to remove the unbound proteins. PARP1-XPC fragments complex was prepared by reacting PARP1 and the XPC fragments at equimolar ratio in the above mentioned reaction buffer at 25 °C for 30 min, followed by PARP1-IP on ice for 1.5 h using the bead bound antibody. Bead bound UV-DDB complex was prepared by incubating agarose bead bound Cul4A/Rbx1 with free UVC-DNA, DDB1 and DDB2 in the reaction buffer with or without PARP1, for 15 min at 25°C. The unreacted proteins were removed by

washing. In experiments where the magnetic and agarose beads were mixed for reaction, the beads were separated and washed post reaction using magnetic stand. The bead bound proteins were eluted, separated on SDS-PAGE and probed with their respective antibodies.

Statistics: For the immunofluorescence studies, three independent experiments were performed and the intensity of fluorescence from at least 200-400 nuclei were analyzed by Axiovert 200 (Zeiss) using the program AutoMeasure Plus of the software Axiovision version 4.7 and expressed as pixel per area. To calculate the amount of accumulation of proteins at UV lesion, the fluorescence intensity at the damage site was measured as described above followed by the subtraction of the background intensity detected outside of the spots from an identic area in the nucleus. Results are expressed as mean ± SEM. The statistical significance of difference was determined by unpaired two-tailed t-tests and * refers to significant *P*-values < 0.05.

Acknowledgments

We are thankful to V. Schreiber for GFP-PARP1 and M. Miwa for permission to receive 10H hybridoma. This work was supported by the Discovery Grants # RGPIN-2016-05868 and Discovery Accelerator Grant # RGPAS-492875-2016 to GMS from the Natural Sciences and Engineering Research Council of Canada. NKP received a foreign student fee-waiver scholarship from Quebec Government and Shastri Indo-Canadian Institute. MR and NKP were recipients of graduate scholarships from the Fonds de recherche du Québec-Santé and Neuroscience Axis of CR-CHU-Q, respectively.

5.10 References

1. Scharer OD (2013) Nucleotide Excision Repair in Eukaryotes. *Cold Spring Harbor perspectives in biology* 5(10):10.1101/cshperspect.a012609.

2. Nemzow L, Lubin A, Zhang L, & Gong F (2015) XPC: Going where no DNA damage sensor has gone before. *DNA Repair (Amst)* 36:19-27.

3. Puumalainen MR, Ruthemann P, Min JH, & Naegeli H (2016) Xeroderma pigmentosum group C sensor: unprecedented recognition strategy and tight spatiotemporal regulation. *Cell Mol Life Sci* 73(3):547-566.

4. Sugasawa K (2016) Molecular mechanisms of DNA damage recognition for mammalian nucleotide excision repair. *DNA Repair (Amst)* 44:110-117.

5. Marteijn JA, Lans H, Vermeulen W, & Hoeijmakers JH (2014) Understanding nucleotide excision repair and its roles in cancer and ageing. *Nat Rev Mol Cell Biol* 15(7):465-481.

6. Hoogstraten D, *et al.* (2008) Versatile DNA damage detection by the global genome nucleotide excision repair protein XPC. *J Cell Sci* 121(Pt 17):2850-2859.

7. Chen X, *et al.* (2015) Kinetic gating mechanism of DNA damage recognition by Rad4/XPC. *Nat Commun* 6:5849.

8. Velmurugu Y, Chen X, Slogoff Sevilla P, Min JH, & Ansari A (2016) Twist-open mechanism of DNA damage recognition by the Rad4/XPC nucleotide excision repair complex. *Proc Natl Acad Sci U S A* 113(16):E2296-2305.

9. Moser J, *et al.* (2005) The UV-damaged DNA binding protein mediates efficient targeting of the nucleotide excision repair complex to UV-induced photo lesions. *DNA Repair* 4(5):571-582.

10. Oh KS, *et al.* (2011) Nucleotide excision repair proteins rapidly accumulate but fail to persist in human XP-E (DDB2 mutant) cells. *Photochem Photobiol* 87(3):729-733.

11. Luijsterburg MS, *et al.* (2007) Dynamic in vivo interaction of DDB2 E3 ubiquitin ligase with UV-damaged DNA is independent of damage-recognition protein XPC. *J. Cell Sci.* 120(Pt 15):2706-2716.

12. Lan L, *et al.* (2012) Monoubiquitinated histone H2A destabilizes photolesion-containing nucleosomes with concomitant release of UV-damaged DNA-binding protein E3 ligase. *J Biol Chem* 287(15):12036-12049.

13. Wang H, *et al.* (2006) Histone H3 and H4 ubiquitylation by the CUL4-DDB-ROC1 ubiquitin ligase facilitates cellular response to DNA damage. *Mol Cell* 22(3):383-394.

14. El-Mahdy MA, *et al.* (2006) Cullin 4A-mediated proteolysis of DDB2 protein at DNA damage sites regulates in vivo lesion recognition by XPC. *J Biol Chem* 281(19):13404-13411.

15. Nishi R, *et al.* (2009) UV-DDB-dependent regulation of nucleotide excision repair kinetics in living cells. *DNA Repair (Amst)* 8(6):767-776.

16. Shell SM, *et al.* (2013) Xeroderma pigmentosum complementation group C protein (XPC) serves as a general sensor of damaged DNA. *DNA Repair (Amst)* 12(11):947-953.

17. Payne A & Chu G (1994) Xeroderma pigmentosum group E binding factor recognizes a broad spectrum of DNA damage. *Mutat Res* 310(1):89-102.

18. Scrima A, *et al.* (2008) Structural basis of UV DNA-damage recognition by the DDB1-DDB2 complex. *Cell* 135(7):1213-1223.

19. Vodenicharov MD, Ghodgaonkar MM, Halappanavar SS, Shah RG, & Shah GM (2005) Mechanism of early biphasic activation of poly(ADP-ribose) polymerase-1 in response to ultraviolet B radiation. *J. Cell Sci.* 118(Pt 3):589-599.

20. Robu M, *et al.* (2013) Role of poly(ADP-ribose) polymerase-1 in the removal of UV-induced DNA lesions by nucleotide excision repair. *Proc. Natl. Acad. Sci. U.S.A.* 110(5):1658-1663.

21. Pines A, *et al.* (2012) PARP1 promotes nucleotide excision repair through DDB2 stabilization and recruitment of ALC1. *J. Cell Biol.* 199(2):235-249.

22. Luijsterburg MS, *et al.* (2012) DDB2 promotes chromatin decondensation at UV-induced DNA damage. *J. Cell Biol.* 197(2):267-281.

23. Fei J, *et al.* (2011) Regulation of nucleotide excision repair by UV-DDB: prioritization of damage recognition to internucleosomal DNA. *PLoS Biol.* 9(10):e1001183.

24. Roux KJ, Kim DI, Raida M, & Burke B (2012) A promiscuous biotin ligase fusion protein identifies proximal and interacting proteins in mammalian cells. *J Cell Biol* 196(6):801-810.

25. Moné MJ, *et al.* (2001) Local UV-induced DNA damage in cell nuclei results in local transcription inhibition. *EMBO Rep.* 2(11):1013-1017.

26. Purohit NK, Robu M, Shah RG, Geacintov NE, & Shah GM (2016) Characterization of the interactions of PARP-1 with UV-damaged DNA in vivo and in vitro. *Sci Rep* 6:19020.

27. Hanssen-Bauer A, *et al.* (2011) XRCC1 coordinates disparate responses and multiprotein repair complexes depending on the nature and context of the DNA damage. *Environ Mol Mutagen* 52(8):623-635.

28. Mortusewicz O, Ame JC, Schreiber V, & Leonhardt H (2007) Feedback-regulated poly(ADP-ribosyl)ation by PARP-1 is required for rapid response to DNA damage in living cells. *Nucleic Acids Res.* 35(22):7665-7675.

29. Pines A, Mullenders LH, van Attikum H, & Luijsterburg MS (2013) Touching base with PARPs: moonlighting in the repair of UV lesions and double-strand breaks. *Trends Biochem Sci* 38(6):321-330.

30. Ghodgaonkar MM, Zacal NJ, Kassam SN, Rainbow AJ, & Shah GM (2008) Depletion of poly(ADP-ribose)polymerase-1 reduces host cell reactivation for UV-treated adenovirus in human dermal fibroblasts. *DNA Repair (Amst)* 7:617-632.

31. Shah RG, Ghodgaonkar MM, Affar EB, & Shah GM (2005) DNA vector-based RNAi approach for stable depletion of poly(ADP-ribose) polymerase-1. *Biochem. Biophys. Res. Commun.* 331(1):167-174.

32. Yasuda G, *et al.* (2007) In vivo destabilization and functional defects of the xeroderma pigmentosum C protein caused by a pathogenic missense mutation. *Mol Cell Biol* 27(19):6606-6614.

33. Godon C, *et al.* (2008) PARP inhibition versus PARP-1 silencing: different outcomes in terms of single-strand break repair and radiation susceptibility. *Nucleic Acids Res* 36(13):4454-4464.

34. Gassman NR & Wilson SH (2015) Micro-irradiation tools to visualize base excision repair and single-strand break repair. *DNA Repair (Amst)* 31:52-63.

35. Fitch ME, Nakajima S, Yasui A, & Ford JM (2003) In vivo recruitment of XPC to UV-induced cyclobutane pyrimidine dimers by the DDB2 gene product. *J. Biol. Chem.* 278(47):46906-46910.

36. Luo X & Kraus WL (2012) On PAR with PARP: cellular stress signaling through poly(ADP-ribose) and PARP-1. *Genes Dev* 26(5):417-432.

37. Pascal JM & Ellenberger T (2015) The rise and fall of poly(ADP-ribose): An enzymatic perspective. *DNA Repair (Amst)* 32:10-16.

38. Langelier MF & Pascal JM (2013) PARP-1 mechanism for coupling DNA damage detection to poly(ADP-ribose) synthesis. *Curr. Opin. Struct. Biol.* 23:134-143.

39. Lonskaya I, *et al.* (2005) Regulation of poly(ADP-ribose) polymerase-1 by DNA structure-specific binding. *J Biol Chem* 280(17):17076-17083.

40. Sugasawa K, *et al.* (2005) UV-induced ubiquitylation of XPC protein mediated by UV-DDB-ubiquitin ligase complex. *Cell* 121(3):387-400.

41. Clark NJ, Kramer M, Muthurajan UM, & Luger K (2012) Alternative modes of binding of poly(ADP-ribose) polymerase 1 to free DNA and nucleosomes. *J. Biol. Chem.* 287(39):32430-32439.

42. Moor NA, Vasil'eva IA, Anarbaev RO, Antson AA, & Lavrik OI (2015) Quantitative characterization of protein-protein complexes involved in base excision DNA repair. *Nucleic Acids Res* 43(12):6009-6022.

43. Wei L, *et al.* (2013) Damage response of XRCC1 at sites of DNA single strand breaks is regulated by phosphorylation and ubiquitylation after degradation of poly(ADP-ribose). *J Cell Sci* 126(Pt 19):4414-4423.

44. Kraus WL & Lis JT (2003) PARP goes transcription. *Cell* 113(6):677-683.

45. Osakabe A, *et al.* (2015) Structural basis of pyrimidine-pyrimidone (6–4) photoproduct recognition by UV-DDB in the nucleosome. *Scientific Reports* 5:16330.

46. Isabelle M, *et al.* (2010) Investigation of PARP-1, PARP-2, and PARG interactomes by affinity-purification mass spectrometry. *Proteome Sci* 8:22.

47. Dubois ML, Bastin C, Levesque D, & Boisvert FM (2016) Comprehensive Characterization of Minichromosome Maintenance Complex (MCM) Protein Interactions Using Affinity and Proximity Purifications Coupled to Mass Spectrometry. *J Proteome Res* 15(9):2924-2934.

Chapitre 6

Discussion générale

Lors de l'exposition au soleil, l'ADN est soumis à l'action des radiations ultraviolettes qui créent des dommages directs à l'ADN par la formation de liaisons covalentes entre les pyrimidines adjacentes et des dommages indirects via des ROS. Deux voies de réparation éliminent ces dommages : la réparation par excision de bases (BER) et la réparation par excision de nucléotides (NER). L'étape limitante de toute voie de réparation est la reconnaissance des dommages. Si la BER emploie des protéines dédiées à trouver un certain type de dommage à l'ADN, les glycosylases, la voie de réparation globale du génome de la NER utilise une seule protéine, la XPC, pour trouver une grande variété de dommages non apparentés structuralement, d'où la question : comment la XPC accomplie-t-elle une tâche si difficile?

Des études récentes ont montré que la XPC cherche les dommages avec ses domaines BHD1/2 en glissant sur l'ADN et s'arrête lorsqu'une distorsion qui altère la structure β de l'ADN. Si l'ADN peut être tordu, la XPC insère son domaine BHD3 [144] et forme une structure stable requise pour le recrutement des autres protéines de la NER [426]. Ceci constitue la base moléculaire des résultats des études biochimiques qui avaient révélé la capacité innée de la XPC à détecter la distorsion de l'ADN causée par plusieurs types de dommages, incluant les dommages de type 6-4PP induites par les UV [66]. Cependant, son immobilisation par les structures qui déforment l'ADN n'est pas une preuve de la présence d'une lésion, car la XPC lie le brin non-endommagé et n'établit aucun contact avec la lésion elle-même. En effet, la XPC lie des dommages qui ne constituent pas de substrats pour la NER, tel que démontré par sa mobilité réduite lors du traitement des cellules avec une grande variété d'agents endommageant l'ADN [140]. Comme la fonction principale de la NER est de reconnaître, exciser et réparer les photolésions sans réparer accidentellement d'autres types de dommages, la NER emploie d'autres facteurs pour vérifier la présence et le type de lésion (voir le paragraphe 1.3.2.2).

Le « talon d'Achille » de ce mécanisme de détection est que les dommages qui altèrent moindrement l'ADN échappent à la XPC. De plus, la chromatine doit être désorganisée pour faciliter son déplacement sur l'ADN en une seule dimension, par glissement. En effet, les facteurs de remodelage de la chromatine facilitent la NER (voir la section 1.4.1), mais plusieurs d'entre eux agissent en aval du recrutement de la XPC. Dans ce cas, comment la XPC trouve-t-elle les lésions moins déformantes dans la chromatine? Une réponse partielle à cette question est le complexe UV-DDB, formé des facteurs DDB2 et DDB1. Contrairement à la XPC, ce complexe se déplace dans la chromatine en trois dimensions, en sautant d'une lésion à une autre [155]. Il reconnaît directement les dimères de pyrimidine situés dans des nucléosomes reconstitués *in vitro* [149] et il réside dans l'eu- et l'hétéro-chromatine [19, 292] avec une préférence pour les régions inter-nucléosomales [162]. Depuis la découverte du DDB2 [435], plusieurs études ont essayé de comprendre pourquoi sa haute affinité pour les dommages induits par les UV [436] ne se traduisait pas par un défaut de réparation *in vitro*. Étonnamment, l'ajout du DDB2 dans des essais de réparation *in vitro* inhibait l'excision de photolésions [147]. Cette inhibition est levée suite à l'ubiquitinylation du DDB2 par le complexe ubiquitine ligase UV-DDB-Cul4A-Rbx1 dont le DDB2 fait partie. Ceci a mené à la proposition que tout le complexe et non seulement le DDB2 est essentiel à la progression de la NER *in vivo*. En effet, les cellules XP-E, déficientes en DDB2, réparent très lentement les dommages induits par les UV [419]. Le complexe UV-DDB est recruté dans la chromatine très rapidement après irradiation aux UV, indépendamment de la présence de la XPC [154]. Par son interaction directe avec la XPC et ses interactions avec les protéines de remodelage de la chromatine [164] ce complexe aide la XPC à trouver les dommages dans un environnement chromatinien répressif (voir aussi la section 1.4.2).

À part l'ubiquitinylation, d'autres modifications post-traductionnelles facilitent la NER *in vivo*, comme l'acétylation, la sumoylation, la neddylation et la phosphorylation [417]. Dans ce contexte, dans une courte période de trois mois, trois laboratoires ont démontré de façon indépendante le nouveau rôle de la PARylation, modification post-traductionnelle catalysée par la PARP1, dans la NER [437-439]. Par des études complémentaires, Pines *et al.*, et notre laboratoire avons montré que la PARP1 coopérait avec

le complexe UV-DDB pour faciliter la réparation par la NER. King *et al*., ont révélé que la PARylation facilitait le recrutement de la protéine du complexe ouvert de la NER, la XPA, au niveau des dommages. Les résultats qui ont conduits à ces conclusions seront présentés et discutés dans les sections suivantes.

6.1 L'absence ou l'inactivation de la PARP1 retarde la réparation des dommages directs induits à l'ADN par les UVC

La majorité (99%) des dommages créés par les rayons UVB et 66% de ceux créés par les UVA sont des dommages directs, n'impliquant pas la formation immédiate de cassures de brin [24, 27]. La liaison de la PARP1 à l'ADN endommagé par les UVB et son activation très rapide, en quelques secondes, par les UVC [338], indiquait sa capacité de détecter les dommages induits par ce type d'activateur dans la chromatine. Malgré ces observations, son rôle direct dans la NER était controversé, en raison de résultats contradictoires dans l'analyse des effets de l'absence ou de l'inhibition pharmacologique de la PARP1 sur la réparation des photolésions induites par les UV [339]. Cette variabilité dans les résultats pourrait être expliquée par les différences entre les méthodes d'inactivation de la PARP1 utilisées, les techniques d'analyse et les modèles cellulaires utilisés, souvent déficients dans des voies de réparation de l'ADN (voir le paragraphe 1.5.4.4). Pour cette raison, le premier *objectif de mon doctorat a été d'analyser si l'effet de la PARP1 sur la cinétique de réparation des photo-lésions était universel.*

Pour séparer le rôle bien connu de la PARP1 dans la BER de ses possibles rôles dans la NER, nous avons utilisé comme source d'UV les UVC, car elles induisent principalement des dommages directs à l'ADN, réparés par la NER. Comme l'activation très rapide de la PARP1 par les UVC a été un des premiers effets observés, nous avons évalué son rôle dans la réparation des dommages directs. Pour ce faire, deux types de fibroblastes normaux pour la NER ont été utilisés: des fibroblastes immortalisés par l'antigène SV40 avec le gène p53 défectueux (GM) et des fibroblastes immortalisés avec hTert, normaux pour p53 (BJ EH2). Nous avons montré par cytofluorimétrie (Figure 3.1A) que l'inhibition de l'activité catalytique de la PARP1 par l'inhibiteur PJ-34 dans les cellules GM retardait la réparation

des dimères de thymine (T-T). Dans les cellules BJ EH2, l'inhibition de la PARP retarde la réparation des 6-4PP à 1h et la réparation des T-T à 63h (Figure 3.1A). Notons qu'à l'instar des cellules GM avec une durée du cycle cellulaire de 24h, celui des cellules BJ EH2 dure 68h. Pines *et al.*, ont confirmé par la technique d'ELISA (« enzyme-linked immunosorbent assay ») le retardement de la réparation des CPD à 24h dans les cellules traitées avec l'inhibiteur AZ12640831-009 de la PARP. Un retardement dans la réparation des 6-4PP a été aussi observé à 1h sans qu'il soit significatif [437]. Ce défaut dans la réparation des dommages directs induits par l'inhibition de la PARP se traduit par une hypersensibilité des cellules, même à une faible dose d'UVC (2 J/m^2) et souligne le rôle primordial de la PARylation dans la NER.

À part la PARP1, d'autres PARP sont activées par les dommages à l'ADN, comme la PARP2 et la PARP3 et l'inhibiteur PJ-34 agit sur tous les membres de la famille des PARP [440]. Afin de déterminer si l'effet observé sur la cinétique de réparation était dû à une ou plusieurs PARP, des cellules déficientes en PARP1 (GMSiP) ont été utilisées [415]. Les cellules GMSiP ne forment pas des PAR suite à l'irradiation aux UVC [339], ce qui est confirmé par immunobuvardage (Figure 3.1C). Le retardement prononcé de la cinétique de réparation des T-T à 24h (Figure 3.1D), similaire à celle obtenue avec l'inhibiteur de PARP soutient l'idée que la PARP1 est probablement le seul membre de la famille impliqué dans la réparation par la NER des dommages directs induits à l'ADN par les UV.

Collectivement, nos résultats et ceux de Pines *et al.* [441], obtenus en utilisant différentes lignées cellulaire, différents inhibiteurs de PARP, différentes techniques d'analyse et des souris sans poil (Figure 3.1B) montrent sans équivoque le rôle critique de la PARP1 et de la PARylation dans la réparation des photolésions par la NER. Cependant, nos études n'indiquent pas quelle étape de la NER est affectée par la PARP1. Pour cette raison, le *deuxième objectif de mon doctorat a été d'analyser l'interaction de la PARP1 avec des protéines de la NER et de vérifier le rôle de l'activité de la PARP dans ces interactions.*

6.2 La PARP1 coopère avec le complexe UV-DDB pour faciliter la reconnaissance des dommages induits par les UV

Comme la PARP1 forme des PAR au site de dommage dans la même période de temps que la protéine DDB2 est recrutée [338], la PARylation a le potentiel de faciliter la phase de reconnaissance de la GG-NER. Pour le démontrer, nous avons utilisé la fraction cellulaire qui représente les protéines liant fortement la chromatine (Figure 3.2A), dans des essais d' immunoprécipitation (IP) [438]. Nous avons observé que suite à l'irradiation aux UVC, DDB2 interagissait fortement avec la PARP1 (Figure 3.2B, D et S3.2), une observation qui corrobore les résultats de spectrométrie de masse obtenus par Pines *et al*. [437]. Que ces protéines interagissent directement et non via l'ADN a été révélé par l'usage du bromure d'éthidium pendant les IP (Figure 3.2C) et par des essais *in vitro* en utilisant des protéines purifiées [437]. Le bromure d'éthidium a été précédemment prouvée comme agent qui permettait de déterminer si une interaction entre deux protéines était faite par intermédiaire de l'ADN ou non [442]. Comme la XPC interagit directement avec DDB2 [162], les IP réalisées dans la fraction chromatinienne des cellules XP-C confirment aussi leur interaction directe (Figure 3.4B). Les PAR jouent un rôle médiateur, car l'utilisation de l'inhibiteur PJ-34 de la PARP brise l'interaction entre DDB2 et la PARP1 (Figure 3.2D et S3.2E). L'autre facteur du complexe UV-DDB, le DDB1 interagit également avec la PARP1, *in vivo* et *in vitro* [437].

En conclusion, en utilisant des techniques complémentaires, nos résultats démontrent que la PARP1 est le nouveau partenaire du complexe UV-DDB dans la phase de reconnaissance des dommages de la GG-NER. *Plusieurs mécanismes par lesquels PARP1 et sa PARylation en coopération avec DDB2 pourraient faciliter la reconnaissance des dommages ont été identifiés et analysés et sont décrits dans les sections suivants.*

6.2.1 Le rôle dépendant de la PARP1 du complexe UV-DDB dans le remodelage de la chromatine

Dans les cellules humaines, le facteur DDB2 sert, entre autres, de médiateur de décondensation de la chromatine afin d'établir un environnement local favorable au recrutement de la protéine XPC aux photolésions [175, 176]. Ce rôle est étroitement lié à son activité dans le complexe ubiquitine ligase UV-DDB-Cul4A-Rbx1. Cependant, le DDB2 peut induire l'ouverture de la chromatine indépendamment de l'ubiquitinylation et en l'absence d'interaction avec les autres membres du complexe ubiquitine ligase UV-DDB-Cul4A-Rbx1 [186]. Pour étendre la structure chromatinienne, le DDB2 nécessite non seulement l'hydrolyse d'ATP mais aussi l'activité de la PARP1. Ceci a été démontré en utilisant un système qui permet de localiser *in vivo* une protéine à une région chromosomique définie. En concordance avec le rôle connu de la PARylation dans le remodelage de la chromatine [282], la déplétion de la PARP1 ou le traitement des cellules avec des inhibiteurs de PARP réduit significativement l'éviction des histones H1 et H4 du site de dommages. Ainsi, le recrutement de la XPC aux lésions induites par les UVC est diminué. Étant donné que la déplétion de l'ATP affectait davantage le recrutement de la XPC que l'inhibition de l'activité de PARP, les auteurs ont conclu que le DDB2, de concert avec la PARP1, facilitait le recrutement de la XPC dans la chromatine par l'intermédiaire d'un facteur de remodelage de la chromatine dépendant de l'ATP.

Dans un article subséquent, la même équipe de recherche a identifiée le facteur ALC1 comme étant responsable de l'effet observé [437]. Il était déjà connu que son recrutement au site de dommages était dépendant des PAR (voir section 1.5.4.1) et son activité ATP-ase était stimulée par la formation des PAR [262]. Pines *et al*., ont démontré qu'ALC1 est également recruté rapidement aux dommages induits par les UV dans les cellules avec une NER normale, mais aussi dans les cellules XP-A, incapables d'exciser l'ADN endommagé. En utilisant ces cellules, ils ont démontré que la présence des cassures d'ADN n'est pas une condition requise pour la formation des PAR et l'accumulation d'ALC1 aux photolésions. Par contre, ce recrutement était réduit au site de micro-irradiation et complètement absent aux sites localisés d'irradiation aux UVC dans les cellules XP-E, ayant une DDB2 non-

fonctionnelle [437]. Par immunobuvardage, nous avons aussi observé que les cellules XP-E forment très peu de PAR après irradiation (Figure 3.3E). Ceci suggère que le DDB2 avait un effet stimulateur sur l'activité catalytique de la PARP1, ce que nous avons prouvé en utilisant plusieurs types d'essais *in vitro* (Figures 3.3C, D et S3.3) et en exprimant le DDB2 couplée à une étiquette myc dans les cellules XP-E (Figure 3.3F) [438]. En observant que les cellules XP-E forment des PAR lorsque la synthèse et la ligation de l'ADN sont inhibées, Pines *et al*., proposent que l'activation de la PARP1 a lieu en deux phases: la première pendant la phase de pré-incision est complètement dépendante du DDB2, alors que la deuxième phase, plus lente, requière la formation de cassures par l'activité des endonucléases. En conclusion, nos études démontrent le rôle stimulateur du DDB2 sur l'activité catalytique de la PARP1 et indirectement sur le recrutement d'ALC1 dans la phase de pré-incision des dommages. Notons que en comparaison avec l'absence de DDB2, l'inhibition de l'activité catalytique de la PARP abolit complétement l'accumulation d'ALC1 au site de micro-irradiation, confirmant les études précédentes [257]. Ceci suggère l'existence d'un mécanisme d'activation de la PARP1 et du recrutement de l'ALC1 indépendant de DDB2. La déplétion d'ALC1 retarde la réparation des CPD jusqu'à 24h, mais pas celle des 6-4PP, ce qui affecte la viabilité cellulaire tel que mesuré par des tests clonogéniques [437]. Cette observation démontre l'importance du remodelage de la chromatine pour la réparation des lésions UV, surtout de type CPD, via un recrutement efficace de la XPC pour initier la réparation.

Dans les cellules XP-E ayant une mutation qui brise la liaison entre le DDB2 et le complexe ubiquitine ligase dont il fait partie, la protéine DDB2 lie toujours l'ADN et ouvre la structure de la chromatine, en stimulant la PARP1 [186]. Cependant, la réparation des photolésions est retardée dans ces cellules [419], et cela démontre que l'activité ubiquitine ligase du complexe UV-DDB-Cul4A-Rbx1 est également importante pour les fonctions du DDB2 dans la NER.

6.2.3 Les rôles de la PARP1 dans les fonctions du complexe ubiquitine ligase UV-DDB-Cul4A-Rbx1

À part leurs rôles dans le remodelage de la chromatine, les PAR formés localement peuvent servir d'échafaudage en attirant des nombreux facteurs de réparation, incluant la PARP1 elle-même [440]. Pour cette raison, nous avons vérifié si l'activité de la PARP1 joue un rôle dans le recrutement du DDB2 au site du dommage. L'inhibition de l'activité catalytique de la PARP par l'inhibiteur PJ-34 ne change pas la cinétique du DDB2 exogène au site local d'irradiation aux UVC (Figure S3.2C) [438] ou au site de microirradiation [437]. Cela démontre que le recrutement du DDB2 est indépendant de l'activité de la PARP. Par contre, le traitement des cellules avec l'inhibiteur PJ-34 retarde le départ du DDB2 de la chromatine jusqu'à 2h (Figure 3.2E). Comme l'ubiquitinylation du DDB2 mène à son extraction de la chromatine et à sa dégradation, sa présence prolongée indique soit que le DDB2 n'a pas été modifié avec des chaînes d'ubiquitines [167], soit que les chaînes d'ubiquitine formées sur le DDB2 ne sont pas assez longues pour qu'il devienne une cible de la ségrégase p97 [166]. Il est connu que la rétention prolongée du DDB2 aux dommages réduit le recrutement de la XPC avec un effet inhibiteur sur la réparation des photolésions [146, 165]. En effet, nous avons trouvé que l'inhibition de la PARP affecte l'interaction de la XPC avec le DDB2 (Figure 3.4D) ainsi que l'accumulation de la XPC aux lésions (Figure 3.4E). Il est possible que la faible interaction entre la XPC et le DDB2 soit due à la quantité réduite de XPC au niveau de la chromatine. Cependant, lorsque l'activité catalytique de la PARP est inhibée, un moins grande nombre des molécules de DDB2 sont immobilisées au niveau de la chromatine [437]. Ainsi, l'accumulation réduite de la XPC aux dommages est le résultat d'une faible ubiquitinylation due à la réduction d'interaction d'entre la XPC et le DDB2 ce qui affectait la stabilisation de la XPC aux lésions. Appuyant cette proposition, les formes modifiées de XPC qui migrent plus lentement dans un gel SDS-PAGE, connues en littérature comme XPC ubiquitinylée, sont aussi absente dans les cellules traitées avec PJ-34 (Figure 3.4F).

À partir de nos résultats indiquant que l'inhibition de la PARP affecte l'activité du complexe ubiquitine ligase UV-DDB-Cul4A-Rbx1 nous avons proposé que la PARylation et

l'ubiquitinylation agissent en synergie pour faciliter la NER. Cette proposition est appuyée par l'observation que la déplétion d'ATP affecte davantage le recrutement de la XPC que celui des inhibiteurs de la PARP. Indépendamment de sa participation dans le complexe ubiquitine ligase, le DDB2 stimule l'activité de la PARP1. En sachant que les PAR peuvent être utilisés comme source locale d'ATP [443], il est tout à fait possible que la PARylation stimule non seulement l'ubiquitinylation, mais aussi le remodelage de la chromatine par des facteurs possédant une activité dépendante de l'ATP. Pines *et al.*, ont aussi proposé une modulation de l'ubiquitinylation par la PARylation [437]. En sachant que la PARylation cible la partie N-terminale du DDB2 et que cette région est un site majeur d'ubiquitinylation [77], ils ont envisagé une compétition entre la PARylation et l'ubiquitinylation pour les mêmes sites lysines. En effet, l'accumulation des PAR dans les cellules déficientes en PARG retardait le départ du DDB2 de la chromatine et à l'envers l'inhibition de la PARP accélérait la dégradation du DDB2 d'un extrait cellulaire total après irradiation aux UVC. La lysine est connue comme un acide aminé accepteur de PAR. Par exemple, toutes les histones acceptent des PAR sur des résidus lysine [281] et dans la structure de la PARP1 un résidu lysine accepteur des PAR a été identifié [215]. Étant donné qu'aucune enzyme capable de cliver la liaison entre la dernière unité d'ADP-ribose et la lysine n'a été identifié [248], d'autres études seront nécessaire afin d'identifier les acides aminées accepteurs des PAR du facteur DDB2 ainsi que leur rôle biologique.

Indifféremment du mécanisme employé, compétition ou coopération entre la PARylation et l'ubiquitinylation, nos résultats suggèrent une modulation de l'activité ubiquitine ligase du complexe UV-DDB-Cul4A-Rbx1 par la PARylation. L'activité enzymatique de plusieurs facteurs impliqués dans la réparation de l'ADN (ALC1, FACT, Iduna, CHFR, p53, etc..) est stimulée ou inhibée après leur modification avec des PAR [199]. Pour ces raisons, nous avons examiné si le DDB2 est PARylée en réponse aux UVC. En utilisant des extraits cellulaires et des protéines pures, nous avons montré que DDB2 est une protéine acceptrice des PAR (Figures 3.3A, B, 3.4B et S3.3A). Le site de PARylation est localisé dans les 90 premiers acides aminés du DDB2, tel que prouvé en utilisant des formes tronquées de la protéine [441]. De façon intéressante, ce site chevauche celui de liaison de

DDB1 qui s'étend entre les acides aminés 1 et 78 [162]. L'effet de la PARylation sur l'interaction entre les facteurs DDB2 et DDB1 reste à déterminer.

6.2.3 Le recrutement de la PARP1 aux dommages directs induits par les UV

L'interaction directe entre la PARP1 et DDB2 indique leur présence sur le même brin, celui qui contient le dommage. Dans ce cas, comment expliquer physiquement leur présence simultanée au niveau de la lésion ? La formation des PAR dans les cellules déficientes en XPC (Figure 3.4A) prouve que le recrutement de la PARP1 ne dépend pas de la formation des cassures ou des autres facteurs de la NER. Dans les cellules XP-C, seul DDB2 est recruté aux dommages, tous les autres facteurs de la NER nécessitant sa présence pour leur recrutement [92]. En sachant que le DDB2 se lie directement aux lésions UV, indépendamment de l'activité de la PARP1, un possible mécanisme était le recrutement de la PARP1 par le DDB2. La stimulation observée de la PARylation par le DDB2 peut être aussi expliquée par un enrichissement des molécules de PARP1 sur la chromatine, recrutées par le DDB2 [438]. Cependant, les cellules XP-E, déficientes en DDB2, forment aussi des PAR (Figure 3.3E) et la PARylation, en contrecarrant l'ubiquitinylation, stabilise le DDB2 sur la chromatine [441]. Dans ce cas, la PARP1 et sa PARylation doit être présente aux dommages avant l'activation du complexe UV-DDB-Cul4A-Rbx1, qui commence avec la liaison du DDB2 à la lésion [441]. En effet, la PARP1 forme des PAR *in vitro* lorsqu'elle est incubé avec des constructions sans cassures de brin, comme des plasmides irradiés aux UVB [338, 437] ou surenroulés [228]. Malgré le fait que l'absence totale des PAR dans les cellules déficientes en PARP1 (Figure 3.1C) suggère qu'ils étaient formés exclusivement par la PARP1 et non par les autres membres de la famille PARP impliqués dans la réparation des dommages à l'ADN, PARP2 et PARP3 [339, 438], aucune étude n'a réussi à le prouver, en raison de l'abondance cellulaire de la PARP1.

Afin de montrer la PARP1 liée à un dommage induit par les UV, nous avons développé deux techniques, le fractionnement in situ des protéines et la création d'un oligonucléotide ayant un seul dommage de type thymine-thymine, entouré de multiples sites de reconnaissance pour des enzymes de restriction. La technique de fractionnement in situ

utilise des détergents et du sel pour extraire les protéines cytoplasmiques et nucléoplasmiques libres tout en gardant les protéines fortement liés à la chromatine. En couplant cette technique à la microscopie confocale nous avons montré la colocalisation de la PARP1 exogène avec un dommage de type CPD *in vivo* (Figure S5.3A, B) et la colocalisation de la PARP1 endogène avec le DDB2 (Figure 4.1E). De plus, nous avons démontré que le domaine N-terminal de la PARP1, celui qui contient les doigts de zinc F1 et F2, était suffisant pour la localisation de la PARP1 aux photolésions (Figure 4.2B). Cependant, les UVC qui passent à travers les pores de 5µm du filtre utilisé induisent plus d'un dommage à l'ADN. Donc, la colocalisation observée entre la PARP1 et le DDB2 n'indique pas forcément leur présence sur le même site de dommage. Pour cette raison, mes collègues ont créé un oligonucléotide avec un seul dommage de type UV. La présence du dommage UV augmente de 1.5 à 1.7 fois l'affinité de la PARP1 pour l'ADN endommagé (Figure 4.3B). De plus, la présence de PARP1 double le nombre de molécules de DDB2 liant l'ADN (Figure 4.4D), ce qui suggère que la PARP1 augmente l'affinité de DDB2 pour la lésion tout comme le DDB2 augmente celle de la XPC [162]. Il sera intéressant de déterminer si l'absence de la PARP1 affectera le recrutement de DDB2 aux dommages *in vivo*. La présence du DDB2 à la lésion [77] n'empêche pas celle de PARP1. La PARP1 a une empreinte asymétrique qui couvre l'ADN de chaque côté de la lésion, du nucléotide -12 au nucléotide +9 (Figure 4.5B). Son activation par les 6-4PP, plus forte que celle obtenue avec des CPD, indique que la PARP1 détecte, comme la XPC, la distorsion de l'ADN induite par le dommage et pas le dommage en soi (Figure 4.5A). Le pliage de l'ADN induit par DDB2 [91] pourrait représenter la base structurale de la stimulation de l'activité catalytique de la PARP1 par le DDB2.

6.3 Le rôle de la PARP1 dans le recrutement de la XPA

La protéine XPA représente le facteur limitant de la NER. Elle interagit avec la grande majorité des facteurs de la NER, jouant un rôle clé dans la formation du complexe ouvert [444]. Plus important, la XPA avec le complexe TFIIH vérifie les dommages [105]. Des études biochimiques ont établi la présence d'un motif de liaison des PAR à l'extrémité C-terminale de la protéine [252] ainsi que sa préférence pour de longs PAR, formés de 40 à 55 unités [263], sans toutefois préciser son importance *in vivo*. King *et al*., ont montré que la

PARylation de la XPA est nécessaire à son recrutement à la chromatine [439]. La PARP1 interagit avec XPA au niveau de la chromatine. Cette association est abolie par l'inhibiteur DPQ de la PARP, impliquant que les PAR agissent comme médiateurs de l'interaction. L'inhibition de la PARP ou la déplétion de la PARP1 empêche la réparation des dommages induits par les UV.

Le recrutement initial de la GFP-XPA au site de micro-irradiation est dépendant de la formation des PAR, mais pas son recrutement ultérieur. Ceci suggère que la protéine PARP1 a un rôle direct dans le recrutement de la XPA [445]. En effet, la PARP1 interagit directement avec la XPA *in vivo* et *in vitro* et leur interaction directe est suffisante pour stimuler l'activation de la PARP1, contrairement au DDB2 qui nécessite la présence d'ADN (Figure 3.3C). L'effet immédiat est probablement le départ du complexe PARP1-XPA de la chromatine, car la XPA modifiée avec des longs polymères perd son affinité pour l'ADN. De ces résultats, Fischer *et al.,* proposent que la modification covalente de la XPA par des PAR joue un rôle mineur dans la modulation de ses fonctions dans la NER [445]. En effet, les dommages directs induits dans les kératinocytes HaCaT déficients en PARP1 sont réparés plus lentement que celle des cellules traitées avec des inhibiteurs de PARP.

6.4 Le rôle direct de la PARP1 dans la fonction de recherche des dommages de la XPC

Le modèle actuel propose que le complexe UV-DDB reconnaît la lésion et recrute la XPC, qui est l'initiateur de la sous-voie GG-NER. L'ubiquitinylation concomitante des histones et le recrutement d'ALC1 par la PARP1 ouvre la chromatine pour lui donner accès aux dommages dispersés dans la chromatine. Ce modèle est basé sur l'observation que les cellules avec une NER normale éliminent 97% des 6-4PP jusqu'à 3h et 75% des CPD jusqu'à 24h, alors que dans la même période de temps, les cellules XP-E éliminent seulement 62-66% des 6-4PP et 22-44% des CPD [419]. En poursuivant l'analyse de la cinétique de 6-4PP jusqu'à 24h, la différence entre les cellules normales et les cellules déficientes en DDB2 s'efface [446]. Des études futures devront déterminer si, comme dans le cas des 6-4PP, les cellules XP-E réparent aussi lentement les CPD et identifier les autres facteurs qui aident la XPC à trouver les dommages peu déformants dans la chromatine.

Comme les cellules XP-E ne réparent que très peu les CPD jusqu'à 24h, plusieurs études ont accordé au DDB2 un rôle primordial dans leur détection [90]. Étonnamment, le DDB2 est dégradé avant que la grande majorité des CPD soit éliminé [182]. Dans ce cas, comment la XPC trouve-t-elle les dommages de type CPD dans la chromatine? Une indication est venue des études de spectrométrie de masse qui avaient identifié la XPC comme protéine acceptrice des PAR [447], observation confirmée ultérieurement par des études *in vitro* [448]. Comme les PAR contribuent au recrutement des protéines au site de lésions, la PARylation et la PARP1 pourraient jouer un rôle direct dans la fonction de recherche des dommages de la XPC.

En utilisant la spectrométrie de masse et les IP comme méthodes d'analyse, nous avons révélé une interaction directe entre XPC et la PARP1 dans le nucléoplasme avant l'induction des dommages (Figure 5.1). Du complexe formé par la PARP1 et la XPC, le DDB2 ne fait pas partie (Figures 5.1 et 5.2). L'ADN n'agit pas comme intermédiaire d'interaction, car le traitement de la fraction cellulaire nucléoplasmique avec une concentration élevée de la nucléase micrococcale ne brise pas le lien entre la PARP1 et la XPC (Figures 5.2A et S5.1). En utilisant différents fragments immunopurifiés ou pures de la protéine XPC, nous avons identifié le fragment situé entre les acides aminés 496-733 comme site d'interaction de la PARP1 avec la XPC. Fait intéressant, ce domaine chevauche les sites de liaison des protéines HR23B et DDB2 avec la XPC [89, 162], ainsi que celui de la liaison entre la XPC et l'ADN [89, 141]. Il a été proposé que l'interaction entre le DDB2 et la XPC au niveau de la chromatine est transitoire pour permettre à la XPC de lier l'ADN [162]. L'interaction de la XPC avec le HR23B est stable, ces deux protéines formant avec la centrine 2 un complexe tri-protéique dans le nucléoplasme. Lorsque l'ADN est endommagé, ce lien doit être brisé [130] afin d'assurer la stabilisation de la XPC sur l'ADN, nécessaire au recrutement des autres protéines de la NER [426].

La PARP1 est une des premières protéines recrutées aux dommages induits par les UV dans le contexte de la chromatine [338]. Pour cette raison, nous avons vérifié si PARP1 escorte la XPC au site des dommages après irradiation. Afin de suivre le mouvement du complexe PARP1-XPC du nucléoplasme vers la chromatine, nous avons utilisé la technique

«proximity dependent biotin identification». Cette technique utilise une biotine ligase promiscue, BIO-ID, qui lors de l'ajout de biotine dans le milieu de culture, modifie avec des résidus biotine les protéines qui se trouvent à proximité ou avec lesquelles elle interagit directement [421]. Nous avons introduit la PARP1 couplée à une étiquette FLAG dans la partie C-terminale de la BIO-ID pour créer les clones BIO-ID-PARP1 (Figure S5.2A). En couplant cette technique à l'IP, nous avons montré que la XPC biotinylée dans le nucléoplasme migre vers la chromatine après irradiation aux UVC (Figure 5.3A et S5.2B). L'inhibition de l'activité catalytique de la PARP bloque ce mouvement de la XPC (Figure 5.3A). Ceci a pour effet une accumulation initiale réduite de la XPC aux dommages marqués avec l'anticorps CPD (Figure 5.3B), confirmant les résultats précédents [186, 438]. La XPC retarde aussi son départ jusqu'à 3h, probablement à cause de sa faible ubiquitinylation (Figure 3.4F). Il a été montré qu'une XPC faiblement ubiquitinylée résidait plus longtemps aux dommages, n'étant pas reconnue par la ségrégase p97 [166]. L'inhibiteur de PARP, PJ-34 réduit également le recrutement de la PARP1 aux dommages, sans toutefois affecter l'intensité de signal des CPD (Figure 5.3C, D). Cet effet des inhibiteurs de PARP sur le recrutement de la PARP1 au site de microirradiation a déjà été rapporté [428, 449] et nous l'avons observé après irradiation aux UVC. Comme le recrutement de la PARP1 n'était pas affecté par l'absence de la XPC (Figure 5.3E), la PARP1 et son activité catalytique sont la force motrice qui déplace le complexe XPC-PARP1 vers la chromatine après irradiation.

Le recrutement réduit de la XPC est la marque des cellules XP-E [419]. Pour pouvoir faire la distinction entre l'effet direct de la PARP sur le recrutement de la XPC et son effet via le DDB2, nous avons utilisé les cellules XP-E. Comme ces cellules ne possèdent pas de DDB2 fonctionnel et ont un niveau bas de PAR [438], le remodelage de la chromatine par ubiquitinylation ou par l'ALC1 est absent [437]. Pour cette raison, l'accumulation réduite de la XPC aux photolésions dans les cellules XP-E traitées avec l'inhibiteur de PARP, ABT-888 (Figure 5.4A), démontre le rôle essentiel de l'interaction directe de la XPC avec la PARP1 et celui de l'activité catalytique de la PARP1 pour leur recrutement. En utilisant des cellules déficientes en DDB2 (CHOU6) ou en PARP1 (GMSiP), nous avons montré que la PARP1 et le DDB2 ont un effet aditif pour recruter la XPC et la stabiliser au niveau de la lésion (Figure 5.4C). La stimulation de la PARylation par DDB2 forme la plateforme

d’échafaudage qui assure le recrutement du complexe PARP1-XPC. Cependant, la présence de la PARP1 dans les cellules déficientes en DDB2 est suffisante pour augmenter de 40% l’intensité du signal de XPC aux photolésions (Figure 5.4C). Donc, la PARP1 pourrait recruter la XPC aux dommages une fois le DDB2 dégradé [182] ou lorsque le nombre de dommages excède celui de molécules de DDB2 disponibles [160]. La PARP1 est localisée dans les régions hétérochromatiniennes suite aux dommages oxydatifs [315] et la XPC, une fois le DDB2 dégradé, migre aussi vers ces régions [162]. Il est donc tout à fait possible que la PARP1 aide la XPC à trouver les dommages dans ces régions inaccessibles.

Le complexe PARP1-XPC se dissocie une fois recruté à la chromatine (Figure 5.5A). Au moyen d’études *in vitro*, nous avons montré que le complexe ubiquitine ligase UV-DDB-Cul4A-Rbx1 est responsable de la dissociation du complexe XPC-PARP1 (Figure 5.5D). Malgré le modèle actuel [162], la présence du DDB2 n’est pas suffisante pour assurer le transfert de la lésion vers la XPC (Figure 5.4C), la présence des autres membres du complexe ubiquitine ligase étant également requise. Ceci réplique les conditions physiologiques qui existent au site des lésions, car le DDB2 est recruté à la chromatine sous la forme du complexe ubiquitine ligase UV-DDB-Cul4A-Rbx1 [78]. Notre modèle *in vitro* reproduit fidèlement la séquence d'événements conduisant à la stabilisation de la XPC aux lésions qui commence par la dissociation de XPC du complexe formé avec la PARP1, suivi de la formation d'un nouveau complexe avec UV-DDB-Cul4A-Rbx1. Le chevauchement du domaine de liaison de la PARP1 et la XPC avec celui du DDB2 et la XPC implique que le transfert de la XPC au site de la lésion est un processus dynamique nécessitant la coopération de la PARP1 avec le complexe UV-DDB. La présence du complexe UV-DDB non seulement positionne la XPC sur le site de la lésion, mais elle favorise aussi la répartition des lésions 6-4PP situées dans les régions inter-nucléosomales. Notre étude n’exclut pas la possibilité que d’autres facteurs, comme la PARylation de la PARP1, de la XPC et d'autres protéines ainsi que des changements dans la structure de l'ADN au site de lésion, puissent jouer un rôle clé dans la séparation de XPC de la PARP1 au site de dommage. Ces facteurs contribuent à la séparation de la PARP1 du complexe formé avec le XRCC1 ou l’APE1 lors de la réparation par excision des bases [47, 428].

6.5 Conclusions

PARP1 a un rôle très bien connu dans plusieurs voies de réparation de l'ADN. Lors de son activation, elle utilise des molécules de NAD^+ pour produire des polymères d'ADP-ribose sur de protéines acceptrices incluant la PARP1 elle-même. Les PAR générés, par leur grande taille et leur charge négative, jouent le rôle d'échafaudage, assurant l'organisation spatiale et temporelle des réponses aux dommages de l'ADN, comme la signalisation de ces dommages, le recrutement de facteurs de réparation et le remodelage de la chromatine. Son rôle dans la BER et la SSBR a été à la base de l'utilisation d'inhibiteurs de la PARP dans la thérapie du cancer [450, 451]. Son rôle dans la réparation des cassures double brin et dans la réparation des mésappariements est bien étudié [320]. La NER est la seule voie de réparation majeure de l'ADN dans laquelle le rôle de PARP1 n'était pas connu en détail et mes études doctorales ont permis de répondre à cette question.

Nous avons démontré le rôle de la PARP1 dans la première étape de la GG-NER, la reconnaissance des dommages. Nos données suggèrent que la PARP1 et son activité participent dans la GG-NER via trois mécanismes qui ne s'excluent pas mutuellement : (1) la modulation de la structure de la chromatine, (2) le recrutement des protéines de la NER aux dommages induits par les UV et (3) la modulation des fonctions de ces protéines par PARylation. En accord avec son rôle direct dans la GG-NER, la PARP1 détecte les dommages de type CPD dans un oligonucléotide double brin *in vitro* et dans la chromatine *in vivo* et stimule la réparation des dommages directs dans les cellules humains.

Nous proposons le modèle suivant pour les rôles de la PARP1 et de la PARylation dans la NER qui englobe les résultats disponibles présentement (Figure 6.1) [437-439, 445]. Avant irradiation, dû à son abondance, PARP1 est libre dans le nucléoplasme, est en complexe avec la XPC et est liée aux régions inter-nucléosomales [389]. Sous ces trois formes, la PARP1 participe à la recherche des dommages dans la chromatine. Le faible niveau d'activation de la PARP1 par l'ADN non-endommagé [60], facilite le glissement de la XPC sur la chromatine [144], probablement via le recrutement de facteurs de remodelage de la

chromatine. Le DDB2 réside aussi dans le nucléoplasme sous la forme inactive du complexe ubiquitine ligase UV-DDB-Cul4A-Rbx1 (Figure 6.1A) [78].

Lorsque l'ADN est irradié aux UV, quelques molécules de PARP1 trouvent et elles sont activées faiblement par les dommages UV (Figure 6.1B). Le complexe UV-DDB est recruté au même site dans les régions inter-nucléosomales. La PARP1 stabilise le DDB2 qui à son tour stimule l'activité de la PARP1. Les PAR formés localement modifieront la PARP1 elle–même, mais aussi des membres du complexe ubiquitine ligase, les facteurs DDB1 et DDB2, et attireront d'autres protéines, incluant l'ALC1, la PARP1 et le complexe XPC-PARP1 vers les lésions. La confluence de ces facteurs de réparation permet l'ouverture de la chromatine et le transfert de XPC de la PARP1 à la lésion ainsi que sa stabilisation par insertion du domaine BHD3 [162]. Dans cette étape, ni l'activité d'ubiquitine ligase du complexe UV-DDB-Cul4A-Rbx1, ni l'activité catalytique de la PARP1 ne sont requises. Par contre, la stabilisation de la XPC aux dommages situés dans les régions inter-nucléosomales va nécessiter son ubiquitinylation par le complexe UV-DDB-Cul4A-Rbx1 [162]. La PARylation du DDB2 change sa cinétique de dissociation. Il devient soit plus mobile et reconnait plus de dommages soit il reste plus longtemps au même endroit et facilite une reconnaissance efficace par la XPC des CPD. La PARylation de la PARP1 située sur le brin endommagé assure probablement son départ de la chromatine. Il reste à déterminer si le complexe UV-DDB-Cul4A-Rbx1 l'accompagne. La XPA est recrutée par les PAR et le complexe TFIIH par la XPC. Une fois le dommage vérifié, la stimulation de l'activité catalytique de la PARP1 par la XPA assure leur départ et font place aux autres facteurs situés en aval de la phase de reconnaissance des dommages de la NER. Suite à la dégradation du DDB2, la PARP1 et son activité catalytique recrute la XPC et la XPA dans les régions intra-nucléosomales, moins permissives à la réparation. Comme résultat, la PARP1 et la PARylation stimulent la réparation des dommages de type 6-4PP et CPD.

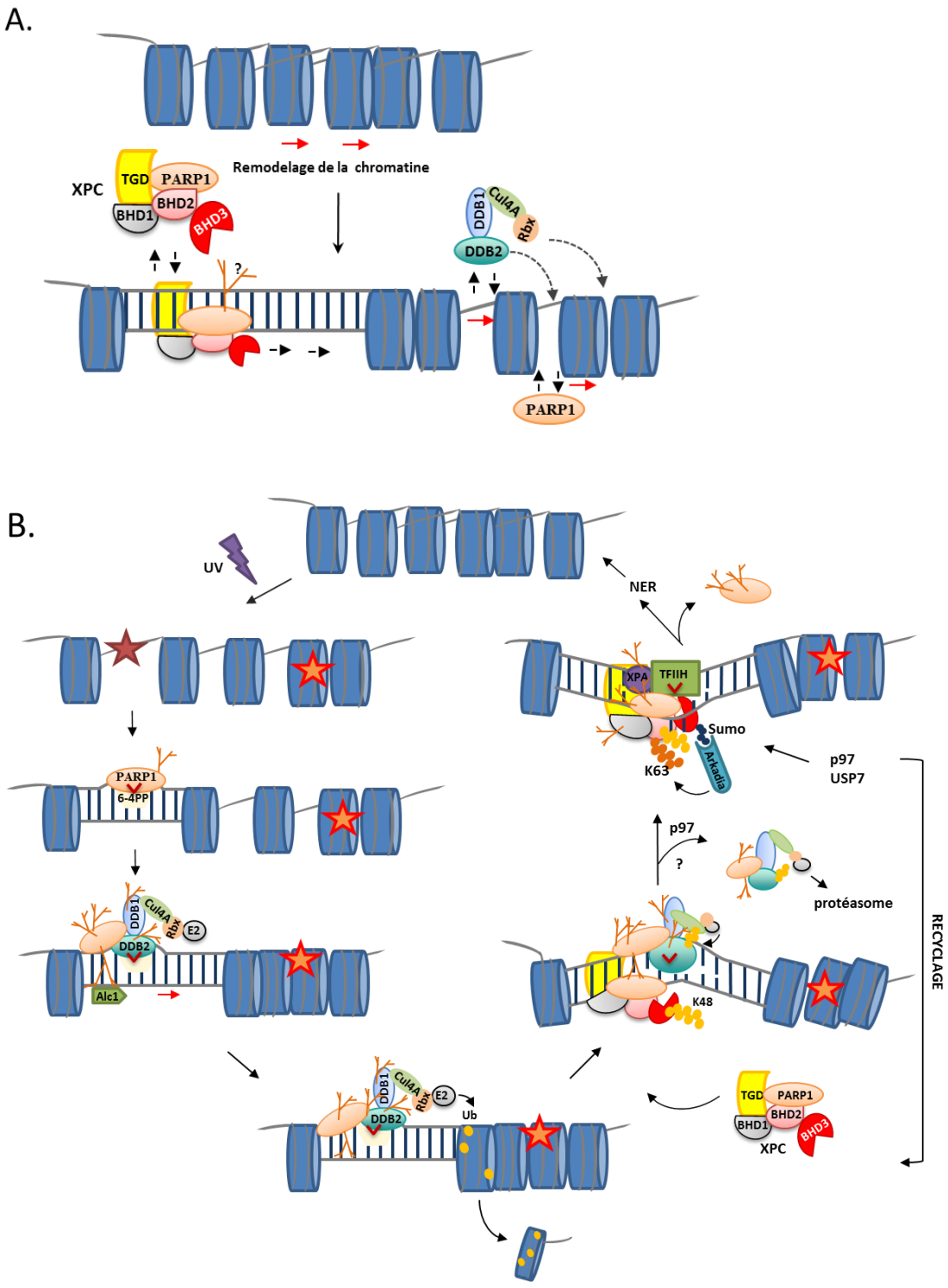

Figure 6.1 Modèle pour les fonctions de la PARP1 dans la NER.

(**A**) La recherche des dommages par les protéines XPC, DDB2 et PARP1 dans les cellules non-irradiées. (**B**) La coopération de ces trois facteurs de réparation lors de l'irradiation des

cellules aux UV. Les détails du modèle sont donnés dans le texte. Les cercles jaune et orange représentent des résidus d'ubiquitine, les cercles bleu, les protéines Sumo, les arbres orange représentent la PARylation et les étoiles, les photolésions.

6.6 Perspectives futures

Les études récentes montrent que les modifications post-traductionnelles jouent des rôles clé dans la régulation du complexe de réparation de la NER [452] et mes études doctorales ajoutent la PARylation à cette liste. Le défi sera de déterminer comment ces modifications collaborent à chaque étape de la phase de reconnaissance des dommages (recherche des dommages, stabilisation, dissociation et dégradation de protéines) pour faciliter la réparation. Agissent-elles successivement, comme la sumoylation-ubiquitinylation pour extraire la XPC de la chromatine et la recycler [170], ou plutôt en parallèle comme l'acétylation-ubiquitinylation qui créent ensemble une zone permissive autour de la lésion permettant ainsi l'accès aux facteurs de réparation?

Des études récentes suggèrent que les protéines qui contiennent des motifs de liaison spécifiques pour ces modifications post-traductionnelles sont des facteurs importants dans ce processus. Nous avons identifié le DDB2, un des composants du complexe ubiquitine ligase UV-DDB-Cul4A-Rbx1, comme étant une protéine acceptrice des PAR. L'étude de Pines *et al*., [437] suggère que même le DDB1 est modifié avec des PAR. Des motifs de liaison des PAR (PBM) dans la structure des protéines DDB1, Cul4A/B et XPC ont été identifiés par des études in silico [351]. Pour confirmer leur présence, les expériences suivantes pourraient être réalisées : l'immobilisation des protéines pures sur une membrane et l'incubation avec des PAR libres [257, 351], et/ou la réaction des protéines avec des PAR suivie par une IP en utilisant des anticorps spécifiques contre les PAR. Les résidus accepteurs des PAR pourront être identifiés par spectrométrie de masse combinée à des analyses bio-informatiques [215]. Une fois les résidus identifiés, l'ADN codant pour ces protéines pourra être modifié par mutagénèse dirigée afin d'obtenir des protéines non-modifiables avec des PAR [260]. Alternativement, des constructions codant pour des protéines tronquées, sans le site de liaison des PAR, seront exprimées dans les cellules normales ou déficientes en NER (XP-E, XP-C, CHO). Pour le DDB2, les lysines situées dans la partie N-terminale de la protéine avaient été proposées comme résidus accepteurs des PAR [437]. Pour déterminer si la perte des Lys affecte la PARylation du DDB2, les résidus Lys seront remplacés par mutation dirigé, avec alanine, tel que décrit [167] et la construction sera utilisée dans des essais de PARylation *in*

vitro. Fait intéressant, ces mutations reproduisent l'effet observé lors de l'inhibition de la PARP dans les fibroblastes, avec le DDB2 qui réside plus longtemps sur la chromatine [167]. Cette construction ne pourra pas être utilisée dans des essais d'ubiquitinylation-PARylation, car les mêmes lysines sont acceptrices d'ubiquitine.

L'identification des sites ou des résidus qui acceptent les PAR offre la base structurale pour tester le rôle de la PARylation pour les fonctions des protéines acceptrices, DDB2, DDB1, Cul4A et XPC. Nous allons pouvoir répondre aux questions suivantes:

(1) *l'absence des sites accepteurs des PAR affecte-il la réparation de l'ADN et la viabilité cellulaire?* Pour ce faire, les cellules exprimant les formes tronquées ou mutées de protéines et leur forme sauvage peuvent être irradiées globalement à 10 J/m2 UVC et la réparation des 6-4PP et CPD peut être analysée par FACS ou immunofluorescence en utilisant des anticorps spécifiques. L'effet sur la viabilité cellulaire peut être déterminé par des tests clonogéniques après irradiation des cellules à différentes doses d'UVC (de 2 à 10 J/m^2).

(2) *l'absence des sites accepteurs de PAR affecte-il le recrutement et ou le départ des protéines acceptrices?* Le DDB2 interagit directement avec la PARP1 sur la chromatine, mais leur interaction augmente significativement après irradiation lors de la formation des PAR. Pour déterminer si les PAR influencent la mobilité du DDB2, son accumulation en temps au site local d'irradiation peut être déterminé par des expériences d'immunofluorescence ou par immunobuvardage de la fraction chromatinienne. Sa présence prolongée au site du dommage indiquera le rôle de la PARylation comme signal de départ. Nous conseillons la technique de la double irradiation développée par le groupe de Maria Fousteri [453] car la technique d'irradiation locale ne permet pas de faire la distinction entre le recrutement et le départ des protéines de la NER depuis le dommage. Cette technique utilise deux doses d'UV séparées par des temps suffisamment longs pour permettre la réparation et deux techniques d'irradiation (globale et locale). Normalement, les facteurs de la NER assemblés aux dommages induits par la première série d'irradiation aux UV doivent être recrutés aux sites des dommages induits par la deuxième série d'irradiation. En

employant cette technique, il est possible de vérifier si la PARP1 et la PARylation influencent aussi la mobilité de la XPC [146]. Pour déterminer si les PAR contribuent au départ du DDB2 en raison de la répulsion de charge, nous pouvons utiliser les oligonucléotides avec un seul dommage définit de type UV et des protéines natives et PARylées, tel que démontré pour la XPA [445] et la XPC [448]. Nous avons déjà déterminé par cette méthode que la présence de PARP1 augmente l'affinité du DDB2 pour l'ADN. Les répercussions d'un départ retardé peuvent être déterminées en suivant la cinétique d'accumulation des facteurs XPB, XPD et XPA qui se trouvent en aval de l'étape de recrutement de la XPC et du DDB2.

(3) *l'absence des sites accepteurs de PAR affecte-elle l'ubiquitinylation des protéines acceptrices?* L'ubiquitinylation du DDB2 diminue son affinité pour l'ADN, ce qui suggère qu'elle joue un rôle important dans son départ [66]. De plus, la mono-ubiquitinylation de l'histone H2A sur la lysine 119 mène à la libération du DDB2 de la chromatine et promeut son mouvement vers d'autres sites de dommages [177]. L'ubiquitinylation de la XPC augmente son affinité pour l'ADN et est requise pour sa sumoylation [170]. Nos résultats montrent que l'inhibition de la PARylation retarde le départ du DDB2 de la chromatine, alors que Pines *et al.,* en observant que l'absence du PARG retarde la dissociation du DDB2, propose que la PARylation prolonge son temps de résidence sur le site de dommage [164]. Afin de bien comprendre le mécanisme et éliminer la controverse, les protéines acceptrices devraient être modifiées avec des PAR et utilisées dans des essais d'ubiquitinylation *in vitro* pour déterminer comment la PARylation affecte l'ubiquitinylation [260]. Aussi la réaction d'ubiquitinylation pourrait se faire en présence de la PARP1, du NAD^+ et des inhibiteurs de PARP ou en utilisant une forme catalytique non-fonctionnelle (E988K) de la PARP1 [449]. Ceci peut déterminer si la PARP1 ou son activité catalytique module la réaction d'ubiquitinylation. En sachant que l'ubiquitinylation change l'affinité de la XPC et du DDB2 pour l'ADN, l'effet de la PARylation devrait aussi être évalué par des expériences d'ubiquitinylation *in vitro* en utilisant comme source d'ADN des oligonucléotides avec un CPD défini. La quantité de protéines liées à l'ADN, comparée à celle présente dans le surnageant, peut être évaluée par immunobuvardage [167]. L'effet de la PARylation sur l'ubiquitinylation pourrait être vérifié *in vivo* par une double IP d'abord contre la protéine d'intérêt suivi d'une autre contre l'ubiquitine dans la fraction chromatinienne des cellules

traitées ou non avec des inhibiteurs de PARP, déficientes en PARP1 ou avec une PARP1 non-fonctionnelle (E988K) [454]. Pour faciliter l'expérience, un plasmide exprimant l'ubiquitine couplée à une étiquette GFP pourrait être utilisée [455]. Par cette méthode, une interconnexion entre l'ubiquitinylation et la sumoylation pour les fonctions de la CSB été prouvé [456].

(4) *l'absence des sites accepteurs de PAR change-t-elle leur interactome?* Nos résultats indiquent que l'inhibition de la PARP réduit l'interaction entre le DDB2 et la XPC et entre le DDB2 et la PARP1. Cependant, des interactions protéine-protéine entre ces facteurs sont aussi décrites [146, 162, 437]. Les extraits cellulaires des clones exprimant des formes tronquées ou non-modifiables des protéines DDB2, XPC, DDB1, Cul4A pourront être fractionnés afin de conduire des expériences d'immunoprécipitation pour déterminer si la PARylation est un médiateur d'interaction et si le site d'interaction protéine-protéine chevauche celui de la PARylation.

(5) *la PARP1 est-elle une cible du complexe ubiquitine ligase UV-DDB-Cul4A-Rbx1?* Via l'ubiquitinylation, l'ubiquitine ligase CHFR assure le départ de la PARP1 de la chromatine pour permettre la réparation des cassures double-brin [294]. L'ubiquitine ligase Iduna est aussi responsable de la dégradation de la PARP1 [260]. Comme la PARP1 est une protéine abondante, il est possible d'utiliser le fractionnement in situ pour détecter des changements dans son niveau cellulaire. Le traitement des cellules avec des inhibiteurs de protéasome, ainsi que des essais d'ubiquitinylation *in vitro* devraient compléter l'expérience.

(6) *l'absence des sites accepteurs des PAR affecte-t-elle la fonction de recherche de la XPC?* Des études *in vivo* et *in vitro* indiquent que la XPC est aussi PARylée [448]. L'inhibition et la déplétion de la PARP1 donne des résultats similaires pour le recrutement de la XPC et de la PARP1 suggérant que la PARylation de la PARP1 est la force motrice du complexe PARP1-XPC. Dans ce cas, quel est le rôle de la PARylation de la XPC? Il a été montré par mutation dirigée que la présence d'un acide aminé acide (acide glutamique 755) est critique pour la fonction de recherche de dommages de la XPC. Son changement avec une acide aminé basique augmente la liaison de la XPC à l'ADN et diminue sa capacité de

se déplacer librement sur la chromatine [141]. La XPC stimule l'activité catalytique de la PARP1 et elle est modifiée à son tour avec des PAR. À noter que l'ADN non-endommagé active faiblement la PARP1 [60] et les petits PAR n'affectent pas la capacité de la XPC de se lier à l'ADN [448]. En raison de leur charge négative, il est envisageable que les PAR augmentent la vitesse de glissement de la XPC en facilitant sa fonction de recherche des dommages ainsi que l'efficacité de la NER. Pour le démontrer, le plasmide codant pour une XPC de pleine longueur, non-modifiable avec des PAR, pourrait être exprimé dans les cellules déficientes en XPC. Son affinité pour l'ADN endommagé pourrait ensuite être évalué par rapport à celle de la XPC modifiée avec des petits PAR (de 3 à 22 unités d'ADP-ribose) dans des expériences de liaison à l'ADN en utilisant les oligonucléotides avec un seul dommage UV définit [423]. Des expériences d'immunofluorescence devraient montrer le changement dans le recrutement et la persistance de la XPC au niveau des dommages, et les expériences de FACS et les tests clonogéniques devraient montrer l'impact de la XPC non-modifiable sur la réparation et la viabilité cellulaire.

Il est probable qu'avec l'avancement des études de protéomique basées sur la spectrométrie de masse et sur les analogues de la PARP1 et du NAD^+, de nouvelles cibles de la PARylation par la PARP1 soient identifiées [245]. Cela permettra de déterminer si la PARP1 joue un rôle aussi en aval, dans les étapes de synthèse et de ligation, de la NER. Les fonctions de la XPA sont modulées par la PARP1 [445]. À son tour, la XPA arrête les protéines XPD/XPB au niveau du dommage pour le vérifier [105] et recrute, via l'ERCC1, l'endonucléase XPF [118]. Il nous reste à déterminer si ces protéines sont PARylée lorsque la XPA stimule la PARP1 et/ou si la PARylation module leurs fonctions. Plus encore, notre étude sur la relation entre la XPC et la PARP1 a relevé que leur interaction en absence des dommages facilitait la fonction de recherche des dommages chez la XPC. Nous pouvons déterminer si des interactions similaires peuvent s'appliquer aux autres facteurs du complexe de réparation de la NER par fractionnement cellulaire suivi des expériences d'IP dans la fraction cellulaire nucléoplasmique ou par des expériences de spectrométrie de masse. Malgré le fait que l'inhibition de la PARP1 avec l'inhibiteur 3-AB n'affecte pas la synthèse de l'ADN [457, 458], plusieurs protéines impliquées dans cette étape interagissent avec la PARP1, comme la PCNA, la RFC et la RPA [459]. PARP1 bloque la synthèse de l'ADN par

la polymérase epsilon, mais elle n'a aucun effet sur l'activité de la polymérase delta [460]. Comme la grande majorité de ces protéines joue un rôle dans la synthèse de l'ADN dans les cellules quiescentes, des études futures seront nécessaires afin de vérifier un possible rôle dépendant du cycle cellulaire de la PARP1 dans la NER. À noter que les protéines impliquées dans la phase de ligation de la NER de cellules quiescentes, le complexe XRCC1-ligase III sont aussi partenaires de la PARP1 [461].

Nos résultats révèlent également un nouveau paradigme, savoir que l'interaction connue de nombreuses protéines avec la PARP1 en conditions de croissance favorable, e.g sans dommages à l'ADN, pourrait avoir une importance fonctionnelle pour ces protéines. En effet, une étude de protéomique avait révélé que plus de 100 protéines interagissaient avec la PARP1 dans des cellules non exposées à des agents endommageant l'ADN [433]. Aussi, les HPF1 et CHD2 interagissent avec la PARP1 en condition contrôle [289, 292] et l'interaction de l'HPF1 avec la PARP1 ne change pas après l'induction des lésions à l'ADN. Cependant, aucune de ces études n'avaient pas attribué à ces interactions une signification biologique. Le fait que les expériences d'immunoprécipitation ont été réalisées en utilisant des extraits cellulaires totaux, a contribué aussi à l'impossibilité de discerner un rôle pour le complexe formé par ces protéines avec la PARP1 avant l'induction des dommages. Nos résultats révèlent que l'interaction de la XPC avec la PARP1 dans le nucléoplasme avant irradiation aux UVC facilite la fonction de recherche des dommages de la XPC. Des rôles fonctionnels similaires sont possibles pour l'interaction de la PARP1 avec d'autres protéines, non seulement dans la réparation de l'ADN, mais également dans d'autres fonctions cellulaires en présence ou absence des dommages à l'ADN. L'utilisation du fractionnement cellulaire facilitera l'interprétation des résultats, car il permettra de suivre le déplacement des protéines d'un compartiment cellulaire vers un autre.

Le rôle de la PARP1 dans la réparation des dommages induits par les UV ouvre la voie de recherche sur ses rôles potentiels dans l'apparition et le développement des cancers de la peau. Chez la PARP1, des études précédentes ont montré un rôle protecteur [462], d'autres ont trouvé un rôle stimulateur [463]. L'utilisation des souris sans poil $PARP1^{-/-}$ permettra de

déterminer le poids de son nouveau rôle dans la réparation de l'ADN par la NER dans l'apparition et la progression des cancers de la peau.

Bibliographie

1. Seebode, C., J. Lehmann, and S. Emmert, *Photocarcinogenesis and Skin Cancer Prevention Strategies.* Anticancer Res, 2016. **36**(3): p. 1371-8.
2. Stapleton, A.E., *Ultraviolet Radiation and Plants: Burning Questions.* Plant Cell, 1992. **4**(11): p. 1353-1358.
3. Svobodova, A., D. Walterova, and J. Vostalova, *Ultraviolet light induced alteration to the skin.* Biomed Pap Med Fac Univ Palacky Olomouc Czech Repub, 2006. **150**(1): p. 25-38.
4. D'Orazio, J., et al., *UV radiation and the skin.* Int J Mol Sci, 2013. **14**(6): p. 12222-48.
5. El Ghissassi, F., et al., *A review of human carcinogens--part D: radiation.* Lancet Oncol, 2009. **10**(8): p. 751-2.
6. Rass, K. and J. Reichrath, *UV damage and DNA repair in malignant melanoma and nonmelanoma skin cancer.* Adv Exp Med Biol, 2008. **624**: p. 162-78.
7. Cadet, J., A. Grand, and T. Douki, *Solar UV radiation-induced DNA Bipyrimidine photoproducts: formation and mechanistic insights.* Top Curr Chem, 2015. **356**: p. 249-75.
8. Cadet, J., E. Sage, and T. Douki, *Ultraviolet radiation-mediated damage to cellular DNA.* Mutat Res, 2005. **571**(1-2): p. 3-17.
9. Schreier, W.J., et al., *Thymine dimerization in DNA model systems: cyclobutane photolesion is predominantly formed via the singlet channel.* J Am Chem Soc, 2009. **131**(14): p. 5038-9.
10. Schreier, W.J., et al., *Thymine dimerization in DNA is an ultrafast photoreaction.* Science, 2007. **315**(5812): p. 625-9.
11. Mouret, S., et al., *Cyclobutane pyrimidine dimers are predominant DNA lesions in whole human skin exposed to UVA radiation.* Proc Natl Acad Sci U S A, 2006. **103**(37): p. 13765-70.
12. Richa, R.P. Sinha, and D.P. Hader, *Physiological aspects of UV-excitation of DNA.* Top Curr Chem, 2015. **356**: p. 203-48.
13. Cadet, J., et al., *Photoinduced damage to cellular DNA: direct and photosensitized reactions.* Photochem Photobiol, 2012. **88**(5): p. 1048-65.
14. Taylor, J.S., H.F. Lu, and J.J. Kotyk, *Quantitative conversion of the (6-4) photoproduct of TpdC to its Dewar valence isomer upon exposure to simulated sunlight.* Photochem Photobiol, 1990. **51**(2): p. 161-7.
15. Douki, T. and J. Cadet, *Individual determination of the yield of the main UV-induced dimeric pyrimidine photoproducts in DNA suggests a high mutagenicity of CC photolesions.* Biochemistry, 2001. **40**(8): p. 2495-501.
16. Kim, J.K., D. Patel, and B.S. Choi, *Contrasting structural impacts induced by cis-syn cyclobutane dimer and (6-4) adduct in DNA duplex decamers: implication in mutagenesis and repair activity.* Photochem Photobiol, 1995. **62**(1): p. 44-50.
17. Gale, J.M. and M.J. Smerdon, *UV induced (6-4) photoproducts are distributed differently than cyclobutane dimers in nucleosomes.* Photochem Photobiol, 1990. **51**(4): p. 411-7.
18. Niggli, H.J. and P.A. Cerutti, *Nucleosomal distribution of thymine photodimers following far- and near-ultraviolet irradiation.* Biochem Biophys Res Commun, 1982. **105**(3): p. 1215-23.
19. Han, C., et al., *Differential DNA lesion formation and repair in heterochromatin and euchromatin.* Carcinogenesis, 2016. **37**(2): p. 129-38.
20. Mouret, S., et al., *Differential repair of UVB-induced cyclobutane pyrimidine dimers in cultured human skin cells and whole human skin.* DNA Repair (Amst), 2008. **7**(5): p. 704-12.

21. Peng, W. and B.R. Shaw, *Accelerated deamination of cytosine residues in UV-induced cyclobutane pyrimidine dimers leads to CC-->TT transitions.* Biochemistry, 1996. **35**(31): p. 10172-81.
22. Hutchinson, F., *Induction of tandem-base change mutations.* Mutat Res, 1994. **309**(1): p. 11-5.
23. Rochette, P.J., et al., *UVA-induced cyclobutane pyrimidine dimers form predominantly at thymine-thymine dipyrimidines and correlate with the mutation spectrum in rodent cells.* Nucleic Acids Res, 2003. **31**(11): p. 2786-94.
24. Douki, T., et al., *Bipyrimidine photoproducts rather than oxidative lesions are the main type of DNA damage involved in the genotoxic effect of solar UVA radiation.* Biochemistry, 2003. **42**(30): p. 9221-6.
25. Courdavault, S., et al., *Larger yield of cyclobutane dimers than 8-oxo-7,8-dihydroguanine in the DNA of UVA-irradiated human skin cells.* Mutat Res, 2004. **556**(1-2): p. 135-42.
26. Greinert, R., et al., *UVA-induced DNA double-strand breaks result from the repair of clustered oxidative DNA damages.* Nucleic Acids Res, 2012. **40**(20): p. 10263-73.
27. Douki, T., et al., *Oxidation of guanine in cellular DNA by solar UV radiation: biological role.* Photochem Photobiol, 1999. **70**(2): p. 184-90.
28. Cadet, J., et al., *Sensitized formation of oxidatively generated damage to cellular DNA by UVA radiation.* Photochem Photobiol Sci, 2009. **8**(7): p. 903-11.
29. Foote, C.S., *Definition of type I and type II photosensitized oxidation.* Photochem Photobiol, 1991. **54**(5): p. 659.
30. Wondrak, G.T., M.K. Jacobson, and E.L. Jacobson, *Endogenous UVA-photosensitizers: mediators of skin photodamage and novel targets for skin photoprotection.* Photochem Photobiol Sci, 2006. **5**(2): p. 215-37.
31. Dedon, P.C., *The chemical toxicology of 2-deoxyribose oxidation in DNA.* Chem Res Toxicol, 2008. **21**(1): p. 206-19.
32. Shibutani, S., M. Takeshita, and A.P. Grollman, *Insertion of specific bases during DNA synthesis past the oxidation-damaged base 8-oxodG.* Nature, 1991. **349**(6308): p. 431-4.
33. Gorrini, C., I.S. Harris, and T.W. Mak, *Modulation of oxidative stress as an anticancer strategy.* Nat Rev Drug Discov, 2013. **12**(12): p. 931-47.
34. Hegde, M.L., T. Izumi, and S. Mitra, *Oxidized base damage and single-strand break repair in mammalian genomes: role of disordered regions and posttranslational modifications in early enzymes.* Prog Mol Biol Transl Sci, 2012. **110**: p. 123-53.
35. Fortini, P., et al., *Different DNA polymerases are involved in the short- and long-patch base excision repair in mammalian cells.* Biochemistry, 1998. **37**(11): p. 3575-80.
36. Scott, T.L., et al., *Repair of oxidative DNA damage and cancer: recent progress in DNA base excision repair.* Antioxid Redox Signal, 2014. **20**(4): p. 708-26.
37. Kim, Y.J. and D.M. Wilson, 3rd, *Overview of base excision repair biochemistry.* Curr Mol Pharmacol, 2012. **5**(1): p. 3-13.
38. Sattler, U., et al., *Long-patch DNA repair synthesis during base excision repair in mammalian cells.* EMBO Rep, 2003. **4**(4): p. 363-7.
39. Campalans, A., et al., *Distinct spatiotemporal patterns and PARP dependence of XRCC1 recruitment to single-strand break and base excision repair.* Nucleic Acids Res, 2013. **41**(5): p. 3115-29.
40. Wiederhold, L., et al., *AP endonuclease-independent DNA base excision repair in human cells.* Mol Cell, 2004. **15**(2): p. 209-20.
41. Vidal, A.E., et al., *XRCC1 coordinates the initial and late stages of DNA abasic site repair through protein-protein interactions.* EMBO J, 2001. **20**(22): p. 6530-9.

42. Della-Maria, J., et al., *The interaction between polynucleotide kinase phosphatase and the DNA repair protein XRCC1 is critical for repair of DNA alkylation damage and stable association at DNA damage sites.* J Biol Chem, 2012. **287**(46): p. 39233-44.
43. Caldecott, K.W., et al., *XRCC1 polypeptide interacts with DNA polymerase beta and possibly poly (ADP-ribose) polymerase, and DNA ligase III is a novel molecular 'nick-sensor' in vitro.* Nucleic Acids Res, 1996. **24**(22): p. 4387-94.
44. Caldecott, K.W., et al., *An interaction between the mammalian DNA repair protein XRCC1 and DNA ligase III.* Mol Cell Biol, 1994. **14**(1): p. 68-76.
45. Carter, R.J. and J.L. Parsons, *Base Excision Repair, a Pathway Regulated by Posttranslational Modifications.* Mol Cell Biol, 2016. **36**(10): p. 1426-37.
46. Odell, I.D., et al., *Nucleosome disruption by DNA ligase III-XRCC1 promotes efficient base excision repair.* Mol Cell Biol, 2011. **31**(22): p. 4623-32.
47. Caldecott, K.W., *Mammalian single-strand break repair: mechanisms and links with chromatin.* DNA Repair (Amst), 2007. **6**(4): p. 443-53.
48. Moor, N.A., et al., *Quantitative characterization of protein-protein complexes involved in base excision DNA repair.* Nucleic Acids Res, 2015. **43**(12): p. 6009-22.
49. Sukhanova, M., S. Khodyreva, and O. Lavrik, *Poly(ADP-ribose) polymerase 1 regulates activity of DNA polymerase beta in long patch base excision repair.* Mutat Res, 2010. **685**(1-2): p. 80-9.
50. Dantzer, F., et al., *Base excision repair is impaired in mammalian cells lacking Poly(ADP-ribose) polymerase-1.* Biochemistry, 2000. **39**(25): p. 7559-69.
51. Schreiber, V., et al., *Poly(ADP-ribose) polymerase-2 (PARP-2) is required for efficient base excision DNA repair in association with PARP-1 and XRCC1.* J Biol Chem, 2002. **277**(25): p. 23028-36.
52. Strom, C.E., et al., *Poly (ADP-ribose) polymerase (PARP) is not involved in base excision repair but PARP inhibition traps a single-strand intermediate.* Nucleic Acids Res, 2011. **39**(8): p. 3166-75.
53. Reynolds, P., et al., *Disruption of PARP1 function inhibits base excision repair of a sub-set of DNA lesions.* Nucleic Acids Res, 2015. **43**(8): p. 4028-38.
54. Wilson, S.H. and T.A. Kunkel, *Passing the baton in base excision repair.* Nat Struct Biol, 2000. **7**(3): p. 176-8.
55. Prasad, R., et al., *Substrate channeling in mammalian base excision repair pathways: passing the baton.* J Biol Chem, 2010. **285**(52): p. 40479-88.
56. Das, A., et al., *NEIL2-initiated, APE-independent repair of oxidized bases in DNA: Evidence for a repair complex in human cells.* DNA Repair (Amst), 2006. **5**(12): p. 1439-48.
57. Pogozelski, W.K. and T.D. Tullius, *Oxidative Strand Scission of Nucleic Acids: Routes Initiated by Hydrogen Abstraction from the Sugar Moiety.* Chem Rev, 1998. **98**(3): p. 1089-1108.
58. Osipov, A.N., et al., *The formation of DNA single-strand breaks and alkali-labile sites in human blood lymphocytes exposed to 365-nm UVA radiation.* Free Radic Biol Med, 2014. **73**: p. 34-40.
59. Caldecott, K.W., *DNA single-strand break repair.* Exp Cell Res, 2014. **329**(1): p. 2-8.
60. Sukhanova, M.V., et al., *Single molecule detection of PARP1 and PARP2 interaction with DNA strand breaks and their poly(ADP-ribosyl)ation using high-resolution AFM imaging.* Nucleic Acids Res, 2016. **44**(6): p. e60.
61. Okano, S., et al., *Spatial and temporal cellular responses to single-strand breaks in human cells.* Mol Cell Biol, 2003. **23**(11): p. 3974-81.

62. Masson, M., et al., *XRCC1 is specifically associated with poly(ADP-ribose) polymerase and negatively regulates its activity following DNA damage.* Mol Cell Biol, 1998. **18**(6): p. 3563-71.
63. El-Khamisy, S.F., et al., *A requirement for PARP-1 for the assembly or stability of XRCC1 nuclear foci at sites of oxidative DNA damage.* Nucleic Acids Res, 2003. **31**(19): p. 5526-33.
64. Fisher, A.E., et al., *Poly(ADP-ribose) polymerase 1 accelerates single-strand break repair in concert with poly(ADP-ribose) glycohydrolase.* Mol Cell Biol, 2007. **27**(15): p. 5597-605.
65. Woodhouse, B.C., et al., *Poly(ADP-ribose) polymerase-1 modulates DNA repair capacity and prevents formation of DNA double strand breaks.* DNA Repair (Amst), 2008. **7**(6): p. 932-40.
66. Scharer, O.D., *Nucleotide excision repair in eukaryotes.* Cold Spring Harb Perspect Biol, 2013. **5**(10): p. a012609.
67. Giordano, C.N., et al., *Understanding photodermatoses associated with defective DNA repair: Syndromes with cancer predisposition.* J Am Acad Dermatol, 2016. **75**(5): p. 855-870.
68. Cleaver, J.E., E.T. Lam, and I. Revet, *Disorders of nucleotide excision repair: the genetic and molecular basis of heterogeneity.* Nat Rev Genet, 2009. **10**(11): p. 756-68.
69. Marteijn, J.A., et al., *Understanding nucleotide excision repair and its roles in cancer and ageing.* Nat Rev Mol Cell Biol, 2014. **15**(7): p. 465-81.
70. Vermeulen, W. and M. Fousteri, *Mammalian transcription-coupled excision repair.* Cold Spring Harb Perspect Biol, 2013. **5**(8): p. a012625.
71. Bohr, V.A., et al., *DNA repair in an active gene: removal of pyrimidine dimers from the DHFR gene of CHO cells is much more efficient than in the genome overall.* Cell, 1985. **40**(2): p. 359-69.
72. Anindya, R., et al., *A ubiquitin-binding domain in Cockayne syndrome B required for transcription-coupled nucleotide excision repair.* Mol Cell, 2010. **38**(5): p. 637-48.
73. Lake, R.J. and H.Y. Fan, *Structure, function and regulation of CSB: a multi-talented gymnast.* Mech Ageing Dev, 2013. **134**(5-6): p. 202-11.
74. Lake, R.J., et al., *UV-induced association of the CSB remodeling protein with chromatin requires ATP-dependent relief of N-terminal autorepression.* Mol Cell, 2010. **37**(2): p. 235-46.
75. Kamiuchi, S., et al., *Translocation of Cockayne syndrome group A protein to the nuclear matrix: possible relevance to transcription-coupled DNA repair.* Proc Natl Acad Sci U S A, 2002. **99**(1): p. 201-6.
76. Sin, Y., K. Tanaka, and M. Saijo, *The C-terminal Region and SUMOylation of Cockayne Syndrome Group B Protein Play Critical Roles in Transcription-coupled Nucleotide Excision Repair.* J Biol Chem, 2016. **291**(3): p. 1387-97.
77. Fischer, E.S., et al., *The molecular basis of CRL4DDB2/CSA ubiquitin ligase architecture, targeting, and activation.* Cell, 2011. **147**(5): p. 1024-39.
78. Groisman, R., et al., *The ubiquitin ligase activity in the DDB2 and CSA complexes is differentially regulated by the COP9 signalosome in response to DNA damage.* Cell, 2003. **113**(3): p. 357-67.
79. Spivak, G., *Transcription-coupled repair: an update.* Arch Toxicol, 2016. **90**(11): p. 2583-2594.
80. Brooks, P.J., *Blinded by the UV light: how the focus on transcription-coupled NER has distracted from understanding the mechanisms of Cockayne syndrome neurologic disease.* DNA Repair (Amst), 2013. **12**(8): p. 656-71.
81. He, J., et al., *Valosin-containing Protein (VCP)/p97 Segregase Mediates Proteolytic Processing of Cockayne Syndrome Group B (CSB) in Damaged Chromatin.* J Biol Chem, 2016. **291**(14): p. 7396-408.

82. Nakazawa, Y., et al., *Mutations in UVSSA cause UV-sensitive syndrome and impair RNA polymerase IIo processing in transcription-coupled nucleotide-excision repair.* Nat Genet, 2012. **44**(5): p. 586-92.
83. Tornaletti, S., D. Reines, and P.C. Hanawalt, *Structural characterization of RNA polymerase II complexes arrested by a cyclobutane pyrimidine dimer in the transcribed strand of template DNA.* J Biol Chem, 1999. **274**(34): p. 24124-30.
84. Fousteri, M., et al., *Cockayne syndrome A and B proteins differentially regulate recruitment of chromatin remodeling and repair factors to stalled RNA polymerase II in vivo.* Mol Cell, 2006. **23**(4): p. 471-82.
85. Schwertman, P., et al., *UV-sensitive syndrome protein UVSSA recruits USP7 to regulate transcription-coupled repair.* Nat Genet, 2012. **44**(5): p. 598-602.
86. Beerens, N., et al., *The CSB protein actively wraps DNA.* J Biol Chem, 2005. **280**(6): p. 4722-9.
87. Kuraoka, I., et al., *Isolation of XAB2 complex involved in pre-mRNA splicing, transcription, and transcription-coupled repair.* J Biol Chem, 2008. **283**(2): p. 940-50.
88. Tornaletti, S., *DNA repair in mammalian cells: Transcription-coupled DNA repair: directing your effort where it's most needed.* Cell Mol Life Sci, 2009. **66**(6): p. 1010-20.
89. Min, J.H. and N.P. Pavletich, *Recognition of DNA damage by the Rad4 nucleotide excision repair protein.* Nature, 2007. **449**(7162): p. 570-5.
90. Sugasawa, K., *Molecular mechanisms of DNA damage recognition for mammalian nucleotide excision repair.* DNA Repair (Amst), 2016. **44**: p. 110-7.
91. Scrima, A., et al., *Structural basis of UV DNA-damage recognition by the DDB1-DDB2 complex.* Cell, 2008. **135**(7): p. 1213-23.
92. Volker, M., et al., *Sequential assembly of the nucleotide excision repair factors in vivo.* Mol Cell, 2001. **8**(1): p. 213-24.
93. Yokoi, M., et al., *The xeroderma pigmentosum group C protein complex XPC-HR23B plays an important role in the recruitment of transcription factor IIH to damaged DNA.* J Biol Chem, 2000. **275**(13): p. 9870-5.
94. Riedl, T., F. Hanaoka, and J.M. Egly, *The comings and goings of nucleotide excision repair factors on damaged DNA.* EMBO J, 2003. **22**(19): p. 5293-303.
95. Buterin, T., et al., *DNA quality control by conformational readout on the undamaged strand of the double helix.* Chem Biol, 2005. **12**(8): p. 913-22.
96. Bernardes de Jesus, B.M., et al., *Dissection of the molecular defects caused by pathogenic mutations in the DNA repair factor XPC.* Mol Cell Biol, 2008. **28**(23): p. 7225-35.
97. Oksenych, V., et al., *Molecular insights into the recruitment of TFIIH to sites of DNA damage.* Embo J, 2009. **28**(19): p. 2971-80.
98. Coin, F., et al., *Mutations in the XPD helicase gene result in XP and TTD phenotypes, preventing interaction between XPD and the p44 subunit of TFIIH.* Nat Genet, 1998. **20**(2): p. 184-8.
99. Mathieu, N., N. Kaczmarek, and H. Naegeli, *Strand- and site-specific DNA lesion demarcation by the xeroderma pigmentosum group D helicase.* Proc Natl Acad Sci U S A, 2010. **107**(41): p. 17545-50.
100. Winkler, G.S., et al., *TFIIH with inactive XPD helicase functions in transcription initiation but is defective in DNA repair.* J Biol Chem, 2000. **275**(6): p. 4258-66.
101. Naegeli, H., L. Bardwell, and E.C. Friedberg, *The DNA helicase and adenosine triphosphatase activities of yeast Rad3 protein are inhibited by DNA damage. A potential mechanism for damage-specific recognition.* J Biol Chem, 1992. **267**(1): p. 392-8.
102. Liu, H., et al., *Structure of the DNA repair helicase XPD.* Cell, 2008. **133**(5): p. 801-12.

103. Wolski, S.C., et al., *Crystal structure of the FeS cluster-containing nucleotide excision repair helicase XPD.* PLoS Biol, 2008. **6**(6): p. e149.
104. Sugasawa, K., et al., *Two-step recognition of DNA damage for mammalian nucleotide excision repair: Directional binding of the XPC complex and DNA strand scanning.* Mol Cell, 2009. **36**(4): p. 642-53.
105. Li, C.L., et al., *Tripartite DNA Lesion Recognition and Verification by XPC, TFIIH, and XPA in Nucleotide Excision Repair.* Mol Cell, 2015. **59**(6): p. 1025-34.
106. Mathieu, N., et al., *DNA quality control by a lesion sensor pocket of the xeroderma pigmentosum group D helicase subunit of TFIIH.* Curr Biol, 2013. **23**(3): p. 204-12.
107. Evans, E., et al., *Mechanism of open complex and dual incision formation by human nucleotide excision repair factors.* EMBO J, 1997. **16**(21): p. 6559-73.
108. Cleaver, J.E. and J.C. States, *The DNA damage-recognition problem in human and other eukaryotic cells: the XPA damage binding protein.* Biochem J, 1997. **328 (Pt 1)**: p. 1-12.
109. Thoma, B.S. and K.M. Vasquez, *Critical DNA damage recognition functions of XPC-hHR23B and XPA-RPA in nucleotide excision repair.* Mol Carcinog, 2003. **38**(1): p. 1-13.
110. Missura, M., et al., *Double-check probing of DNA bending and unwinding by XPA-RPA: an architectural function in DNA repair.* EMBO J, 2001. **20**(13): p. 3554-64.
111. Naegeli, H. and K. Sugasawa, *The xeroderma pigmentosum pathway: decision tree analysis of DNA quality.* DNA Repair (Amst), 2011. **10**(7): p. 673-83.
112. Krasikova, Y.S., et al., *Localization of xeroderma pigmentosum group A protein and replication protein A on damaged DNA in nucleotide excision repair.* Nucleic Acids Res, 2010. **38**(22): p. 8083-94.
113. Camenisch, U., et al., *Recognition of helical kinks by xeroderma pigmentosum group A protein triggers DNA excision repair.* Nat Struct Mol Biol, 2006. **13**(3): p. 278-84.
114. de Laat, W.L., et al., *DNA-binding polarity of human replication protein A positions nucleases in nucleotide excision repair.* Genes Dev, 1998. **12**(16): p. 2598-609.
115. Wang, Q.E., et al., *Ubiquitylation-independent degradation of Xeroderma pigmentosum group C protein is required for efficient nucleotide excision repair.* Nucleic Acids Res, 2007. **35**(16): p. 5338-50.
116. Zotter, A., et al., *Recruitment of the nucleotide excision repair endonuclease XPG to sites of UV-induced dna damage depends on functional TFIIH.* Mol Cell Biol, 2006. **26**(23): p. 8868-79.
117. Ito, S., et al., *XPG stabilizes TFIIH, allowing transactivation of nuclear receptors: implications for Cockayne syndrome in XP-G/CS patients.* Mol Cell, 2007. **26**(2): p. 231-43.
118. Li, L., et al., *Specific association between the human DNA repair proteins XPA and ERCC1.* Proc Natl Acad Sci U S A, 1994. **91**(11): p. 5012-6.
119. Li, L., et al., *Mutations in XPA that prevent association with ERCC1 are defective in nucleotide excision repair.* Mol Cell Biol, 1995. **15**(4): p. 1993-8.
120. Wakasugi, M., J.T. Reardon, and A. Sancar, *The non-catalytic function of XPG protein during dual incision in human nucleotide excision repair.* J Biol Chem, 1997. **272**(25): p. 16030-4.
121. Mocquet, V., et al., *Sequential recruitment of the repair factors during NER: the role of XPG in initiating the resynthesis step.* Embo J, 2008. **27**(1): p. 155-67.
122. Ogi, T., et al., *Three DNA polymerases, recruited by different mechanisms, carry out NER repair synthesis in human cells.* Mol Cell, 2010. **37**(5): p. 714-27.
123. Staresincic, L., et al., *Coordination of dual incision and repair synthesis in human nucleotide excision repair.* Embo J, 2009. **28**(8): p. 1111-20.
124. Han, C., et al., *Cdt2-mediated XPG degradation promotes gap-filling DNA synthesis in nucleotide excision repair.* Cell Cycle, 2015. **14**(7): p. 1103-15.

125. Kemp, M.G. and A. Sancar, *DNA excision repair: where do all the dimers go?* Cell Cycle, 2012. **11**(16): p. 2997-3002.
126. Moser, J., et al., *Sealing of chromosomal DNA nicks during nucleotide excision repair requires XRCC1 and DNA ligase III alpha in a cell-cycle-specific manner.* Mol Cell, 2007. **27**(2): p. 311-23.
127. Sugasawa, K., et al., *HHR23B, a human Rad23 homolog, stimulates XPC protein in nucleotide excision repair in vitro.* Mol Cell Biol, 1996. **16**(9): p. 4852-61.
128. Ng, J.M., et al., *A novel regulation mechanism of DNA repair by damage-induced and RAD23-dependent stabilization of xeroderma pigmentosum group C protein.* Genes Dev, 2003. **17**(13): p. 1630-45.
129. Dantuma, N.P., C. Heinen, and D. Hoogstraten, *The ubiquitin receptor Rad23: at the crossroads of nucleotide excision repair and proteasomal degradation.* DNA Repair (Amst), 2009. **8**(4): p. 449-60.
130. Bergink, S., et al., *Recognition of DNA damage by XPC coincides with disruption of the XPC-RAD23 complex.* J Cell Biol, 2012. **196**(6): p. 681-8.
131. Nishi, R., et al., *Centrin 2 stimulates nucleotide excision repair by interacting with xeroderma pigmentosum group C protein.* Mol Cell Biol, 2005. **25**(13): p. 5664-74.
132. Sugasawa, K., et al., *Xeroderma pigmentosum group C protein complex is the initiator of global genome nucleotide excision repair.* Mol Cell, 1998. **2**(2): p. 223-32.
133. Hey, T., et al., *The XPC-HR23B complex displays high affinity and specificity for damaged DNA in a true-equilibrium fluorescence assay.* Biochemistry, 2002. **41**(21): p. 6583-7.
134. Sugasawa, K., et al., *A multistep damage recognition mechanism for global genomic nucleotide excision repair.* Genes Dev, 2001. **15**(5): p. 507-21.
135. Shell, S.M., et al., *Xeroderma pigmentosum complementation group C protein (XPC) serves as a general sensor of damaged DNA.* DNA Repair (Amst), 2013. **12**(11): p. 947-53.
136. Sugasawa, K., et al., *A molecular mechanism for DNA damage recognition by the xeroderma pigmentosum group C protein complex.* DNA Repair (Amst), 2002. **1**(1): p. 95-107.
137. Maillard, O., S. Solyom, and H. Naegeli, *An aromatic sensor with aversion to damaged strands confers versatility to DNA repair.* PLoS Biol, 2007. **5**(4): p. e79.
138. Maillard, O., et al., *DNA repair triggered by sensors of helical dynamics.* Trends Biochem Sci, 2007. **32**(11): p. 494-9.
139. Chen, X., et al., *Kinetic gating mechanism of DNA damage recognition by Rad4/XPC.* Nat Commun, 2015. **6**: p. 5849.
140. Hoogstraten, D., et al., *Versatile DNA damage detection by the global genome nucleotide excision repair protein XPC.* J Cell Sci, 2008. **121**(Pt 17): p. 2850-9.
141. Camenisch, U., et al., *Two-stage dynamic DNA quality check by xeroderma pigmentosum group C protein.* EMBO J, 2009. **28**(16): p. 2387-99.
142. Mu, H., et al., *Recognition of Damaged DNA for Nucleotide Excision Repair: A Correlated Motion Mechanism with a Mismatched cis-syn Thymine Dimer Lesion.* Biochemistry, 2015. **54**(34): p. 5263-7.
143. Velmurugu, Y., et al., *Twist-open mechanism of DNA damage recognition by the Rad4/XPC nucleotide excision repair complex.* Proc Natl Acad Sci U S A, 2016. **113**(16): p. E2296-305.
144. Kong, M., et al., *Single-Molecule Imaging Reveals that Rad4 Employs a Dynamic DNA Damage Recognition Process.* Mol Cell, 2016. **64**(2): p. 376-387.
145. Kusumoto, R., et al., *Diversity of the damage recognition step in the global genomic nucleotide excision repair in vitro.* Mutat Res, 2001. **485**(3): p. 219-27.
146. Sugasawa, K., et al., *UV-induced ubiquitylation of XPC protein mediated by UV-DDB-ubiquitin ligase complex.* Cell, 2005. **121**(3): p. 387-400.

147. Reardon, J.T. and A. Sancar, *Recognition and repair of the cyclobutane thymine dimer, a major cause of skin cancers, by the human excision nuclease.* Genes Dev, 2003. **17**(20): p. 2539-51.
148. Luijsterburg, M.S., et al., *Stochastic and reversible assembly of a multiprotein DNA repair complex ensures accurate target site recognition and efficient repair.* J Cell Biol, 2010. **189**(3): p. 445-63.
149. Osakabe, A., et al., *Structural basis of pyrimidine-pyrimidone (6-4) photoproduct recognition by UV-DDB in the nucleosome.* Sci Rep, 2015. **5**: p. 16330.
150. Wittschieben, B.O., S. Iwai, and R.D. Wood, *DDB1-DDB2 (xeroderma pigmentosum group E) protein complex recognizes a cyclobutane pyrimidine dimer, mismatches, apurinic/apyrimidinic sites, and compound lesions in DNA.* J Biol Chem, 2005. **280**(48): p. 39982-9.
151. Kulaksiz, G., J.T. Reardon, and A. Sancar, *Xeroderma pigmentosum complementation group E protein (XPE/DDB2): purification of various complexes of XPE and analyses of their damaged DNA binding and putative DNA repair properties.* Mol Cell Biol, 2005. **25**(22): p. 9784-92.
152. He, Y.J., et al., *DDB1 functions as a linker to recruit receptor WD40 proteins to CUL4-ROC1 ubiquitin ligases.* Genes Dev, 2006. **20**(21): p. 2949-54.
153. Wakasugi, M., et al., *DDB accumulates at DNA damage sites immediately after UV irradiation and directly stimulates nucleotide excision repair.* J Biol Chem, 2002. **277**(3): p. 1637-40.
154. Fitch, M.E., et al., *In vivo recruitment of XPC to UV-induced cyclobutane pyrimidine dimers by the DDB2 gene product.* J Biol Chem, 2003. **278**(47): p. 46906-10.
155. Ghodke, H., et al., *Single-molecule analysis reveals human UV-damaged DNA-binding protein (UV-DDB) dimerizes on DNA via multiple kinetic intermediates.* Proc Natl Acad Sci U S A, 2014. **111**(18): p. E1862-71.
156. Moser, J., et al., *The UV-damaged DNA binding protein mediates efficient targeting of the nucleotide excision repair complex to UV-induced photo lesions.* DNA Repair (Amst), 2005. **4**(5): p. 571-82.
157. Batty, D., et al., *Stable binding of human XPC complex to irradiated DNA confers strong discrimination for damaged sites.* J Mol Biol, 2000. **300**(2): p. 275-90.
158. Yeh, J.I., et al., *Damaged DNA induced UV-damaged DNA-binding protein (UV-DDB) dimerization and its roles in chromatinized DNA repair.* Proc Natl Acad Sci U S A, 2012. **109**(41): p. E2737-46.
159. Wang, Q.E., et al., *UV radiation-induced XPC translocation within chromatin is mediated by damaged-DNA binding protein, DDB2.* Carcinogenesis, 2004. **25**(6): p. 1033-43.
160. Nishi, R., et al., *UV-DDB-dependent regulation of nucleotide excision repair kinetics in living cells.* DNA Repair (Amst), 2009. **8**(6): p. 767-76.
161. Wakasugi, M., et al., *Damaged DNA-binding protein DDB stimulates the excision of cyclobutane pyrimidine dimers in vitro in concert with XPA and replication protein A.* J Biol Chem, 2001. **276**(18): p. 15434-40.
162. Fei, J., et al., *Regulation of nucleotide excision repair by UV-DDB: prioritization of damage recognition to internucleosomal DNA.* PLoS Biol, 2011. **9**(10): p. e1001183.
163. Yang, Y., et al., *Autophagic UVRAG Promotes UV-Induced Photolesion Repair by Activation of the CRL4(DDB2) E3 Ligase.* Mol Cell, 2016. **62**(4): p. 507-19.
164. Puumalainen, M.R., et al., *Xeroderma pigmentosum group C sensor: unprecedented recognition strategy and tight spatiotemporal regulation.* Cell Mol Life Sci, 2016. **73**(3): p. 547-66.

165. El-Mahdy, M.A., et al., *Cullin 4A-mediated proteolysis of DDB2 protein at DNA damage sites regulates in vivo lesion recognition by XPC.* J Biol Chem, 2006. **281**(19): p. 13404-11.
166. Puumalainen, M.R., et al., *Chromatin retention of DNA damage sensors DDB2 and XPC through loss of p97 segregase causes genotoxicity.* Nat Commun, 2014. **5**: p. 3695.
167. Matsumoto, S., et al., *Functional regulation of the DNA damage-recognition factor DDB2 by ubiquitination and interaction with xeroderma pigmentosum group C protein.* Nucleic Acids Res, 2015. **43**(3): p. 1700-13.
168. Wang, Q.E., et al., *DNA repair factor XPC is modified by SUMO-1 and ubiquitin following UV irradiation.* Nucleic Acids Res, 2005. **33**(13): p. 4023-34.
169. Poulsen, S.L., et al., *RNF111/Arkadia is a SUMO-targeted ubiquitin ligase that facilitates the DNA damage response.* J Cell Biol, 2013. **201**(6): p. 797-807.
170. van Cuijk, L., et al., *SUMO and ubiquitin-dependent XPC exchange drives nucleotide excision repair.* Nat Commun, 2015. **6**: p. 7499.
171. He, J., et al., *Ubiquitin-specific protease 7 regulates nucleotide excision repair through deubiquitinating XPC protein and preventing XPC protein from undergoing ultraviolet light-induced and VCP/p97 protein-regulated proteolysis.* J Biol Chem, 2014. **289**(39): p. 27278-89.
172. Luijsterburg, M.S., et al., *Dynamic in vivo interaction of DDB2 E3 ubiquitin ligase with UV-damaged DNA is independent of damage-recognition protein XPC.* J Cell Sci, 2007. **120**(Pt 15): p. 2706-16.
173. Krasikova, Y.S., et al., *Human and yeast DNA damage recognition complexes bind with high affinity DNA structures mimicking in size transcription bubble.* J Mol Recognit, 2013. **26**(12): p. 653-61.
174. Bertolaet, B.L., et al., *UBA domains of DNA damage-inducible proteins interact with ubiquitin.* Nat Struct Biol, 2001. **8**(5): p. 417-22.
175. Kapetanaki, M.G., et al., *The DDB1-CUL4ADDB2 ubiquitin ligase is deficient in xeroderma pigmentosum group E and targets histone H2A at UV-damaged DNA sites.* Proc Natl Acad Sci U S A, 2006. **103**(8): p. 2588-93.
176. Wang, H., et al., *Histone H3 and H4 ubiquitylation by the CUL4-DDB-ROC1 ubiquitin ligase facilitates cellular response to DNA damage.* Mol Cell, 2006. **22**(3): p. 383-94.
177. Lan, L., et al., *Monoubiquitinated histone H2A destabilizes photolesion-containing nucleosomes with concomitant release of UV-damaged DNA-binding protein E3 ligase.* J Biol Chem, 2012. **287**(15): p. 12036-49.
178. Smerdon, M.J., et al., *Sodium butyrate stimulates DNA repair in UV-irradiated normal and xeroderma pigmentosum human fibroblasts.* J Biol Chem, 1982. **257**(22): p. 13441-7.
179. Ramanathan, B. and M.J. Smerdon, *Enhanced DNA repair synthesis in hyperacetylated nucleosomes.* J Biol Chem, 1989. **264**(19): p. 11026-34.
180. Martinez, E., et al., *Human STAGA complex is a chromatin-acetylating transcription coactivator that interacts with pre-mRNA splicing and DNA damage-binding factors in vivo.* Mol Cell Biol, 2001. **21**(20): p. 6782-95.
181. Datta, A., et al., *The p48 subunit of the damaged-DNA binding protein DDB associates with the CBP/p300 family of histone acetyltransferase.* Mutat Res, 2001. **486**(2): p. 89-97.
182. Rapic-Otrin, V., et al., *Sequential binding of UV DNA damage binding factor and degradation of the p48 subunit as early events after UV irradiation.* Nucleic Acids Res, 2002. **30**(11): p. 2588-98.
183. Jiang, Y., et al., *INO80 chromatin remodeling complex promotes the removal of UV lesions by the nucleotide excision repair pathway.* Proc Natl Acad Sci U S A, 2010. **107**(40): p. 17274-9.

184. Zhang, L., et al., *The chromatin remodeling factor BRG1 stimulates nucleotide excision repair by facilitating recruitment of XPC to sites of DNA damage.* Cell Cycle, 2009. **8**(23): p. 3953-9.
185. Zhao, Q., et al., *Modulation of nucleotide excision repair by mammalian SWI/SNF chromatin-remodeling complex.* J Biol Chem, 2009. **284**(44): p. 30424-32.
186. Luijsterburg, M.S., et al., *DDB2 promotes chromatin decondensation at UV-induced DNA damage.* J Cell Biol, 2012. **197**(2): p. 267-81.
187. Chambon, P., J.D. Weill, and P. Mandel, *Nicotinamide mononucleotide activation of new DNA-dependent polyadenylic acid synthesizing nuclear enzyme.* Biochem Biophys Res Commun, 1963. **11**: p. 39-43.
188. Sugimura, T., et al., *Polymerization of the adenosine 5'-diphosphate ribose moiety of NAD by rat liver nuclear enzyme.* Biochim Biophys Acta, 1967. **138**(2): p. 438-41.
189. Nishizuka, Y., et al., *Studies on the polymer of adenosine diphosphate ribose. I. Enzymic formation from nicotinamide adenine dinuclotide in mammalian nuclei.* J Biol Chem, 1967. **242**(13): p. 3164-71.
190. Chambon, P., et al., *On the formation of a novel adenylic compound by enzymatic extracts of liver nuclei.* Biochemical and Biophysical Research Communications, 1966. **25**(6): p. 638-643.
191. Brightwell, M. and S. Shall, *Poly(adenosine diphosphate ribose) polymerase in Physarum polycephalum nuclei.* Biochem J, 1971. **125**(3): p. 67P.
192. Krishnakumar, R. and W.L. Kraus, *The PARP side of the nucleus: molecular actions, physiological outcomes, and clinical targets.* Mol Cell, 2010. **39**(1): p. 8-24.
193. Barkauskaite, E., G. Jankevicius, and I. Ahel, *Structures and Mechanisms of Enzymes Employed in the Synthesis and Degradation of PARP-Dependent Protein ADP-Ribosylation.* Mol Cell, 2015. **58**(6): p. 935-46.
194. Alvarez-Gonzalez, R. and M.K. Jacobson, *Characterization of polymers of adenosine diphosphate ribose generated in vitro and in vivo.* Biochemistry, 1987. **26**(11): p. 3218-24.
195. Minaga, T. and E. Kun, *Spectral analysis of the conformation of polyadenosine diphosphoribose. Evidence indicating secondary structure.* J Biol Chem, 1983. **258**(2): p. 725-30.
196. Daniels, C.M., S.E. Ong, and A.K. Leung, *The Promise of Proteomics for the Study of ADP-Ribosylation.* Mol Cell, 2015. **58**(6): p. 911-24.
197. Hassa, P.O., et al., *Nuclear ADP-ribosylation reactions in mammalian cells: where are we today and where are we going?* Microbiol Mol Biol Rev, 2006. **70**(3): p. 789-829.
198. Schreiber, V., et al., *Poly(ADP-ribose): novel functions for an old molecule.* Nat Rev Mol Cell Biol, 2006. **7**(7): p. 517-528.
199. Teloni, F. and M. Altmeyer, *Readers of poly(ADP-ribose): designed to be fit for purpose.* Nucleic Acids Res, 2016. **44**(3): p. 993-1006.
200. Vyas, S., et al., *Family-wide analysis of poly(ADP-ribose) polymerase activity.* Nature Communications, 2014. **5**: p. 4426.
201. Hottiger, M.O., et al., *Toward a unified nomenclature for mammalian ADP-ribosyltransferases.* Trends Biochem Sci, 2010. **35**(4): p. 208-19.
202. Yamanaka, H., et al., *Characterization of human poly(ADP-ribose) polymerase with autoantibodies.* J Biol Chem, 1988. **263**(8): p. 3879-83.
203. Ludwig, A., et al., *Immunoquantitation and size determination of intrinsic poly(ADP-ribose) polymerase from acid precipitates. An analysis of the in vivo status in mammalian species and in lower eukaryotes.* J Biol Chem, 1988. **263**(15): p. 6993-9.

204. Kameshita, I., et al., *Poly (ADP-Ribose) synthetase. Separation and identification of three proteolytic fragments as the substrate-binding domain, the DNA-binding domain, and the automodification domain.* J Biol Chem, 1984. **259**(8): p. 4770-6.
205. Menissier-de Murcia, J., et al., *Zinc-binding domain of poly(ADP-ribose)polymerase participates in the recognition of single strand breaks on DNA.* J Mol Biol, 1989. **210**(1): p. 229-33.
206. Gradwohl, G., et al., *The second zinc-finger domain of poly(ADP-ribose) polymerase determines specificity for single-stranded breaks in DNA.* Proc Natl Acad Sci U S A, 1990. **87**(8): p. 2990-4.
207. Soldani, C. and A.I. Scovassi, *Poly(ADP-ribose) polymerase-1 cleavage during apoptosis: an update.* Apoptosis, 2002. **7**(4): p. 321-8.
208. Langelier, M.F., et al., *Structural basis for DNA damage-dependent poly(ADP-ribosyl)ation by human PARP-1.* Science, 2012. **336**(6082): p. 728-32.
209. Langelier, M.F., et al., *Crystal structures of poly(ADP-ribose) polymerase-1 (PARP-1) zinc fingers bound to DNA: structural and functional insights into DNA-dependent PARP-1 activity.* J Biol Chem, 2011. **286**(12): p. 10690-701.
210. Langelier, M.F. and J.M. Pascal, *PARP-1 mechanism for coupling DNA damage detection to poly(ADP-ribose) synthesis.* Curr Opin Struct Biol, 2013. **23**(1): p. 134-43.
211. Eustermann, S., et al., *The DNA-binding domain of human PARP-1 interacts with DNA single-strand breaks as a monomer through its second zinc finger.* J Mol Biol, 2011. **407**(1): p. 149-70.
212. Eustermann, S., et al., *Structural Basis of Detection and Signaling of DNA Single-Strand Breaks by Human PARP-1.* Mol Cell, 2015. **60**(5): p. 742-54.
213. Langelier, M.F., et al., *A third zinc-binding domain of human poly(ADP-ribose) polymerase-1 coordinates DNA-dependent enzyme activation.* J Biol Chem, 2008. **283**(7): p. 4105-14.
214. Langelier, M.F., et al., *The Zn3 domain of human poly(ADP-ribose) polymerase-1 (PARP-1) functions in both DNA-dependent poly(ADP-ribose) synthesis activity and chromatin compaction.* J Biol Chem, 2010. **285**(24): p. 18877-87.
215. Gagne, J.P., et al., *Quantitative site-specific ADP-ribosylation profiling of DNA-dependent PARPs.* DNA Repair (Amst), 2015. **30**: p. 68-79.
216. Altmeyer, M., et al., *Molecular mechanism of poly(ADP-ribosyl)ation by PARP1 and identification of lysine residues as ADP-ribose acceptor sites.* Nucleic Acids Res, 2009. **37**(11): p. 3723-38.
217. Dawicki-McKenna, J.M., et al., *PARP-1 Activation Requires Local Unfolding of an Autoinhibitory Domain.* Mol Cell, 2015. **60**(5): p. 755-68.
218. Clark, N.J., et al., *Alternative modes of binding of poly(ADP-ribose) polymerase 1 to free DNA and nucleosomes.* J Biol Chem, 2012. **287**(39): p. 32430-9.
219. Kim, M.Y., T. Zhang, and W.L. Kraus, *Poly(ADP-ribosyl)ation by PARP-1: 'PAR-laying' NAD+ into a nuclear signal.* Genes Dev, 2005. **19**(17): p. 1951-67.
220. Trucco, C., et al., *Mutations in the amino-terminal domain of the human poly(ADP-ribose) polymerase that affect its catalytic activity but not its DNA binding capacity.* FEBS Lett, 1996. **399**(3): p. 313-6.
221. Steffen, J.D., M.M. McCauley, and J.M. Pascal, *Fluorescent sensors of PARP-1 structural dynamics and allosteric regulation in response to DNA damage.* Nucleic Acids Res, 2016.
222. Ali, A.A.E., et al., *The zinc-finger domains of PARP1 cooperate to recognize DNA strand breaks.* Nat Struct Mol Biol, 2012. **19**(7): p. 685-692.
223. Sousa, F.G., et al., *PARPs and the DNA damage response.* Carcinogenesis, 2012. **33**(8): p. 1433-40.

224. Pinnola, A., et al., *Nucleosomal core histones mediate dynamic regulation of poly(ADP-ribose) polymerase 1 protein binding to chromatin and induction of its enzymatic activity.* J Biol Chem, 2007. **282**(44): p. 32511-9.
225. Mao, Z., et al., *SIRT6 promotes DNA repair under stress by activating PARP1.* Science, 2011. **332**(6036): p. 1443-6.
226. Cohen-Armon, M., et al., *DNA-independent PARP-1 activation by phosphorylated ERK2 increases Elk1 activity: a link to histone acetylation.* Mol Cell, 2007. **25**(2): p. 297-308.
227. Pion, E., et al., *Poly(ADP-ribose) polymerase-1 dimerizes at a 5' recessed DNA end in vitro: a fluorescence study.* Biochemistry, 2003. **42**(42): p. 12409-17.
228. Lonskaya, I., et al., *Regulation of poly(ADP-ribose) polymerase-1 by DNA structure-specific binding.* J Biol Chem, 2005. **280**(17): p. 17076-83.
229. Alvarez-Gonzalez, R. and F.R. Althaus, *Poly(ADP-ribose) catabolism in mammalian cells exposed to DNA-damaging agents.* Mutat Res, 1989. **218**(2): p. 67-74.
230. David, K.K., et al., *Parthanatos, a messenger of death.* Front Biosci (Landmark Ed), 2009. **14**: p. 1116-28.
231. Koh, D.W., et al., *Failure to degrade poly(ADP-ribose) causes increased sensitivity to cytotoxicity and early embryonic lethality.* Proc Natl Acad Sci U S A, 2004. **101**(51): p. 17699-704.
232. Woodhouse, B.C. and G.L. Dianov, *Poly ADP-ribose polymerase-1: an international molecule of mystery.* DNA Repair (Amst), 2008. **7**(7): p. 1077-86.
233. Meyer-Ficca, M.L., et al., *Human poly(ADP-ribose) glycohydrolase is expressed in alternative splice variants yielding isoforms that localize to different cell compartments.* Exp Cell Res, 2004. **297**(2): p. 521-32.
234. Mortusewicz, O., et al., *PARG is recruited to DNA damage sites through poly(ADP-ribose)-and PCNA-dependent mechanisms.* Nucleic Acids Res, 2011. **39**(12): p. 5045-56.
235. Rack, J.G., D. Perina, and I. Ahel, *Macrodomains: Structure, Function, Evolution, and Catalytic Activities.* Annu Rev Biochem, 2016. **85**: p. 431-54.
236. Slade, D., et al., *The structure and catalytic mechanism of a poly(ADP-ribose) glycohydrolase.* Nature, 2011. **477**(7366): p. 616-20.
237. Patel, C.N., et al., *Identification of three critical acidic residues of poly(ADP-ribose) glycohydrolase involved in catalysis: determining the PARG catalytic domain.* Biochem J, 2005. **388**(Pt 2): p. 493-500.
238. Brochu, G., et al., *Mode of action of poly(ADP-ribose) glycohydrolase.* Biochim Biophys Acta, 1994. **1219**(2): p. 342-50.
239. Barkauskaite, E., et al., *Visualization of poly(ADP-ribose) bound to PARG reveals inherent balance between exo- and endo-glycohydrolase activities.* Nat Commun, 2013. **4**: p. 2164.
240. Mashimo, M., J. Kato, and J. Moss, *ADP-ribosyl-acceptor hydrolase 3 regulates poly (ADP-ribose) degradation and cell death during oxidative stress.* Proc Natl Acad Sci U S A, 2013. **110**(47): p. 18964-9.
241. Jankevicius, G., et al., *A family of macrodomain proteins reverses cellular mono-ADP-ribosylation.* Nat Struct Mol Biol, 2013. **20**(4): p. 508-514.
242. Rosenthal, F., et al., *Macrodomain-containing proteins are new mono-ADP-ribosylhydrolases.* Nat Struct Mol Biol, 2013. **20**(4): p. 502-7.
243. Sharifi, R., et al., *Deficiency of terminal ADP-ribose protein glycohydrolase TARG1/C6orf130 in neurodegenerative disease.* EMBO J, 2013. **32**(9): p. 1225-37.
244. Wielckens, K., et al., *DNA fragmentation and NAD depletion. Their relation to the turnover of endogenous mono(ADP-ribosyl) and poly(ADP-ribosyl) proteins.* J Biol Chem, 1982. **257**(21): p. 12872-7.

245. Gibson, B.A., et al., *Chemical genetic discovery of PARP targets reveals a role for PARP-1 in transcription elongation.* Science, 2016. **353**(6294): p. 45-50.
246. Cervantes-Laurean, D., E.L. Jacobson, and M.K. Jacobson, *Glycation and glycoxidation of histones by ADP-ribose.* J Biol Chem, 1996. **271**(18): p. 10461-9.
247. Martello, R., et al., *Proteome-wide identification of the endogenous ADP-ribosylome of mammalian cells and tissue.* Nat Commun, 2016. **7**: p. 12917.
248. Hottiger, M.O., *ADP-ribosylation of histones by ARTD1: an additional module of the histone code?* FEBS Lett, 2011. **585**(11): p. 1595-9.
249. Krietsch, J., et al., *Reprogramming cellular events by poly(ADP-ribose)-binding proteins.* Mol Aspects Med, 2013. **34**(6): p. 1066-87.
250. Robert, I., et al., *Functional aspects of PARylation in induced and programmed DNA repair processes: preserving genome integrity and modulating physiological events.* Mol Aspects Med, 2013. **34**(6): p. 1138-52.
251. Malanga, M. and F.R. Althaus, *The role of poly(ADP-ribose) in the DNA damage signaling network.* Biochem Cell Biol, 2005. **83**(3): p. 354-64.
252. Pleschke, J.M., et al., *Poly(ADP-ribose) binds to specific domains in DNA damage checkpoint proteins.* J Biol Chem, 2000. **275**(52): p. 40974-80.
253. Cayrol, C. and B. Ducommun, *Interaction with cyclin-dependent kinases and PCNA modulates proteasome-dependent degradation of p21.* Oncogene, 1998. **17**(19): p. 2437-44.
254. Kanai, M., et al., *Inhibition of Crm1-p53 interaction and nuclear export of p53 by poly(ADP-ribosyl)ation.* Nat Cell Biol, 2007. **9**(10): p. 1175-83.
255. Haince, J.F., et al., *PARP1-dependent kinetics of recruitment of MRE11 and NBS1 proteins to multiple DNA damage sites.* J Biol Chem, 2008. **283**(2): p. 1197-208.
256. Li, G.Y., et al., *Structure and identification of ADP-ribose recognition motifs of APLF and role in the DNA damage response.* Proc Natl Acad Sci U S A, 2010. **107**(20): p. 9129-34.
257. Ahel, D., et al., *Poly(ADP-ribose)-dependent regulation of DNA repair by the chromatin remodeling enzyme ALC1.* Science, 2009. **325**(5945): p. 1240-3.
258. Wang, Z., et al., *Recognition of the iso-ADP-ribose moiety in poly(ADP-ribose) by WWE domains suggests a general mechanism for poly(ADP-ribosyl)ation-dependent ubiquitination.* Genes Dev, 2012. **26**(3): p. 235-40.
259. DaRosa, P.A., et al., *Allosteric activation of the RNF146 ubiquitin ligase by a poly(ADP-ribosyl)ation signal.* Nature, 2015. **517**(7533): p. 223-6.
260. Kang, H.C., et al., *Iduna is a poly(ADP-ribose) (PAR)-dependent E3 ubiquitin ligase that regulates DNA damage.* Proc Natl Acad Sci U S A, 2011. **108**(34): p. 14103-8.
261. Kim, I.K., et al., *A quantitative assay reveals ligand specificity of the DNA scaffold repair protein XRCC1 and efficient disassembly of complexes of XRCC1 and the poly(ADP-ribose) polymerase 1 by poly(ADP-ribose) glycohydrolase.* J Biol Chem, 2015. **290**(6): p. 3775-83.
262. Gottschalk, A.J., et al., *Activation of the SNF2 family ATPase ALC1 by poly(ADP-ribose) in a stable ALC1.PARP1.nucleosome intermediate.* J Biol Chem, 2012. **287**(52): p. 43527-32.
263. Fahrer, J., et al., *Quantitative analysis of the binding affinity of poly(ADP-ribose) to specific binding proteins as a function of chain length.* Nucleic Acids Res, 2007. **35**(21): p. e143.
264. Malanga, M., et al., *Poly(ADP-ribose) binds to specific domains of p53 and alters its DNA binding functions.* J Biol Chem, 1998. **273**(19): p. 11839-43.
265. Simbulan-Rosenthal, C.M., et al., *Poly(ADP-ribosyl)ation of p53 in vitro and in vivo modulates binding to its DNA consensus sequence.* Neoplasia, 2001. **3**(3): p. 179-88.
266. Simbulan-Rosenthal, C.M., et al., *Poly(ADP-ribosyl)ation of p53 during apoptosis in human osteosarcoma cells.* Cancer Res, 1999. **59**(9): p. 2190-4.

267. Hatakeyama, K., et al., *Purification and characterization of poly(ADP-ribose) glycohydrolase. Different modes of action on large and small poly(ADP-ribose).* J Biol Chem, 1986. **261**(32): p. 14902-11.
268. Burkle, A. and L. Virag, *Poly(ADP-ribose): PARadigms and PARadoxes.* Mol Aspects Med, 2013. **34**(6): p. 1046-65.
269. Ryu, K.W., D.S. Kim, and W.L. Kraus, *New facets in the regulation of gene expression by ADP-ribosylation and poly(ADP-ribose) polymerases.* Chem Rev, 2015. **115**(6): p. 2453-81.
270. Haince, J.F., et al., *Ataxia telangiectasia mutated (ATM) signaling network is modulated by a novel poly(ADP-ribose)-dependent pathway in the early response to DNA-damaging agents.* J Biol Chem, 2007. **282**(22): p. 16441-53.
271. Kedar, P.S., et al., *Interaction between PARP-1 and ATR in mouse fibroblasts is blocked by PARP inhibition.* DNA Repair (Amst), 2008. **7**(11): p. 1787-98.
272. Talhaoui, I., et al., *Poly(ADP-ribose) polymerases covalently modify strand break termini in DNA fragments in vitro.* Nucleic Acids Res, 2016.
273. Tallis, M., et al., *Poly(ADP-ribosyl)ation in regulation of chromatin structure and the DNA damage response.* Chromosoma, 2014. **123**(1-2): p. 79-90.
274. Soria, G., S.E. Polo, and G. Almouzni, *Prime, repair, restore: the active role of chromatin in the DNA damage response.* Mol Cell, 2012. **46**(6): p. 722-34.
275. Poirier, G.G., et al., *Poly(ADP-ribosyl)ation of polynucleosomes causes relaxation of chromatin structure.* Proc Natl Acad Sci U S A, 1982. **79**(11): p. 3423-7.
276. de Murcia, G., et al., *Modulation of chromatin superstructure induced by poly(ADP-ribose) synthesis and degradation.* J Biol Chem, 1986. **261**(15): p. 7011-7.
277. Thoma, F., R. Losa, and T. Koller, *Involvement of the domains of histones H1 and H5 in the structural organization of soluble chromatin.* J Mol Biol, 1983. **167**(3): p. 619-40.
278. Panzeter, P.L., C.A. Realini, and F.R. Althaus, *Noncovalent interactions of poly(adenosine diphosphate ribose) with histones.* Biochemistry, 1992. **31**(5): p. 1379-85.
279. Wesierska-Gadek, J. and G. Sauermann, *The effect of poly(ADP-ribose) on interactions of DNA with histones H1, H3 and H4.* Eur J Biochem, 1988. **173**(3): p. 675-9.
280. Burzio, L.O., P.T. Riquelme, and S.S. Koide, *ADP ribosylation of rat liver nucleosomal core histones.* J Biol Chem, 1979. **254**(8): p. 3029-37.
281. Messner, S., et al., *PARP1 ADP-ribosylates lysine residues of the core histone tails.* Nucleic Acids Res, 2010. **38**(19): p. 6350-62.
282. Rouleau, M., R.A. Aubin, and G.G. Poirier, *Poly(ADP-ribosyl)ated chromatin domains: access granted.* J Cell Sci, 2004. **117**(Pt 6): p. 815-25.
283. Wacker, D.A., et al., *The DNA binding and catalytic domains of poly(ADP-ribose) polymerase 1 cooperate in the regulation of chromatin structure and transcription.* Mol Cell Biol, 2007. **27**(21): p. 7475-85.
284. Althaus, F.R., *Poly ADP-ribosylation: a histone shuttle mechanism in DNA excision repair.* J Cell Sci, 1992. **102 (Pt 4)**: p. 663-70.
285. Tulin, A. and A. Spradling, *Chromatin loosening by poly(ADP)-ribose polymerase (PARP) at Drosophila puff loci.* Science, 2003. **299**(5606): p. 560-2.
286. Kreimeyer, A., et al., *DNA repair-associated ADP-ribosylation in vivo. Modification of histone H1 differs from that of the principal acceptor proteins.* J Biol Chem, 1984. **259**(2): p. 890-6.
287. Kawaichi, M., K. Ueda, and O. Hayaishi, *Multiple autopoly(ADP-ribosyl)ation of rat liver poly(ADP-ribose) synthetase. Mode of modification and properties of automodified synthetase.* J Biol Chem, 1981. **256**(18): p. 9483-9.

288. Muthurajan, U.M., et al., *Automodification switches PARP-1 function from chromatin architectural protein to histone chaperone.* Proc Natl Acad Sci U S A, 2014. **111**(35): p. 12752-7.
289. Gibbs-Seymour, I., et al., *HPF1/C4orf27 Is a PARP-1-Interacting Protein that Regulates PARP-1 ADP-Ribosylation Activity.* Mol Cell, 2016. **62**(3): p. 432-42.
290. Realini, C.A. and F.R. Althaus, *Histone shuttling by poly(ADP-ribosylation).* J Biol Chem, 1992. **267**(26): p. 18858-65.
291. Strickfaden, H., et al., *Poly(ADP-ribosyl)ation-dependent Transient Chromatin Decondensation and Histone Displacement following Laser Microirradiation.* J Biol Chem, 2016. **291**(4): p. 1789-802.
292. Luijsterburg, M.S., et al., *PARP1 Links CHD2-Mediated Chromatin Expansion and H3.3 Deposition to DNA Repair by Non-homologous End-Joining.* Mol Cell, 2016. **61**(4): p. 547-62.
293. Smeenk, G., et al., *Poly(ADP-ribosyl)ation links the chromatin remodeler SMARCA5/SNF2H to RNF168-dependent DNA damage signaling.* J Cell Sci, 2013. **126**(Pt 4): p. 889-903.
294. Kashima, L., et al., *CHFR protein regulates mitotic checkpoint by targeting PARP-1 protein for ubiquitination and degradation.* J Biol Chem, 2012. **287**(16): p. 12975-84.
295. Liu, C., et al., *CHFR is important for the first wave of ubiquitination at DNA damage sites.* Nucleic Acids Res, 2013. **41**(3): p. 1698-710.
296. Iles, N., et al., *APLF (C2orf13) is a novel human protein involved in the cellular response to chromosomal DNA strand breaks.* Mol Cell Biol, 2007. **27**(10): p. 3793-803.
297. Mehrotra, P.V., et al., *DNA repair factor APLF is a histone chaperone.* Mol Cell, 2011. **41**(1): p. 46-55.
298. Grundy, G.J., et al., *APLF promotes the assembly and activity of non-homologous end joining protein complexes.* EMBO J, 2013. **32**(1): p. 112-25.
299. Timinszky, G., et al., *A macrodomain-containing histone rearranges chromatin upon sensing PARP1 activation.* Nat Struct Mol Biol, 2009. **16**(9): p. 923-9.
300. Chou, D.M., et al., *A chromatin localization screen reveals poly (ADP ribose)-regulated recruitment of the repressive polycomb and NuRD complexes to sites of DNA damage.* Proc Natl Acad Sci U S A, 2010. **107**(43): p. 18475-80.
301. Polo, S.E., et al., *Regulation of DNA-damage responses and cell-cycle progression by the chromatin remodelling factor CHD4.* EMBO J, 2010. **29**(18): p. 3130-9.
302. Belotserkovskaya, R., et al., *FACT facilitates transcription-dependent nucleosome alteration.* Science, 2003. **301**(5636): p. 1090-3.
303. Huang, J.Y., et al., *Modulation of nucleosome-binding activity of FACT by poly(ADP-ribosyl)ation.* Nucleic Acids Res, 2006. **34**(8): p. 2398-407.
304. De Vos, M., V. Schreiber, and F. Dantzer, *The diverse roles and clinical relevance of PARPs in DNA damage repair: current state of the art.* Biochem Pharmacol, 2012. **84**(2): p. 137-46.
305. Khodyreva, S.N., et al., *Apurinic/apyrimidinic (AP) site recognition by the 5'-dRP/AP lyase in poly(ADP-ribose) polymerase-1 (PARP-1).* Proc Natl Acad Sci U S A, 2010. **107**(51): p. 22090-5.
306. Allinson, S.L., Dianova, II, and G.L. Dianov, *Poly(ADP-ribose) polymerase in base excision repair: always engaged, but not essential for DNA damage processing.* Acta Biochim Pol, 2003. **50**(1): p. 169-79.
307. Lindahl, T., et al., *Post-translational modification of poly(ADP-ribose) polymerase induced by DNA strand breaks.* Trends Biochem Sci, 1995. **20**(10): p. 405-11.
308. Satoh, M.S., G.G. Poirier, and T. Lindahl, *NAD(+)-dependent repair of damaged DNA by human cell extracts.* J Biol Chem, 1993. **268**(8): p. 5480-7.

309. Parsons, J.L., et al., *Poly(ADP-ribose) polymerase-1 protects excessive DNA strand breaks from deterioration during repair in human cell extracts.* Febs J, 2005. **272**(8): p. 2012-21.
310. Prasad, R., et al., *Mammalian Base Excision Repair: Functional Partnership between PARP-1 and APE1 in AP-Site Repair.* PLoS One, 2015. **10**(5): p. e0124269.
311. Cistulli, C., et al., *AP endonuclease and poly(ADP-ribose) polymerase-1 interact with the same base excision repair intermediate.* DNA Repair (Amst), 2004. **3**(6): p. 581-91.
312. Prasad, R., et al., *Suicidal cross-linking of PARP-1 to AP site intermediates in cells undergoing base excision repair.* Nucleic Acids Res, 2014. **42**(10): p. 6337-51.
313. Kleppa, L., et al., *Kinetics of endogenous mouse FEN1 in base excision repair.* Nucleic Acids Res, 2012. **40**(18): p. 9044-59.
314. Horton, J.K., et al., *XRCC1 and DNA polymerase beta in cellular protection against cytotoxic DNA single-strand breaks.* Cell Res, 2008. **18**(1): p. 48-63.
315. Lan, L., et al., *Novel method for site-specific induction of oxidative DNA damage reveals differences in recruitment of repair proteins to heterochromatin and euchromatin.* Nucleic Acids Res, 2014. **42**(4): p. 2330-45.
316. Noren Hooten, N., et al., *Poly(ADP-ribose) polymerase 1 (PARP-1) binds to 8-oxoguanine-DNA glycosylase (OGG1).* J Biol Chem, 2011. **286**(52): p. 44679-90.
317. Durkacz, B.W., et al., *(ADP-ribose)n participates in DNA excision repair.* Nature, 1980. **283**(5747): p. 593-6.
318. Kupper, J.H., et al., *trans-dominant inhibition of poly(ADP-ribosyl)ation sensitizes cells against gamma-irradiation and N-methyl-N'-nitro-N-nitrosoguanidine but does not limit DNA replication of a polyomavirus replicon.* Mol Cell Biol, 1995. **15**(6): p. 3154-63.
319. Vodenicharov, M.D., et al., *Base excision repair is efficient in cells lacking poly(ADP-ribose) polymerase 1.* Nucleic Acids Res, 2000. **28**(20): p. 3887-96.
320. Pines, A., et al., *Touching base with PARPs: moonlighting in the repair of UV lesions and double-strand breaks.* Trends Biochem Sci, 2013. **38**(6): p. 321-30.
321. Bryant, H.E., et al., *PARP is activated at stalled forks to mediate Mre11-dependent replication restart and recombination.* Embo J, 2009. **28**(17): p. 2601-15.
322. Yang, Y.G., et al., *Ablation of PARP-1 does not interfere with the repair of DNA double-strand breaks, but compromises the reactivation of stalled replication forks.* Oncogene, 2004. **23**(21): p. 3872-82.
323. Li, M. and X. Yu, *The Role of Poly(ADP-ribosyl)ation in DNA Damage Response and Cancer Chemotherapy.* Oncogene, 2015. **34**(26): p. 3349-3356.
324. Ying, S., F.C. Hamdy, and T. Helleday, *Mre11-dependent degradation of stalled DNA replication forks is prevented by BRCA2 and PARP1.* Cancer Res, 2012. **72**(11): p. 2814-21.
325. Illuzzi, G., et al., *PARG is dispensable for recovery from transient replicative stress but required to prevent detrimental accumulation of poly(ADP-ribose) upon prolonged replicative stress.* Nucleic Acids Res, 2014. **42**(12): p. 7776-92.
326. Hochegger, H., et al., *Parp-1 protects homologous recombination from interference by Ku and Ligase IV in vertebrate cells.* EMBO J, 2006. **25**(6): p. 1305-14.
327. Ray Chaudhuri, A., et al., *Topoisomerase I poisoning results in PARP-mediated replication fork reversal.* Nat Struct Mol Biol, 2012. **19**(4): p. 417-23.
328. Schultz, N., et al., *Poly(ADP-ribose) polymerase (PARP-1) has a controlling role in homologous recombination.* Nucleic Acids Res, 2003. **31**(17): p. 4959-64.
329. Claybon, A., et al., *PARP1 suppresses homologous recombination events in mice in vivo.* Nucleic Acids Res, 2010. **38**(21): p. 7538-45.
330. Cheng, Q., et al., *Ku counteracts mobilization of PARP1 and MRN in chromatin damaged with DNA double-strand breaks.* Nucleic Acids Research, 2011. **39**(22): p. 9605-9619.

331. Wang, M., et al., *PARP-1 and Ku compete for repair of DNA double strand breaks by distinct NHEJ pathways.* Nucleic Acids Res, 2006. **34**(21): p. 6170-82.
332. Rybanska, I., et al., *PARP1 and DNA-PKcs synergize to suppress p53 mutation and telomere fusions during T-lineage lymphomagenesis.* Oncogene, 2013. **32**(14): p. 1761-1771.
333. Rosidi, B., et al., *Histone H1 functions as a stimulatory factor in backup pathways of NHEJ.* Nucleic Acids Res, 2008. **36**(5): p. 1610-23.
334. McCurry, L.S. and M.K. Jacobson, *Poly(ADP-ribose) synthesis following DNA damage in cells heterozygous or homozygous for the xeroderma pigmentosum genotype.* J Biol Chem, 1981. **256**(2): p. 551-3.
335. Berger, N.A., et al., *Defective poly(adenosine diphosphoribose) synthesis in xeroderma pigmentosum.* Biochemistry, 1980. **19**(2): p. 289-93.
336. Jacobson, E.L., et al., *Poly(ADP-ribose) metabolism in ultraviolet irradiated human fibroblasts.* J Biol Chem, 1983. **258**(1): p. 103-7.
337. Benjamin, R.C. and D.M. Gill, *ADP-ribosylation in mammalian cell ghosts. Dependence of poly(ADP-ribose) synthesis on strand breakage in DNA.* J Biol Chem, 1980. **255**(21): p. 10493-501.
338. Vodenicharov, M.D., et al., *Mechanism of early biphasic activation of poly(ADP-ribose) polymerase-1 in response to ultraviolet B radiation.* J Cell Sci, 2005. **118**(Pt 3): p. 589-99.
339. Ghodgaonkar, M.M., et al., *Depletion of poly(ADP-ribose) polymerase-1 reduces host cell reactivation of a UV-damaged adenovirus-encoded reporter gene in human dermal fibroblasts.* DNA Repair (Amst), 2008. **7**(4): p. 617-32.
340. Molinete, M., et al., *Overproduction of the poly(ADP-ribose) polymerase DNA-binding domain blocks alkylation-induced DNA repair synthesis in mammalian cells.* EMBO J, 1993. **12**(5): p. 2109-17.
341. Schreiber, V., et al., *A dominant-negative mutant of human poly(ADP-ribose) polymerase affects cell recovery, apoptosis, and sister chromatid exchange following DNA damage.* Proc Natl Acad Sci U S A, 1995. **92**(11): p. 4753-7.
342. Wang, Z.Q., et al., *Mice lacking ADPRT and poly(ADP-ribosyl)ation develop normally but are susceptible to skin disease.* Genes Dev, 1995. **9**(5): p. 509-20.
343. Stevnsner, T., et al., *Inhibition of gene-specific repair of alkylation damage in cells depleted of poly(ADP-ribose) polymerase.* Nucleic Acids Res, 1994. **22**(22): p. 4620-4.
344. Flohr, C., et al., *Poly(ADP-ribosyl)ation accelerates DNA repair in a pathway dependent on Cockayne syndrome B protein.* Nucleic Acids Res, 2003. **31**(18): p. 5332-7.
345. Hastak, K., E. Alli, and J.M. Ford, *Synergistic chemosensitivity of triple-negative breast cancer cell lines to poly(ADP-Ribose) polymerase inhibition, gemcitabine, and cisplatin.* Cancer Res, 2010. **70**(20): p. 7970-80.
346. Tang, J.Y., et al., *Xeroderma pigmentosum p48 gene enhances global genomic repair and suppresses UV-induced mutagenesis.* Mol Cell, 2000. **5**(4): p. 737-44.
347. Hartman, A.R. and J.M. Ford, *BRCA1 induces DNA damage recognition factors and enhances nucleotide excision repair.* Nat Genet, 2002. **32**(1): p. 180-4.
348. Robu, M., *Rôle de la poly(ADP-ribose) polymérase-1 (PARP-1) dans la réparation de l'ADN par excision des nucléotides.* Memoire de maîtrise, 2010.
349. Robu, M., Petitclerc,N., Brind'Amour J., Kandan-Kulangara, F., Shah, R.G. and Shah G.M., *Role of poly(ADP-ribose) polymerase-1 in the removal of UV-induced DNA lesions by nucleotide excision repair.* PNAS, 2012. **accepted with revision**.
350. Thorslund, T., et al., *Cooperation of the Cockayne syndrome group B protein and poly(ADP-ribose) polymerase 1 in the response to oxidative stress.* Mol Cell Biol, 2005. **25**(17): p. 7625-36.

351. Gagne, J.P., et al., *Proteome-wide identification of poly(ADP-ribose) binding proteins and poly(ADP-ribose)-associated protein complexes.* Nucleic Acids Res, 2008. **36**(22): p. 6959-76.
352. Lord, C.J., A.N. Tutt, and A. Ashworth, *Synthetic lethality and cancer therapy: lessons learned from the development of PARP inhibitors.* Annu Rev Med, 2015. **66**: p. 455-70.
353. De Lorenzo, S.B., et al., *The Elephant and the Blind Men: Making Sense of PARP Inhibitors in Homologous Recombination Deficient Tumor Cells.* Front Oncol, 2013. **3**: p. 228.
354. Farmer, H., et al., *Targeting the DNA repair defect in BRCA mutant cells as a therapeutic strategy.* Nature, 2005. **434**(7035): p. 917-21.
355. Bryant, H.E., et al., *Specific killing of BRCA2-deficient tumours with inhibitors of poly(ADP-ribose) polymerase.* Nature, 2005. **434**(7035): p. 913-7.
356. Montoni, A., et al., *Resistance to PARP-Inhibitors in Cancer Therapy.* Front Pharmacol, 2013. **4**: p. 18.
357. Helleday, T., *The underlying mechanism for the PARP and BRCA synthetic lethality: clearing up the misunderstandings.* Mol Oncol, 2011. **5**(4): p. 387-93.
358. Gottipati, P., et al., *Poly(ADP-ribose) polymerase is hyperactivated in homologous recombination-defective cells.* Cancer Res, 2010. **70**(13): p. 5389-98.
359. Satoh, M.S. and T. Lindahl, *Role of poly(ADP-ribose) formation in DNA repair.* Nature, 1992. **356**(6367): p. 356-8.
360. Li, M. and X. Yu, *Function of BRCA1 in the DNA damage response is mediated by ADP-ribosylation.* Cancer cell, 2013. **23**(5): p. 693-704.
361. Patel, A.G., J.N. Sarkaria, and S.H. Kaufmann, *Nonhomologous end joining drives poly(ADP-ribose) polymerase (PARP) inhibitor lethality in homologous recombination-deficient cells.* Proc Natl Acad Sci U S A, 2011. **108**(8): p. 3406-11.
362. Feng, F.Y., et al., *Chromatin to Clinic: The Molecular Rationale for PARP1 Inhibitor Function.* Mol Cell, 2015. **58**(6): p. 925-34.
363. Statistics., C.C.S.s.A.C.o.C., *Canadian Cancer Statistics 2014.* Toronto, ON: Canadian Cancer Society; 2014., 2014.
364. Sims, J.L., et al., *Poly(adenosinediphosphoribose) polymerase inhibitors stimulate unscheduled deoxyribonucleic acid synthesis in normal human lymphocytes.* Biochemistry, 1982. **21**(8): p. 1813-21.
365. Krishnakumar, R. and W.L. Kraus, *The PARP Side of the Nucleus: Molecular Actions, Physiological Outcomes, and Clinical Targets.* Mol. Cell, 2010. **39**(1): p. 8-24.
366. Yélamos, J., et al., *PARP-1 and PARP-2: New players in tumor development.* Am. J. Cancer Res., 2011. **1**(3): p. 328-346.
367. Fei, J., et al., *Regulation of nucleotide excision repair by UV-DDB: prioritization of damage recognition to internucleosomal DNA.* PLoS Biol., 2011. **9**(10): p. e1001183.
368. Ciccia, A. and S.J. Elledge, *The DNA damage response: making it safe to play with knives.* Mol. Cell, 2010. **40**(2): p. 179-204.
369. Stevnsner, T., et al., *Inhibition of gene-specific repair of alkylation damage in cells depleted of poly(ADP-ribose) polymerase.* Nucl. Acids Res., 1994. **22**(22): p. 4620-4.
370. Flohr, C., et al., *Poly(ADP-ribosyl)ation accelerates DNA repair in a pathway dependent on Cockayne syndrome B protein.* Nucl. Acids Res., 2003. **31**(18): p. 5332-5337.
371. Auclair, Y., et al., *ATR kinase is required for global genomic nucleotide excision repair exclusively during S phase in human cells.* Proc Natl Acad Sci U S A, 2008. **105**(46): p. 17896-901.
372. Shah, R.G., et al., *DNA vector-based RNAi approach for stable depletion of poly(ADP-ribose) polymerase-1.* Biochem Biophys Res Commun, 2005. **331**(1): p. 167-174.

373. Shah, G.M., et al., *Approaches to detect PARP-1 activation in vivo, in situ, and in vitro.* Methods Molec Biol, 2011. **780**: p. 3-34.
374. Fitch, M.E., I.V. Cross, and J.M. Ford, *p53 responsive nucleotide excision repair gene products p48 and XPC, but not p53, localize to sites of UV-irradiation-induced DNA damage, in vivo.* Carcinogenesis, 2003. **24**(5): p. 843-50.
375. Luijsterburg, M.S., et al., *Dynamic in vivo interaction of DDB2 E3 ubiquitin ligase with UV-damaged DNA is independent of damage-recognition protein XPC.* J. Cell Sci., 2007. **120**(Pt 15): p. 2706-16.
376. Pleschke, J.M., et al., *Poly(ADP-ribose) binds to specific domains in DNA checkpoint proteins.* J. Biol. Chem., 2000. **275**(52): p. 40974-40980.
377. Epstein, J.H. and J.E. Cleaver, *3-Aminobenzamide can act as a cocarcinogen for ultraviolet light-induced carcinogenesis in mouse skin.* Cancer Res., 1992. **52**(14): p. 4053-4054.
378. Ghodgaonkar, M.M., et al., *Depletion of poly(ADP-ribose)polymerase-1 reduces host cell reactivation for UV-treated adenovirus in human dermal fibroblasts.* DNA Repair (Amst), 2008. **7**: p. 617-632.
379. Gibson, B.A. and W.L. Kraus, *New insights into the molecular and cellular functions of poly(ADP-ribose) and PARPs.* Nature Reviews: Molec. Cell Biol., 2012. **13**(7): p. 411-24.
380. Lukas, J., C. Lukas, and J. Bartek, *More than just a focus: The chromatin response to DNA damage and its role in genome integrity maintenance.* Nat. Cell Biol., 2011. **13**(10): p. 1161-9.
381. Sugasawa, K., *Regulation of damage recognition in mammalian global genomic nucleotide excision repair.* Mutat Res, 2010. **685**(1-2): p. 29-37.
382. Midgley, C.A., et al., *Coupling between gamma irradiation, p53 induction and the apoptotic response depends upon cell type in vivo.* J Cell Sci, 1995. **108 (Pt 5)**: p. 1843-8.
383. Zhu, Q., et al., *Chromatin restoration following nucleotide excision repair involves the incorporation of ubiquitinated H2A at damaged genomic sites.* DNA Repair, 2009. **8**(2): p. 262-73.
384. Rouget, R., et al., *A sensitive flow cytometry-based nucleotide excision repair assay unexpectedly reveals that mitogen-activated protein kinase signaling does not regulate the removal of UV-induced DNA damage in human cells.* J Biol Chem, 2008. **283**(9): p. 5533-41.
385. Krishnakumar, R. and W.L. Kraus, *PARP-1 regulates chromatin structure and transcription through a KDM5B-dependent pathway.* Molecular Cell, 2010. **39**(5): p. 736-49.
386. Wu, X., et al., *ATR-dependent checkpoint modulates XPA nuclear import in response to UV irradiation.* Oncogene, 2007. **26**(5): p. 757-64.
387. Robert, I., et al., *Functional aspects of PARylation in induced and programmed DNA repair processes: Preserving genome integrity and modulating physiological events.* Mol. Aspects Med., 2013. **34**(6): p. 1138-52.
388. Pascal, J.M. and T. Ellenberger, *The rise and fall of poly(ADP-ribose): An enzymatic perspective.* DNA Repair (Amst), 2015. **32**: p. 10-16.
389. Kim, M.Y., et al., *NAD+-dependent modulation of chromatin structure and transcription by nucleosome binding properties of PARP-1.* Cell, 2004. **119**(6): p. 803-14.
390. Pines, A., et al., *PARP1 promotes nucleotide excision repair through DDB2 stabilization and recruitment of ALC1.* J. Cell Biol., 2012. **199**(2): p. 235-49.
391. Luijsterburg, M.S., et al., *DDB2 promotes chromatin decondensation at UV-induced DNA damage.* J. Cell Biol., 2012. **197**(2): p. 267-81.
392. Robu, M., et al., *Role of poly(ADP-ribose) polymerase-1 in the removal of UV-induced DNA lesions by nucleotide excision repair.* Proc. Natl. Acad. Sci. U.S.A. , 2013. **110**(5): p. 1658-1663.

393. King, B.S., et al., *Poly(ADP-ribose) contributes to an association between Poly(ADP-ribose)polymerase-1 and Xeroderma pigmentosum complementation group A in nucleotide excision repair.* J. Biol. Chem., 2012. **287**: p. 39824-33.
394. Fischer, J.M., et al., *Poly(ADP-ribose)-mediated interplay of XPA and PARP1 leads to reciprocal regulation of protein function.* FEBS J., 2014. **281**(16): p. 3625-41.
395. Maltseva, E.A., et al., *Poly(ADP-ribose)polymerase 1 Modulates Interaction of the Nucleotide Excision Repair Factor XPC-RAD23B with DNA via Poly(ADP-ribosyl)ation.* J. Biol. Chem., 2015. **290**(36): p. 21811-20.
396. Vodenicharov, M.D., et al., *Mechanism of early biphasic activation of poly(ADP-ribose) polymerase-1 in response to ultraviolet B radiation.* J. Cell Sci., 2005. **118**(Pt 3): p. 589-99.
397. Berger, N.A. and G.W. Sikorski, *Poly(adenosine diphosphoribose) synthesis in ultraviolet-irradiated xeroderma pigmentosum cells reconstituted with Micrococcus luteus UV endonuclease.* Biochemistry, 1981. **20**(12): p. 3610-4.
398. Kawamitsu, H., et al., *Monoclonal antibodies to poly(adenosine diphosphate ribose) recognize different structures.* Biochemistry, 1984. **23**: p. 3771-3777.
399. Shah, G.M., et al., *Approaches to detect PARP-1 activation in vivo, in situ, and in vitro.* Methods Mol. Biol., 2011. **780**: p. 3-34.
400. Mirzoeva, O.K. and J.H. Petrini, *DNA damage-dependent nuclear dynamics of the Mre11 complex.* Mol. Cell. Biol., 2001. **21**(1): p. 281-8.
401. Balajee, A.S. and C.R. Geard, *Chromatin-bound PCNA complex formation triggered by DNA damage occurs independent of the ATM gene product in human cells.* Nucleic Acids Res., 2001. **29**(6): p. 1341-51.
402. Fey, E.G., K.M. Wan, and S. Penman, *Epithelial cytoskeletal framework and nuclear matrix-intermediate filament scaffold: three-dimensional organization and protein composition.* J. Cell Biol., 1984. **98**(6): p. 1973-84.
403. Kaufmann, S.H., et al., *Association of poly(ADP-ribose) polymerase with the nuclear matrix: the role of intermolecular disulfide bond formation, RNA retention, and cell type.* Exp. Cell Res., 1991. **192**(2): p. 524-35.
404. Mortusewicz, O., et al., *Feedback-regulated poly(ADP-ribosyl)ation by PARP-1 is required for rapid response to DNA damage in living cells.* Nucleic Acids Res., 2007. **35**(22): p. 7665-75.
405. Ali, A.A., et al., *The zinc-finger domains of PARP1 cooperate to recognize DNA strand breaks.* Nat. Struct. Mol. Biol., 2012. **19**(7): p. 685-92.
406. Hall, R.K. and L.L. Larcom, *Blockage of restriction endonuclease cleavage by thymine dimers.* Photochem. Photobiol., 1982. **36**(4): p. 429-32.
407. Cleaver, J.E., *Restriction enzyme cleavage of ultraviolet-damaged simian virus 40 and pBR322 DNA.* J. Mol. Biol., 1983. **170**(2): p. 305-17.
408. Wittschieben, B.O., S. Iwai, and R.D. Wood, *DDB1-DDB2 (xeroderma pigmentosum group E) protein complex recognizes a cyclobutane pyrimidine dimer, mismatches, apurinic/apyrimidinic sites, and compound lesions in DNA.* J. Biol. Chem., 2005. **280**(48): p. 39982-9.
409. Clark, N.J., et al., *Alternative modes of binding of poly(ADP-ribose) polymerase 1 to free DNA and nucleosomes.* J. Biol. Chem., 2012. **287**(39): p. 32430-9.
410. Menissier-de Murcia, J., et al., *Zinc-binding domain of poly(ADP-ribose)polymerase participates in the recognition of single strand breaks on DNA.* J. Mol. Biol., 1989. **210**(1): p. 229-33.
411. Sancar, A. and G.B. Sancar, *DNA repair enzymes.* Annu. Rev. Biochem., 1988. **57**: p. 29-67.
412. Fitch, M.E., et al., *In vivo recruitment of XPC to UV-induced cyclobutane pyrimidine dimers by the DDB2 gene product.* J. Biol. Chem., 2003. **278**(47): p. 46906-46910.

413. Hendel, A., et al., *Reduced efficiency and increased mutagenicity of translesion DNA synthesis across a TT cyclobutane pyrimidine dimer, but not a TT 6-4 photoproduct, in human cells lacking DNA polymerase eta.* DNA Repair (Amst), 2008. **7**(10): p. 1636-46.
414. Langelier, M.F. and J.M. Pascal, *PARP-1 mechanism for coupling DNA damage detection to poly(ADP-ribose) synthesis.* Curr. Opin. Struct. Biol., 2013. **23**: p. 134-43.
415. Shah, R.G., et al., *DNA vector-based RNAi approach for stable depletion of poly(ADP-ribose) polymerase-1.* Biochem Biophys Res Commun, 2005. **331**(1): p. 167-74.
416. Scharer, O.D., *Nucleotide Excision Repair in Eukaryotes.* Cold Spring Harb Perspect Biol, 2013. **5**(10): p. 10.1101/cshperspect.a012609.
417. Nemzow, L., et al., *XPC: Going where no DNA damage sensor has gone before.* DNA Repair (Amst), 2015. **36**: p. 19-27.
418. Moser, J., et al., *The UV-damaged DNA binding protein mediates efficient targeting of the nucleotide excision repair complex to UV-induced photo lesions.* DNA Repair, 2005. **4**(5): p. 571-82.
419. Oh, K.S., et al., *Nucleotide excision repair proteins rapidly accumulate but fail to persist in human XP-E (DDB2 mutant) cells.* Photochem Photobiol, 2011. **87**(3): p. 729-33.
420. Payne, A. and G. Chu, *Xeroderma pigmentosum group E binding factor recognizes a broad spectrum of DNA damage.* Mutat Res, 1994. **310**(1): p. 89-102.
421. Roux, K.J., et al., *A promiscuous biotin ligase fusion protein identifies proximal and interacting proteins in mammalian cells.* J Cell Biol, 2012. **196**(6): p. 801-10.
422. Moné, M.J., et al., *Local UV-induced DNA damage in cell nuclei results in local transcription inhibition.* EMBO Rep., 2001. **2**(11): p. 1013-1017.
423. Purohit, N.K., et al., *Characterization of the interactions of PARP-1 with UV-damaged DNA in vivo and in vitro.* Sci Rep, 2016. **6**: p. 19020.
424. Hanssen-Bauer, A., et al., *XRCC1 coordinates disparate responses and multiprotein repair complexes depending on the nature and context of the DNA damage.* Environ Mol Mutagen, 2011. **52**(8): p. 623-35.
425. Shah, R.G., et al., *DNA vector-based RNAi approach for stable depletion of poly(ADP-ribose) polymerase-1.* Biochem. Biophys. Res. Commun., 2005. **331**(1): p. 167-174.
426. Yasuda, G., et al., *In vivo destabilization and functional defects of the xeroderma pigmentosum C protein caused by a pathogenic missense mutation.* Mol Cell Biol, 2007. **27**(19): p. 6606-14.
427. Godon, C., et al., *PARP inhibition versus PARP-1 silencing: different outcomes in terms of single-strand break repair and radiation susceptibility.* Nucleic Acids Res, 2008. **36**(13): p. 4454-64.
428. Gassman, N.R. and S.H. Wilson, *Micro-irradiation tools to visualize base excision repair and single-strand break repair.* DNA Repair (Amst), 2015. **31**: p. 52-63.
429. Luo, X. and W.L. Kraus, *On PAR with PARP: cellular stress signaling through poly(ADP-ribose) and PARP-1.* Genes Dev, 2012. **26**(5): p. 417-32.
430. Wei, L., et al., *Damage response of XRCC1 at sites of DNA single strand breaks is regulated by phosphorylation and ubiquitylation after degradation of poly(ADP-ribose).* J Cell Sci, 2013. **126**(Pt 19): p. 4414-23.
431. Kraus, W.L. and J.T. Lis, *PARP goes transcription.* Cell, 2003. **113**(6): p. 677-683.
432. Osakabe, A., et al., *Structural basis of pyrimidine-pyrimidone (6–4) photoproduct recognition by UV-DDB in the nucleosome.* Scientific Reports, 2015. **5**: p. 16330.
433. Isabelle, M., et al., *Investigation of PARP-1, PARP-2, and PARG interactomes by affinity-purification mass spectrometry.* Proteome Sci, 2010. **8**: p. 22.

434. Dubois, M.L., et al., *Comprehensive Characterization of Minichromosome Maintenance Complex (MCM) Protein Interactions Using Affinity and Proximity Purifications Coupled to Mass Spectrometry.* J Proteome Res, 2016. **15**(9): p. 2924-34.
435. Chu, G. and E. Chang, *Xeroderma pigmentosum group E cells lack a nuclear factor that binds to damaged DNA.* Science, 1988. **242**(4878): p. 564-7.
436. Fujiwara, Y., et al., *Characterization of DNA recognition by the human UV-damaged DNA-binding protein.* J Biol Chem, 1999. **274**(28): p. 20027-33.
437. Pines, A., et al., *PARP1 promotes nucleotide excision repair through DDB2 stabilization and recruitment of ALC1.* J Cell Biol, 2012. **199**(2): p. 235-49.
438. Robu, M., et al., *Role of poly(ADP-ribose) polymerase-1 in the removal of UV-induced DNA lesions by nucleotide excision repair.* Proc Natl Acad Sci U S A, 2013. **110**(5): p. 1658-63.
439. King, B.S., et al., *Poly(ADP-ribose) contributes to an association between Poly(ADP-ribose)polymerase-1 and Xeroderma pigmentosum complementation group A in nucleotide excision repair.* J Biol Chem, 2012.
440. Pascal, J.M. and T. Ellenberger, *The Rise and Fall of Poly (ADP-ribose). An Enzymatic Perspective.* DNA repair, 2015. **32**: p. 10-16.
441. Pines, A., et al., *PARP1 promotes nucleotide excision repair through DDB2 stabilization and recruitment of ALC1.* J Cell Biol, 2012.
442. Lai, J.S. and W. Herr, *Ethidium bromide provides a simple tool for identifying genuine DNA-independent protein associations.* Proc Natl Acad Sci U S A, 1992. **89**(15): p. 6958-62.
443. Wright, R.H., et al., *ADP-ribose-derived nuclear ATP synthesis by NUDIX5 is required for chromatin remodeling.* Science, 2016. **352**(6290): p. 1221-5.
444. Koberle, B., V. Roginskaya, and R.D. Wood, *XPA protein as a limiting factor for nucleotide excision repair and UV sensitivity in human cells.* DNA Repair (Amst), 2006. **5**(5): p. 641-8.
445. Fischer, J.M., et al., *Poly(ADP-ribose)-mediated interplay of XPA and PARP1 leads to reciprocal regulation of protein function.* FEBS J, 2014. **281**(16): p. 3625-41.
446. Hwang, B.J., et al., *Expression of the p48 xeroderma pigmentosum gene is p53-dependent and is involved in global genomic repair.* Proc Natl Acad Sci U S A, 1999. **96**(2): p. 424-8.
447. Jungmichel, S., et al., *Proteome-wide Identification of Poly(ADP-Ribosyl)ation Targets in Different Genotoxic Stress Responses.* Molecular Cell. **52**(2): p. 272-285.
448. Maltseva, E.A., et al., *Poly(ADP-ribose) Polymerase 1 Modulates Interaction of the Nucleotide Excision Repair Factor XPC-RAD23B with DNA via Poly(ADP-ribosyl)ation.* J Biol Chem, 2015. **290**(36): p. 21811-20.
449. Mortusewicz, O., et al., *Feedback-regulated poly(ADP-ribosyl)ation by PARP-1 is required for rapid response to DNA damage in living cells.* Nucleic Acids Research, 2007. **35**(22): p. 7665-7675.
450. Helleday, T., et al., *DNA repair pathways as targets for cancer therapy.* Nat Rev Cancer, 2008. **8**(3): p. 193-204.
451. Rouleau, M., et al., *PARP inhibition: PARP1 and beyond.* Nat Rev Cancer, 2010. **10**(4): p. 293-301.
452. Park, J.M. and T.H. Kang, *Transcriptional and Posttranslational Regulation of Nucleotide Excision Repair: The Guardian of the Genome against Ultraviolet Radiation.* Int J Mol Sci, 2016. **17**(11).
453. Overmeer, R.M., et al., *Replication protein A safeguards genome integrity by controlling NER incision events.* J Cell Biol, 2011. **192**(3): p. 401-15.
454. Patel, A.G., et al., *Enhanced killing of cancer cells by poly(ADP-ribose) polymerase inhibitors and topoisomerase I inhibitors reflects poisoning of both enzymes.* J Biol Chem, 2012. **287**(6): p. 4198-210.

455. Dantuma, N.P., et al., *Short-lived green fluorescent proteins for quantifying ubiquitin/proteasome-dependent proteolysis in living cells.* Nat Biotech, 2000. **18**(5): p. 538-543.
456. Ranes, M., et al., *A ubiquitylation site in Cockayne syndrome B required for repair of oxidative DNA damage, but not for transcription-coupled nucleotide excision repair.* Nucleic Acids Research, 2016. **44**(11): p. 5246-5255.
457. Cleaver, J.E., et al., *Differences in the regulation by poly(ADP-ribose) of repair of DNA damage from alkylating agents and ultraviolet light according to cell type.* J Biol Chem, 1983. **258**(15): p. 9059-68.
458. Durkacz, B.W., J. Irwin, and S. Shall, *Inhibition of (ADP-ribose)n biosynthesis retards DNA repair but does not inhibit DNA repair synthesis.* Biochem Biophys Res Commun, 1981. **101**(4): p. 1433-41.
459. Liu, Y., F.A. Kadyrov, and P. Modrich, *PARP-1 enhances the mismatch-dependence of 5'-directed excision in human mismatch repair in vitro.* DNA Repair (Amst), 2011. **10**(11): p. 1145-53.
460. Eki, T., *Poly (ADP-ribose) polymerase inhibits DNA replication by human replicative DNA polymerase alpha, delta and epsilon in vitro.* FEBS Lett, 1994. **356**(2-3): p. 261-6.
461. Caldecott, K.W., *Protein ADP-ribosylation and the cellular response to DNA strand breaks.* DNA Repair (Amst), 2014. **19**: p. 108-13.
462. Epstein, J.H. and J.E. Cleaver, *3-Aminobenzamide can act as a cocarcinogen for ultraviolet light-induced carcinogenesis in mouse skin.* Cancer Res, 1992. **52**(14): p. 4053-4.
463. Farkas, B., et al., *Reduction of acute photodamage in skin by topical application of a novel PARP inhibitor.* Biochem Pharmacol, 2002. **63**(5): p. 921-32.

Annexes

Annexe 1: Role of poly(ADP-ribose) polymerase-1 in the removal of UV-induced DNA lesions by nucleotide excision repair

Annexe 2: Characterization of the interactions of PARP-1 with UV-damaged DNA in vivo and in vitro

Annexe 3: Resistance to PARP-Inhibitors in Cancer Therapy

Annexe 4: PARP Inhibitors in Cancer Therapy: Magic Bullets but Moving Targets

Role of poly(ADP-ribose) polymerase-1 in the removal of UV-induced DNA lesions by nucleotide excision repair

Mihaela Robu, Rashmi G. Shah, Nancy Petitclerc, Julie Brind'Amour[1], Febitha Kandan-Kulangara, and Girish M. Shah[2]

Laboratory for Skin Cancer Research, Hospital Research Centre of Laval University (CHUL) and Centre Hospitalier Universitaire du Quebec (CHUQ), Laval University, Quebec, QC, Canada G1V 4G2

Edited* by James E. Cleaver, University of California, San Francisco, CA, and approved December 12, 2012 (received for review June 6, 2012)

Among the earliest responses of mammalian cells to DNA damage is catalytic activation of a nuclear enzyme poly(ADP-ribose) polymerase-1 (PARP-1). Activated PARP-1 forms the polymers of ADP-ribose (pADPr or PAR) that posttranslationally modify its target proteins, such as PARP-1 and DNA repair–related proteins. Although this metabolism is known to be implicated in other repair pathways, here we show its role in the versatile nucleotide excision repair pathway (NER) that removes a variety of DNA damages including those induced by UV. We show that PARP inhibition or specific depletion of PARP-1 decreases the efficiency of removal of UV-induced DNA damage from human skin fibroblasts or mouse epidermis. Using NER-proficient and -deficient cells and in vitro PARP-1 assays, we show that damaged DNA-binding protein 2 (DDB2), a key lesion recognition protein of the global genomic subpathway of NER (GG-NER), associates with PARP-1 in the vicinity of UV-damaged chromatin, stimulates its catalytic activity, and is modified by pADPr. PARP inhibition abolishes UV-induced interaction of DDB2 with PARP-1 or xeroderma pigmentosum group C (XPC) and also decreases localization of XPC to UV-damaged DNA, which is a key step that leads to downstream events in GG-NER. Thus, PARP-1 collaborates with DDB2 to increase the efficiency of the lesion recognition step of GG-NER.

Mammalian cells respond very rapidly to different types of DNA damage by activation of an abundant and ubiquitous nuclear enzyme poly(ADP-ribose) polymerase-1 (PARP-1). The activated PARP-1 uses NAD^+ to form polymers of ADP-ribose (pADPr or PAR) that modify PARP-1 itself and selected target proteins, such as histones and DNA repair proteins (1). This posttranslational modification, i.e., PARylation, has been implicated in cellular responses ranging from DNA repair to cell death. Among mammalian DNA repair pathways, PARP-1 has been implicated in base excision repair, homologous recombination, and nonhomologous end-joining pathways (2, 3), but we do not know its role in the most versatile nucleotide excision repair (NER) pathway that removes a wide variety of DNA lesions, including UV-induced thymine dimers (T-T) and other cyclobutane pyrimidine dimers (CPD), as well as 6–4 photoproducts (6-4PP) (4).

The core mammalian NER pathway uses more than 30 proteins to recognize the damaged site on DNA, remove 24- to 32-nucleotide-long single-stranded DNA containing the lesion, fill the gap using the nondamaged strand as a template, and finally ligate the nick (4). There are two subpathways of NER: the transcription-coupled NER (TC-NER) removes lesions from the actively transcribed strands of the genes and the global genomic NER (GG-NER) repairs lesions from the entire genome. These two pathways differ in the initial step of lesion recognition: TC-NER is initiated when elongating RNA polymerase II stalls at the lesion, whereas GG-NER is initiated when the lesion is recognized in the chromatin context by DDB2 (XPE), which through its participation in the UV-DDB-E3 ligase complex ubiquitinates and localizes the key GG-NER protein XPC to the damaged site (5–7).

Although the roles for different core NER proteins have been well characterized with bacterial and yeast model systems, we still cannot fully explain the accuracy and rapidity with which mammalian NER is targeted to a very few damaged bases that are surrounded by a large number of unmodified bases in chromatin. In this context, some of the posttranslational modifications, such as phosphorylation, acetylation, ubiquitination, and sumoylation, are known to help different steps of NER (8). Here, we examined whether PARylation that occurs rapidly after PARP-1 is activated by UV-induced DNA lesions (9) could be involved in improving the efficiency of mammalian NER. Earlier studies examined the effect of impaired PARP-1 function on mammalian NER but obtained contradictory results (10–12), because the repair of UV-induced CPD was unaffected by PARP inhibition in HeLa cells (10), whereas it was reduced in transdominantly PARP-1–inhibited CHO cells (11) or in the PARP-1–impaired triple negative breast cancer cell lines (12). In view of other confounding factors such as DNA repair defects in CHO or breast cancer cells, we used RNAi or PARP inhibition approaches in multiple mammalian NER-proficient models to show that PARP-1 is required for an efficient removal of UV-induced T-T and 6-4PP from genomic DNA. We also show that the catalytic activity of PARP-1 in collaboration with DDB2 leads to an improved function of DDB2 and XPC during the lesion recognition step of mammalian GG-NER.

Results

PARP Inhibitors Delay Removal of UV-Induced DNA Lesions. To explore the role of catalytic activation of PARP-1 in NER, we first examined the effect of PARP inhibitor PJ-34 on the efficiency of removal of UVC-induced T-T or 6-4PP from genomic DNA of two different human skin fibroblasts using a flow cytometry–based assay (13) (Fig. 1*A*). In this assay, the histograms for T-T or 6-4PP at early time points after irradiation (5–15 min) represent initial damage, and movement of histograms at later time points (6–63 h) toward untreated cells represents the extent of repair. In the SV-40–immortalized GMU6 human skin fibroblasts, a significant removal of T-T at 24 h was seen only in the normal but not in the PJ-34–treated cells (Fig. 1*A*, *Left*). The quantification of the average T-T signal confirmed that 43% of damage removed by 24 h from normal GMU6 cells was significantly more than 27% of the damage removed by PJ-34–treated cells ($n = 4–7$; $P < 0.05$). Next, we examined the effect of PJ-34 on the capacity of hTert-immortalized BJ-EH2 human foreskin fibroblasts (BJ-hTert) to remove UVC-induced T-T and 6-4PP lesions up to 63 and 6 h, respectively (Fig. 1*A*, *Center* and *Right*). Unlike normal BJ-hTert cells that removed all of the T-T signal by 63 h, PJ-34–treated

Author contributions: M.R., R.G.S., N.P., J.B., F.K.-K., and G.M.S. designed research; M.R., R.G.S., N.P., J.B., and F.K.-K. performed research; M.R., R.G.S., N.P., J.B., F.K.-K., and G.M.S. analyzed data; and M.R., R.G.S., N.P., J.B., F.K.-K., and G.M.S. wrote the paper.

The authors declare no conflict of interest.

*This Direct Submission article had a prearranged editor.

Freely available online through the PNAS open access option.

[1]Present address: Terry Fox Laboratory, Vancouver, BC, Canada V5Z 1L3.

[2]To whom correspondence should be addressed. E-mail: girish.shah@crchul.ulaval.ca.

This article contains supporting information online at www.pnas.org/lookup/suppl/doi:10.1073/pnas.1209507110/-/DCSupplemental.

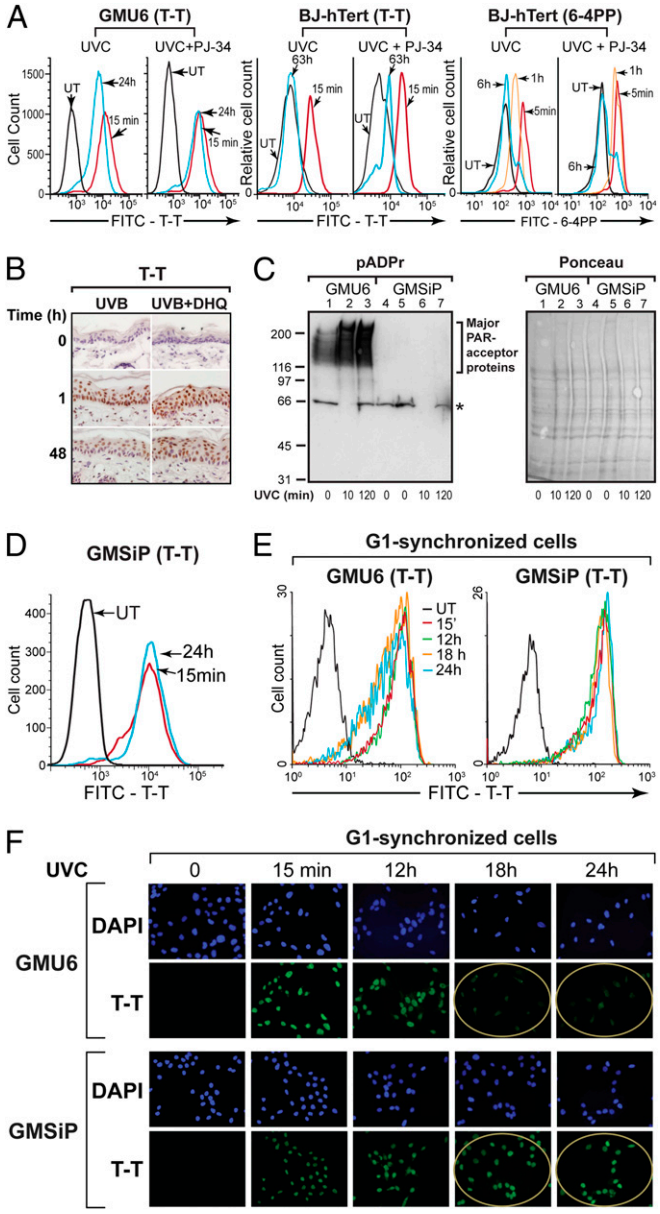

Fig. 1. Impaired PARP-1 function delays removal of T-T and 6-4PP from genomic DNA. (*A*) PARP inhibition decreases repair of T-T and 6-4PP. The GMU6 and BJ-hTert fibroblasts were treated with 10 μM PJ-34 (or control) before UVC irradiation at 10 (for T-T) or 30 (for 6-4PP) J/m^2. Repair was monitored before (untreated: UT) or after irradiation at specified times. Representative histograms from one of four to six experiments with similar results are shown. (*B*) PARP inhibition delays removal of UV-induced DNA lesions from mouse epidermis. Mice were exposed to 1,600 J/m^2 UVB, and the PARP inhibitor DHQ was applied every 3 h to inhibit PARP activation up to 12 h. Skin was processed for immunohistological analysis of T-T. Data shown here are from one of four experiments with identical results. (*C*) PARP-1–depleted GMSiP cells are deficient in formation of pADPr after UV exposure. The chromatin-bound protein fractions from GMSiP and PARP-1–replete GMU6 cells at specified time after irradiation with 30 J/m^2 UVC were immunoblotted for PARylated proteins, as shown here for one of three experiments with identical results. Asterisk indicates nonspecific reaction with BSA, and Ponceau staining was a loading control. (*D*–*F*) PARP-1 depletion decreases repair of UV-induced T-T in nonsynchronized or in G1 synchronized human skin fibroblasts. GMU6 and GMSiP cells were nonsynchronized (*D*) or synchronized in G1 phase with 0.5 μM mimosine (*E* and *F*) before irradiation with 10 (*D* and *E*) or 100 (*F*) J/m^2 UVC. Repair was monitored at specified times by flow cytometry (*D* and *E*) or fluorescence microscopy (*F*). Data are from one of three to four experiments with similar results.

cells removed significantly less (50%) damage, which was further confirmed by quantifying the average T-T signal from multiple assays ($n = 6$; $P < 0.05$). For removal of 6-4PP lesions, although the final repair by 6 h was not affected, the early phase of removal of damage at 1 h was significantly suppressed by PJ-34, and quantification of the signal confirmed that 45% of damage removed by normal BJ cells was significantly more than 20% of the damage removed by PJ-34–treated cells ($n = 3$; $P < 0.01$). Last, the removal of UVB-induced T-T from the epidermis of SKH-1 hairless mice was also reduced up to 48 h by the PARP inhibitor 1,5-dihydroxyisoquinoline (Fig. 1*B*). Thus, PARP inhibitors significantly decreased the efficiency of removal of UV-induced DNA photolesions in multiple models.

PARP-1 Depletion Decreases Efficiency of Removal of UV-Induced DNA Damage. PARP inhibitors affect activity of all of the members of the PARP family; hence, we examined whether the effect of PARP inhibition on repair of UV-damaged DNA was caused by its effect on PARP-1 or on other PARPs. We used GMSiP human skin fibroblasts, in which PARP-1 has been stably and significantly depleted by shRNA without affecting the expression of PARP-2 (14). We assessed their capacity to (*i*) form PAR in response to UVC and (*ii*) repair the UVC-induced T-T lesions. In the pADPr immunoblot, a strong signal for heterogeneous bands of PARylated proteins above 116 kDa (15) could be seen in the matched PARP-1–replete GMU6 cells but not in the GMSiP cells (Fig. 1*C*), confirming that PARP-1 is the major, if not the only, producer of pADPr in UV-treated cells. Using flow cytometry assay, we noted a marked failure of GMSiP cells to remove T-T from 15 min to 24 h (Fig. 1*D*), which is in stark contrast to the significant repair seen in GMU6 cell (Fig. 1*A*, *Left*). To exclude the possible differences in the cell cycle phases influencing the repair capacity of these cells (13), we synchronized GMU6 and GMSiP cells in the G1 phase and compared their time course of removal of T-T up to 24 h by flow cytometry (Fig. 1*E*) and immunofluorescence microscopy (Fig. 1*F*). By both techniques, we observed that PARP-1–depleted cells were inefficient at removal of T-T damage. The quantification of T-T signal from flow-cytometry assays confirmed that, although GMU6 cells removed 54% of the initial damage, GMSiP cells barely removed any damage (~2%; $n = 3$; $P < 0.01$). The immunofluorescence microscopy confirmed this trend because GMU6 cells removed 58% of the T-T signal per nuclei by 24 h compared with 15% damage removed by GMSiP cells ($n > 125$ nuclei; $P < 0.01$). Because PARP-1 depletion was sufficient to abolish UV-induced PAR synthesis and impair repair of UV-induced DNA damage, similar to that seen in PARP-inhibited cells, PARP-1 is likely to be the main PARP implicated in this repair process.

Characterization of UV-Induced Interaction Between PARP-1 and DDB2. We showed earlier that PARP-1 rapidly binds to UV-damaged DNA in vitro or in UV-irradiated cells, and it is activated to form PAR within seconds after irradiation at the site of DNA damage (9). Because DDB2, the early GG-NER protein, is also known to translocate very rapidly at the site of UV-damaged DNA (16), we examined whether DDB2 and PARP-1 interact with each other in the vicinity of UV-damaged chromatin using cellular fractions that represent chromatin-bound proteins (Ch-fraction) rather than the whole cell extract in coimmunoprecipitation (co-IP) studies (Fig. S1*A*). The cell fractionation technique to isolate the Ch-fraction was validated by confirming the expected UV-induced relocalization of DDB2 to this fraction in both NER-proficient GM637 and NER-deficient XP-C cells (Fig. 2*A*, lanes 4, 8, and 12), although total cellular DDB2 levels remained unchanged before and after irradiation (Fig. 2*A*, lanes 1, 5, and 9). We further confirmed that UV irradiation promoted the recruitment of downstream NER proteins XPC and xeroderma pigmentosum group A (XPA) to the Ch-fraction of GM637 cells, whereas XP-C cells did not relocalize XPA to the Ch-fraction (Fig. 2*A*). For the IP studies, we used GMRSiP cells that express FLAG-tagged human PARP-1 (Fig. S1*B*). The IP of equal amounts of Ch-extracts (input, Fig. S1*C*) of these cells prepared

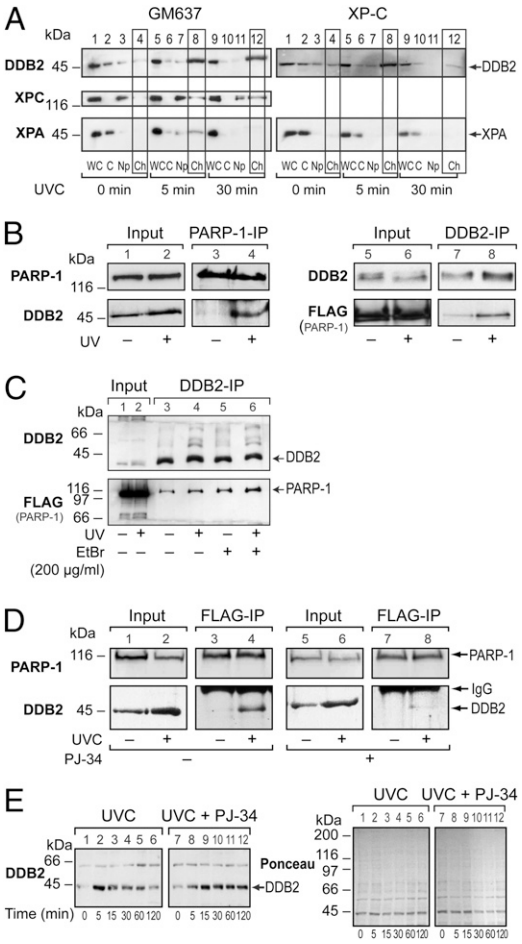

Fig. 2. Cooperation between PARP-1 and DDB2 at UVC-irradiated chromatin. (*A*) UVC-induced recruitment of NER proteins to chromatin-bound protein (Ch) fractions. Different cellular fractions (WC, whole cells; C, cytoplasm; Np, nucleoplasm; Ch, chromatin-bound) prepared from the NER-proficient GM637 and NER-deficient XP-C cells at 0 (unirradiated), 5, and 30 min after UVC irradiation were immunoblotted for DDB2, XPC, and XPA. (*B*) UV-induced association of PARP-1 and DDB2. The co-IPs were carried out with Ch-fractions (input) derived from control or UVC (30 J/m^2) irradiated FLAG-PARP-1 expressing GMRSiP cells with antibodies to PARP-1 or DDB2. Input and IP eluates were immunoblotted for the presence of PARP-1/FLAG and DDB2. Results are from one of six experiments with identical results. (*C*) Interaction of PARP-1 and DDB2 is not mediated via DNA. The Ch-fractions (input) of GMRSiP cells prepared before or 10 min after exposure to 30 J/m^2 UVC were incubated with or without ethidium bromide before and during IP for DDB2, followed by immunoblotting for DDB2 and FLAG (PARP-1). Results are representative of two experiments with identical results. (*D*) PARP inhibitor disrupts co-IP of PARP-1 and DDB2. GMRSiP were treated with 10 μM PJ-34 (or control) before UVC irradiation at 30 J/m^2. The Ch-fractions (input) prepared at 10 min after irradiation were subjected to IP for FLAG followed by detection of PARP-1 and DDB2. Data are from one of three experiments with identical results. (*E*) PARP inhibition delays the departure of DDB2. The Ch-fractions isolated from GMU6 cells at specified times after UVC irradiation with 10 J/m^2 (or control) in the presence or absence of 10 μM PJ-34 were immunoblotted for DDB2. Ponceau staining was used as a loading control.

before or 10 min after UVC irradiation with the PARP-1 antibody revealed a significant UV-induced association of DDB2 with PARP-1, which was confirmed in an inverse co-IP with DDB2 antibody (Fig. 2*B*, lanes 4 and 8). Mock IPs with control IgGs confirmed specificity of antibody-based IPs (Fig. S1*D*). To determine whether the interaction between these two proteins is direct or mediated via DNA, DDB2-IP was carried out in the presence of 200 μg/mL ethidium bromide to loosen the protein–DNA interactions. The failure of ethidium bromide to prevent co-IP of PARP-1 with DDB2 indicated a direct interaction between these two proteins (Fig. 2*C*; mock control: Fig. S1*E*).

To determine the possible role of catalytic activation of PARP-1 in this interaction, the GMRSiP cells were irradiated in the presence or absence of the PARP inhibitor PJ-34. The FLAG-IP of Ch-fractions before or after irradiation confirmed UV-induced interaction of DDB2 and PARP-1 without the PARP inhibitor (Fig. 2*D*, DDB2, lane 4). Interestingly, although PJ-34 treatment did not prevent UV-induced accumulation of DDB2 in the input Ch-fraction before IP, it significantly suppressed its ability to associate with PARP-1 (Fig. 2*D*, DDB2, lanes 6 and 8). In an independent model of GMU6 cells expressing mycDDB2 (Fig. S2 *A*–*C*), we confirmed by local UVC irradiation (Fig. S2*D*) and co-IP of Ch-fractions with PARP-1 or myc antibodies (Fig. S2*E*) that the PARP inhibitor PJ-34 did not affect early accumulation of mycDDB2 but blocked its co-IP with PARP-1. We examined whether the PARP inhibitor that disrupts the interaction between DDB2 and PARP-1 also affects the departure of DDB2 from the damaged site, which is a necessary step for the continuation of GG-NER (17). Immunoblotting for DDB2 in the Ch-fractions isolated up to 2 h after irradiation revealed that DDB2 levels that accumulated from 5 to 15 min declined rapidly by 60 min in the normal cells but remained high until 120 min in PARP-inhibited cells (Fig. 2*E*). Thus, although the initial recruitment of DDB2 to UV-induced chromatin is independent of PARP-1, its subsequent direct association with PARP-1, as well as its eventual departure from the damaged site, is dependent on the catalytic activity of PARP-1 that would PARylate proteins near the damaged DNA.

DDB2 Stimulates Catalytic Activity of PARP-1 and Becomes a Target for PARylation. The influence of catalytic activity of PARP-1 on DDB2 prompted us to examine whether DDB2 is PARylated in response to UV (Fig. 3 *A* and *B*). First, the pADPr-IP of GMU6-mycDDB2 cells pulled down more mycDDB2 after UVC exposure, indicating that it is either PARylated or interacts with other PARylated proteins (Fig. 3*A*). That DDB2 could be directly PARylated was tested in an in vitro Dot-blot assay, which showed that pADPr could bind to mycDDB2 (Fig. 3*B*, *Upper*). The binding of pADPr to its known acceptors PARP-1 and XPA (18) served as positive controls. To confirm that the recipient of pADPr was indeed the designated protein in the immunopurified mycDDB2 preparation, we ran a SouthWestern type of blot in which immunopurified mycDDB2 and purified GST-DDB2 were resolved on SDS/PAGE, blotted, and reacted with pADPr (Fig. 3*B*, *Lower*). The mycDDB2 and purified GST-DDB2 displayed one major pADPr-accepting band at 50 or 75 kDa, which corresponds to their respective bands in the DDB2 immunoblots. A strong signal for PARylated PARP-1 at 113 kDa was a positive control, and lack of pADPr binding by proteinase K (Fig. 3*B*) or DNase I and myc antibody (Fig. S3*A*) served as negative controls. Thus, DDB2 is an acceptor of pADPr.

We next examined whether interaction of DDB2 with PARP-1 has any influence on the activity of PARP-1. In an in vitro PARP-1 activation assay (15), we first observed using bovine PARP-1 and nonlabeled NAD (Fig. S3*B*) or immunopurified human FLAG-PARP-1 and biotinylated NAD (Fig. S3*C*), that the catalytic activation of PARP-1 by UV-damaged DNA was stimulated in the presence of mycDDB2, as seen from a heterogeneous smear above 113 kDa for PARylated PARP-1. Moreover, the effect of DDB2 on stimulating PARP-1 activation and formation of pADPr-modified PARP-1 was more pronounced with UV-damaged DNA than with the unirradiated DNA (Fig. 3*C*, lanes 2 and 3). Interestingly, the PARylation of mycDDB2 (50 kDa) was evident from the smearing of signal between 50 and 75 kDa in both pADPr and myc-blots in this reaction (lane 3). Controls show that PJ-34 suppressed PARP-1 activation (lanes 4–6), and mycDDB2 could not activate PARP-1 without DNA (lane 1). A dose–response for purified GST-DDB2 in the assay showed that ~1/12th of the amount of GST-DDB2 gave an optimum activation of PARP-1, i.e., 67 pmol GST-DDB2 for 860 pmol PARP-1 per assay (Fig. 3*D*; Fig. S3*D*).

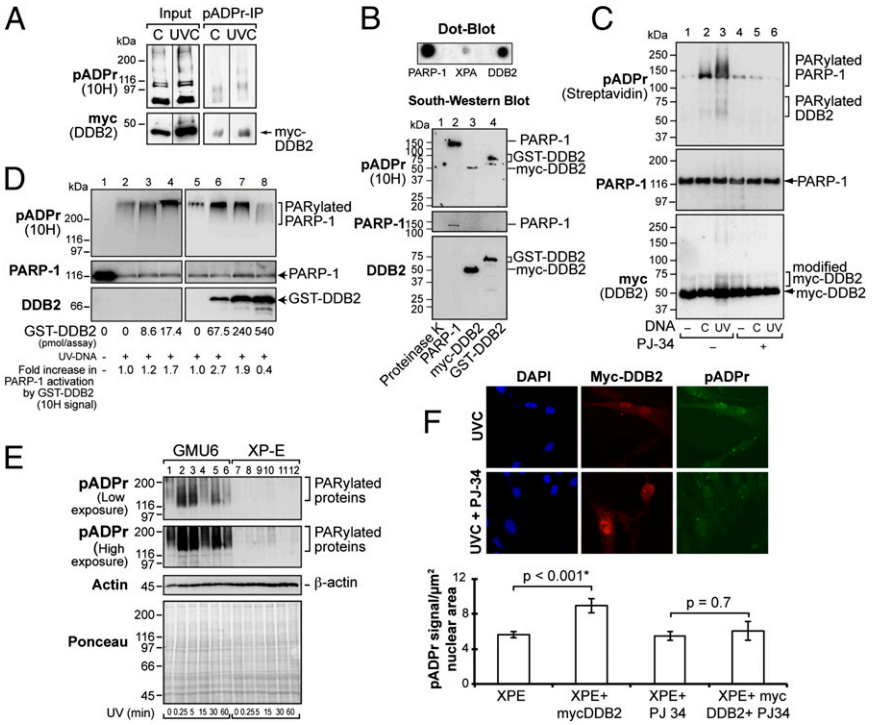

Fig. 3. DDB2 stimulates PARP-1 activation and is a target for PARylation. (*A*) The pADPr IP was carried out with Ch-fractions isolated from GMU6-mycDDB2 cells before or 10 min after exposure to 10 J/m^2 UVC and immunoblotted for PARylated proteins and myc. (*B*) DDB2 binds to pADPr. (*Upper*) Dot-blot: Purified bovine PARP-1 and immunopurified XPA and DDB2 were spotted and reacted with pADPr before immunoprobing for pADPr. (*Lower*) South-Western blot: Immunopurified mycDDB2, purified GST-DDB2, purified bovine PARP-1, and proteinase K were resolved on SDS/PAGE, blotted, and reacted with pADPr followed by immunoprobing for pADPr, PARP-1, and DDB2. The results are representative of two experiments with similar results. (*C* and *D*) DDB2 stimulates catalytic activity of PARP-1 in response to UVC-damaged DNA. In vitro PARP-1 activation assays were performed with purified bovine PARP-1, immunopurified mycDDB2 (*C*), or different amounts of purified GST-DDB2 (*D*), control, or UV-irradiated covalently closed circular DNA, untagged or biotinylated NAD, and PJ-34, as specified. Aliquots were immunoblotted for PARP-1 (PARP-1), pADPr (10H or streptavidin), and DDB2 (myc or DDB2). Purified GST-DDB2 is undetectable by antibody at lower concentrations and shows minor degradation bands at higher levels. The results are representative of three experiments with similar results. (*E*) XP-E cells are inefficient at forming pADPr after UV exposure. GMU6 and XP-E cells were irradiated with 10 J/m^2 UVC, and whole cell extracts prepared at various times were immunoblotted for pADPr. Actin probing and Ponceau staining served as loading controls. (*F*) DDB2 stimulates catalytic activation of PARP-1 in vivo. XP-E cells were transiently transfected with myc-DDB2 expression vector for 24 h and treated with 10 μM PJ-34 (or control) before irradiation with 10 J/m^2 UVC. Samples were processed at 5 min for immunofluorescent visualization of mycDDB2 (red), pADPr (green), and DNA (DAPI-blue). The chart provides an average pADPr signal per unit nuclear area (mean ± SE) of XP-E cells that expressed the transfected mycDDB2 or not. The image and chart are derived from the data of multiple nuclei from different fields of two independent experiments.

Next, we examined whether the interaction with DDB2 stimulates activity of PARP-1 in UV-irradiated cells. In the pADPr immunoblot, the signal for PARylated proteins in the first 60 min after UVC irradiation was extremely weak in DDB2-deficient XP-E cells compared with DDB2-replete GMU6 cells (Fig. 3*E*), although PARP-1 levels were comparable in both the cell types (Fig. S3*E*). This deficiency could be rescued in XP-E cells by transient transfection of the mycDDB2 expression vector, because despite being irradiated with UVC at the same time, the XP-E cells that did not express transfected mycDDB2 (nonred nuclei) showed a basal level of pADPr synthesis (green signal), which was significantly stimulated in the cells that expressed mycDDB2 (red nuclei) (Fig. 3*F*). The PJ-34 treatment abolished this additional pADPr synthesis. Collectively, these results indicate that DDB2 stimulates the catalytic activity of PARP-1 by UVC-damaged DNA and, in turn, PARP-1 PARylates DDB2.

XPC and the Interaction of PARP-1 with DDB2. To determine whether XPC that is known to co-IP with DDB2 (5) plays a role in the PARP-1 and DDB2 interaction, we used XP-C cells because they could recruit DDB2 to the damaged DNA but not XPA and other downstream GG-NER proteins due to nonfunctional XPC (Fig. 2*A*). Because PARP-1 activation and pADPr synthesis played a key role in the DDB2–PARP-1 interaction, we first examined whether XP-C cells could make pADPr in response to UVC. The time course of the pADPr immunoblot revealed that the appearance and extent of PARylated proteins in UV-irradiated XP-C and NER-proficient GM637 cells was comparable (Fig. 4*A*). Using co-IP studies in XP-C cells for PARP-1 (Fig. 4*B*) or pADPr (Fig. 4*C*), we observed that UVC irradiation promoted an interaction between PARP-1 and DDB2 (Fig. 4*B*) and caused direct or indirect PARylation of DDB2 (Fig. 4*C*). Because these interactions were not as robust as in normal cells (Figs. 2 *B* and *C* and 3*A*), our results indicate that there may be an XPC-dependent and -independent interaction between PARP-1 and DDB2.

Because the PARP inhibitor disrupts the interaction between DDB2 and PARP-1 and blocks the departure of DDB2 from the UV-damaged DNA, we determined whether it would also affect the downstream actions of DDB2, such as its interaction with XPC or modification and stabilization of XPC to UV-damaged DNA (5, 6). Using DDB2-IP of GMU6 cells, we observed that PJ-34 significantly suppressed UV-induced association of DDB2 with XPC (Fig. 4*D*, lanes 6 and 8). Moreover, a slowly migrating heterogeneously modified XPC, often characterized as ubiquitinated XPC (5), was significantly increased in response to UV and suppressed in the PJ-34–treated cells (Fig. 4*D*, lanes 6 and 8). A possible consequence of this effect of PARP inhibition was evident on the recruitment and stabilization of XPC at the site of DNA damage after local UVC irradiation. In the normal GMU6 cells, the signal for XPC colocalized with subnuclear T-T by 10 min and sharply intensified by 30 min. In the PJ-34–treated cells, XPC was weakly localized with T-T at 10 min and failed to focus properly by 30 min (Fig. 4*E*). The quantification of XPC and T-T in the subnuclear spots revealed that PARP inhibition significantly reduced the colocalization of XPC with T-T (Fig. 4*E*). This influence of the catalytic function of PARP on the movement of XPC to the UV-damaged chromatin DNA was further confirmed by the effect of the PARP inhibitor on the presence of XPC in Ch-fractions of UV-irradiated GMU6 cells (Fig. 4*F*). In the normal cells, the XPC levels gradually declined from the peak values at 5–15 min up to 4 h, whereas in PARP-inhibited cells, XPC levels declined rapidly by 30–60 min. In addition, the band for modified XPC was significantly increased from 5 to 15 min in the normal cells but not in the PJ-34–treated cells (Fig. 4*F*). Thus, PARP inhibition disrupted the interaction of XPC with DDB2 and decreased its stabilization at the lesion site.

Discussion

We showed that, in response to UV irradiation, PARP-inhibited cells have (*i*) an impaired capacity to remove UV-induced DNA

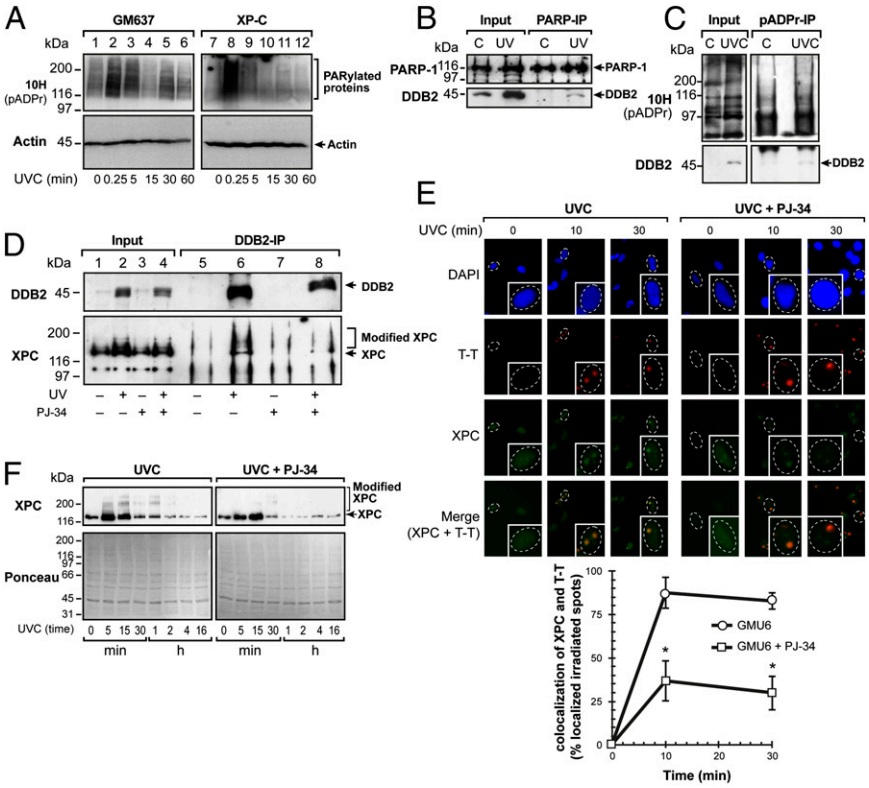

Fig. 4. Effect of PARP inhibition on XPC-related events in response to UV. (*A*) UV-induced pADPr synthesis in XP-C cells. GM637 and XP-C cells were irradiated with 10 J/m^2 UVC, and whole cell extracts prepared at various time points were immunoblotted for pADPr. Actin was used as a loading control. (*B* and *C*) UV-induced interaction of PARP-1 with DDB2 and pADPr modification of DDB2 in XP-C cells. The Ch-fractions (input) derived from control or UVC (30 J/m^2) irradiated XP-C cells were subjected to IP for PARP-1 or pADPr and immunoblotted for PARP-1, pADPr (10H), and DDB2. Results shown here are from one of three experiments with identical results. (*D*) PARP inhibitor disrupts UV-induced co-IP of DDB2 with XPC. GMU6 cells were treated with 10 μM PJ-34 (or control), and Ch-fractions prepared before or 10 min after UVC irradiation at 30 J/m^2 were subjected to IP for DDB2 followed by detection of XPC. Results are representative of two to three experiments with similar results. (*E*) Aberrant XPC localization in PARP-inhibited cells. GMU6 cells were locally irradiated with 100 J/m^2 UVC with or without PJ-34. Immunofluorescence microscopy allowed detection of XPC (green) and T-T (red) in DAPI-stained nuclei. The chart represents the percent of T-T spots, which are also positive for XPC, as pooled from three experiments, each in triplicate (n = 100–150 spots, data points are mean ± SE). (*F*) PARP inhibition decreases UVC-induced modification and stabilization of XPC. GMU6 cells treated with 10 μM PJ-34 (or control) were irradiated with 10 J/m^2 UVC, and Ch-fractions prepared at different time points were immunoblotted to detect unmodified and modified forms of XPC. Ponceau staining served as a loading control. Results shown here are from one of four experiments with identical results.

photolesions; (*ii*) a decreased level of interaction of DDB2 with XPC or PARP-1; (*iii*) an increased tendency for DDB2 to persist at the UV-damaged chromatin; and (*iv*) a decreased level of recruitment, modification, and localization of XPC to the damaged site. In addition, we show that (*v*) DDB2 and PARP-1 directly interact in the vicinity of the DNA lesion; (*vi*) DDB2 stimulates catalytic activity of PARP-1; and (*vii*) DDB2 is modified by PAR. Our results strongly indicate that PARP-1 is the principle player in the above responses, because cells specifically depleted of PARP-1 do not form detectable amounts of PARylated proteins in response to UV and are also inefficient at repair of UV-damaged genomic DNA. Our results are consistent with earlier reports that impaired PARP-1 function increases UV-induced skin cancer in mice (19), decreases cellular capacity to repair UV-induced DNA damage from viral reporter gene (20) or genomic DNA of CHO or triple negative breast cancer cells (11, 12), and decreases the clonogenicity in response to UV (20).

Our results together with previous reports suggest several possible ways in which PARP-1 can collaborate with DDB2 to increase the efficiency of GG-NER. (*i*) The PARylated PARP-1 or free PAR chains could serve as a scaffold on which PARylated DDB2 can interact with XPC, such as that suggested for their role with X-ray repair cross-complementing protein 1 (XRCC-1) in the base excision repair (21). Hence, PARP inhibitor or absence of PARP-1 could reduce participation of XPC in NER. (*ii*) The catalytic activation of PARP-1 and resultant PARylation of DDB2 could promote chromatin remodeling by DDB2. In fact, PARP inhibitor or PARP-1 depletion was recently shown to block chromatin remodeling of UV-damaged chromatin (7). In addition, the departure of DDB2 from the UV-induced lesion site was shown to be dependent on chromatin remodeling (22); hence, our result showing a delayed departure of DDB2 from the UV-damaged chromatin in PARP-inhibited cells supports an argument that catalytic function of PARP-1 plays a role in DDB2-mediated chromatin remodeling. This role of PARP-1 in chromatin remodelling would be in agreement with the reported role of PARylated proteins, such as amplified in liver cancer 1 (ALC-1) and aprataxin and PNKP like factor 1 (APLF-1) in stimulating their chromatin remodeling activity in DNA repair (23). (*iii*) The catalytic activity of PARP-1 and PAR formed locally around the lesion could be

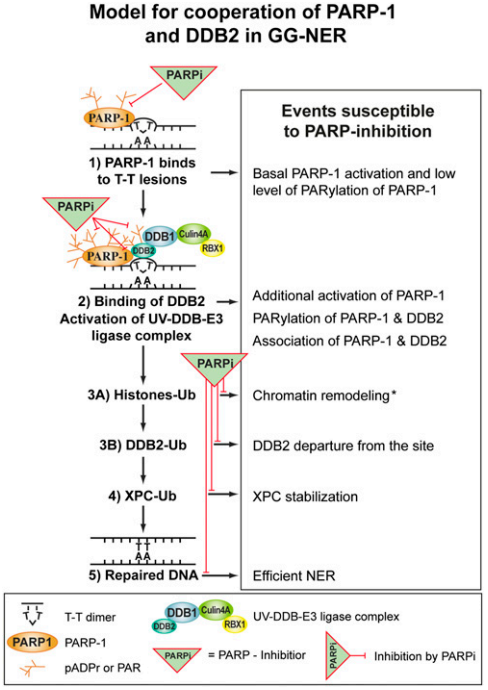

Fig. 5. Model for cooperation of PARP-1 and DDB2 in GG-NER. See *Discussion* for details. Based on the present data and previous study (*ref. 7), different NER-related end results that are susceptible to PARP inhibition are indicated in the box.

involved in the ubiquitination activity of the UV-DDB-E3 ligase complex, just as PARylation of targets has been shown to facilitate their modification by ubiquitin E3 ligase RNF146/Iduna (21). The ubiquitination of different proteins by UV-DDB-E3 ligase produces varying end results, e.g., ubiquitination of its own members DDB2, cullin 4A, and Rbx1 leads to a disengagement of the ligase complex from the damaged site; that of the histones H2A, H3, and H4 leads to chromatin remodeling (22, 24); and that of XPC helps in its recruitment and stabilization at the damaged site (24). Although a previous study has shown a chromatin destabilization effect of PARP inhibition (7), here we show its effect on reduced mobility of DDB2 and decreased modification and stabilization of XPC, all of which could be explained by inefficient ubiquitination activity of the UV-DDB-E3 ligase complex. (*iv*) Finally, a strong effect of PARP inhibition in suppression of the initial phase of repair of 6-4PP in BJ-hTert cells could be due to a specific influence of PARP-1 activation on NER at a given site of chromatin, because ubiquitination of XPC was recently shown to promote its relocalization from the intra- to the internucleosomal region to prioritize the repair at the latter site (6).

Based on our results and previous work, we propose a model for the role of PARP-1 and DDB2 at the lesion recognition step of GG-NER (Fig. 5). Immediately after UV irradiation, PARP-1, due to its sheer abundance and known capacity to be rapidly activated in response to different types of DNA damage (8), is likely to be one of the first proteins to arrive at the lesion and be basally activated within seconds of DNA damage (step 1). The arrival of DDB2, which occurs in a similar time frame as PARP-1, will cause a stronger activation of PARP-1, which will result in PARylation of many proteins including PARP-1 and DDB2. This PARylation will foster a direct association of DDB2 and PARP-1 that resists separation by ethidium bromide during IP (step 2). Because both proteins are known to independently bind to DNA containing CPD lesions, it is likely that these proteins would interact with the damaged DNA and with each other (step 2). One possible scenario to explain the downstream events is that the PARylated DDB2 as part of the UV-DDB-E3 complex will remodel the chromatin (step 3A), ubiquitinate DDB2 to reduce its affinity for the lesion (step 3B), and ubiquitinate XPC to promote its stabilization at the damaged site (step 4), which will result in an efficient GG-NER (step 5). As indicated in the model, many of the steps in this model have been shown by us and others (7), implying the role for PARP-1 in collaboration with DDB2 at the lesion recognition step to improve the efficiency of mammalian GG-NER. It will be interesting to examine whether PARP-1 also plays other roles in NER.

Materials and Methods

Full details are provided in *SI Materials and Methods*.

Cells, Clones, Transient Transfections, and Mice. SV-40–immortalized GM637 and XP-C (GM15983) human skin fibroblasts and untransformed XP-E (GM01389) cells were obtained from Coriell. The hTert-immortalized human skin fibroblasts were a gift from W. Hahn, Dana Farber Cancer Institute, Boston. PARP-1–replete GMU6 and PARP-1–depleted GMSiP cells have been reported (14). Details for FLAG-hPARP-1–expressing GMRSiP or mycDDB2 and FLAG-XPA–expressing GMU6-derived clones are in *SI Materials and Methods*. XP-E cells were transfected with pcDNA3-mycDDB2 plasmid for 24 h before irradiation. Four-week-old female SKH-1 hairless mice were from Charles River.

UV Irradiation, Analyses of DNA Repair, and Recruitment of NER Factors. Global and local UVC irradiation of cells has been reported (9). The repair kinetics assays for T-T and 6-4PP in cellular genomic DNA by flow cytometry and immunofluorescence microscopy and detection of NER proteins after local irradiation are detailed in *SI Materials and Methods*. SKH-1 hairless mice were irradiated with 1,600 J/m^2 of UVB, and immunohistological analysis was performed on paraffin sections of skin.

Immunopurification, Cell Fractionation, and co-IP. FLAG-hPARP-1, mycDDB2, and FLAG-XPA were expressed in cells and immunopurified from whole cell extracts using suitable antibodies and beads. Purified human GST-DDB2 was purchased from Abnova. Cell fractionation protocol to extract chromatin-bound proteins (Ch-fraction) is detailed in *SI Materials and Methods*. IP was carried out with 100–300 μg protein of Ch-fractions.

In Vitro PARP-1 Activation Reactions, pADPr Dot-Blot, and SouthWestern Blot. The pADPr immunodot-blot (18) and in vitro PARP-1 activation reaction (15) were performed as described. The SouthWestern blot method was derived from the Activity-Western blot of PARP-1 (15).

ACKNOWLEDGMENTS. We thank W. Hahn and P. Lee for BJ-hTert cells and E. Drobetksy, H. Naegeli, and M. Ghodgaonkar for helpful suggestions. Scholarship support was received from Natural Sciences and Engineering Research Council of Canada (M.R., N.P., and F.K.K.), Laval University (M.R.), and Fonds de la recherche en santé du Québec (N.P.). This work was supported by National Cancer Institute of Canada with the finds from the Canadian Cancer Society Grant 16407 (to G.M.S.).

1. Krishnakumar R, Kraus WL (2010) The PARP side of the nucleus: Molecular actions, physiological outcomes, and clinical targets. *Mol Cell* 39(1):8–24.
2. De Vos M, Schreiber V, Dantzer F (2012) The diverse roles and clinical relevance of PARPs in DNA damage repair: Current state of the art. *Biochem Pharmacol* 84(2):137–146.
3. Yélamos J, Farrés J, Llacuna L, Ampurdanés C, Martin-Caballero J (2011) PARP-1 and PARP-2: New players in tumour development. *Am J Cancer Res* 1(3):328–346.
4. Cleaver JE, Lam ET, Revet I (2009) Disorders of nucleotide excision repair: The genetic and molecular basis of heterogeneity. *Nat Rev Genet* 10(11):756–768.
5. Sugasawa K, et al. (2005) UV-induced ubiquitylation of XPC protein mediated by UV-DDB-ubiquitin ligase complex. *Cell* 121(3):387–400.
6. Fei J, et al. (2011) Regulation of nucleotide excision repair by UV-DDB: Prioritization of damage recognition to internucleosomal DNA. *PLoS Biol* 9(10):e1001183.
7. Luijsterburg MS, et al. (2012) DDB2 promotes chromatin decondensation at UV-induced DNA damage. *J Cell Biol* 197(2):267–281.
8. Ciccia A, Elledge SJ (2010) The DNA damage response: Making it safe to play with knives. *Mol Cell* 40(2):179–204.
9. Vodenicharov MD, Ghodgaonkar MM, Halappanavar SS, Shah RG, Shah GM (2005) Mechanism of early biphasic activation of poly(ADP-ribose) polymerase-1 in response to ultraviolet B radiation. *J Cell Sci* 118(Pt 3):589–599.
10. Stevnsner T, Ding R, Smulson M, Bohr VA (1994) Inhibition of gene-specific repair of alkylation damage in cells depleted of poly(ADP-ribose) polymerase. *Nucleic Acids Res* 22(22):4620–4624.
11. Flohr C, Bürkle A, Radicella JP, Epe B (2003) Poly(ADP-ribosyl)ation accelerates DNA repair in a pathway dependent on Cockayne syndrome B protein. *Nucleic Acids Res* 31(18):5332–5337.
12. Hastak K, Alli E, Ford JM (2010) Synergistic chemosensitivity of triple-negative breast cancer cell lines to poly(ADP-Ribose) polymerase inhibition, gemcitabine, and cisplatin. *Cancer Res* 70(20):7970–7980.
13. Auclair Y, Rouget R, Affar B, Drobetsky EA (2008) ATR kinase is required for global genomic nucleotide excision repair exclusively during S phase in human cells. *Proc Natl Acad Sci USA* 105(46):17896–17901.
14. Shah RG, Ghodgaonkar MM, Affar B, Shah GM (2005) DNA vector-based RNAi approach for stable depletion of poly(ADP-ribose) polymerase-1. *Biochem Biophys Res Commun* 331(1):167–174.
15. Shah GM, et al. (2011) Approaches to detect PARP-1 activation in vivo, in situ, and in vitro. *Methods Mol Biol* 780:3–34.
16. Fitch ME, Cross IV, Ford JM (2003) p53 responsive nucleotide excision repair gene products p48 and XPC, but not p53, localize to sites of UV-irradiation-induced DNA damage, in vivo. *Carcinogenesis* 24(5):843–850.
17. Luijsterburg MS, et al. (2007) Dynamic in vivo interaction of DDB2 E3 ubiquitin ligase with UV-damaged DNA is independent of damage-recognition protein XPC. *J Cell Sci* 120(Pt 15):2706–2716.
18. Pleschke JM, Kleczkowska HE, Strohm M, Althaus FR (2000) Poly(ADP-ribose) binds to specific domains in DNA damage checkpoint proteins. *J Biol Chem* 275(52): 40974–40980.
19. Epstein JH, Cleaver JE (1992) 3-Aminobenzamide can act as a cocarcinogen for ultraviolet light-induced carcinogenesis in mouse skin. *Cancer Res* 52(14):4053–4054.
20. Ghodgaonkar MM, Zacal NJ, Kassam SN, Rainbow AJ, Shah GM (2008) Depletion of poly(ADP-ribose)polymerase-1 reduces host cell reactivation for UV-treated adenovirus in human dermal fibroblasts. *DNA Repair (Amst)* 7:617–632.
21. Gibson BA, Kraus WL (2012) New insights into the molecular and cellular functions of poly(ADP-ribose) and PARPs. *Nat Rev Mol Cell Biol* 13(7):411–424.
22. Lan L, et al. (2012) Monoubiquitinated histone H2A destabilizes photolesion-containing nucleosomes with concomitant release of UV-damaged DNA-binding protein E3 ligase. *J Biol Chem* 287(15):12036–12049.
23. Lukas J, Lukas C, Bartek J (2011) More than just a focus: The chromatin response to DNA damage and its role in genome integrity maintenance. *Nat Cell Biol* 13(10): 1161–1169.
24. Sugasawa K (2010) Regulation of damage recognition in mammalian global genomic nucleotide excision repair. *Mutat Res* 685(1-2):29–37.

SCIENTIFIC REPORTS

OPEN

Characterization of the interactions of PARP-1 with UV-damaged DNA *in vivo* and *in vitro*

Received: 05 August 2015
Accepted: 02 December 2015
Published: 12 January 2016

Nupur K. Purohit[1,*], Mihaela Robu[1,*], Rashmi G. Shah[1,*], Nicholas E. Geacintov[2] & Girish M. Shah[1]

The existing methodologies for studying robust responses of poly (ADP-ribose) polymerase-1 (PARP-1) to DNA damage with strand breaks are often not suitable for examining its subtle responses to altered DNA without strand breaks, such as UV-damaged DNA. Here we describe two novel assays with which we characterized the interaction of PARP-1 with UV-damaged DNA *in vivo* and *in vitro*. Using an *in situ* fractionation technique to selectively remove free PARP-1 while retaining the DNA-bound PARP-1, we demonstrate a direct recruitment of the endogenous or exogenous PARP-1 to the UV-lesion site *in vivo* after local irradiation. In addition, using the model oligonucleotides with single UV lesion surrounded by multiple restriction enzyme sites, we demonstrate *in vitro* that DDB2 and PARP-1 can simultaneously bind to UV-damaged DNA and that PARP-1 casts a bilateral asymmetric footprint from −12 to +9 nucleotides on either side of the UV-lesion. These techniques will permit characterization of different roles of PARP-1 in the repair of UV-damaged DNA and also allow the study of normal housekeeping roles of PARP-1 with undamaged DNA.

The abundance of poly (ADP-ribose) polymerase-1 (PARP-1) in mammalian cells and its rapid catalytic activation to form polymers of ADP-ribose (PAR) in the presence of various types of DNA damages with or without strand breaks has made it an ideal first responder at the lesion site to influence downstream events[1,2]. Apart from DNA damages, PARP-1 is also recruited to DNA during normal physiological processes such as transcription and chromatin remodeling[3], which do not involve overt DNA damage but just altered DNA structures. While we know much more about how PARP-1 rapidly recognizes and binds to single or double strand breaks in DNA, we know very little about how PARP-1 interacts with DNA damages or altered DNA structures without strand breaks. The key reason is that the existing methodologies that readily identify interactions of PARP-1 with DNA strand breaks are not sufficiently sensitive to study the relatively weaker responses of PARP-1 to DNA damage without strand breaks. The response of PARP-1 to UVC-induced direct photolesions, such as cyclobutane pyrimidine dimers (CPD) that are formed without any DNA strand breaks exemplifies this problem.

Recent studies from others and our team have shown the involvement of PARP-1 in the host cell reactivation[4] and specifically in the nucleotide excision repair (NER) of UV-damaged DNA through its interaction with early NER protein DDB2[5–7]. Additional studies have shown that downstream NER proteins XPA[8,9] and XPC[10] are PARylated. Thus, PARP-1 possibly has multiple roles in NER, but we do not yet fully understand its interactions with UV-damaged DNA or other NER proteins due to two major challenges. The first challenge is that unlike for many NER proteins, the abundance of endogenous PARP-1 in the nucleus makes it nearly impossible to visualize its dynamics of recruitment to UV-damaged DNA *in situ* using conventional immunocytological methods. To circumvent this challenge, the detection of its activation product PAR has been used as a proxy for PARP-1 recruitment at UV-lesion[5,11]. However, PAR may underestimate the role of PARP-1 in response to UV-damage due to weak activation of PARP-1 by UV[4,12], short half-life of PAR[2], and technical limitations in combining the detection of PAR with other proteins[13,14]. PAR detection will also not reveal participation of PARP-1 in protein-protein interactions without formation of PAR. Thus, there is a need for methods that permit direct visualization of recruitment of PARP-1 to UV-induced DNA lesions.

[1]Laboratory for Skin Cancer Research, CHU-Q (CHUL) Quebec University Hospital Research Centre & Laval University, 2705, Laurier Boulevard, Québec (QC) Canada G1V 4G2. [2]New York University, Department of Chemistry, New York, NY, USA. *These authors contributed equally to this work. Correspondence and requests for materials should be addressed to G.M.S. (email: girish.shah@crchul.ulaval.ca)

The second major challenge is that we do not know the exact footprint of PARP-1 at the UV-lesion site that could explain its interaction with different NER proteins. We have earlier shown that PARP-1 binds to UV-damaged large oligonucleotide *in vitro* or to chromatin fragments containing T-T lesions *in vivo*[11]. We also showed that PARP-1 and DDB2 associate with each other on the chromatin of UV-irradiated cells and that DDB2 stimulates catalytic activity of PARP-1 in the presence of UV-damaged DNA[7]. However, these assays lack the nucleotide level resolution to reveal whether PARP-1 was bound directly to the UV-damaged bases or to any other base in those long pieces of DNA and whether PARP-1 and DDB2 have sufficient space to co-exist around UV-induced DNA lesion. To address these challenges, here, we describe two novel assays. The first assay is an *in situ* fractionation technique that allows a direct visualization of PARP-1 recruited to UV-damaged DNA *in vivo*. The second assay involves use of model oligonucleotides with a defined UV-damage surrounded by multiple restriction enzyme sites that reveals a bilateral asymmetric footprint of PARP-1 around the UV-lesion.

Results and Discussion

Novel *in situ* fractionation protocol to reveal recruitment of endogenous PARP-1 to UV-induced DNA lesion. We first determined whether different permeabilization-fixation protocols conventionally used for PARP-1 could reveal a direct recruitment of PARP-1 to UVC-induced DNA photolesions *in situ*. There was no change in the pattern of abundant PARP-1 signal before or after global UVC-irradiation using formaldehyde-methanol protocol despite using three different antibodies to PARP-1 (Fig. 1a, left panel). Unlike global irradiation, local UVC-irradiation produces defined subnuclear spots of UV-damaged DNA that could be identified either by immunodetection of T-T lesions or DDB2 that is recruited very rapidly to these lesions (Supplementary Fig. S1a). Therefore, we examined whether the formaldehyde-methanol protocol could reveal localization of PARP-1 to subnuclear UV-damaged DNA spots after local irradiation. Once again, we could not observe colocalization of PARP-1 with the subnuclear spots of DDB2 (Fig. 1a, right panel). Next, we tried previously described formaldehyde-Triton protocol[8] which was shown to display a punctate pattern of PARP-1. However, we noted that this pattern did not correlate with recruitment of PARP-1 to UV-damaged DNA, because it was observed in both the unirradiated control and globally UVC-irradiated cells; and none of the spots of PARP-1 were co-incident with DDB2, i.e., UV-damaged DNA in the cells after local UVC-irradiation (Supplementary Fig. S1b).

In view of these challenges in the immunocytological detection of PARP-1 bound to UV-damaged DNA due to the background "noise" created by rest of the nuclear PARP-1, we designed a novel *in situ* fractionation technique to selectively deplete unbound or "free" PARP-1 from the nuclei while leaving behind the PARP-1 that is bound and cross-linked to the UV-damaged DNA. We used CSK buffer (C) with Triton (C+T) as the basic conditions, which have been used earlier to extract majority of the cellular proteins without destroying the cellular architecture and permit visualization of NER and other repair proteins recruited to the damaged DNA[15–18]. To this buffer, we added 0.42 M NaCl (C+T+S), since we had earlier seen that 0.42 M NaCl retained chromatin-bound PARP-1 during cell fractionation *in vitro*[7] whereas 1.6 M NaCl was shown to strip almost all PARP-1 from cells[19]. We first compared the efficiency of these three protocols (i.e., C, C+T and C+T+S) for the extraction of PARP-1 and DDB2 from unirradiated control cells. The immunoblotting of cell pellet and supernatant from each protocol revealed that while C+T protocol could efficiently remove majority of the free DDB2, a significant extraction of the free PARP-1 from cell pellet required C+T+S protocol (Fig. 1c). Next, we compared the capacity of these three protocols for the *in situ* extraction of PARP-1 from control and global UVC-irradiated cells. The immunocytological visualization confirmed that C+T+S buffer extracted most of the "free" PARP-1 from the control and UVC-irradiated cells, while leaving behind residual PARP-1 that would be interacting with DNA for normal physiological functions in control cells and relatively stronger punctate pattern of PARP-1 in UV-irradiated nuclei (Fig. 1d).

When the three protocols were compared after local irradiation, we observed that the C+T+S protocol offered the best extraction condition for visualization of the recruitment of PARP-1 to the subnuclear spots of DDB2 (Fig. 1e, left panel). The pooled data from at least 100 subnuclear spots revealed that each additional step of extraction with detergent and salt improved our ability to discern colocalization of PARP-1 with DDB2 (Fig. 1e, left chart). Since the initial irradiation conditions were identical prior to extraction with each of the protocols, the improved detection of colocalization of PARP-1 with DDB2 could only be due to a more efficient removal of rest of the nuclear "free PARP-1" by the C+T+S protocol. This was evident when PARP-1 signal at the irradiated site was corrected for the background signal from an equivalent area of the unirradiated part of the same nucleus for all techniques (Fig. 1e, right chart).

Validation of the *in situ* fractionation protocol with GFP-tagged exogenous PARP-1 or its N-terminal DNA binding domain. We compared the efficiency of each of the three protocols in revealing the recruitment of exogenous GFP-tagged PARP-1 to UV-induced T-T lesion in locally UV-irradiated cells (Fig. 2a). The C protocol was inefficient in revealing the co-localization of GFP signal with T-T spots especially in the cells expressing higher levels of exogenous PARP-1. The C+T and C+T+S protocols increasingly resolved this problem by removing "free" PARP-1, thus giving a background-corrected signal for GFP-PARP-1 at T-T lesion that was 1.9 and 2.7 times better than the C protocol, respectively (Fig. 2a, chart). The additional advantage was that this co-localization could be readily observed whether these cells initially expressed high or low levels of GFP-PARP-1.

The N-terminal DNA binding domain (DBD) of PARP-1 containing first two zinc fingers was shown to be sufficient for its recruitment to different types of DNA damages caused by laser irradiation of cells[20,21]. In the cells transiently transfected with GFP-DBD, the colocalization of DBD with T-T was evident only in low DBD-expressers, as shown in low and high exposure panels of C-protocol (Fig. 2b). The ability to discern co-localization of GFP-DBD to T-T lesion sites was significantly improved by 1.5 and 2.1 times with C+T protocol and C+T+S protocol, respectively (Fig. 2b, chart). Immunoblotting for GFP-DBD and endogenous untagged

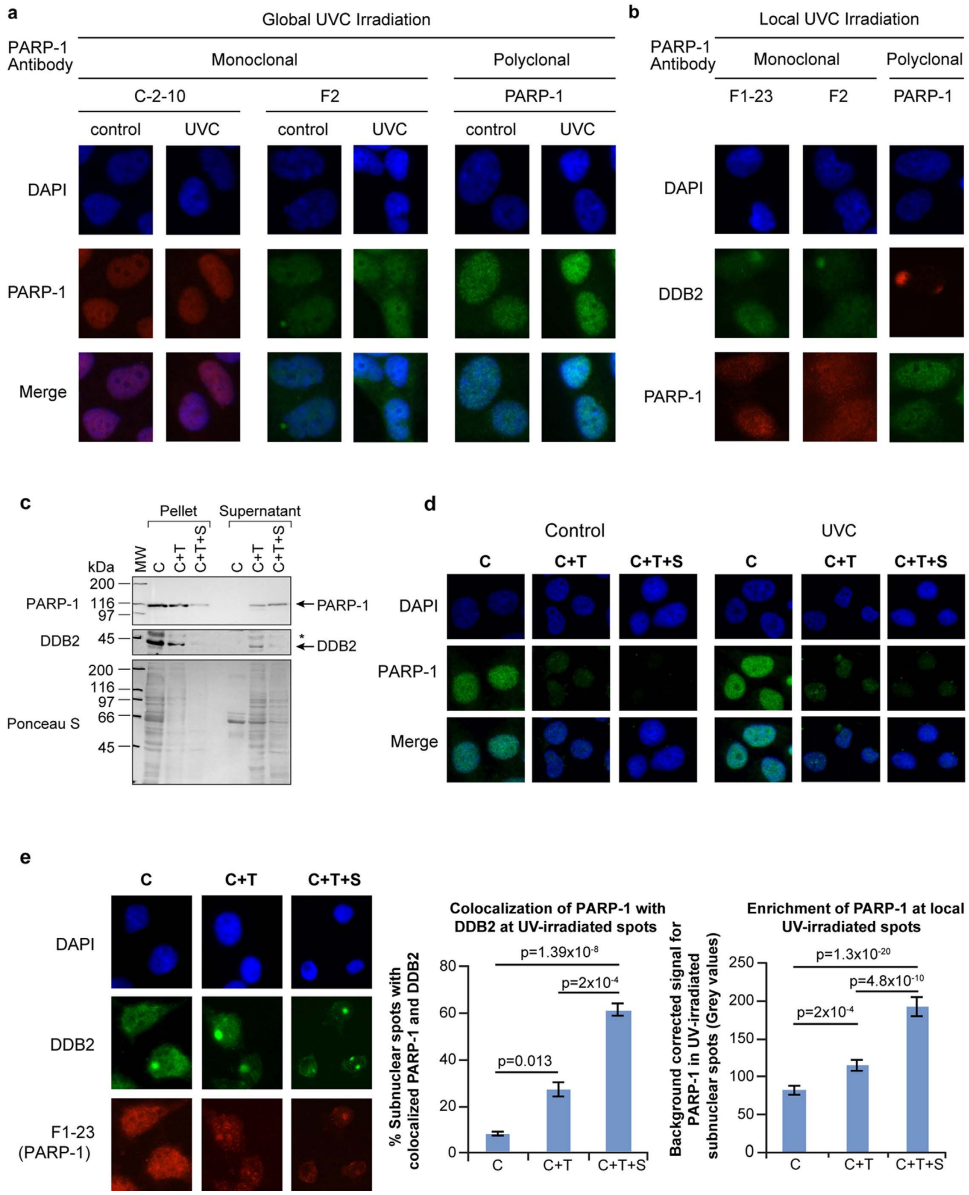

Figure 1. ***In situ*** **fractionation to reveal the recruitment of endogenous PARP-1 to UV-induced DNA lesion site.** (**a,b**) Unchanged pattern of nuclear staining for PARP-1 after global or local UVC-irradiation of cells processed with conventional immunocytological techniques. Human skin fibroblasts were exposed either to global (panel a) or local (panel b) irradiation with UVC, fixed with formaldehyde-methanol and probed for PARP-1 (global and local UVC) and DDB2 (local UVC) using specified antibodies. DAPI staining was carried out to define nuclei. **(c)** Efficiency of extraction of free PARP-1 and DDB2 from adherent control GMU6 cells. The pellets and supernatants obtained from equivalent cell numbers after extraction with CSK buffer (C), CSK+0.5% Triton (C+T) or CSK + 0.5% Triton + 0.42 M NaCl (C+T+S) were immunoblotted for PARP-1 and DDB2. The *refers to non-specific signal in DDB2 probing and Ponceau S staining reflected the residual protein content in cell pellets and supernatant at the end of each protocol. **(d)** Comparison of the efficiency of three protocols for extraction of the endogenous PARP-1 from adherent control and UV-irradiated cells. The GMU6 human skin fibroblasts were globally irradiated with 10 J/m^2 UVC (or control), extracted 10 min later with the three protocols and probed for PARP-1 using polyclonal PARP-1 antibody. **(e)** Colocalization of endogenous PARP-1 with DDB2 at local UVC-induced DNA damage. GMU6 cells were irradiated locally with 100 J/m^2 and after 10 min subjected to the three protocols (C, C+T and C+T+S) followed by visualization of PARP-1 (F1-23, red) and DDB2 (green). The left chart represents the percent of subnuclear PARP-1 spots that colocalize with DDB2. The right chart represents the quantification of the PARP-1 intensity at the DDB2 spots after subtraction of background signal intensity for PARP-1 from an equivalent area of unirradiated part of the same nucleus. Data of the charts are pooled from three experiments ($n = 120–150$ spots, data points are mean ± s.e.).

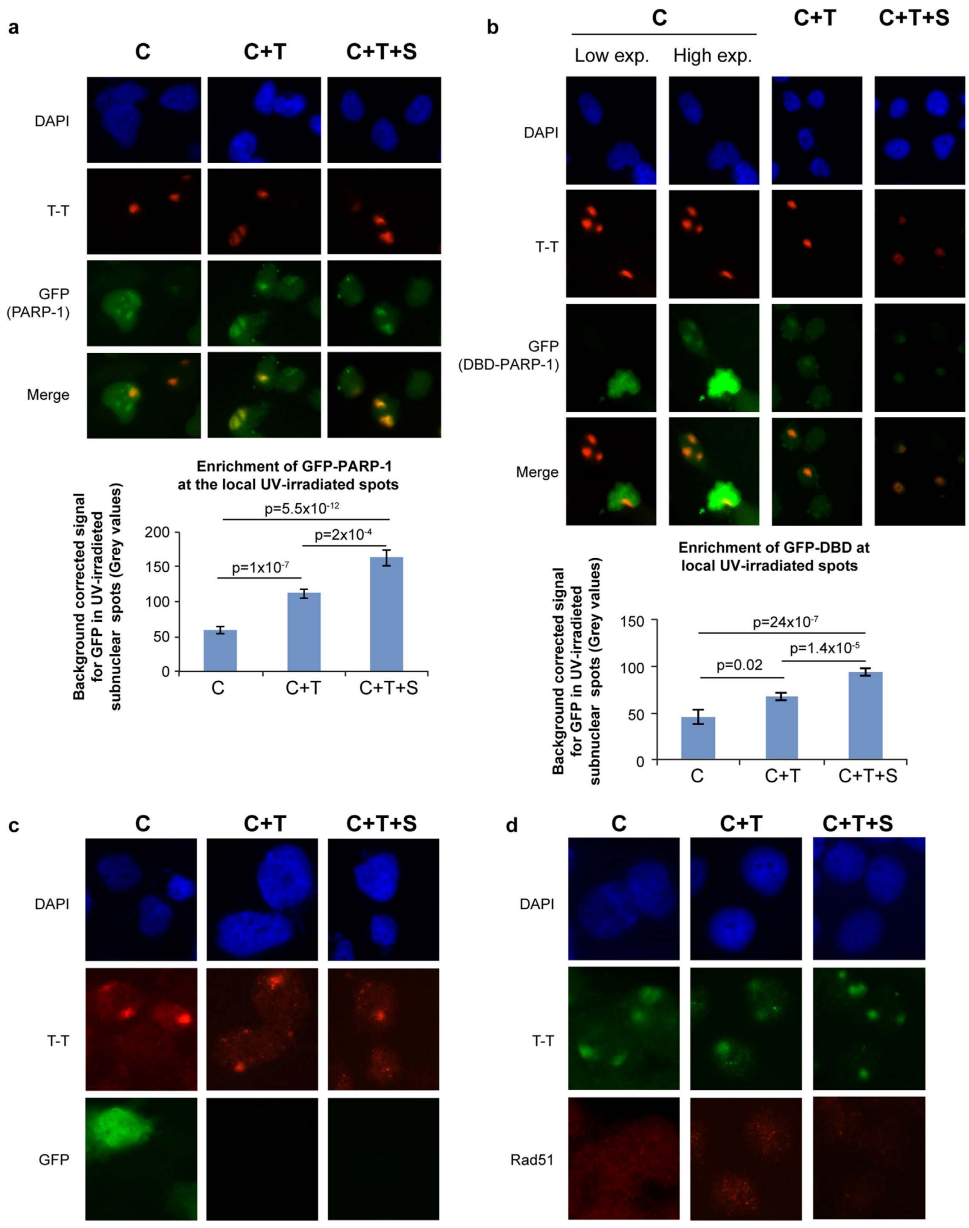

Figure 2. ***In situ*** **fractionation improves detection of exogenous GFP-PARP-1 or its DNA binding domain at local UV-irradiated spots. (a,b)** Recruitment of GFP-PARP-1 or its DBD to UV-induced T-T lesions. GMU6 cells were transfected with GFP- PARP-1 or GFP-DBD of PARP-1 for 24 h. The cells were locally irradiated and processed by C, C+T or C+T+S protocols. GFP-PARP-1 or GFP-DBD (green) and T-T (red) were visualized in DAPI-stained nuclei by immunofluorescence microscopy. The charts represent the quantification of GFP intensity for GFP- PARP-1 or GFP-DBD of PARP-1 at the T-T spots after background correction. ($n = 80–150$ spots, data points are mean ± s.e.). **(c,d)** Specificity of *in situ* extraction protocol: unrelated nuclear proteins (GFP and Rad51) do not colocalize with UV-damaged DNA. GMU6 cells were locally irradiated with 100 J/m^2 UVC and subjected 10 min later to *in situ* fractionation using the three protocols. For panel-c, the cells were transfected with GFP expressing plasmid 24 h before irradiation and protein extraction. The cells were processed for immunofluorescence detection of GFP, Rad51 (green) and T-T (red). DAPI staining was carried out to define nuclei.

PARP-1 in control cell pellets in these extraction protocols revealed that the extent of removal of exogenous GFP-DBD at each step was similar to that of the endogenous cellular PARP-1 (Supplementary Fig. S1c). Our results show that the N-terminal DBD of PARP-1 is sufficient to recognize and bind to UVC-induced DNA damage.

To assess the specificity of the new protocol, we examined the status of UV-induced colocalization of unrelated proteins, such as the exogenous tag protein GFP (Fig. 2c) or the cellular DNA double strand break-repair protein Rad51 (Fig. 2d) at UV-lesion spots after processing with all three protocols. Although C+T and C+T+S protocols progressively removed both of these proteins from the cells, neither GFP nor Rad51 colocalized with UV-induced T-T lesions. Thus, our results show that the C+T+S protocol does not cause an artifact of random

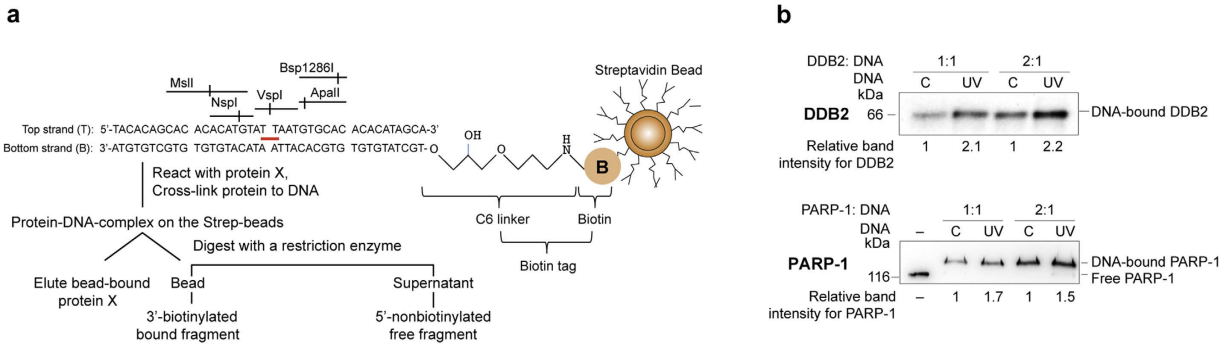

Figure 3. Strategy to study binding and footprint of proteins on UV-DNA. (a) The experimental design for determining the extent of binding of proteins to UV-DNA and analyses of protection of DNA during restriction digestion. The control and UV-DNA were immobilized on streptavidin beads via their biotin tag and reacted with purified PARP-1 or DDB2. The unreacted proteins were removed and bound proteins were cross-linked. The beads were then either analysed for bound-proteins by eluting the protein in Laemmli buffer, followed by SDS-PAGE, transfer and probe with specific antibodies or they were subjected to restriction digestion followed by analyses of the released DNA fragments on 10–15% native PAGE stained with gel red. **(b)** DDB2 and PARP-1 bind more to UV-DNA than control DNA. PARP-1 and DDB2 were reacted with 50 ng of control or UV-DNA at 1:1 or 1:2 (DNA:protein) molar ratios. The proteins were eluted from the beads, resolved on SDS-PAGE and analyzed by immunoblotting as shown in (**a**). The band intensities of protein bound to UV-DNA are shown as relative to signal for protein bound to control DNA.

colocalization of unrelated proteins with UV-damaged DNA. This simple yet selective *in situ* fractionation protocol to reveal PARP-1 at UV-lesion site would be useful in studying other NER-related roles of PARP-1 with or without its catalytic activation at the site of UV-damaged DNA.

An oligo with defined UV-lesion for restriction mapping of PARP-1. To determine the exact footprint of PARP-1 at the UV-lesion site, we created biotin-tagged 40 mer oligonucleotides with or without a single defined UV-lesion surrounded by multiple unique restriction enzyme sites (Fig. 3a and Supplementary Fig. S2a). The UVC-irradiation of the top strand of the oligo, which has only one pair of adjacent Ts and no other adjacent pyrimidines (T or C), resulted largely in the formation of T-T rather than 6–4PP lesions (Supplementary Fig. S2b). The inability of restriction enzymes to digest through UV-induced CPD[22,23] was exploited for purification of UV-DNA with VspI enzyme to remove all DNA molecules that did not form T-T at this site (Supplementary Fig. S2c). The biotin-tagged complementary strand for both control and UV-DNA allowed a common procedure for their immobilization to streptavidin beads (Fig. 3a). We reasoned that any protein bound at or around the UV-lesion site would prevent the restriction enzyme from digesting the DNA at that site; and thus decrease the quantity of non-biotinylated 5′-restriction fragment released from bead-bound DNA into the supernatant. This model allowed us to compare the extent of binding of proteins to control versus UV-DNA and also provide a non-isotopic method to footprint proteins on UV-DNA.

PARP-1 and DDB2 bind more to UV-DNA than control DNA. We had shown in the cells and *in vitro* that PARP-1 not only binds to UV-damaged DNA[11], but also interacts with DDB2 in the vicinity of UV-induced DNA lesions[7]. Using the model oligo described in Fig. 3a, we examined the extent of binding of PARP-1 and DDB2 to control and UV-DNA at two different molar ratios of protein : DNA (Fig. 3b). The 2.1−2.2× fold higher binding of DDB2 to UV-DNA than the control-DNA at these two molar ratios is in agreement with a previous report[24]. The binding of PARP-1 to UV-DNA was also 1.5−1.7× fold more than the control-DNA (Fig. 3b). We confirmed that PARP-1 did not bind to the beads per se unless DNA was attached to it (Supplementary Fig. S3a: left panel). To determine the site of PARP-1 binding to the control DNA without UV-lesion, we digested PARP-1-bound control DNA with VspI or NspI and noted that PARP-1 was attached more to the bead-bound 3′-end than to the 5′-end that is released after the restriction digestion (Supplementary Fig. S3a: right panel). This could be due to the linker attached biotin providing a pseudo-overhang at the 3′-end unlike blunt 5′-end, because PARP-1 has higher affinity for overhangs as compared to the blunt ends of DNA[25]. However, since the same 3′ and 5′-ends exist in both control and UV-DNA, any increase in PARP-1 binding to UV-DNA as compared to control-DNA must be due to the interaction of PARP-1 with UV-lesion, which we footprinted using a series of restriction enzymes that digest on either side of the lesion.

Restriction protection profile of PARP-1 is distinct from that of DDB2 on either side of the T-T lesion. We established the optimal amount of DNA required in the assay for detection of DNA fragments released after digestion with restriction enzyme (Supplementary Fig. S3b) and also confirmed that both the control and UV-DNA without bound protein could be digested by all the restriction enzymes used in our footprinting assays (Supplementary Fig. S3c,d). Thus, any restriction protection offered to DNA after reaction with protein could be attributed to the footprint of the protein. During the restriction digestion by NspI and MslI that recognize sequences from −2 to −12nt on the 5′-side of the T-T lesion, PARP-1 offered more protection to UV-DNA than control DNA, as seen from a significant PARP-1 dose-dependent decrease in the corresponding

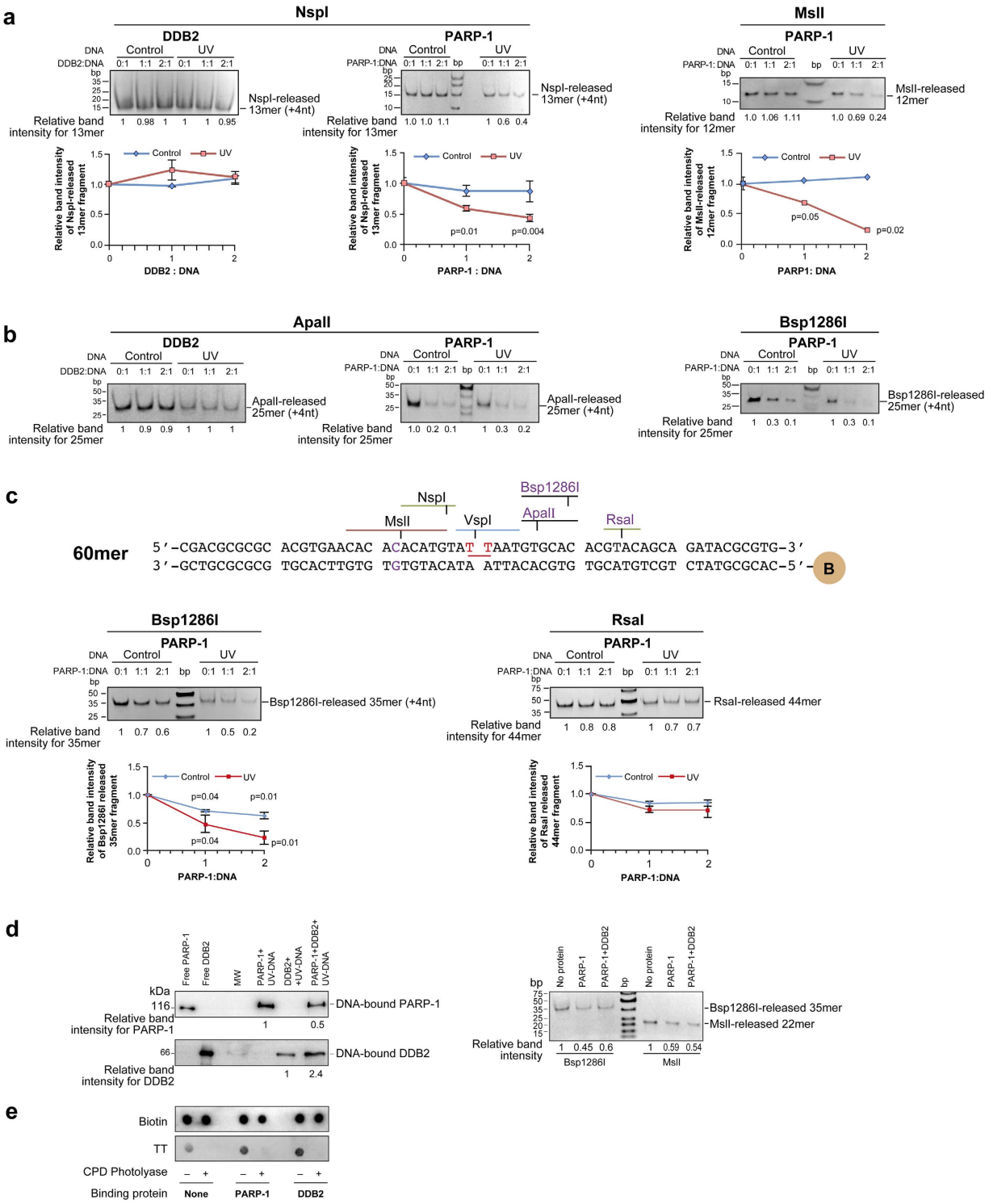

Figure 4. Footprinting of PARP-1 and DDB2 at UV-lesion site. (a) Restriction mapping of proteins on the 5′of the UV-lesion on 40mer DNA. 100 ng of bead-bound control or UV-DNA were reacted with DDB2 or PARP-1 at different DNA: protein ratios and digested at 37 °C with NspI (30 min) or MslI (15 min). The released 5′-fragments were resolved on 15% native PAGE and band intensities were measured. Each data point derived from three independent experiments represents mean ± s.d. for relative band intensity from three experiments for the fragment released from protein-bound versus protein-free DNA, with *P* values shown in the chart. **(b)** Mapping of proteins on the 3′-side of the UV-lesion on 40mer DNA. The protein-bound DNA was digested with ApaII (60 min) and Bsp1286I (20 min), and released 5′-fragments were resolved on 12% native PAGE. The data derived from two independent experiments is represented in the chart as described in panel-a. **(c)** *Top panel*-Structure of 60mer oligo with defined UV-damage. The 60mer oligo sequence was based on 40mer oligo but with a new RsaI site near 3′-end. *Bottom panels*- Restriction mapping of proteins on the 3′-side of the UV-lesion on 60mer DNA. The protein-bound DNA was digested with Bsp1286I (20 min) and

RsaI (30 min) and released 5′-fragments were analysed by 12% native PAGE. The data derived from three independent experiments is represented in the chart as described in panel-a. **(d)** Simultaneous binding and footprint of DDB2 and PARP-1 on 60mer UV-DNA. PARP-1 and DDB2 were reacted either separately or together with bead-bound UV-DNA (50 ng), at 2:1 molar ratio of protein:DNA. The proteins bound to the beads were detected by immunoblotting (left panels), and footprint of proteins on DNA was examined by restriction digestion with Bsp1286I and MslI (right panels). **(e)** Repair of T-T by CPD photolyase despite binding of DDB2 or PARP-1 to UV-DNA. Bead-bound 40mer UV-DNA was reacted (or not) with DDB2 or PARP-1, and subjected to repair (or not) by CPD photolyase. The DNA was eluted and immunodot-blotted for T-T. The data represents identical results obtained in three independent experiments.

5′-fragments released by these enzymes (Fig. 4a). Thus, the footprint of PARP-1 on UV-DNA extended from 2–12nt upstream of the lesion site. In contrast, DDB2 failed to protect UV-DNA against NspI (−2 to −7 nt), indicating that its footprint stays within 2nt on the 5′-side of T-T, as reported earlier[26].

PARP-1 has been shown to have a bilateral footprint of 7nt on either side of DNA single strand breaks[27]. Therefore, we compared the protections offered by PARP-1 and DDB2 against the restriction enzymes ApaII and Bsp1286I that target from 3 to 9nt on the 3′-side of the T-T lesion. The DDB2 did not offer any protection to control or UV-DNA against ApaII (Fig. 4b), indicating that its footprint does not exceed beyond 3nt on 3′-side of T-T, as reported earlier[26]. In contrast, PARP-1 offered a strong but equal protection to both UV and control oligos against both the enzymes, possibly due to PARP-1 bound to 3′-ends of both types of DNA, as noted earlier (Supplementary Fig. S3a: right panel). Thus using 40mer oligo, it was difficult to discern additional protection, if any, offered by PARP-1 that is bound at or near T-T site from the protection offered by PARP-1 that is bound to the 3′-end of the oligo.

To resolve this issue, we extended the size of 40 mer oligo on either ends to create a 60 mer, in which 3′-end was significantly separated from these two restriction sites and added a new RsaI restriction site at +11 nt from T-T (Fig. 4c, top panel). PARP-1 significantly protected 60mer UV-DNA against digestion by Bsp1286I as compared to control DNA, confirming its footprint up to +9nt from T-T lesion. Moreover, the lack of any additional protection by PARP-1 to UV-DNA against digestion by RsaI defined that PARP-1 footprint does not reach up to +11nt from T-T site (Fig. 4c). Thus using restriction-mapping technique on our model oligo, we show that PARP-1 bound at or near the T-T lesion extends asymmetric bilateral protection against restriction digestion from −12 to +9nt around the lesion.

Next, we examined whether PARP-1 and DDB2 can simultaneously bind to UV-DNA and whether DDB2 bound at the T-T lesion would alter the footprint of PARP-1 around the lesion. Using 60mer oligo, we noted that when incubated together, both DDB2 and PARP-1 could bind to UV-DNA (Fig. 4d, left panel). We observed in two independent experiments that the presence of PARP-1 increased the binding of DDB2 to UV-DNA, whereas that of DDB2 reduced the binding of PARP-1. However, the presence of DDB2 did not affect the restriction footprint of PARP-1 on UV-DNA, because PARP-1 offered identical protection to UV-DNA against restriction digestion on either side of the lesion site by MslI and Bsp1286I in the absence or the presence of DDB2 (Fig. 4d, right panel). Thus, the footprint of PARP-1 around the lesion was not compromised in the presence of DDB2 whereas DDB2 was more stabilized in the presence of PARP-1.

No effect of PARP-1 and DDB2 binding on CPD-photolyase mediated repair of T-T in UV-DNA. Unlike restriction enzymes that cleave the DNA in the sugar phosphate backbone, the CPD photolyase directly removes the cross-linking of adjacent pyrimidines in the CPD photolesions such as T-T[28]. Structural studies have revealed that DDB2 has a protein fold that flips out and maintains contact with T-T[26], and our results indicate that PARP-1 also remains in the vicinity of T-T lesion. Hence, we examined whether binding of DDB2 or PARP-1 to UV-DNA could influence the repair of T-T by CPD photolyase (Fig. 4e). The immunodot-blot of DNA with or without photolyase treatment revealed that binding of DDB2 or PARP-1 to DNA could not inhibit the ability of photolyase to repair the T-T lesions, indicating that these two proteins do not exclude other repair proteins from accessing the lesion. This is also in agreement with a previous report that binding of DDB2 to UV-DNA does not prevent CPD photolyase from repairing the UV-lesion[29].

Catalytic activation of PARP-1 is stronger with 6–4PP than T-T lesion. We used the model oligos for further characterization of the interaction of PARP-1 with UV-damaged DNA. Since the catalytic activation of PARP-1 is more with damaged DNA than with undamaged DNA[14], we examined the extent of activation of PARP-1 with 40mer control or UV-oligo *in vitro* as an additional indicator of the extent of binding of PARP-1 to these DNA. A stronger PARP-1 activation with UV-DNA was observed as compared to control-DNA at two different molar ratios of PARP-1 to DNA (Fig. 5a, left panel). Thus the binding of PARP-1 to UV-lesion caused stronger stimulation of its catalytic activity as compared to its binding to either the 3′ or 5′-ends of both the control and UV-DNA. To compare the capacity of different UV-induced direct damages for activation of PARP-1, we assessed the efficacy of 24mer oligo containing a single chemically synthesized T-T or 6–4PP lesion[30] in the PARP-1 activation assay *in vitro* (Fig. 5a, right panel). Both the DNA containing defined UV-lesions were stronger activator of PARP-1 than the 24mer control-DNA at two different molar ratios of PARP-1 to DNA. Moreover, 6–4PP, which is known to cause a higher degree of helical distortion, was a stronger stimulator of the catalytic activity of PARP-1 than T-T.

Model for the interaction of PARP-1 and DDB2 with UV-damaged DNA. Based on the current results of *in situ* visualization and footprinting of PARP-1 and DDB2 at UV-induced DNA lesion site, we propose

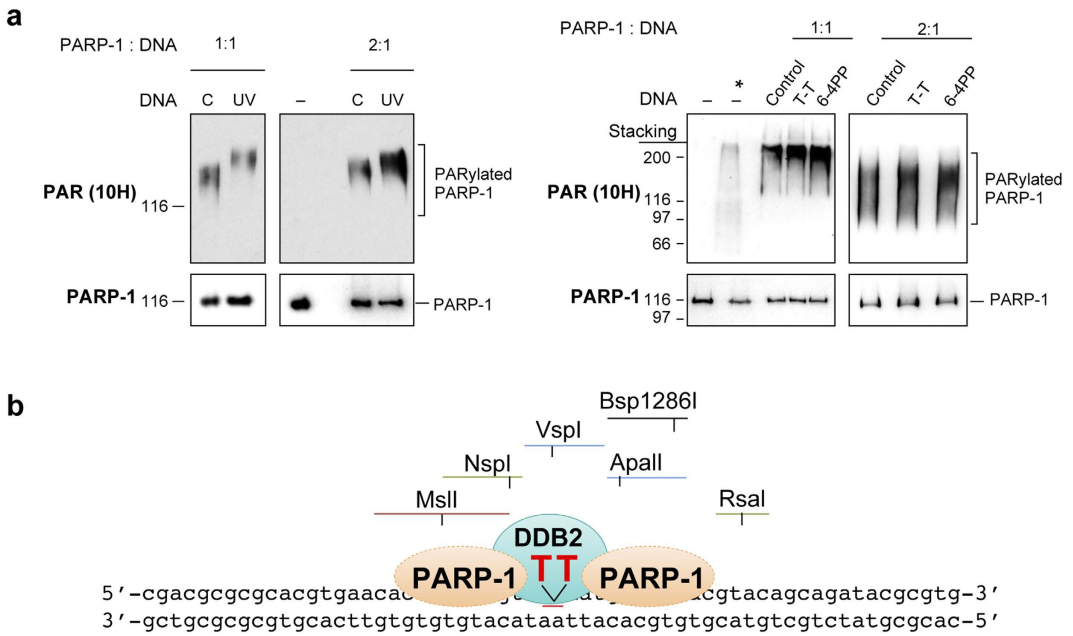

Figure 5. Catalytic activation of PARP-1 with defined UV-damaged DNA and a model for footprint of PARP-1 and DDB2 on UV-lesion site. **(a)** Stimulation of catalytic activity of PARP-1 by various defined UV-damaged DNA *in vitro*. PARP-1 activation assay was performed using 40 mer control or UV-DNA (left panel) or using 24mer DNA with no damage (control) or with a single defined T-T and 6–4PP (right panel) at 1:1 or 1:2 molar ratio of DNA:protein. After resolution on SDS-PAGE, immunoprobing for PARP-1 and PARylated PARP-1 (10H antibody) was carried out. The *refers to the cell extract containing H_2O_2-activated PARP-1. Panel represents one of three identical experiments. **(b)** Model for binding of PARP-1 and DDB2 to the UV-lesion site on 60mer oligo (see Results and Discussion section for details).

that DDB2 attaches directly at the UV-lesion site whereas PARP-1 makes an asymmetric bilateral contact from −12 to +9nt around the lesion (Fig. 5b). This footprint is compatible with either one or two PARP-1 molecules enveloping around the UV-lesion, similar to the reported binding of either one[31] or two[21] PARP-1 molecules at the site of DNA strand breaks. The N-terminal DNA binding domain of PARP-1 that is known to be recruited to DNA strand breaks[20] was also recruited to UV-lesions without strand breaks, indicating more general property of this domain of PARP-1 to bind to different types of DNA damages. Our model is also consistent with previously reported interactions of DDB2 and PARP-1 at the UV-lesion site[5,7]. We have earlier shown that PARP-1 and DDB2 co-immunoprecipitate at the UV-damaged chromatin in the presence of ethidium bromide, indicating their direct interaction on the same DNA strand[7]. Here, we confirm that PARP-1 and DDB2 can co-exist at the UV-lesion site and the presence of DDB2 does not alter the footprint of PARP-1 around the lesion. Our results do not exclude the possibility that PARP-1 footprint may vary when the damaged DNA is in the context of chromatin or when there are multiple UV-lesions in close proximity. We had earlier shown that PARP-1 is weakly activated by UV in the DDB2-deficient XP-E cells, but introduction of DDB2 in these cells strongly stimulates PARP-1 catalytic activity in response to UV[7]. Moreover, we had also observed that DDB2 stimulates catalytic activity of PARP-1 *in vitro* with UV-damaged DNA that largely contains T-T lesions[7], and here we show that PARP-1 activation was much stronger with 6–4PP than with T-T. Since the 6–4PP by itself causes larger distortion of DNA as compared to T-T, whereas the binding of DDB2 to T-T increases the distortion of DNA[26], collectively these results indicate that the extent of DNA distortion could be the determinant for PARP-1 activation with UV-damaged DNA. Our results show that PARP-1 and DDB2 do not prevent access to the lesion site by other repair proteins such as CPD photolyase, and may even be more flexible and accommodating in the *in vivo* conditions as compared to our *in vitro* condition in which damaged DNA is anchored to beads and interacting proteins are cross-linked to the DNA. Together, these two novel assays will open new avenues to study the ever-expanding roles of PARP-1 in NER and housekeeping functions in which PARP-1 shows subtle interactions with DNA without strand breaks.

Material and Methods

Antibodies. For Western blotting: Monoclonal 6–4PP (KTM50) and T-T (KTM53) (1:5,000), polyclonal PARP-1 (1:5,000), PARP-1 monoclonal (F2, 1:500), GFP monoclonal (1:5,000), DDB2 anti goat (1:500), PAR monoclonal (10H, 1:1,000), HRP-conjugated secondary antibodies (1:2,500). For immunocytology: T-T (KTM53, 1:2,000), polyclonal PARP-1 (1:5,000), PARP-1 monoclonal F2 (1:500), PARP-1 monoclonal C2-10 (1:500), F1-23 monoclonal (1:500), DDB2 anti goat (1:200), Rad51 polyclonal (1:500) and secondary fluorescent antibodies (1:500).

Cell culture. Cells were grown in 5% humidified incubator at 37 °C in αMEM medium supplemented with 10% FBS, penicillin and streptomycin and 200 μg/ml hygromycin. The creation of GM637-derived PARP-1 replete GMU6 cells were described earlier[32].

Expression Plasmids. The pGFP-hPARP-1 was a gift from V. Schreiber, pGFP-DBD of PARP-1 was generated by subcloning the 0.7 kb SacI (blunted) and HindIII-fragment of PARP31 cDNA into NheI (blunt)/HindIII sites of pEGFP-N1 plasmid.

Transfection and UVC-irradiation. GMU6 cells were transfected with pEGFP-hPARP-1, pEGFP-DBD-PARP-1 and pEGFP-N1 plasmid using Turbofect reagent. After 24 h, cells were irradiated for global UVC (10 J/m^2) or through polycarbonate filter with 5 μm pores for local (100 J/m^2) UVC[11].

Indirect immunofluorescence detection *in situ*. The cells adherent on the coverslip were processed by one of the three protocols: *C protocol:* After washing with CSK buffer (100 mM NaCl, 300 mM sucrose, 10 mM PIPES pH 6.8, 3 mM $MgCl_2$, 1 mM EGTA), cells were fixed with 3% formaldehyde (10 min, ambient temperature), rinsed with PBS, permeabilized with 100% methanol (−30 °C, 10 min), rinsed with PBS, blocked for 30 min with 5% BSA in PBS-0.1% Triton-X-100 followed by reaction with primary antibodies given below. *C+T protocol:* Cells were washed twice with CSK buffer, extracted with 0.5% Triton in CSK buffer for 8 min at ambient temperature, fixed and blocked as in C protocol. *C+T+S protocol:* After C+T protocol fixation step, cells were washed and extracted with 0.5% Triton in high salt CSK buffer (420 mM NaCl, 300 mM sucrose, 10 mM PIPES pH 6.8, 3 mM $MgCl_2$, 1 mM EGTA) for 20 min on ice. After DNA denaturation in 0.07 N NaOH for 8 min at ambient temperature, immunoprobing was carried out for all three protocols as follows: The cells were incubated for 1 h with primary antibodies in the blocking buffer, washed with PBS containing 0.1% Tween 20 and incubated for 30 min with Alexa 488 or 594-linked secondary antibodies. After washing with PBS-0.1% Tween 20, coverslips were incubated in PBS-0.25 μg/ml DAPI for 5 min and mounted with ProLong Gold Antifade. Images were captured with Zeiss Axiovert 200 and AxioCam MRm and the brightness and contrast were uniformly adjusted across the panels with Photoshop CS5.5. The fluorescent intensity of PARP-1 at the irradiated spots was analyzed with AxioVision 4.7 and corrected for background signal for similar area in the unirradiated zone of nucleus, where specified.

Statistical analyses for immunocytology. Data for intensity of at least 100 foci from three independent experiments were pooled to create mean ± s.e., and subjected to the unpaired two-tailed t-tests to determine the significance of difference. The significant P-values <0.05 are stated in the charts.

Oligos. The ss-24mer oligos with T-T or 6–4PP were chemically synthesized and hybridized with the complementary ss-24mer to get 24mer ds oligo with T-T or 6–4PP lesions. The creation of 40 or 60mer oligos are described in Figs. 3a, 4c, and Supplementary Fig. S2a.

VspI-purification of 25 kJ/m^2 UVC irradiated oligo. The UVC irradiated 40mer or 60mer ds oligos were digested with VspI for 1 h at 37 °C, followed by VspI-inactivation at 65 °C for 5 min. The VspI-resistant 40 or 60mer UV-DNA were separated on 12% PAGE from the digested fragments of DNA without UV-damage, cut from the gel and eluted with PAGE elution buffer (0.5 M ammonium acetate, 10 mM magnesium acetate and 1 mM EDTA) overnight at 37 °C. The eluted UV-DNA were cleaned by passage through ULTRAFREE–DA filter units, concentrated in Microcon YM-10 followed by purification in Zymo Research oligo clean and concentrator columns.

The protein-DNA interactions, restriction mapping and CPD photolyase assays for bead-bound oligos with proteins. The control or UV-DNA with biotin tag was immobilized on Dynabeads MyOne streptavidin T1. (i) The binding of PARP-1 or DDB2 to control or UV-oligos immobilized on the magnetic streptavidin beads: The bead-bound oligos (50–100 ng) were reacted with PARP-1 or DDB2 at 1:1 or 1:2 molar ratio. PARP-1 was reacted at 25 °C for 15 min in 10 μL of Na-PO_4 reaction mixture (20 mM of Na-PO_4 buffer pH 7.4, 5 mM $MgCl_2$, 150 mM NaCl, 5% glycerol, 1 mM DTT, 0.01% Triton, 20 μM Zn-acetate and 1× protease inhibitor). DDB2 was reacted at 25 °C for 30 min in Tris reaction mixture (100 mM Tris buffer pH 8.0, 10 mM $MgCl_2$, 10% glycerol, 150 mM NaCl, 1.5 mM DTT and 1× protease inhibitor). The simultaneous binding of PARP-1 and DDB2 was carried out in Tris reaction mixture for 15 min at 25 °C. The unbound proteins were removed and the bound proteins were crosslinked to oligo with 1% formalin in Na-PO_4 reaction mixture for 10 min at ambient temperature. After quenching formalin with 250 mM Tris-HCl pH 8.0, the beads were washed twice with Tris-reaction mixture and subjected to following steps.

(ii) Assessment of binding of proteins with DNA: The proteins that were attached to bead-bound DNA were extracted with Laemmli buffer at 95 °C for 10 min. The eluted proteins were resolved on SDS-PAGE for immunoblotting of the protein. The band quantification for immunoblots was carried out with ChemiGenius 2 using SynGene software.

(iii) Restriction protection assay of protein-bound oligos: For the restriction protection assay, the magnetic streptavidin beads bound control or UV-DNA with or without bound protein were digested with the specified Fast-digest or CutSmart restriction enzyme in 10 μL reaction buffer at 37 °C for specified time. The DNA fragments released in the supernatant were resolved on 10–15% native PAGE and stained with gel red for identification and quantification with ChemiGenius2 using SynGene software. The relative band intensities were derived by comparing the intensities of the fragments released from the protein-bound DNA with that from protein-free

DNA. The significance was calculated by unpaired two-tailed t-test and the P values <0.05 were considered significant.

(iv) CPD photolyase repair assays: The bead-bound UV-DNA with or without attached proteins was split into two aliquots; one subjected to repair by CPD photolyase and the other was mock-treated. The CPD repair was carried out in 20 μL CPD photolyase binding mix (20 mM Tris buffer pH 7.5, 1 mM DTT, 0.2 mg/ml BSA, 125 mM NaCl) with 0.2 μL Oryza sativa CPD photolyase and incubated for 15 min in dark at ambient temperature, followed by exposure for 15 min to UVA (Spectrolinker XL-1500, 363 nm, 15 watts). DNA was eluted with 95% formamide, 10 mM EDTA pH 8.0 for 5 min at 95 °C, dot-blotted on the Hybond N^+ and probed for T-T.

PARP-1 activation assay *in vitro*. In a 10 μL reaction mixture containing 100 mM Tris-HCl pH 8.0, 10 mM $MgCl_2$, 10% glycerol, 1.5 mM DTT, 1× protease inhibitor and 10 μM NAD, purified PARP-1 was reacted at 25 °C for 30 min with specified DNA for each reaction. After adding an equal volume of 2× Laemmli buffer, samples were resolved on SDS-PAGE and immunoblotted for PAR (10H) and PARP-1 [14].

Immuno-Dot-blot. DNA samples were heated at 95 °C for 5 min, chilled on ice for 5 min and adjusted to final concentration of 6× SSC. Samples were dot-blotted on Hybond N+ membrane, baked at 80 °C for 1–2 h and processed for antibody probing.

References

1. Robert, I., Karicheva, O., Reina San Martin, B., Schreiber, V. & Dantzer, F. Functional aspects of PARylation in induced and programmed DNA repair processes: Preserving genome integrity and modulating physiological events. *Mol. Aspects Med.* **34,** 1138–1152 (2013).
2. Pascal, J. M. & Ellenberger, T. The rise and fall of poly(ADP-ribose): An enzymatic perspective. *DNA Repair (Amst)* **32,** 10–16 (2015).
3. Kim, M. Y., Mauro, S., Gevry, N., Lis, J. T. & Kraus, W. L. NAD+-dependent modulation of chromatin structure and transcription by nucleosome binding properties of PARP-1. *Cell* **119,** 803–814 (2004).
4. Ghodgaonkar, M. M., Zacal, N. J., Kassam, S. N., Rainbow, A. J. & Shah, G. M. Depletion of poly(ADP-ribose) polymerase-1 reduces host cell reactivation for UV-treated adenovirus in human dermal fibroblasts. *DNA Repair (Amst)* **7,** 617–632 (2008).
5. Pines, A. *et al.* PARP1 promotes nucleotide excision repair through DDB2 stabilization and recruitment of ALC1. *J. Cell Biol.* **199,** 235–249 (2012).
6. Luijsterburg, M. S. *et al.* DDB2 promotes chromatin decondensation at UV-induced DNA damage. *J. Cell Biol.* **197,** 267–281 (2012).
7. Robu, M. *et al.* Role of poly(ADP-ribose) polymerase-1 in the removal of UV-induced DNA lesions by nucleotide excision repair. *Proc. Natl. Acad. Sci. USA* **110,** 1658–1663 (2013).
8. King, B. S., Cooper, K. L., Liu, K. J. & Hudson, L. G. Poly (ADP-ribose) contributes to an association between Poly(ADP-ribose) polymerase-1 and Xeroderma pigmentosum complementation group A in nucleotide excision repair. *J. Biol. Chem.* **287,** 39824–39833 (2012).
9. Fischer, J. M. *et al.* Poly(ADP-ribose)-mediated interplay of XPA and PARP1 leads to reciprocal regulation of protein function. *FEBS J.* **281,** 3625–3641 (2014).
10. Maltseva, E. A., Rechkunova, N. I., Sukhanova, M. V. & Lavrik, O. I. Poly(ADP-ribose) polymerase 1 Modulates Interaction of the Nucleotide Excision Repair Factor XPC-RAD23B with DNA via Poly(ADP-ribosyl) ation. *J. Biol. Chem.* **290,** 21811–21820 (2015).
11. Vodenicharov, M. D., Ghodgaonkar, M. M., Halappanavar, S. S., Shah, R. G. & Shah, G. M. Mechanism of early biphasic activation of poly(ADP-ribose) polymerase-1 in response to ultraviolet B radiation. *J. Cell Sci.* **118,** 589–599 (2005).
12. Berger, N. A. & Sikorski, G. W. Poly(adenosine diphosphoribose) synthesis in ultraviolet-irradiated xeroderma pigmentosum cells reconstituted with Micrococcus luteus UV endonuclease. *Biochemistry* **20,** 3610–3614 (1981).
13. Kawamitsu, H. *et al.* Monoclonal antibodies to poly(adenosine diphosphate ribose) recognize different structures. *Biochemistry* **23,** 3771–3777 (1984).
14. Shah, G. M. *et al.* Approaches to detect PARP-1 activation *in vivo*, *in situ*, and *in vitro*. *Methods Mol. Biol.* **780,** 3–34 (2011).
15. Mirzoeva, O. K. & Petrini, J. H. DNA damage-dependent nuclear dynamics of the Mre11 complex. *Mol. Cell. Biol.* **21,** 281–288 (2001).
16. Balajee, A. S. & Geard, C. R. Chromatin-bound PCNA complex formation triggered by DNA damage occurs independent of the ATM gene product in human cells. *Nucleic Acids Res.* **29,** 1341–1351 (2001).
17. Zhu, Q. *et al.* Chromatin restoration following nucleotide excision repair involves the incorporation of ubiquitinated H2A at damaged genomic sites. *DNA Repair* **8,** 262–273 (2009).
18. Fey, E. G., Wan, K. M. & Penman, S. Epithelial cytoskeletal framework and nuclear matrix-intermediate filament scaffold: three-dimensional organization and protein composition. *J. Cell Biol.* **98,** 1973–1984 (1984).
19. Kaufmann, S. H. *et al.* Association of poly(ADP-ribose) polymerase with the nuclear matrix: the role of intermolecular disulfide bond formation, RNA retention, and cell type. *Exp. Cell Res.* **192,** 524–535 (1991).
20. Mortusewicz, O., Ame, J. C., Schreiber, V. & Leonhardt, H. Feedback-regulated poly(ADP-ribosyl) ation by PARP-1 is required for rapid response to DNA damage in living cells. *Nucleic Acids Res.* **35,** 7665–7675 (2007).
21. Ali, A. A. *et al.* The zinc-finger domains of PARP1 cooperate to recognize DNA strand breaks. *Nat. Struct. Mol. Biol.* **19,** 685–692 (2012).
22. Hall, R. K. & Larcom, L. L. Blockage of restriction endonuclease cleavage by thymine dimers. *Photochem. Photobiol.* **36,** 429–432 (1982).
23. Cleaver, J. E. Restriction enzyme cleavage of ultraviolet-damaged simian virus 40 and pBR322 DNA. *J. Mol. Biol.* **170,** 305–317 (1983).
24. Wittschieben, B. O., Iwai, S. & Wood, R. D. DDB1-DDB2 (xeroderma pigmentosum group E) protein complex recognizes a cyclobutane pyrimidine dimer, mismatches, apurinic/apyrimidinic sites, and compound lesions in DNA. *J. Biol. Chem.* **280,** 39982–39989 (2005).
25. Clark, N. J., Kramer, M., Muthurajan, U. M. & Luger, K. Alternative modes of binding of poly(ADP-ribose) polymerase 1 to free DNA and nucleosomes. *J. Biol. Chem.* **287,** 32430–32439 (2012).
26. Fischer, E. S. *et al.* The molecular basis of CRL4DDB2/CSA ubiquitin ligase architecture, targeting, and activation. *Cell* **147,** 1024–1039 (2011).
27. Menissier-de Murcia, J., Molinete, M., Gradwohl, G., Simonin, F. & de Murcia, G. Zinc-binding domain of poly(ADP-ribose) polymerase participates in the recognition of single strand breaks on DNA. *J. Mol. Biol.* **210,** 229–233 (1989).
28. Sancar, A. & Sancar, G. B. DNA repair enzymes. *Annu. Rev. Biochem.* **57,** 29–67 (1988).
29. Fitch, M. E., Nakajima, S., Yasui, A. & Ford, J. M. *In vivo* recruitment of XPC to UV-induced cyclobutane pyrimidine dimers by the DDB2 gene product. *J. Biol. Chem.* **278,** 46906–46910 (2003).

30. Hendel, A., Ziv, O., Gueranger, Q., Geacintov, N. & Livneh, Z. Reduced efficiency and increased mutagenicity of translesion DNA synthesis across a TT cyclobutane pyrimidine dimer, but not a TT 6–4 photoproduct, in human cells lacking DNA polymerase eta. *DNA Repair (Amst)* **7,** 1636–1646 (2008).
31. Langelier, M. F. & Pascal, J. M. PARP-1 mechanism for coupling DNA damage detection to poly(ADP-ribose) synthesis. *Curr. Opin. Struct. Biol.* **23,** 134–143 (2013).
32. Shah, R. G., Ghodgaonkar, M. M., Affar el, B. & Shah, G. M. DNA vector-based RNAi approach for stable depletion of poly(ADP-ribose) polymerase-1. *Biochem Biophys Res Commun* **331,** 167–174 (2005).

Acknowledgements

We are thankful to V. Schreiber for GFP-PARP-1, K. Hitomi for the CPD photolyase and J. Brind'Amour for creating cDNA for GFP-DBD. We thank M. Miwa, National Cancer Center Research Institute, Tokyo, for permission to receive 10H hybridoma through the Riken cell bank. This work was supported equally by the two grant to GMS: Discovery Grant 155257-2011 from NSERC, Canada and Grant IMH-131569 from the Canadian Institutes of Health Research: Priority Announcement of Musculoskeletal Health, Arthritis, Skin and Oral Health. The work related to the site-specifically modified oligonucleotides was supported by the National Institutes of Health Grant CA-168469 to NEG. NP received the scholarship support from Quebec Government and Shastri Indo-Canadian Institute from foreign student fee waiver program and MR received graduate scholarship from the Fonds de recherche du Québec-Santé.

Author Contributions

The first three authors (N.K.P., M.R. and R.G.S.) contributed equally to performing all the experiments and preparing the figures. N.E.G. provided material support and guidance in planning the experiments with synthetically defined UV-damaged oligo. All authors contributed towards writing and reviewing the manuscript.

Additional Information

Supplementary information accompanies this paper at http://www.nature.com/srep

Competing financial interests: The authors declare no competing financial interests.

How to cite this article: Purohit, N. K. *et al.* Characterization of the interactions of PARP-1 with UV-damaged DNA *in vivo* and *in vitro*. *Sci. Rep.* **6**, 19020; doi: 10.1038/srep19020 (2016).

frontiers in
PHARMACOLOGY

MINI REVIEW ARTICLE
published: 27 February 2013
doi: 10.3389/fphar.2013.00018

Resistance to PARP-inhibitors in cancer therapy

Alicia Montoni, Mihaela Robu, Émilie Pouliot and Girish M. Shah*

Laboratory for Skin Cancer Research, (CHU-Q) Hospital Research Centre of Laval University, Laval University, Québec, QC, Canada

Edited by:
Gerald Batist, McGill University, Canada

Reviewed by:
Hu Liu, Anhui Medical University, China
Michael Witcher, McGill University, Canada

****Correspondence:***
Girish M. Shah, Laboratory for Skin, Cancer Research, (CHU-Q) Hospital, Research Centre of Laval University, Laval University, 2705, Laurier Boulevard, Québec, QC G1V 4G2, Canada.
e-mail: girish.shah@crchul.ulaval.ca

The pharmacological inhibitors of poly(ADP-ribose) polymerase (PARP) family of proteins have shown promising results in preclinical studies and clinical trials as a monotherapy or in combination therapy for some cancers. Thus, usage of PARP-inhibitors (PARPi) in cancer therapy is bound to increase with time, but resistance of cancer cells to PARPi is also beginning to be observed. Here we review different known and potential mechanisms by which: (i) PARPi kill cancer cells; and (ii) cancer cells develop resistance to PARPi. Understanding the lethality caused by PARPi and the countermeasures deployed by cancers cells to survive PARPi will help us rationalize the use of this new class of drugs in cancer therapy.

Keywords: poly(ADP-ribose) polymerase, PARP-inhibitors, synthetic lethality, potentiation of anti-cancer therapy, resistance to PARP-inhibitors, DNA damage, DNA repair

Recent clinical trials with poly(ADP-ribose) polymerase-inhibitors as a monotherapy or in combination therapy have shown promising results against different cancers (Lord and Ashworth, 2012). Therefore, their use in cancer therapy is likely to increase, resulting in the inevitable appearance of PARPi-resistant cancers (Chiarugi, 2012). Here, we first discuss different mechanisms by which PARPi can kill cancer cells and then review several known and potential mechanisms by which cancers can become resistant to PARPi.

MECHANISMS OF ACTION OF PARPi IN CANCER THERAPY

PARP-1 AS THE PRINCIPLE TARGET FOR THERAPEUTIC ACTIVITY OF PARPi

There are 18 members of the PARP family of proteins, but therapeutic effect of PARPi on cancer cells is observed only in conjunction with DNA damage; hence DNA damage-responsive PARPs are the most likely mediators of PARPi effect. Among three such PARPs, PARP-1 is the principle responder to DNA damage, as it rapidly reaches the damaged site and mounts a robust catalytic activation response that influences different cellular responses to DNA damage (Javle and Curtin, 2011; Yélamos et al., 2011; Gibson and Kraus, 2012). The activated PARP-1 splits the substrate nicotinamide adenine dinucleotide (NAD^+) to release ADP-ribose, nicotinamide, and protons (Affar et al., 2002; Shah et al., 2011). PARP-1 then forms polymers of ADP-ribose (PAR) that post-translationally modify (i.e., PARylate) PARP-1 itself and selected target proteins to control a wide array of cellular processes, such as cell death, transcription, cell division, and DNA repair (Krishnakumar and Kraus, 2010). Among the DNA repair pathways, PARP-1 is widely recognized for its impact on the base excision repair (BER) and single strand break (SSB) repair pathways, but it also influences homologous recombination (HR) and non-homologous end-joining (NHEJ) repair of double strand breaks (DSB; Yélamos et al., 2011; De Vos et al., 2012). In addition, it also plays a role in mismatch repair (Liu et al., 2012) and more recently the nucleotide excision repair pathways (King et al., 2012; Luijsterburg et al., 2012; Pines et al., 2012; Robu et al., 2013).

In contrast to PARP-1, the other two DNA damage-responsive PARPs play a limited role in DNA damage responses. For example, PARP-2, in conjunction with PARP-1, has been shown to affect BER (Schreiber et al., 2002) and restart the stalled replication forks (Bryant et al., 2009). PARP-3 plays a role in NHEJ pathway in conjunction with APLF (Rulten et al., 2011) or PARP-1 (Boehler et al., 2011) and helps activation of PARP-1 (Loseva et al., 2010). In the context of the role of PARPi in inhibiting PARylation activity of PARPs, it is pertinent to note that PARP-2 has a very weak PARylation activity as compared to PARP-1, and many functions of PARP-2 and 3 are associated with PARP-1. Therefore, one could argue that the main target for PARPi is on the role of PARP-1 in DNA repair with possibly some effect on the roles of PARP-2 and 3. Finally, we should not exclude the possibility that the roles of PARP-1 in cell death and transcription are also involved in the therapeutic effect of PARPi.

COMPETITIVE PARPi HAVE CONSISTENT THERAPEUTIC ACTIVITY

Most consistent results in clinical trials have been obtained with competitive PARPi, which are analogs of nicotinamide that compete with the substrate NAD^+ to bind to the enzyme. Unlike weak inhibitory activity of nicotinamide, its derivatives ranging from the first generation 3-aminobenzamide to the third generation Olaparib and Rucaparib are better inhibitors of PARP-1 and PARP-2 (**Table 1**). The Iniparib, originally developed as a non-competitive inhibitor of PARP-1, showed early successes in clinical trials, but it is a non-specific and weak inhibitor of PARP-1 (Patel et al., 2012). Hence this review will focus on the results obtained with competitive PARPi.

Table 1 | Different PARPi currently in clinical trials and their relative inhibitory potential against PARP-1 and PARP-2 (adapted from Davar et al., 2012).

Inhibitor	Other name(s)	IC_{50}/Ki	IC_{50}/Ki for PARP-1	IC_{50}/Ki for PARP-2	Trial status	Type of cancer(s)
Olaparib	AZD2281 KU0059436	IC50	5 nM	1 nM	Phase I/II singly or combination	Breast, ovarian, colorectal, solid tumors, pancreatic, prostate, carcinoma of esophagus, head and neck squamous cells carcinoma, gastric, NSCLC, brain, CNS, Ewing's sarcoma, uterine, fallopian tube, etc.
Veliparib	ABT-888	Ki	5.2 nM	2.9 nM	Phase I/II singly or combination	Breast, colorectal, GBM, melanoma, solid tumors, pancreatic, fallopian tube, peritoneal cavity, pancreatic, brain, CNS, lymphoma, multiple myeloma, etc.
Rucaparib	AG014699 PF01367338	Ki	1.4 nM	–	Phase I combined with chemotherapy/phase II singly in BRCA associated status	Breast, ovarian, solid tumors (also diabetes mellitus)
INO-1001	–	IC50	50 nM	–	Phase I/II	Cardiovascular disease/combination with TMZ in melanoma
MK-4827	–	IC50	3.8 nM	2.1 nM	Phase I singly or with chemotherapy/phase II	Ovarian, solid tumors, glioblastoma multiform, melanoma, lymphoma, chronic lymphocytic leukemia, T-cell-pro-lymphocytic leukemia

PARPi AS SYNTHETIC LETHAL MONOTHERAPY FOR DSB REPAIR DEFECTIVE TUMORS

It was suggested that two mutations should be considered synthetic lethal if cells with either mutation are viable but those with both mutations are non-viable (Dobzhansky, 1946). The first success of this approach was observed in 2005, when two groups showed that PARPi, which is non-toxic to normal cells, is lethal to BRCA1/2 cancer cells that are deficient in HR-mediated repair of DSB (Bryant et al., 2005; Farmer et al., 2005; Helleday et al., 2005). Several clinical trials for different cancers have since been launched with PARPi, and a list of current trials is shown in **Table 1**.

There are different possible mechanisms by which PARPi kill HR-deficient tumor cells (Helleday, 2011). It was initially suggested that constant DNA damage induced by endogenous factors, such as oxidants needs to be repaired by BER in which PARP-1 participates either by binding to SSB or by collaborating with XRCC-1 (**Figure 1**, steps A and B). Thus, when PARPi block BER, the unrepaired SSB would stall and collapse the replication fork to create DSB (**Figure 1**, step C). The normal cells would survive by readily repairing these DSB by error-free HR or error-prone NHEJ (**Figure 1**, steps D or E). However, the DSB would be lethal to HR-deficient BRCA1/2 tumors with an excessive reliance on the error-prone NHEJ repair pathway (Aly and Ganesan, 2011). This scenario is most plausible and is supported by significant evidence, but it does not explain many things, such as lack of accumulation of SSB in PARPi-treated cells or the absence of synthetic lethality by targeting XRCC-1 in BRCA-deficient cells (Helleday, 2011).

Therefore, alternative explanations have been offered for synthetic lethality of PARPi in HR-deficient cells. In brief, it has been shown that PARP-1 binds to and is activated by SSB-intermediates formed during BER, which results in release of PARylated PARP-1 from SSB, which are then repaired (Strom et al., 2011). Thus, it is proposed that in the presence of PARPi, SSB bound to PARP-1 would collapse the replication fork and DSB-mediated lethality will occur in HR-deficient cells (Helleday, 2011). It is also possible that the role of PARP-1 in suppressing the error-prone NHEJ is the target for PARPi-induced lethality in HR-deficient cells, because inhibition or downregulation of multiple components of NHEJ, such as Ku80, Artemis, and DNA-PK, made HR-deficient cells resistant to PARPi (Patel et al., 2011). Finally, it has been suggested that since PARP-1 plays a role in reactivating the stalled replication forks, this step could be a target for PARPi-induced lethality in HR-deficient cells (Helleday, 2011).

Cancer cells are known to carry other conditions that create HR-deficiency or BRCAness, which can make them susceptible to synthetic lethality by PARPi. Three such examples are listed here (**Figure 1**, step D). (i) The protein kinase ataxia telangiectasia mutated (ATM), a key regulator that senses DNA damage, initiates the protein kinase cascade (Wang and Weaver, 2011) and plays a role in HR, is frequently mutated in lymphoid malignancies. Interestingly, PARPi is synthetic lethal to the ATM mutant lymphoid tumor cells (Weston et al., 2010). (ii) Aurora-1 is frequently amplified and overexpressed in breast cancers (Staff et al., 2010). An overexpression of Aurora-1 induces BRCAness in an otherwise HR-competent PIR12 pancreatic tumor cells by causing an impaired recruitment of key HR-protein RAD51, and sensitizes them to synthetic lethality by PARPi (Sourisseau et al., 2010). (iii) PTEN (phosphatase and tensin homolog), which plays a crucial role in regulating PI3K/Akt-1-mTOR signaling pathway, is frequently mutated or decreased in a wide range of human tumors (Salmena et al., 2008). The PTEN-*null* cancer cells, which are HR-defective due to reduced expression and nuclear localization of RAD51, are sensitive to PARPi (Mendes-Pereira et al., 2009; Dedes et al., 2010; McEllin et al., 2010; **Figure 1**, step D). Although

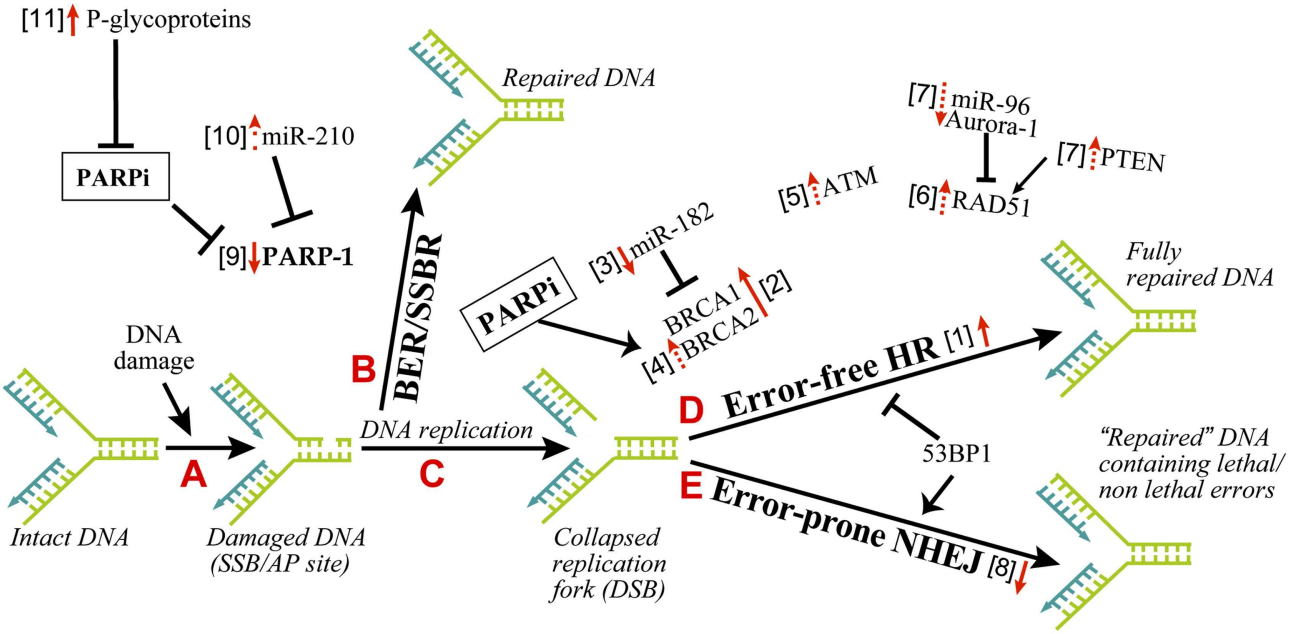

FIGURE 1 | Mechanisms of resistance to PARPi in cancer therapy. The principle explanation for the efficacy of PARPi as synthetic lethal therapy in DNA double strand break (DSB) repair defective cancer cells or as a combination therapy with other agents for other cancers rests on the role of PARP-1 in BER and SSBR. As shown in the series of A–E steps, the inefficient repair of DNA single strand breaks by PARP-1-mediated BER in the presence of PARPi would lead to DSB. An inefficient repair of DSB by HR-deficient cancer cells will kill these cells, whereas normal cells with proper DSB repair capacity will survive. The resistance to PARPi can occur in cancer cells by alteration of various parameters, which influence different steps in this pathway. The changes in these factors, i.e., upregulation or downregulation as pointed by the direction of red arrows, is associated with resistance to PARPi. The solid or dashed arrows indicate known or hypothesized mechanisms of resistance to PARPi, respectively. The numbers within square bracket next to the arrows refer to the explanation in the text for this mechanism of PARPi-resistance.

another study reported that PTEN deficiency in prostate cancer cells is not associated with BRCAness or sensitivity to PARPi (Fraser et al., 2012), suggesting a need for more work in this model.

Finally, PARPi sensitivity has also been reported under circumstances without BRCAness. For example, the depletion of NHEJ components DNA-PK or Ku80 made HR-proficient cells more sensitive to PARPi (Bryant and Helleday, 2006). PARPi sensitivity is also observed in conditions with no apparent defect in any of the DNA repair pathway. The sporadic breast cancer cells overexpressing HER2 (human epidermal growth factor receptor 2) are addicted to overexpression of NF-κB-mediated transcription for survival. Since PARP-1 is a co-activator of NF-κB, the treatment with PARPi abrogates NF-κB-mediated transcription and kills these cancer cells (Nowsheen et al., 2012).

Overall, the ability of PARPi to cause synthetic lethality in cancer cells with BRCAness as well as many other conditions indicates a potential for their use as monotherapy for a wide variety of cancers.

PARPi IN COMBINATION THERAPY FOR DNA REPAIR PROFICIENT TUMORS

All of the above studies dealing with synthetic lethal effect of PARPi rely on the DNA damage induced by endogenous factors, such as oxidants created during metabolism. Therefore, it is not surprising that PARPi also potentiates lethality of exogenous DNA damaging agents, such as chemotherapeutic agents or ionising radiations (Javle and Curtin, 2011). Such combination therapy has the potential to kill cancer cells with no apparent defect in DNA repair, because chemotherapy induced SSB will be amplified by PARPi to make a large flux of DSB that will overwhelm the normal DSB repair capacity of these tumors and cause death (**Figure 1**, steps B–E). In the actual clinical conditions for treatment of cancer patients, it is highly likely that PARPi will be used most frequently in combination therapy for DNA repair proficient and even for DNA repair deficient tumors.

MECHANISMS OF RESISTANCE TO PARPi IN CANCER THERAPY

There are four categories of known and potential mechanisms of resistance to PARPi in cancer cells, which are described below: (i) increased HR capacity; (ii) altered NHEJ capacity; (iii) decreased levels or activity of PARP-1, and (iv) decreased intracellular availability of PARPi.

INCREASED HR CAPACITY

Since pre-existing HR defect is the initial lesion that allows PARPi to kill HR-deficient tumors, any of the following conditions that restore HR could result in the resistance to PARPi (**Figure 1**, step D, arrow #1).

Reverse mutation of brca

The resistance of BRCA tumors or cells to PARPi was initially identified to be due to reverse mutations in *brca1/2* and restoration of HR (**Figure 1**, step D, arrow #2; Ashworth, 2008; Edwards et al., 2008; Sakai et al., 2008; Swisher et al., 2008; Norquist et al., 2011; Barber et al., 2013). For BRCA2, reverse mutation was in part due to intragenic deletion of the c.6174delT mutation and restoration of the open reading frame (Ashworth, 2008). The genomic instability associated with BRCA loss could be a cause for reverse mutations of *brca* (Aly and Ganesan, 2011). Certain BRCA1-deficient tumors carry hypomorphic BRCA1 mutations within its population (Drost et al., 2011); hence a selection of cells with restored BRCA function could confer resistance to PARPi.

Overexpression of BRCA via downregulation of miR-182 or PARP-1

BRCA1 expression is negatively regulated by the microRNA miR-182; hence miR-182 overexpression sensitizes BRCA1-proficient breast cancer cells to PARPi, whereas its downregulation made them resistant to PARPi (Moskwa et al., 2011; **Figure 1**, step D, arrow #3). PARP-1 and its activity is a negative modulator of BRCA2, because PARP-1 binds to the silencer-binding region of the *brca2* promoter (Wang et al., 2008). Hence PARPi mediated suppression of PARP-1 activity could lead to overexpression of BRCA2 and resistance to PARPi (**Figure 1**, step D, arrow #4).

ATM-mediated HR during loss of 53BP1 in BRCA-deficient background

53BP1 is a nuclear protein that plays a key role in DNA repair responses and checkpoint control (Bunting et al., 2010). Together, BRCA1 and 53BP1 determine the balance between NHEJ and HR, because the loss of BRCA1 results in a profound defect in HR and increased NHEJ repair, whereas loss of 53BP1 suppresses NHEJ and promotes HR (**Figure 1**, steps D–E). While cells with defect in BRCA1 alone were susceptible to PARPi, an additional loss of 53BP1 allowed a partial ATM-dependent HR repair (Aly and Ganesan, 2011), making these cells resistant to PARPi (Cao et al., 2009; Bouwman et al., 2010; Bunting et al., 2010; Brandsma and Gent, 2012; Oplustilova et al., 2012). Thus, increased ATM alone could induce resistance to PARPi (**Figure 1**, steps D–E, arrow #5).

Increased activity of RAD51

RAD51 is a key HR-protein; therefore any factor that increases RAD51 levels or activity can potentially lead to a resistance to PARPi (**Figure 1**, step D, arrow #6). The levels of RAD51 are suppressed by miR-96 (Wang et al., 2012) and Aurora-1 (Sourisseau et al., 2010) and increased by PTEN (Dedes et al., 2010). Hence, we hypothesize that decreased miR-96 and Aurora-1 or increased PTEN can increase RAD51 and HR activity leading to the resistance to PARPi (**Figure 1**, step D, arrows #7). This is indirectly supported by the observation that increased RAD51 levels make colon carcinoma cells resistant to the combined treatment of PARPi and temozolomide (Liu et al., 2009).

ALTERED NHEJ CAPACITY

One of the causes for synthetic lethality of PARPi in HR-deficient cells is an upregulation of the error-prone NHEJ pathway that is normally suppressed by PARP-1. Hence any decrease in NHEJ capacity in these cells could increase their resistance to PARPi, as shown in BRCA2-deficient cells by inhibition or downregulation of Ku80, Artemis, or DNA-PK (**Figure 1**, step E, arrow #8; Patel et al., 2011). On the flip side, it has been suggested that normal NHEJ function and the genomic instability mediated by NHEJ could be one of the causes for reversion of the mutation of *brca1/2*, restoration of partial HR capacities and development of resistance to PARPi in HR-deficient tumors (Chiarugi, 2012; **Figure 1**, step D, arrow #2). Thus, both increased and decreased NHEJ capacity of cells could lead to resistance to PARPi in different contexts.

DECREASED LEVELS OR ACTIVITY OF PARP-1

The effectiveness of PARPi in anti-cancer therapy requires that its target PARP-1 is available for inhibition; because in PARPi-treated cells, PARP-1 will still bind to DNA strand breaks but will not be activated to form PAR or facilitate DNA repair events. Hence reduced levels of PARP-1 could result in resistance to PARPi (**Figure 1**, step B, arrow #9). In fact, PARP-1 levels are significantly decreased in the PARPi and temozolomide-resistant clones of colorectal carcinoma HCT116 cells (Liu et al., 2009). Therefore, it will be interesting to see if alterations in PARP-1 levels during different stages in tumor development are also associated with a corresponding change in sensitivity to PARPi. For example, levels of miR-210, which suppresses PARP-1 expression, are initially decreased when normal breast cells are transformed to ductal carcinoma *in situ*, and they are increased during further transition to the invasive ductal carcinoma stage (Volinia et al., 2012). It will be interesting to test in such a series of samples, whether these changes in miR-210 are inversely associated with alterations in the levels of PARP-1 and directly correlated with the resistance to PARPi (**Figure 1**, step B, arrow #10). There have been reports of a correlation between the abundance of cytoplasmic PARP-1 and higher sensitivity to chemotherapy in breast cancer samples (Domagala et al., 2011; von Minckwitz et al., 2011; Klauke et al., 2012). However, cytoplasmic PARP-1 was detected at a very low frequency in these tumors, and since we do not know any role for cytoplasmic PARP-1 in DNA damage responses, it is difficult at this moment to rationalize the link between cytoplasmic PARP-1 and resistance to PARPi.

The effectiveness of PARPi is also linked to the catalytic activity of PARP-1. Hence any factor that decreases the activity of PARP-1 could influence the efficacy of PARPi. The cancer cells with normal levels of PARP-1 but decreased enzymatic activity as noted by reduced level of endogenous PARylation are more resistant to PARPi (Oplustilova et al., 2012; **Figure 1**, step B, arrow #9). As a corollary, HR-deficient tumor cells with higher endogenous PARylation activity are more sensitive to PARPi (Gottipati et al., 2010).

Variant forms of PARP-1 with decreased catalytic activity, such as those created by small nucleotide polymorphism (SNP), could make cancer cells resistant to PARPi. In human cancers, some SNP have indeed been found to some extent, such as V^{762}/A (Lockett et al., 2004; Wang et al., 2007; Zaremba et al., 2009) or M^{129}/T and E^{251}/K (Ogino et al., 2010). However, there is no consensus as to whether V^{762}/A reduces enzyme activity and other mutants do not have significant effect on enzyme function. Thus,

it is difficult to predict the effect of SNP on the effectiveness of PARPi.

DECREASED INTRACELLULAR AVAILABILITY OF PARPi

A cancer cell that can efficiently throw PARPi out of the cell can become relatively resistant to this therapy. The p-glycoproteins (P-gp) also called multi-drug resistance proteins are involved in the efflux of PARPi (**Figure 1**, step A, arrow #11), because P-gp inhibitors prevent the decrease of PARPi in HCT116 colon cancer cells (Oplustilova et al., 2012) and re-sensitize PARPi-resistant BRCA-1 deficient cells to PARPi (Rottenberg et al., 2008). In the mouse mammary tumor models, PARPi was more effective when P-gp knockout condition was added to BRCA-1 deficient cells (Jaspers et al., 2012). The P-gp belong to ABC transporter family which is inhibited by ADP-ribose, a product of catalytic activity of PARP-1 (Dumitriu et al., 2004). Therefore, it is feasible that PARPi that would prevent formation of ADP-ribose can permit full activity of P-gp to eliminate PARPi from the cells. Nonetheless, more work is needed in this domain because the resistance to drug via upregulation of P-gp has not yet been shown in human tumoral tissues (Borst, 2012).

CONCLUSION

In cancer treatment with PARPi, the personalization of therapy is important because many factors can influence the efficiency of PARPi, such as HR and NHEJ status, PARP-1 levels or its activity and finally other factors that influence intracellular concentrations of PARPi. Therefore, it would be necessary to assess the status of these controlling factors before beginning the treatment with PARPi (Lord and Ashworth, 2012; Ratner et al., 2012). A thorough understanding of different mechanisms for the resistance to PARPi will permit us to design better PARPi monotherapy as well as combination therapy, and will allow us to identify conditions that can re-sensitize tumor cells to PARPi; and thus treat cancer patients more efficiently.

ACKNOWLEDGMENTS

We wish to acknowledge very useful comments made by the reviewers. The scholarship support was received from NSERC and Laval University (Émilie Pouliot and Mihaela Robu). This work was supported by the CIHR operating grant#89964 to Girish M. Shah.

REFERENCES

Affar, E. B., Shah, R. G., Dallaire, A.-K., Castonguay, V., and Shah, G. M. (2002). Role of poly(ADP-ribose) polymerase in rapid intracellular acidification induced by alkylating DNA damage. *Proc. Natl. Acad. Sci. U.S.A.* 99, 245–250.

Aly, A., and Ganesan, S. (2011). BRCA1, PARP, and 53BP1: conditional synthetic lethality and synthetic viability. *J. Mol. Cell Biol.* 3, 66–74.

Ashworth, A. (2008). A synthetic lethal therapeutic approach: poly(ADP) ribose polymerase inhibitors for the treatment of cancers deficient in DNA double-strand break repair. *J. Clin. Oncol.* 26, 3785–3790.

Barber, L. J., Sandhu, S., Chen, L., Campbell, J., Kozarewa, I., Fenwick, K., et al. (2013). Secondary mutations in BRCA2 associated with clinical resistance to a PARP inhibitor. *J. Pathol.* 229, 422–429.

Boehler, C., Gauthier, L. R., Mortusewicz, O., Biard, D. S., Saliou, J. M., Bresson, A., et al. (2011). Poly(ADP-ribose) polymerase 3 (PARP3), a newcomer in cellular response to DNA damage and mitotic progression. *Proc. Natl. Acad. Sci. U.S.A.* 108, 2783–2788.

Borst, P. (2012). Cancer drug pan-resistance: pumps, cancer stem cells, quiescence, epithelial to mesenchymal transition, blocked cell death pathways, persisters or what? *Open Biol.* 2, 120066.

Bouwman, P., Aly, A., Escandell, J. M., Pieterse, M., Bartkova, J., van der Gulden, H., et al. (2010). 53BP1 loss rescues BRCA1 deficiency and is associated with triple-negative and BRCA-mutated breast cancers. *Nat. Struct. Mol. Biol.* 17, 688–695.

Brandsma, I., and Gent, D. C. (2012). Pathway choice in DNA double strand break repair: observations of a balancing act. *Genome Integr.* 3, 9.

Bryant, H. E., and Helleday, T. (2006). Inhibition of poly (ADP-ribose) polymerase activates ATM which is required for subsequent homologous recombination repair. *Nucleic Acids Res.* 34, 1685–1691.

Bryant, H. E., Petermann, E., Schultz, N., Jemth, A. S., Loseva, O., Issaeva, N., et al. (2009). PARP is activated at stalled forks to mediate Mre11-dependent replication restart and recombination. *EMBO J.* 28, 2601–2615.

Bryant, H. E., Schultz, N., Thomas, H. D., Parker, K. M., Flower, D., Lopez, E., et al. (2005). Specific killing of BRCA2-deficient tumours with inhibitors of poly(ADP-ribose) polymerase. *Nature* 434, 913–917.

Bunting, S. F., Callen, E., Wong, N., Chen, H. T., Polato, F., Gunn, A., et al. (2010). 53BP1 inhibits homologous recombination in Brca1-deficient cells by blocking resection of DNA breaks. *Cell* 141, 243–254.

Cao, L., Xu, X., Bunting, S. F., Liu, J., Wang, R. H., Cao, L. L., et al. (2009). A selective requirement for 53BP1 in the biological response to genomic instability induced by Brca1 deficiency. *Mol. Cell* 35, 534–541.

Chiarugi, A. (2012). A snapshot of chemoresistance to PARP inhibitors. *Trends Pharmacol. Sci.* 33, 42–48.

Davar, D., Beumer, J. H., Hamieh, L., and Tawbi, H. (2012). Role of PARP inhibitors in cancer biology and therapy. *Curr. Med. Chem.* 19, 3907–3921.

De Vos, M., Schreiber, V., and Dantzer, F. (2012). The diverse roles and clinical relevance of PARPs in DNA damage repair: current state of the art. *Biochem. Pharmacol.* 84, 137–146.

Dedes, K. J., Wetterskog, D., Mendes-Pereira, A. M., Natrajan, R., Lambros, M. B., Geyer, F. C., et al. (2010). PTEN deficiency in endometrioid endometrial adenocarcinomas predicts sensitivity to PARP inhibitors. *Sci. Transl. Med.* 2, 53ra75.

Dobzhansky, T. (1946). Genetics of natural populations. Xiii. Recombination and variability in populations of Drosophila pseudoobscura. *Genetics* 31, 269–290.

Domagala, P., Huzarski, T., Lubinski, J., Gugala, K., and Domagala, W. (2011). PARP-1 expression in breast cancer including BRCA1-associated, triple negative and basal-like tumors: possible implications for PARP-1 inhibitor therapy. *Breast Cancer Res. Treat.* 127, 861–869.

Drost, R., Bouwman, P., Rottenberg, S., Boon, U., Schut, E., Klarenbeek, S., et al. (2011). BRCA1 RING function is essential for tumor suppression but dispensable for therapy resistance. *Cancer Cell* 20, 797–809.

Dumitriu, I. E., Voll, R. E., Kolowos, W., Gaipl, U. S., Heyder, P., Kalden, J. R., et al. (2004). UV irradiation inhibits ABC transporters via generation of ADP-ribose by concerted action of poly(ADP-ribose) polymerase-1 and glycohydrolase. *Cell Death Differ.* 11, 314–320.

Edwards, S. L., Brough, R., Lord, C. J., Natrajan, R., Vatcheva, R., Levine, D. A., et al. (2008). Resistance to therapy caused by intragenic deletion in BRCA2. *Nature* 451, 1111–1115.

Farmer, H., McCabe, N., Lord, C. J., Tutt, A. N., Johnson, D. A., Richardson, T. B., et al. (2005). Targeting the DNA repair defect in BRCA mutant cells as a therapeutic strategy. *Nature* 434, 917–921.

Fraser, M., Zhao, H., Luoto, K. R., Lundin, C., Coackley, C., Chan, N., et al. (2012). PTEN deletion in prostate cancer cells does not associate with loss of RAD51 function: implications for radiotherapy and chemotherapy. *Clin. Cancer Res.* 18, 1015–1027.

Gibson, B. A., and Kraus, W. L. (2012). New insights into the molecular and cellular functions of poly(ADP-ribose) and PARPs. *Nat. Rev. Mol. Cell Biol.* 13, 411–424.

Gottipati, P., Vischioni, B., Schultz, N., Solomons, J., Bryant, H. E., Djureinovic, T., et al. (2010). Poly(ADP-ribose) polymerase is hyperactivated in homologous recombination-defective cells. *Cancer Res.* 70, 5389–5398.

Helleday, T. (2011). The underlying mechanism for the PARP and BRCA synthetic lethality: clearing up the misunderstandings. *Mol. Oncol.* 5, 387–393.

Helleday, T., Bryant, H. E., and Schultz, N. (2005). Poly(ADP-ribose) polymerase (PARP-1) in homologous recombination and as a target for cancer therapy. *Cell Cycle* 4, 1176–1178.

Jaspers, J. E., Kersbergen, A., Boon, U., Sol, W., van Deemter, L., Zander, S. A., et al. (2012). Loss of 53BP1 causes PARP inhibitor resistance in BRCA1-mutated mouse mammary tumors. *Cancer Discov.* 3, 68–81.

Javle, M., and Curtin, N. J. (2011). The role of PARP in DNA repair and its therapeutic exploitation. *Br. J. Cancer* 105, 1114–1122.

King, B. S., Cooper, K. L., Liu, K. J., and Hudson, L. G. (2012). Poly(ADP-ribose) contributes to an association between Poly(ADP-ribose)polymerase-1 and xeroderma pigmentosum complementation group A in nucleotide excision repair. *J. Biol. Chem.* 287, 39824–39833.

Klauke, M. L., Hoogerbrugge, N., Budczies, J., Bult, P., Prinzler, J., Radke, C., et al. (2012). Higher cytoplasmic and nuclear poly(ADP-ribose) polymerase expression in familial than in sporadic breast cancer. *Virchows Arch.* 461, 425–431.

Krishnakumar, R., and Kraus, W. L. (2010). The PARP side of the nucleus: molecular actions, physiological outcomes, and clinical targets. *Mol. Cell* 39, 8–24.

Liu, X., Han, E. K., Anderson, M., Shi, Y., Semizarov, D., Wang, G., et al. (2009). Acquired resistance to combination treatment with temozolomide and ABT-888 is mediated by both base excision repair and homologous recombination DNA repair pathways. *Mol. Cancer Res.* 7, 1686–1692.

Liu, Y., Kadyrov, F. A., and Modrich, P. (2012). PARP-1 enhances the mismatch-dependence of 5′-directed excision in human mismatch repair in vitro. *DNA Repair (Amst.)* 10, 1145–1153.

Lockett, K. L., Hall, M. C., Xu, J., Zheng, S. L., Berwick, M., Chuang, S. C., et al. (2004). The ADPRT V762A genetic variant contributes to prostate cancer susceptibility and deficient enzyme function. *Cancer Res.* 64, 6344–6348.

Lord, C. J., and Ashworth, A. (2012). The DNA damage response and cancer therapy. *Nature* 481, 287–294.

Loseva, O., Jemth, A. S., Bryant, H. E., Schuler, H., Lehtio, L., Karlberg, T., et al. (2010). PARP-3 is a mono-ADP-ribosylase that activates PARP-1 in the absence of DNA. *J. Biol. Chem.* 285, 8054–8060.

Luijsterburg, M. S., Lindh, M., Acs, K., Vrouwe, M. G., Pines, A., van Attikum, H., et al. (2012). DDB2 promotes chromatin decondensation at UV-induced DNA damage. *J. Cell Biol.* 197, 267–281.

McEllin, B., Camacho, C. V., Mukherjee, B., Hahm, B., Tomimatsu, N., Bachoo, R. M., et al. (2010). PTEN loss compromises homologous recombination repair in astrocytes: implications for glioblastoma therapy with temozolomide or poly(ADP-ribose) polymerase inhibitors. *Cancer Res.* 70, 5457–5464.

Mendes-Pereira, A. M., Martin, S. A., Brough, R., McCarthy, A., Taylor, J. R., Kim, J. S., et al. (2009). Synthetic lethal targeting of PTEN mutant cells with PARP inhibitors. *EMBO Mol. Med.* 1, 315–322.

Moskwa, P., Buffa, F. M., Pan, Y., Panchakshari, R., Gottipati, P., Muschel, R. J., et al. (2011). miR-182-mediated downregulation of BRCA1 impacts DNA repair and sensitivity to PARP inhibitors. *Mol. Cell* 41, 210–220.

Norquist, B., Wurz, K. A., Pennil, C. C., Garcia, R., Gross, J., Sakai, W., et al. (2011). Secondary somatic mutations restoring BRCA1/2 predict chemotherapy resistance in hereditary ovarian carcinomas. *J. Clin. Oncol.* 29, 3008–3015.

Nowsheen, S., Cooper, T., Bonner, J. A., Lobuglio, A. F., and Yang, E. S. (2012). HER2 overexpression renders human breast cancers sensitive to PARP inhibition independently of any defect in homologous recombination DNA repair. *Cancer Res.* 72, 4796–4806.

Ogino, H., Nakayama, R., Sakamoto, H., Yoshida, T., Sugimura, T., and Masutani, M. (2010). Analysis of poly(ADP-ribose) polymerase-1 (PARP1) gene alteration in human germ cell tumor cell lines. *Cancer Genet. Cytogenet.* 197, 8–15.

Oplustilova, L., Wolanin, K., Mistrik, M., Korinkova, G., Simkova, D., Bouchal, J., et al. (2012). Evaluation of candidate biomarkers to predict cancer cell sensitivity or resistance to PARP-1 inhibitor treatment. *Cell Cycle* 11, 3837–3850.

Patel, A. G., De Lorenzo, S. B., Flatten, K. S., Poirier, G. G., and Kaufmann, S. H. (2012). Failure of iniparib to inhibit poly(ADP-Ribose) polymerase in vitro. *Clin. Cancer Res.* 18, 1655–1662.

Patel, A. G., Sarkaria, J. N., and Kaufmann, S. H. (2011). Nonhomologous end joining drives poly(ADP-ribose) polymerase (PARP) inhibitor lethality in homologous recombination-deficient cells. *Proc. Natl. Acad. Sci. U.S.A.* 108, 3406–3411.

Pines, A., Vrouwe, M. G., Marteijn, J. A., Typas, D., Luijsterburg, M. S., Cansoy, M., et al. (2012). PARP1 promotes nucleotide excision repair through DDB2 stabilization and recruitment of ALC1. *J. Cell Biol.* 199, 235–249.

Ratner, E. S., Sartorelli, A. C., and Lin, Z. P. (2012). Poly (ADP-ribose) polymerase inhibitors: on the horizon of tailored and personalized therapies for epithelial ovarian cancer. *Curr. Opin. Oncol.* 24, 564–571.

Robu, M., Shah, R. G., Petitclerc, N., Brind'Amour, J., Kandan-Kulangara, F., and Shah, G. M. (2013). Role of poly(ADP-ribose) polymerase-1 in the removal of UV-induced DNA lesions by nucleotide excision repair. *Proc. Natl. Acad. Sci. U.S.A.* 110, 1658–1663.

Rottenberg, S., Jaspers, J. E., Kersbergen, A., van der Burg, E., Nygren, A. O., Zander, S. A., et al. (2008). High sensitivity of BRCA1-deficient mammary tumors to the PARP inhibitor AZD2281 alone and in combination with platinum drugs. *Proc. Natl. Acad. Sci. U.S.A.* 105, 17079–17084.

Rulten, S. L., Fisher, A. E., Robert, I., Zuma, M. C., Rouleau, M., Ju, L., et al. (2011). PARP-3 and APLF function together to accelerate nonhomologous end-joining. *Mol. Cell* 41, 33–45.

Sakai, W., Swisher, E. M., Karlan, B. Y., Agarwal, M. K., Higgins, J., Friedman, C., et al. (2008). Secondary mutations as a mechanism of cisplatin resistance in BRCA2-mutated cancers. *Nature* 451, 1116–1120.

Salmena, L., Carracedo, A., and Pandolfi, P. P. (2008). Tenets of PTEN tumor suppression. *Cell* 133, 403–414.

Schreiber, V., Ame, J. C., Dolle, P., Schultz, I., Rinaldi, B., Fraulob, V., et al. (2002). Poly(ADP-ribose) polymerase-2 (PARP-2) is required for efficient base excision DNA repair in association with PARP-1 and XRCC1. *J. Biol. Chem.* 277, 23028–23036.

Shah, G. M., Kandan-Kulangara, F., Montoni, A., Shah, R. G., Brind'Amour, J., Vodenicharov, M. D., et al. (2011). Approaches to detect PARP-1 activation in vivo, in situ, and in vitro. *Methods Mol. Biol.* 780, 3–34.

Sourisseau, T., Maniotis, D., McCarthy, A., Tang, C., Lord, C. J., Ashworth, A., et al. (2010). Aurora-A expressing tumour cells are deficient for homology-directed DNA double strand-break repair and sensitive to PARP inhibition. *EMBO Mol. Med.* 2, 130–142.

Staff, S., Isola, J., Jumppanen, M., and Tanner, M. (2010). Aurora-A gene is frequently amplified in basal-like breast cancer. *Oncol. Rep.* 23, 307–312.

Strom, C. E., Johansson, F., Uhlen, M., Szigyarto, C. A., Erixon, K., and Helleday, T. (2011). Poly (ADP-ribose) polymerase (PARP) is not involved in base excision repair but PARP inhibition traps a single-strand intermediate. *Nucleic Acids Res.* 39, 3166–3175.

Swisher, E. M., Sakai, W., Karlan, B. Y., Wurz, K., Urban, N., and Taniguchi, T. (2008). Secondary BRCA1 mutations in BRCA1-mutated ovarian carcinomas with platinum resistance. *Cancer Res.* 68, 2581–2586.

Volinia, S., Galasso, M., Sana, M. E., Wise, T. F., Palatini, J., Huebner, K., et al. (2012). Breast cancer signatures for invasiveness and prognosis defined by deep sequencing of microRNA. *Proc. Natl. Acad. Sci. U.S.A.* 109, 3024–3029.

von Minckwitz, G., Muller, B. M., Loibl, S., Budczies, J., Hanusch, C., Darb-Esfahani, S., et al. (2011). Cytoplasmic poly(adenosine diphosphate-ribose) polymerase expression is predictive and prognostic in patients with breast cancer treated with neoadjuvant chemotherapy. *J. Clin. Oncol.* 29, 2150–2157.

Wang, J., Bian, C., Li, J., Couch, F. J., Wu, K., and Zhao, R. C. (2008). Poly(ADP-ribose) polymerase-1 down-regulates BRCA2 expression through the BRCA2 promoter. *J. Biol. Chem.* 283, 36249–36256.

Wang, X., and Weaver, D. T. (2011). The ups and downs of DNA repair biomarkers for PARP inhibitor therapies. *Am. J. Cancer Res.* 1, 301–327.

Wang, X. G., Wang, Z. Q., Tong, W. M., and Shen, Y. (2007). PARP1 Val762Ala polymorphism reduces enzymatic activity. *Biochem. Biophys. Res. Commun.* 354, 122–126.

Wang, Y., Huang, J. W., Calses, P., Kemp, C. J., and Taniguchi, T. (2012). MiR-96 downregulates REV1 and RAD51 to promote cellular sensitivity to cisplatin and PARP inhibition. *Cancer Res.* 72, 4037–4046.

Weston, V. J., Oldreive, C. E., Skowronska, A., Oscier, D. G., Pratt, G., Dyer, M. J., et al. (2010). The PARP inhibitor olaparib induces significant killing of ATM-deficient lymphoid tumor cells in vitro and in vivo. *Blood* 116, 4578–4587.

Yélamos, J., Farrés, J., Llacuna, L., Ampurdanés, C., and Martin-Caballero, J. (2011). PARP-1 and PARP-2: new players in tumor development. *Am. J. Cancer Res.* 1, 328–346.

Zaremba, T., Ketzer, P., Cole, M., Coulthard, S., Plummer, E. R., and Curtin, N. J. (2009). Poly(ADP-ribose) polymerase-1 polymorphisms, expression and activity in selected human tumour cell lines. *Br. J. Cancer* 101, 256–262.

Conflict of Interest Statement: The authors declare that the research was conducted in the absence of any commercial or financial relationship that could be construed as a potential conflict of interest.

Received: 29 December 2012; paper pending published: 21 January 2013; accepted: 05 February 2013; published online: 27 February 2013.

Citation: Montoni A, Robu M, Pouliot É and Shah GM (2013) Resistance to PARP-inhibitors in cancer therapy. Front. Pharmacol. ***4****:18. doi: 10.3389/fphar.2013.00018*

This article was submitted to Frontiers in Pharmacology of Anti-Cancer Drugs, a specialty of Frontiers in Pharmacology.

frontiers in ONCOLOGY

OPINION ARTICLE
published: 14 November 2013
doi: 10.3389/fonc.2013.00279

PARP inhibitors in cancer therapy: magic bullets but moving targets

Girish M. Shah[1], Mihaela Robu[1], Nupur K. Purohit[1], Jyotika Rajawat[1], Lucio Tentori[2] and Grazia Graziani[2]*

[1] Laboratory for Skin Cancer Research, CHU-Q (CHUL) Research Centre, Laval University, Quebec City, QC, Canada
[2] Department of System Medicine, University of Rome "Tor Vergata", Rome, Italy
*Correspondence: girish.shah@crchul.ulaval.ca

Edited by:
Christina Annunziata, National Cancer Institute, USA

Reviewed by:
Daekyu Sun, University of Arizona, USA
Michael Witcher, McGill University, Canada

Keywords: poly(ADP-ribose) polymerase (PARP), PARP inhibitors (PARPi), cancer therapy, BRCA-mutant cancers, synthetic lethality, combination therapy, multiple targets of PARPi

The pharmacological inhibitors of poly(ADP-ribose) polymerase-1 (PARP-1) have reached the first milestone toward their inclusion in the arsenal of anti-cancer drugs by showing consistent benefits in clinical trials against BRCA-mutant cancers that are deficient in the homologous recombination repair (HRR) of DNA double strand breaks (DSB) (1, 2). PARP inhibitors (PARPi) also potentiate therapeutic efficacy of ionizing radiation and some chemotherapeutic agents (1). These effects of PARPi were initially linked to inhibition of the role of PARP-1 in base excision repair (BER) of DNA damaged by endogenous or exogenous agents, resulting in accumulation of single strand breaks (SSB), which upon conversion to toxic DSB lesions would kill cancer cells deficient in DSB repair (1, 3, 4). However, PARPi lethality in HRR-deficient cancers can also be explained by other mechanisms not involving a direct effect of PARPi on BER [reviewed in Ref. (5, 6)]. In addition, therapeutic benefits of PARPi with agents such as carboplatin in HRR-proficient and -deficient tumors [reviewed in Ref. (1, 7)], simply cannot be explained by BER inhibitory effect of PARPi. Therefore, PARPi are like magic bullets that can kill cancer cells under different circumstances, but to comprehend their global scope and limitations, here we discuss the full range of their targets and the possible impact of broad specificity of current PARPi during prolonged therapy of cancer patients.

MECHANISMS OF ACTION OF PARPi IN CANCER THERAPY: MAGIC BULLETS BUT MOVING TARGETS

It is not surprising that the mechanism of action of PARPi in killing cancer cells still remains an open question, because its principal target PARP-1 is a multifunctional protein implicated in various cellular responses to DNA damage ranging from different pathways of DNA repair and cell death to stress signaling, transcription, and genomic stability (8, 9), all of which could be affected by PARPi and thus influence outcome of cancer therapies. Following are various possibly overlapping mechanisms for the anti-cancer effect of PARPi.

BER/HRR NEXUS FOR SYNTHETIC LETHALITY OF PARPi IN BRCA-MUTANT CANCERS

It was first demonstrated by two teams (3, 4) that two individually non-lethal conditions, i.e., PARPi-mediated inhibition of PARP-1 and BRCA mutation-induced HRR deficiency in cancer cell, would become synthetic lethal when combined in a single cell [reviewed in Ref. (1, 5, 10, 11)] (**Figure 1A**). This model focuses on the role of PARP-1 in BER, the pathway that repairs abasic sites and SSB that are constantly created in the mammalian genome by endogenous oxidants. When PARPi suppress the role of PARP-1 in BER, the unrepaired SSB would accumulate and collapse the DNA replication fork to form potentially lethal DSB. The normal cells would survive by repairing these DSB by HRR, but the HRR-deficient BRCA-mutants would die due to unrepaired DSB or possibly due to excessive reliance on the error-prone non-homologous end-joining (NHEJ) repair pathway to remove DSB (**Figure 1A**). This model also covers minor variations of the central theme as reviewed recently (1, 10) (**Figure 1A**). For example, tumors with other conditions that cause HRR deficiency or "BRCAness" phenotype would also be susceptible to PARPi. It permits inclusion of PARP-2 and its role in BER as target of PARPi, because most current PARPi also inhibit PARP-2 (10). It also explains the potentiating effect of PARPi in the combination therapy with radiation or chemicals, such as temozolomide, irinotecan, or topotecan, because DNA damage caused by these agents is also repaired by BER.

ALTERNATIVE TARGETS OF PARPi IN BRCA-MUTANT CANCERS

However, the above mechanism is inadequate to explain all the effects of PARPi seen in BRCA-mutant cancers, which could be explained by the effect of PARPi on alternate targets, as reviewed earlier (5, 6, 10) (**Figure 1A**). In brief, (i) PARPi could be trapping PARP-1 or PARP-2 to SSB with resultant PARP-SSB complex that would be more toxic than unrepaired SSB or even knockdown of PARPs (5, 12). (ii) PARPi could act via upregulation of NHEJ pathway, which would presumably cause genomic instability and eventual lethality (13). (iii) PARPi could suppress the role of PARP-1 in reactivating DNA replication forks (5). Thus, apart from BER/HRR nexus, there could be NHEJ/HRR or DNA replication/HRR nexus to explain PARPi lethality in BRCA-mutant cancers.

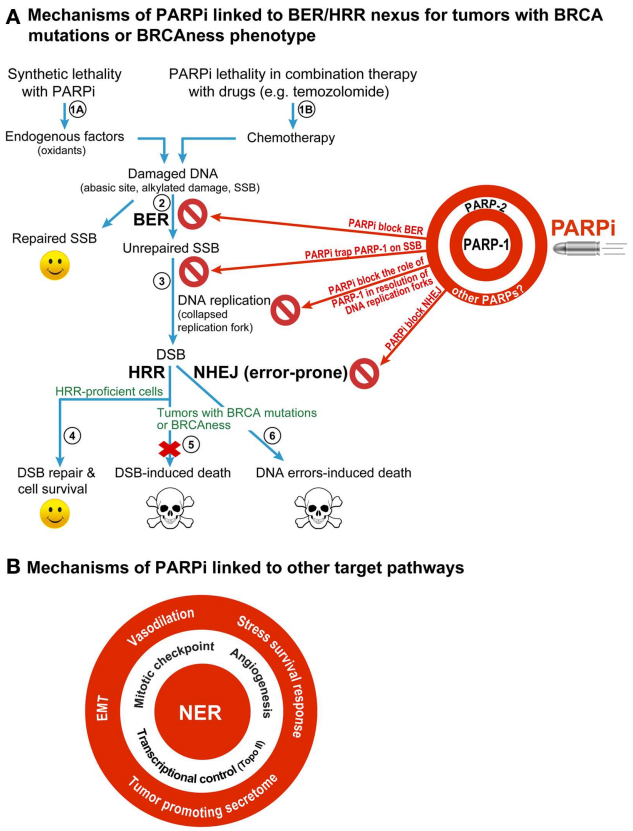

FIGURE 1 | Different mechanisms for therapeutic efficacy of PARPi in cancers. **(A)** BER/HRR model: this model focuses on the role of PARP-1, the principal target of PARPi, in BER that removes abasic sites and SSB created constantly in the mammalian genome by endogenous oxidants (steps 1A). During BER, the binding of PARP-1 to SSB leads to stimulation of its catalytic activity of forming polymers of ADP-ribose (PAR) from its substrate NAD^+. The PAR and PARP-1 interact with and recruit the key BER scaffold protein XRCC1, whereas PAR-modified PARP-1 loses its affinity to bind to SSB and vacates the site for BER to continue. When PARPi suppress the role of PARP-1 in BER (step 2), the unrepaired SSB would accumulate and collapse the DNA replication fork to form potentially lethal DSB (step 3). The normal cells would survive by repairing these DSB by HRR (step 4), but the HRR-deficient BRCA-mutants would die due to unrepaired DSB (step 5) or possibly due to excessive reliance on the error-prone NHEJ repair pathway to remove DSB (step 6). This BER/HRR nexus also explains the effectiveness of combination therapy of PARPi with drugs that cause DNA damage that is repaired by BER (step 1B). Since PARP-2 is also known to play a role in BER, and since current PARPi are also known to inhibit PARP-2, the effect of PARPi may also be mediated by targeting of the functions of PARP-2 in BER, as shown on the target board along with PARP-1. In addition, the inhibitory effect of PARPi on other PARPs could also influence therapeutic efficacy of PARPi (see target board), although their contribution to BER/HRR mediated therapeutic effect of PARPi is not yet fully assessed. **(B)** Other targets of PARPi that can confer therapeutic benefits of PARPi: PARPi could also be effective anticancer agents by targeting the role of PARP-1 in other DNA repair pathways, such as NER; or other cellular pathways, such as control over cell cycle, tumor angiogenesis, transcription, epithelial-mesenchymal transition (EMT), stress survival response, vasodilation, or tumor-promoting secretome.

EXPANDING UNIVERSE OF POTENTIAL TARGETS OF PARPi

Therapeutic effectiveness of PARPi seen with some drugs cannot be explained by any of the above models, e.g., the potentiating effects of PARPi on the platinum-based drugs such as carboplatin, cisplatin, or oxaliplatin on HRR-deficient or -proficient tumors [reviewed in Ref. (1, 7)] (**Figure 1B**). These observations were further supported by recent studies showing the potentiating effect of PARPi veliparib on carboplatin treatment of patients with BRCA-mutant breast cancers (14) or carboplatin and phosphoinositide 3-kinase mTOR inhibitor treatment of mouse xenografts of BRCA-competent triple negative breast cancer cells (15). Since platinum compounds cause DNA damage that is largely repaired by the nucleotide excision repair (NER) pathway and not BER, we need to think beyond BER for an explanation. Moreover, BER was shown to mediate toxicity of cisplatin by competing with the repair of cisplatin inter-strand cross-links and DSB caused by these links (16). Therefore, if PARPi effect was mainly via inhibition of BER, we should have observed less and not more toxicity of cisplatin.

One possible explanation is that PARPi could be causing vasodilation (**Figure 1B**) to improve intra-tumoral delivery of platinum drugs (1), although it needs to be confirmed if this generalized effect could also potentiate other drugs. On the other hand, recently discovered roles of PARP-1 in improving the efficiency of NER-mediated removal of UV-induced DNA damage (17–19) provides a more handy explanation for the PARPi-induced potentiation of platinum compound-based drugs, which also cause DNA damage that is repaired by NER (**Figure 1B**). This NER targeting effect of PARPi alone can account for death of HRR-proficient tumors, as seen in clinical trials [reviewed in Ref. (1, 7)] and supported by *in vitro* results showing that PARP-1 depletion (20) or inhibition (19) decreases clonogenic survival of UV-exposed human skin fibroblasts with no reported HRR-deficiencies. Of course, PARPi could have an additional effect in this model due to suppression of the role of PARP-1 in HRR pathway (21). In addition, in the PARPi-treated BRCA-mutant HRR-deficient tumors, the unrepaired DNA damage by platinum drugs could collapse the DNA replication fork to form DSB and cause lethality. Thus, the NER effect alone or NER-HRR nexus could be possible explanations for the lethality of PARPi/platinum compounds in HRR-proficient or -deficient tumors.

The clinical and preclinical studies have also revealed other targets of PARPi in cancer therapies that are linked to various roles of their multifunctional target PARP-1 in following cellular processes (**Figure 1B**). (i) Transcriptional control of drug-target genes: PARPi have been shown to increase toxicity of topoisomerase II-poison doxorubicin *in vitro* (22) or in xenografted tumors in mice (23). This effect could be

due to doxorubicin-induced decrease in expression and activity of PARP-1 (24) or PARPi-mediated increase in expression of topoisomerase II, because the transcription activator Sp1 loses its affinity for the topoisomerase II-promoter region upon modification by polymer of ADP-ribose (PAR) created by the activated PARP-1 (22). (ii) Mitotic checkpoint: the beneficial effects of PARPi with microtubule stabilizing mitotic inhibitor paclitaxel in patients with recurrent metastatic gastric cancers with BRCAness phenotype (25) could be linked to suppression of the role of PARP-1 in maintaining the mitotic checkpoint via PARylation of itself or the mitotic checkpoint protein CHFR (26, 27). An abrogation of mitotic checkpoint would kill cancer cells, because they will be forced to divide before resolution of the damage. (iii) Tumor-promoting secretome: PARPi-mediated suppression of the role of PARP-1 in elaborating tumor-promoting secretome containing cytokines and growth factors has been suggested as a cause for decreasing the resistance to another mitotic inhibitor docetaxel (28). (iv) Angiogenesis: the role of PARP-1 in promoting angiogenesis that fuels the growth of tumors can also be target of PARPi, because PARP-1 depletion or PARPi reduce vessel formation (29) and expression of markers of angiogenesis in melanoma (30) or endothelial cells (31). (v) Epithelial-mesenchymal transition (EMT) and metastasis: PARPi or PARP-1 depletion-induced reduction in aggressiveness and growth of metastatic melanoma in animal studies (30, 31) along with decreased markers for EMT (31, 32) suggest that the increase in progression-free survival of PARPi-treated patients could be due to reduction in the proliferation rate of the primary tumor and repression of its metastatic potential. (vi) Stress survival response: finally, cancer cells respond to any therapy by elaborating various stress responses to survive; and PARP-1 and its product PAR play key roles in these stress responses (9). Hence the suppression of pro-survival stress responses could explain the effectiveness of PARPi with any anti-cancer drug. An expanding list of potential targets of PARPi provides us with a much larger vision of the future applications of PARPi in cancer therapy.

BROAD SPECIFICITY OF PARPi: A KEY ISSUE FOR THE FUTURE OF PARPi THERAPY

There are two basic issues arising from the broad specificity of current PARPi.

(a) PARPi can inhibit more than one PARP ("they are bazookas not bullets"): many of the current PARPi in clinical trials display strong binding to PARPs 1–4 (33), and inhibit both PARP-1 and 2 at clinically relevant concentrations (10). Most studies assume that the effect of PARPi on both PARP-1 and 2 is important for therapy; however, this may not be the case. In fact, some studies using specific knockdown of PARPs showed that only the knockdown of PARP-1, but not PARP-2, replicates: (i) the synthetic lethal effect of PARPi on BRCA2 mutant cells (3); (ii) potentiation of cisplatin by PARPi in BRCA-proficient triple negative breast cancer cells (34); and (iii) sensitization of melanoma cells *in vitro* to temozolomide (35). On the other hand, the effect of PARPi on gemcitabine in the above breast cancer cells was replicated by PARP-2 knockdown and not PARP-1 knockdown (34). In contrast, the siRNA for PARP-1 could specifically prevent the growth of BRCA-deficient ovarian cancer cell-derived tumors in mice (36). Since the double knockout of PARP-1 and PARP-2 is embryonic lethal (37), we must verify the assumption that gratuitous inhibition of unrelated PARPs has no effect on the end-results.

(b) Indiscriminate inhibition of all the roles of a given PARP by PARPi ("we are nuking the entire PARP-landscape"): PARP-1, the principal target of PARPi, is a multifunctional protein that is implicated not only in DNA repair but also in various forms of cell death, transcription, epigenetic control of gene expression, and chromatin remodeling (8, 38). Hence even if we were to develop novel PARPi to specifically inhibit only PARP-1, it will still shut down most if not all the functions of PARP-1. Similar arguments can be made for PARPi-mediated suppression of different roles of PARP-2. Although adverse genomic consequences of PARPi therapy have not yet been reported, we need to consider that prolonged PARPi therapy may cause genome instability because PARP-$1^{-/-}$ mouse embryonic fibroblasts have a tendency to become tetraploid (39, 40), and the susceptibility of PARP-$1^{-/-}$ female mice to develop mammary carcinoma is enhanced if p53 is also mutated, a phenomenon frequently observed in cancers (41). In effect, PARPi are the magic bullets, but instead of doing precision targeting with them for the desired effect, we are simply nuking the entire spectrum of functions of that target PARP, which could result in unintended consequence during maintenance (prolonged) therapy with PARPi including survival of damaged cancer cells, development of secondary tumors as a consequence of genomic instability and resistance to PARPi. Thus, while the current broad specificity PARPi work properly for short-term cancer therapy, there is a need for development of new and more specific PARPi that are unique not only for a given PARP but also for a given function of that PARP related to its anti-cancer effect.

It is heartening that PARPi have shown some clinical benefit for BRCA-mutant cancer patients in clinical trials as monotherapy or as a combination therapy, but we need to do a lot more to understand the therapeutic effect of PARPi to establish them firmly in the arsenal of anti-tumor agents against variety of cancers.

ACKNOWLEDGMENTS

Mihaela Robu was recipient of the Pierre J. Durand doctoral scholarship award from Faculty of Medicine Laval University (2011–12) the Doctoral scholarship award Fonds de recherche Santé Québec (FRQ-S, # 27896 since 2013). Nupur K. Purohit was recipient of the foreign student supplemental fee waiver scholarship from Laval University and from the Shastri Indo-Canadian Institute (since 2012). This work was supported by the CIHR operating grant #89964 to Girish M. Shah.

REFERENCES

1. Curtin NJ, Szabo C. Therapeutic applications of PARP inhibitors: anticancer therapy and beyond. *Mol Aspects Med* (2013) **34**(6):1217–56. doi:10.1016/j.mam.2013.01.006
2. Do K, Chen AP. Molecular pathways: targeting PARP in cancer treatment. *Clin Cancer Res* (2013) **19**(5):977–84. doi:10.1158/1078-0432.CCR-12-0163
3. Bryant HE, Schultz N, Thomas HD, Parker KM, Flower D, Lopez E, et al. Specific killing of BRCA2-deficient tumours with inhibitors of poly(ADP-ribose) polymerase. *Nature* (2005) **434**(7035):913–7. doi:10.1038/nature03443
4. Farmer H, McCabe N, Lord CJ, Tutt AN, Johnson DA, Richardson TB, et al. Targeting the DNA repair defect in BRCA mutant cells as a therapeutic strategy. *Nature* (2005) **434**(7035):917–21. doi:10.1038/nature03445
5. Helleday T. The underlying mechanism for the PARP and BRCA synthetic lethality: clearing up the misunderstandings. *Mol Oncol* (2011) **5**(4):387–93. doi:10.1016/j.molonc.2011.07.001
6. De Lorenzo SB, Patel AG, Hurley RM, Kaufmann SH. The elephant and the blind men: making sense of PARP inhibitors in homologous recombination deficient tumor cells. *Front Oncol* (2013) **3**:228. doi:10.3389/fonc.2013.00228
7. Tentori L, Muzi A, Dorio AS, Dolci S, Campolo F, Vernole P, et al. MSH3 expression does not influence the sensitivity of colon cancer HCT116 cell line to oxaliplatin and poly(ADP-ribose) polymerase (PARP) inhibitor as monotherapy or in combination. *Cancer Chemother Pharmacol* (2013) **72**(1):117–25. doi:10.1007/s00280-013-2175-0
8. Gibson BA, Kraus WL. New insights into the molecular and cellular functions of poly(ADP-ribose) and PARPs. *Nat Rev Mol Cell Biol* (2012) **13**(7):411–24. doi:10.1038/nrm3376
9. Luo X, Kraus WL. On PAR with PARP: cellular stress signaling through poly(ADP-ribose) and PARP-1. *Genes Dev* (2012) **26**(5):417–32. doi:10.1101/gad.183509.111
10. Montoni A, Robu M, Pouliot E, Shah GM. Resistance to PARP-inhibitors in cancer therapy. *Front Pharmacol* (2013) **4**:18. doi:10.3389/fphar.2013.00018
11. Lord CJ, Ashworth A. The DNA damage response and cancer therapy. *Nature* (2012) **481**(7381):287–94. doi:10.1038/nature10760
12. Murai J, Huang SY, Das BB, Renaud A, Zhang Y, Doroshow JH, et al. Trapping of PARP1 and PARP2 by clinical PARP inhibitors. *Cancer Res* (2012) **72**(21):5588–99. doi:10.1158/0008-5472.CAN-12-2753
13. Patel AG, Sarkaria JN, Kaufmann SH. Nonhomologous end joining drives poly(ADP-ribose) polymerase (PARP) inhibitor lethality in homologous recombination-deficient cells. *Proc Natl Acad Sci U S A* (2011) **108**(8):3406–11. doi:10.1073/pnas.1013715108
14. Somlo G, Frankel PH, Luu TH, Ma C, Arun B, Garcia A, et al. Efficacy of the combination of ABT-888 (veliparib) and carboplatin in patients with BRCA-associated breast cancer. *J Clin Oncol* (2013) **31**(15-Suppl):1024.
15. Dey N, Sun Y, Carlson J, Friedman L, De P, Leyland-Jones B. A combination of dual PI3K-mTOR inhibitor, GDC-0980, with PARP inhibitor plus carboplatin blocked tumor growth of BRCA-competent triple-negative breast cancer cells. *J Clin Oncol* (2013) **31**(15-Suppl):2613.
16. Kothandapani A, Dangeti VS, Brown AR, Banze LA, Wang XH, Sobol RW, et al. Novel role of base excision repair in mediating cisplatin cytotoxicity. *J Biol Chem* (2011) **286**(16):14564–74. doi:10.1074/jbc.M111.225375
17. Robu M, Shah RG, Petitclerc N, Brind'Amour J, Kandan-Kulangara F, Shah GM. Role of poly(ADP-ribose) polymerase-1 in the removal of UV-induced DNA lesions by nucleotide excision repair. *Proc Natl Acad Sci U S A* (2013) **110**(5):1658–63. doi:10.1073/pnas.1209507110
18. Luijsterburg MS, Lindh M, Acs K, Vrouwe MG, Pines A, van Attikum H, et al. DDB2 promotes chromatin decondensation at UV-induced DNA damage. *J Cell Biol* (2012) **197**(2):267–81. doi:10.1083/jcb.201106074
19. Pines A, Vrouwe MG, Marteijn JA, Typas D, Luijsterburg MS, Cansoy M, et al. PARP1 promotes nucleotide excision repair through DDB2 stabilization and recruitment of ALC1. *J Cell Biol* (2012) **199**(2):235–49. doi:10.1083/jcb.201112132
20. Ghodgaonkar MM, Zacal NJ, Kassam SN, Rainbow AJ, Shah GM. Depletion of poly(ADP-ribose)polymerase-1 reduces host cell reactivation for UV-treated adenovirus in human dermal fibroblasts. *DNA Repair (Amst)* (2008) **7**:617–32. doi:10.1016/j.dnarep.2008.01.001
21. Helleday T, Bryant HE, Schultz N. Poly(ADP-ribose) polymerase (PARP-1) in homologous recombination and as a target for cancer therapy. *Cell Cycle* (2005) **4**(9):1176–8. doi:10.4161/cc.4.9.2031
22. Magan N, Isaacs RJ, Stowell KM. Treatment with the PARP-inhibitor PJ34 causes enhanced doxorubicin-mediated cell death in HeLa cells. *Anticancer Drugs* (2012) **23**(6):627–37. doi:10.1097/CAD.0b013e328350900f
23. Mason KA, Valdecanas D, Hunter NR, Milas L. INO-1001, a novel inhibitor of poly(ADP-ribose) polymerase, enhances tumor response to doxorubicin. *Invest New Drugs* (2008) **26**(1):1–5. doi:10.1007/s10637-007-9072-5
24. Zaremba T, Ketzer P, Cole M, Coulthard S, Plummer ER, Curtin NJ. Poly(ADP-ribose) polymerase-1 polymorphisms, expression and activity in selected human tumour cell lines. *Br J Cancer* (2009) **101**(2):256–62. doi:10.1038/sj.bjc.6605166
25. Bang Y-J, Im S-A, Lee K-W, Cho JY, Song E-K, Lee KH, et al. Olaparib plus paclitaxel in patients with recurrent or metastatic gastric cancer: a randomized, double-blind phase II study. *J Clin Oncol* (2013) **31**(15-Suppl):4013.
26. Ahel I, Ahel D, Matsusaka T, Clark AJ, Pines J, Boulton SJ, et al. Poly(ADP-ribose)-binding zinc finger motifs in DNA repair/checkpoint proteins. *Nature* (2008) **451**(7174):81–5. doi:10.1038/nature06420
27. Kashima L, Idogawa M, Mita H, Shitashige M, Yamada T, Ogi K, et al. CHFR protein regulates mitotic checkpoint by targeting PARP-1 protein for ubiquitination and degradation. *J Biol Chem* (2012) **287**(16):12975–84. doi:10.1074/jbc.M111.321828
28. Zhao S, Coleman I, Coleman R, Nelson P. Association of PARP inhibitors and docetaxel resistance through suppressing a tumor microenvironment-associated secretory program. *J Clin Oncol* (2013) **31**(15-Suppl):e22212.
29. Tentori L, Lacal PM, Muzi A, Dorio AS, Leonetti C, Scarsella M, et al. Poly(ADP-ribose) polymerase (PARP) inhibition or PARP-1 gene deletion reduces angiogenesis. *Eur J Cancer* (2007) **43**(14):2124–33. doi:10.1016/j.ejca.2007.07.010
30. Tentori L, Muzi A, Dorio AS, Bultrini S, Mazzon E, Lacal PM, et al. Stable depletion of poly (ADP-ribose) polymerase-1 reduces in vivo melanoma growth and increases chemosensitivity. *Eur J Cancer* (2008) **44**(9):1302–14. doi:10.1016/j.ejca.2008.03.019
31. Rodríguez MI, Peralta-Leal A, O'Valle F, Rodriguez-Vargas JM, Gonzalez-Flores A, Majuelos-Melguizo J, et al. PARP-1 regulates metastatic melanoma through modulation of vimentin-induced malignant transformation. *PLoS Genet* (2013) **9**(6):e1003531. doi:10.1371/journal.pgen.1003531
32. McPhee TR, McDonald PC, Oloumi A, Dedhar S. Integrin-linked kinase regulates E-cadherin expression through PARP-1. *Dev Dyn* (2008) **237**(10):2737–47. doi:10.1002/dvdy.21685
33. Wahlberg E, Karlberg T, Kouznetsova E, Markova N, Macchiarulo A, Thorsell AG, et al. Family-wide chemical profiling and structural analysis of PARP and tankyrase inhibitors. *Nat Biotechnol* (2012) **30**(3):283–8. doi:10.1038/nbt.2121
34. Hastak K, Alli E, Ford JM. Synergistic chemosensitivity of triple-negative breast cancer cell lines to poly(ADP-Ribose) polymerase inhibition, gemcitabine, and cisplatin. *Cancer Res* (2010) **70**(20):7970–80. doi:10.1158/0008-5472.CAN-09-4521
35. Tentori L, Muzi A, Dorio AS, Scarsella M, Leonetti C, Shah GM, et al. Pharmacological inhibition of poly(ADP-ribose) polymerase (PARP) activity in PARP-1 silenced tumour cells increases chemosensitivity to temozolomide and to a N3-adenine selective methylating agent. *Curr Cancer Drug Targets* (2010) **10**(4):368–83. doi:10.2174/156800910791208571
36. Goldberg MS, Xing D, Ren Y, Orsulic S, Bhatia SN, Sharp PA. Nanoparticle-mediated delivery of siRNA targeting Parp1 extends survival of mice bearing tumors derived from Brca1-deficient ovarian cancer cells. *Proc Natl Acad Sci U S A* (2011) **108**(2):745–50. doi:10.1073/pnas.1016538108
37. Menissier de Murcia J, Ricoul M, Tartier L, Niedergang C, Huber A, Dantzer F, et al. Functional interaction between PARP-1 and PARP-2 in chromosome stability and embryonic development in mouse. *EMBO J* (2003) **22**(9):2255–63. doi:10.1093/emboj/cdg206
38. Zampieri M, Guastafierro T, Calabrese R, Ciccarone F, Bacalini MG, Reale A, et al. ADP-ribose polymers localized on Ctcf-Parp1-Dnmt1 complex prevent methylation of Ctcf target sites. *Biochem J* (2012) **441**(2):645–52. doi:10.1042/BJ20111417

39. Simbulan-Rosenthal CM, Haddad BR, Rosenthal DS, Weaver Z, Coleman A, Luo R, et al. Chromosomal aberrations in PARP(-/-) mice: genome stabilization in immortalized cells by reintroduction of poly(ADP-ribose) polymerase cDNA. *Proc Natl Acad Sci U S A* (1999) **96**(23):13191–6. doi:10.1073/pnas.96.23.13191
40. Halappanavar S, Shah GM. Defective control of mitotic and post-mitotic checkpoints in Poly(ADP-ribose) polymerase-1(-/-) fibroblasts after mitotic spindle disruption. *Cell Cycle* (2004) **3**(3):335–42. doi:10.4161/cc.3.3.670
41. Tong WM, Yang YG, Cao WH, Galendo D, Frappart L, Shen Y, et al. Poly(ADP-ribose) polymerase-1 plays a role in suppressing mammary tumourigenesis in mice. *Oncogene* (2006) **26**(26):3857–67. doi:10.1038/sj.onc.1210156

Received: 16 October 2013; accepted: 29 October 2013; published online: 14 November 2013.
*Citation: Shah GM, Robu M, Purohit NK, Rajawat J, Tentori L and Graziani G (2013) PARP inhibitors in cancer therapy: magic bullets but moving targets. Front. Oncol. **3**:279. doi: 10.3389/fonc.2013.00279*